REGULATION OF CONNEXIN43 AND ASTROCYTIC GAP JUNCTIONAL INTERCELLULAR COMMUNICATION IN THE CENTRAL NERVOUS SYSTEM

A Thesis

Submitted to the Faculty of Graduate Studies

in Partial Fulfillment of the Requirements

for the Degree of

Doctor of Philosophy

in Physiology

by

Wei Li

5372615

Department of Physiology

University of Manitoba

Winnipeg, Manitoba

THE UNIVERSITY OF MANITOBA

FACULTY OF GRADUATE STUDIES

*****

COPYRIGHT PERMISSION PAGE

Regulation of Connexin43 and Astrocytic Gap Junctional Intercellular Communication in the Central Nervous System

BY

Wei Li

A Thesis/Practicum submitted to the Faculty of Graduate Studies of The University of Manitoba in partial fulfillment of the requirements of the degree of Doctor of Philosophy

TABLE OF CONTENTS

ACKNOWLEDGEMENTS

I would like to thank my supervisor, Dr. James I. Nagy, for providing me the opportunity to pursue a career of scientific research in Canada, for his extreme patience in guiding me through this six and half year program and for all the responsibilities he has taken in helping me to live and study in Canada. From him, I learned how much it can take to be a successful scientist.

I will be forever grateful to the members of my advisory committee- Dr. David McCrea, Dr. Marc R. Del Bigio and Dr. Larry M. Jordan. They have helped me more than they probably realize. From them, I learned what I shall do, as a scientist as well as a member of a great society, to help a person in his difficult times.

I would like to thank technicians in our laboratory, Bernard Boguski, Jerry Stelmack, Andrew Ochalski and Mike Sawchuk, for teaching me various experimental techniques, for their contributions to the works included in this thesis and for their friendship that greatly enriched my life in Winnipeg.

I would also like to express my gratitude to Jian Li, Bruce Lynn, Xinbo Li, Norm Haughey, Daywin Patel, Uta Frankenstein for having made the past years more endurable and enjoyable for me.

I am thankful to Dr. William Staines for reading this thesis and providing his helpful comments.

Special credit goes to my wife, Yanchun Zhang, for walking me through these years with great understanding, appreciation and love.

I would like to dedicate this thesis to my mother, Zhao Yunying, the greatest person in my life.

Abstract

The objective of this project was to determine the functional states of astrocytic gap junctions under physiological and pathological conditions by analyzing the expression, localization, phosphorylation and immunorecognition of a major astrocytic gap junction protein, connexin43 (Cx43). These studies were aided by antibody 13-8300 that selectively recognizes the non-phosphorylated form, but not the multiply phosphorylated forms of Cx43 in several cell types in vitro and in vivo. The failure of 13-8300 to recognize phosphorylated Cx43 is likely due to blockade of phosphate groups, suggesting that the epitope recognized by 13-8300 contains an early phosphorylation site. Non-phosphorylated Cx43 was seen primarily in the cytoplasm, whereas phosphorylated Cx43 was seen at gap junctions as well as in the cytoplasm. Sciatic nerve stimulation induced preferential dephosphorylation of junctional Cx43 in spinal cord astrocytes, suggesting that junctional Cx43 is more vulnerable to dephosphorylation than cytoplasmic Cx43 and that astrocytic gap junctional intercellular communication (GJIC) can be regulated by neuronal activity. Dephosphorylation of astrocytic Cx43 was also seen in ischemic rat brain. Thus, Cx43 dephosphorylation may represent a common mechanism of the regulation of astrocytic GJIC under physiological and pathological conditions. Mild brain ischemia induced rapid and reversible Cx43 dephosphorylation, whereas severe ischemia led to total removal of Cx43 gap junctions in the lesion center surrounded by a zone of dephosphorylated Cx43 in the penumbral region, indicating distinct functional states of astrocytes in these regions. Reactive astrocytes appear in injured rat CNS at a later survival time and in the vicinity of senile and amyloid plaques in human Alzheimer's disease brain. These cells may express Cx43 and form gap junctions, indicating the re-establishment of GJIC in damaged tissue. Chemical hypoxia induced immediate reduction of astrocytic GJIC in vitro, which was followed by massive Cx43 dephosphorylation. Inhibition of Cx43 dephosphorylation by calcineurin inhibitors led to partial preservation of GJIC, indicating that Cx43 dephosphorylation is related to further reduction of GJIC in hypoxic astrocytes. These results suggest that astrocytes regulate GJIC in a programmed manner under physiological and pathological conditions.

Abbreviations

AD	Alzheimer's disease
BSA	bovine serum albumin
CaMKII	Ca^{2+}/calmodulin-dependent protein kinase II
CNS	central nervous system
Cx	connexin
DAB	3,3-diaminobenzidine
DMEM	Dulbecco's modified essential medium
DMSO	dimethyl sulfoxide
DTT	dithiothreitol
EGF	epidermal growth factor
EM	electron microscopy
ER	endoplasmic reticulum
FBS	fatal bovine serum
FITC	fluorescein isothiocyanates
GFAP	glial fibrillary acidic protein
GJIC	gap junctional intercellular communication
HBSS	Hank's balanced salt solution
H&E	hematoxylin and eosin
HSR	heavy sarcoplasmic reticulum
ir	immunoreactivity
kDa	kilodalton
LM	light microscopy
LSR	light sarcoplasmic reticulum
LY	lucifer yellow
MAP kinase	mitogen-activated protein kinase
MCA	middle cerebral artery

Mr	relative molecular weight
NMDA	N-methyl-D-aspartate
nS	nanosiemens
PAP	peroxidase anti-peroxidase
PB	0.1 M sodium phosphate buffer
PBS	phosphate-buffered saline
PBSF	PBS containing 0.1% Photo-Flo
PBST	phosphate-buffered saline with Triton X-100
PDGF	platelet-derived growth factor
PKA	cAMP-dependent protein kinase
PKC	protein kinase C
PKG	cGMP-dependent protein kinase
PMSF	phenylmethanesulfonyl fluoride
PP-1	type-1 protein phosphatases
PP-2	type-2 protein phosphatases
PP-2A	type-2A protein phosphatases
PP-2B	type-2B protein phosphatases
PP-2C	type-2C protein phophatases
pS	picosiemens
PVDF	polyvinylinene difluoride
RER	rough endoplasmic reticulum
SDS-PAGE	sodium dodecyl sulphate polyacrylamide gel electrophoresis
SCSL	single-cell-scrape-loading
S.E.M.	standard error of mean
Ser	serine
SL	sarcolemma
SR	sarcoplasmic reticulum
TBS	20 mM Tris-HCl buffered saline

TBS-T	TBS containing 0.2% Tween-20
Thr	threonine
TPA	12-O-tetradecanoylphorbol-13-acetate
TSM	tracheal smooth muscle
Tyr	tyrosine
ZO-1	zona occludens-1

GENERAL INTRODUCTION

I. Gap Junctions

In multicellular organisms, physiological functions of specific organs require intercellular communication to coordinate cellular responses to external stimuli. A rapid way of cell-cell communication is by direct transfer of messenger molecules between adjacent cells. Thus, intercellular channels that connect groups of specially differentiated cells would greatly facilitate the coordination or synchronization of the activity of these cells. Gap junctions are the best candidate for providing intercellular passage of molecules such as ions, metabolites and secondary messengers. On the other hand, deleterious cellular activities need to be isolated from the rest of the group to limit the hazardous effect on the organ or the whole organism. Therefore, direct intercellular channels have to be regulated to accommodate the needs of dynamic cellular activity. Recent studies have demonstrated that GJIC can be regulated at several levels including junction protein synthesis and trafficking, channel assembly and gating, and channel internalization and degradation. Phosphorylation and dephosphorylation of gap junction proteins are believed to be important for channel assembly and gating. Thus, regulation of the phosphorylation state of gap junction proteins may have a direct impact on intercellular communication and cellular activities. This thesis describes the phosphorylation state of Cx43 and the effect of Cx43 dephosphorylation on junctional coupling in astrocytes under physiological and pathological conditions.

I.1. Low-resistance intercellular channels

The first physiological observation of these channels was reported by Weidman in 1952. He found that intercellular resistance between Purkinje fibers in heart tissue was less than one tenth of the membrane resistance of these cells. This was followed by the first observation of intercellular electrical coupling in neural tissue, the giant motor synapses of the abdominal nerve cord of the crayfish (Furshpan and Potter, 1959). The synaptic transmission from the presynaptic lateral giant fiber to the postsynaptic giant motor fiber displayed only 0.1 ms

delay, a period much less than the 0.5 ms delay in ordinary chemical synaptic transmission. Intercellular resistance was one seventh that of a similar area of axon membrane (Furshpan and Potter, 1959). Following these reports, numerous observations of low resistance intercellular channels in excitable tissues were published, and this type of electronic coupling was believed to be a special feature of excitable cells and might serve primarily to facilitate the propagation of action potentials (Loewenstein, 1981; Peracchia, 1980). This opinion was not challenged till 1964 when Kanno and Loewenstein demonstrated that sodium fluorescein could enter neighboring epithelial cells without a detectable presence in the extracellular space. (Kanno and Loewenstein, 1964; Loewenstein and Kanno, 1964). These observations were followed by the discovery of intercellular transfer of this fluorescent molecule in glia (Kuffler and Potter, 1964) and at the electrical synapse in crayfish (Pappas and Bennett, 1966; Payton et al., 1969). Thus, it is clear that direct intercellular channels exist in both non-excitable and excitable cells. It was subsequently determined that these channels are permeable to molecules up to 1.2 kilodalton (kDa) (Loewenstein, 1981), which corresponds to an estimated channel diameter of 1.4 nm (Simpson et al. 1977).

I.2. Characterization of gap junctions

It would not have been possible to determine the fine structure of gap junctions without electron microscopy (EM). Gap junctions were reported using EM for the first time by Dewey and Barr (1962) in smooth muscle cells in the jejunum. These structures were named "nexus". The clear description of the extracellular gap in these junctional structures was made in an ultrastructural study of Mauthner cell synapses in goldfish brain by Robertson (1963). In this study, he noticed a constant gap separating the pre- and postsynaptic membranes of the synaptic discs, suggesting the presence of specialized intercellular junctions, which are different from chemical synapses. Robertson also noticed ~9.5 nm hexagonal profiles on the plasma membrane in transverse sections. In 1967, Revel and Karnovsky applied the uranyl staining technique in preparations of thin sections from

Fig. 1. Gap junction structures. A. The cross-sectional profile of vertebrate gap junctions, showing the gap (arrow) between two apposing plasma membranes. B. An isolated liver gap junction plaque viewed above the membrane plane, showing the hexagonal array of gap junction particles. The area around the channels and in the pores was darkened by colloidal lanthanum negative staining. C. A three dimensional model of gap junctions based on X-ray diffraction studies. A gap junction channel is formed by two hemichannels, also termed connexons, from apposing plasma membranes. Each connexon consists of six connexin molecules. Magnifications are 241,000 in A and 307,800 in B. A was taken from Peracchia, 1980, B was from Kandel et al., 1991 and C was from Makowski et al., 1977.

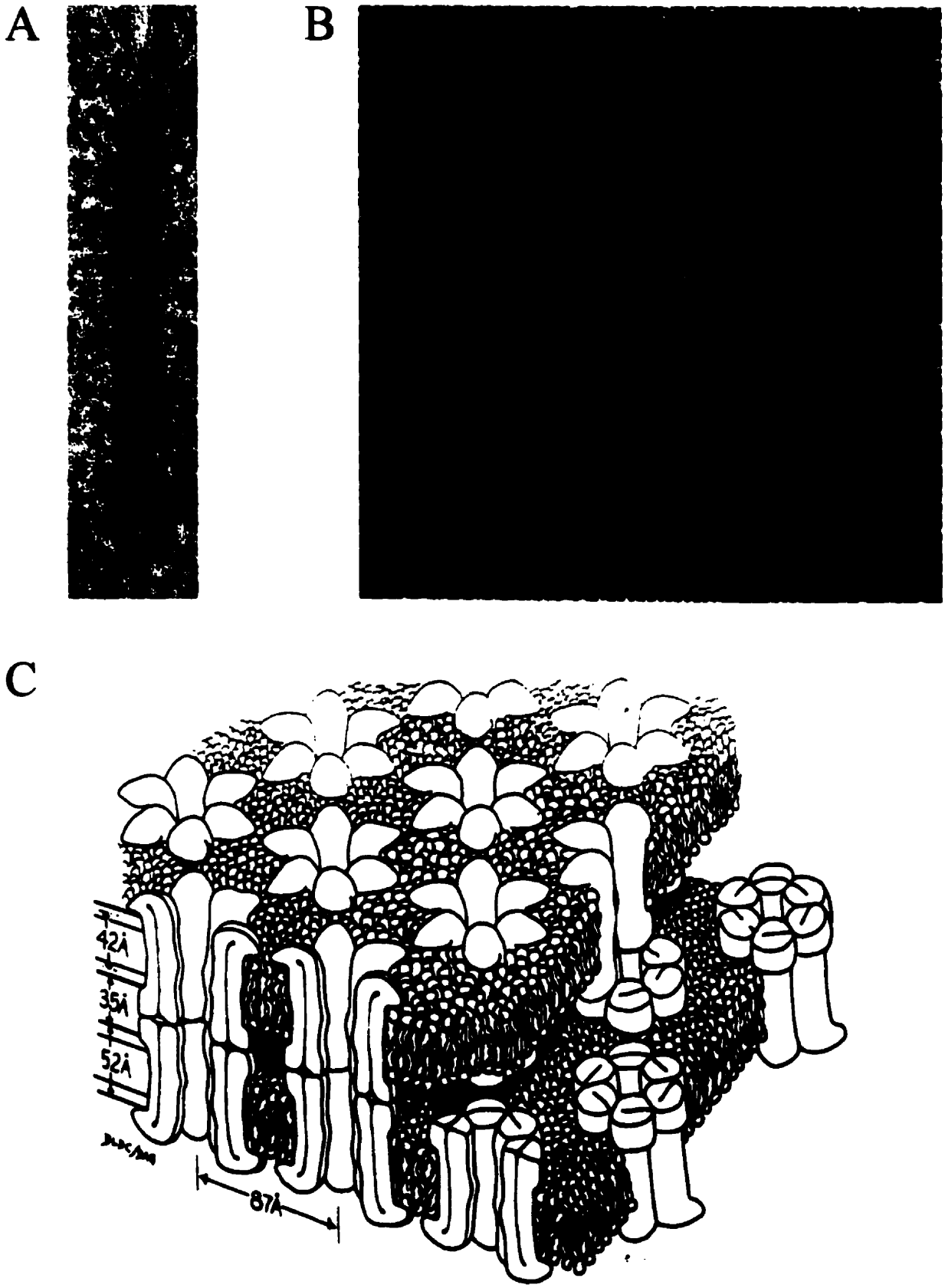

Fig. 1

cardiac and liver cells for electron microscopic study. Uranyl staining effectively increased membrane electronic density and enabled them to visualize a 2-3 nm wide extracellular space at the specialized membrane region between adjacent cells. This space was confirmed by its permeability to the electron-opaque element lanthanum that does not permeate cell membranes. In contrast, tight junctions, another type of intercellular junction, were not stained by lanthanum, suggesting that the intercellular junctions with a gap were different from tight junctions. The characteristic "gap" was included in the new term to describe these membrane junctions, gap junctions (Goodenough and Revel, 1970). The 15-19 nm thick septilaminar structure with a 2 nm gap between apposing membranes has since been the fundamental characteristic of gap junctions (Fig. 1A). Moreover, lanthanum staining also delineated the hexagonally packed structures (Fig. 1B) in the junctional membrane in transverse sections (Robertson, 1963; Revel and Karnovsky, 1967). In the center of each hexagonal structure, there is an electron-opaque core of about 1 nm in diameter, which indicates that these structures might be intercellular channels (Revel and Karnovsky, 1967). With freeze-fracture techniques, Kreutziger (1968) found that, corresponding to the hexagonal lattice, there were intra-membrane particles penetrating deep into the hydrophobic regions of the junctional membranes on both sides of the 2-nm gap. These hexagonal particles were later termed connexons (Goodenough, 1975). Connexons protrude from opposite membrane surfaces, come in contact with each other to bridge the gap and constitute membrane continuity between connected cells. The principal junction protein in connexons was termed connexin (Goodenough, 1974).

Proteolytic degradation failed to split the apposing membranes at gap junctions, suggesting that this 2 nm intercellular gap was too narrow for the penetration of proteases. Gap junctions were also found to be resistant to destruction by detergents (Goodenough, 1974,1975). These properties of gap junctions facilitated the isolation of sufficient amounts of relatively pure gap junctions for biochemical and biophysical analysis. After analyzing the EM and X-ray diffraction data from isolated liver gap junctions (Caspar et al., 1977), in conjunction with the "lipid globular protein mosaic model" (Singer and Nicolson, 1972),

Makowski et al. proposed a model for the structure of gap junctions in 1977 (Fig. 1C). In this model, each gap junction channel is composed of a pair of connexons from two apposing membranes of adjacent cells. Each connexon is formed by six protein subunits, connexins. Connexons are tightly packed in the plane of the membrane, and adjacent connexons are associated with each other by intercellular forces. The diameters of connexons and junction channels were later determined to be 6.5 and 1.7 nm, respectively (Unger et al., 1997). Therefore, gap junctions are now described as aggregates of intercellular aqueous channels at specialized membrane regions formed by hemichannels, connexons (Beyer et al., 1987) from apposing cells. These channels were subsequently identified in nearly all tissues (Peracchia, 1980; Loewenstein, 1981).

I.3.Gap junctions are intercellular communication channels

The concept that gap junction channels are the only intercellular communication channels emerged from a number of observations. The membrane regions forming gap junctions were found to be the regions in which cells are known to be in electrical interconnection, indicating that these structures may be necessary for electrical coupling (Robertson, 1963; Furshpan and Potter, 1959; Revel and Karnovsky, 1967). The initial evidence for the role of gap junctions in cell coupling came from studies by Barr et al. (1965). These investigators found that gap junctional membranes in vertebrate cardiac cells became separated, being mechanically pulled apart as a result of cell shrinkage in hypertonic solutions. Simultaneously, the intercellular resistance increased to completely cell uncoupling, suggesting that the integrity of gap junctions is necessary for the preservation of normal cell-to-cell communication via small ions. This process proved to be reversible since electrical coupling recovered after the tonicity of the solution was returned to the normal range. These results indicated that electrical coupling is dependent on the integrity of gap junctions. In 1972, Gilula et al. studied the involvement of gap junctions in both metabolic and electrical coupling by using three types of cells. They found that metabolic and electrical coupling occurred only in cells that could form gap junctions. In cells that did not form gap junctions,

there was no coupling of either kind even though these cells contacted each other physically and formed tight junctions and other types of cell-cell junctions. This study strongly suggested that intercellular electrical and metabolic coupling requires gap junctions and also indicated that gap junctions may be the only communication channels between these cells. The role of gap junctions in intercellular communication was further supported by another study in which normal human cells capable of electrical coupling were fused with mouse malignant cells incapable of electrical coupling (Azarnia et al., 1974). The resulting hybrid cells displayed electrical coupling and gap junctions. Once the clone lost the human chromosomes, these cells were uncoupled and gap junctions were no longer detectable. Results of these and many other studies have provided convincing evidence supporting the notion that gap junctions are the only intercellular junctions suited for direct intercellular communication. Thus, gap junctions are also called communication channels.

I.4. Gap junction coupling Assays

Based on the understanding that gap junctions are the only intercellular communication channels and that these channels are permeable to small molecules, a number of methods have been developed to assay the efficacy of GJIC. These methods can be classified into two categories. One is to measure the transfer of exogenous tracer molecules between adjacent cells and the other is to measure the intercellular electrical currents carried by intracellular ions. In the first category, metabolically labeled molecules, fluorescent dyes and other tracers are used to indicate the passive diffusion from the loaded cell(s) to adjacent cells. These tracer molecules must be membrane impermeable, gap junction permeable, nontoxic to the cells and have low affinity to cytoplasmic components. Fluorescein was the first fluorescent dye extensively used to characterize direct intercellular coupling (Loewenstein, 1981). However, this dye was found to be permeable to non-junctional membrane (Peracchia, 1980) and was thus gradually replaced by lucifer yellow (LY) (Stewart, 1978), which is still widely used. Biocytin and neurobiotin are suggested to have much higher junction permeability than LY and have been successfully used to unveil gap junctions

impermeable to LY (Kandler and Katz, 1995; Yuste et al., 1995; Goodenough et al., 1996). It is now believed to be necessary to re-examine all tissues previously considered to be junctionally uncoupled based on LY transfer assay (Kandler and Katz, 1995; Yuste et al., 1995).

The second category of assaying GJIC is to measure electrical current between junctionally coupled cells. This was first performed in excitable cells and subsequently also in non-excitable cells. Initial measurements involved two recording microelectrodes in two cells and a third electrode for passing current in one of the two cells. Injection of a current into one cell elicits pre-junctional and post-junctional voltages recorded by two voltage electrodes. The transjunctional resistance and conductance is then calculated. In well-coupled cells, the amplitude of the voltage changes is almost identical in both cells, which indicates the presence of low-resistance intercellular channels. Junctional resistance was estimated at 3 - 12 x 10^{-3} Ω/cm^2, while the resistance of non-junctional membranes is of the order of 1 - 2.6 x $10^3\Omega/cm^2$ (Loewenstein, 1981). Based on the value of specific junctional resistance and the assumption that these channels are hexagonally packed at 10 nm spacing, Loewenstein (1975) estimated the resistance of a single channel to be of the order of 10^{10} Ω. The estimated conductance of a single channel of about 100 pS, is comparable to the junction unitary conductance measured by the patch clamp technique (Dermietzel and Spray, 1993; Veenstra, 1996). Advances in electrophysiology have made it possible to measure single channel conductance with voltage-clamp and patch-clamp techniques. The single channel conductance of gap junctions formed by different connexins varies from tens of picosiemens (pS) to over two hundred pS (Dermietzel and Spray, 1993). This value also fits well with the resistance expected for a channel 1 - 2 nm in diameter and 20 nm in length, dimensions that are close to the structure of gap junctions suggested by ultrastructural, crystallographic, and tracer-transfer studies (Unger et al., 1999). The values of single channel conductance have been accepted by some investigators as a signature of gap

junctions formed by specific types of connexins (see discussions in Bruzzone et al., 1996; Veenstra, 1996; Dermietzel et al., 1997).

Measurement of intercellular current is much more sensitive than dye-transfer assays. Junctional conductance below 1-2 nanosiemens (nS) may not be detectable by LY transfer (Dermietzel and Spray, 1993). For example, the average unitary conductance of gap junction channels between cultured astrocytes is about 50-60 pS (Dermietzel et al., 1991; Giaume et al., 1991a), which means that gap junctions have to contain at least 20-40 open channels to be detected by LY transfer assay (Dermietzel and Spray, 1993). Moreover, if the unitary conductance represents the channel size, it is likely that gap junctions with a small unitary conductance may preferentially allow the passage of small particles such as ions. Therefore, it should be kept in mind that the absence of dye-coupling should not be taken as evidence of cell uncoupling because it may just reflect a specific coupling state with selective permeability. On the other hand, the available data on the characterization of channel conductance does not allow us to reliably correlate the channel permeability to specific substances.

II. Gap Junction Proteins

II.1. Connexins

II.1.1. Nomenclature

Two connexin nomenclatures have been proposed (Beyer et al., 1987; Kumar, 1999). One uses the predicted polypeptide molecular mass in kDa to distinguish between different members of the connexin family (e.g. connexin32, connexin43). The other one uses Greek letters to represent groups of connexins based on the overall connexin sequence similarities and the order that they are cloned, e.g. $\alpha 1$, $\alpha 2$... and $\beta 1$, $\beta 2$... (Kumar, 1999). Consensus on connexin nomenclature has not been reached. However, the former seems to be accepted by more investigators. In the following discussion, I will use the first nomenclature.

Table 1 Mammalian Connexin Multigene Family

Connexins	Predicted Mr (kDa)	Examples of tissue expression	References for gene cloning
Cx26	26.2	Hepatocytes, leptomeninges et al.	Zhang and Nicholson, 1989
Cx30	30.4	Astrocytes, leptominges	Dahl et al., 1996
Cx30.3	30.3	Kidney, skin	Hennemann et al., 1992b
Cx31	31	Keratinocytes	Hoh et al., 1991
Cx31.1	31.1	Keratinocytes,	Haefliger et al., 1992
Cx32	32	Oligodendrocytes, Schwann cells	Paul, 1986; Kumar and Gilula, 1986
Cx33	32.9	Sertoli cells	Haefliger et al., 1992
Cx36	36.1	Neurons	Condorelli et al., 1998
Cx37	37.2	Cortical neuroblasts, endothelium	Willecke et al., 1991
Cx40	40.6	Endothelium, conductive myocardium	Haefliger et al., 1992
Cx43	43	Astrocytes, heart, fibroblasts	Beyer et al., 1987
Cx45	45.5	Oligodendrocytes, heart	Hennemann et al., 1992a
Cx46	46	Heart, lens fibers, Schwann cells	Paul et al., 1991
Cx50	48.2	Lens fibers, corneal epithelium	White et al., 1992
Cx57	57.1	Skin, heart, kidney, testis	Manthey et al., 1999
Cx60	60	Ovary, spleen, colon	Itahana et al., 1998

II.1.2. Connexins are a multigene family

The first connexin was cloned almost simultaneously by two independent groups using different methods (Kumar and Gilula, 1986; Paul, 1986). A mouse liver cDNA library was screened by Paul (1986) by using antibodies generated against a polypeptide of a liver gap junction protein. Kumar and Gilula (1986) employed the microsequensing data generated by Nicholson et al. (1981) to generate oligonucleotides to screen a human liver cDNA library. Both groups obtained virtually identical cDNA and deduced amino acid sequences, suggesting that connexin sequences in different species are highly conserved. The predicted molecular weight of this connexin was 32,007 dalton and it was therefore termed Cx32. One year later, rat Cx43 was cloned by screening a rat heart cDNA library using a Cx32 cDNA probe at low stringency hybridization (Beyer et al., 1987).

Successful cloning of Cx32 and Cx43 settled the debate whether gap junctions are formed by identical connexins and consequently stimulated the expedition for cloning other connexins. Two strategies have been used in the search for other connexin family members. One strategy is to screen a target cDNA library by low stringency hybridization with a full-length cDNA probe and the other one is PCR amplification using degenerate oligonucleotide primers corresponding to the most conserved domains among previously cloned connexins. So far, sixteen connexins have been cloned in mammals (Table 1, page 10) and there are possibly more to come. These connexins share sufficient amino acid homology (50-80%) to be considered members of the connexin family. But there is also substantial heterogeneity among these connexins such that they can not be considered to be products of alternative splicing of the same gene (Bruzzone et al., 1996; Goodenough et al., 1996; Kumar and Gilula, 1996). Chromosome mapping studies have demonstrated that connexin genes have different chromosomal locations (Table 2, page 23).

II.1.3. Connexins are gap junction proteins

Evidence supporting that connexins are gap junction proteins includes: 1) immunolabeling of gap junctions by antibodies generated against synthetic connexin peptides (Beyer et al.,

1987; Milks et al., 1988; Hertzberg et al., 1988; Dermietzel et al., 1989; Yancey et al., 1989; Yamamoto et al., 1990a,b); 2) hemichannel formation in liposomes by connexins (Ahmad et al., 1999; Kim et al., 1999); 3) increased GJIC in gap junction deficient cells after connexin transfection (Zhu et al., 1991); 4) inhibition of GJIC in connexin transfected cells by conventional gap junction blockers (Cotrina et al., 1998b); 5) inhibition of gap junction formation by intracellular and extracellular applications of anti-connexin antibodies (Meyer et al., 1992; Hofer and Dermietzel, 1998); 6) inhibition of gap junction formation by synthetic peptides homologous to extracellular loops of connexins (Dahl et al., 1992, 1994; Warner et al., 1995; Kwak and Jongsma, 1999); 7) inhibition of gap junction formation in transfected cells by replacement or misplacement of the cysteine residues in connexin extracellular loops (Dahl et al., 1992; Foote et al., 1998); 8) reduction of GJIC after antisense ablation of connexins (Li et al., 1996; Singh et al., 1997); 9) reduction of GJIC after deletion of a specific type of connexin (Reaume et al., 1995; Gong et al., 1998); 10) recovery of GJIC after reintroduction of the connexin gene that was deleted (Huang et al., 1998). Collectively, these findings have convincingly established connexins as major gap junction proteins.

II.1.4. Connexins have a common membrane topology

Peptide antibodies generated against predicted amino acid sequences of Cx32 and Cx43 have been used to analyze the topology of these connexins in conjunction with site-specific protease digestion, EM and hydrophobicity plots (Paul, 1986; Kumar and Gilula, 1986; Beyer et al., 1987, 1989; Zimmer et al., 1987; Goodenough et al., 1988; Hertzberg et al., 1988; Milks et al., 1988; Yancey et al., 1989). Results from these studies suggest that connexins have four transmembrane domains and cytoplasmic N- and C-termini (Fig. 2, page 13). Two extracellular and one intracellular loops are formed by these four transmembrane domains. Three cysteine residues are found in each of the two extracellular loops and are believed to be essential for interlocking connexons from apposing cell membranes (Dahl et al., 1992, 1994; Foote et al., 1998). Due to the presence of a number of

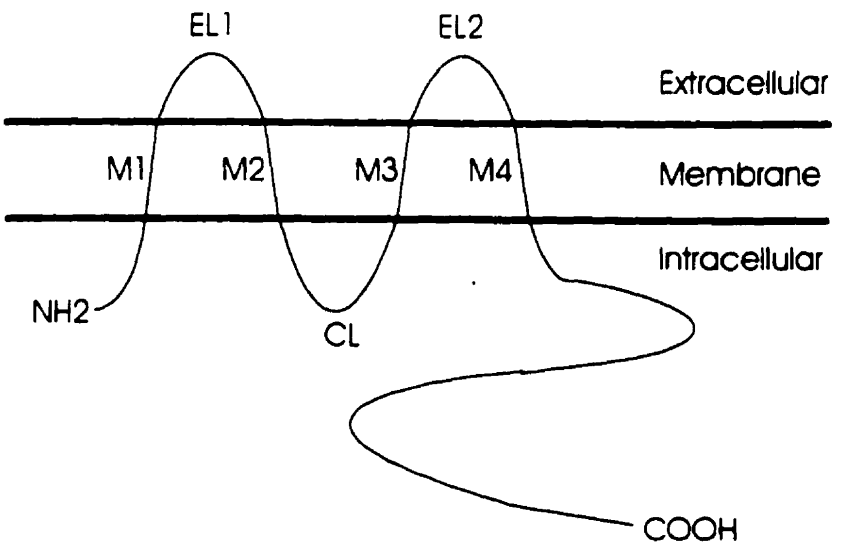

Fig. 2. Schematic diagram showing the membrane topology of a connexin molecule. A connexin molecule is believed to cross lipid bilayer four times and contain four trans-membrane domains (M1, M2, M3 and M4), and cytoplasmic N- and C-terminals. Two extracellular (EL1 and EL2) and one intracellular (CL) loops are formed by these trans-membrane domains.

negatively charged amino acids, the third transmembrane domain (M3) is believed to be the pore-lining domain which, in conjunction with the M3 domains from five other connexins, constitutes the inner wall of the hemichannel (Kumar and Gilula, 1996).

Although the membrane topology of other connexins has not been comprehensively studied, sequence analysis suggests that all connexins have a similar topology. The transmembrane domains and extracellular loops are the most conserved regions and are believed to be responsible for channel structure, whereas the cytoplasmic domains are highly variable and represent regions unique to a specific type of connexin.

II.1.5. Connexin expression and gap junction subtypes

Rapid progress in connexin cloning accelerated studies of the distribution and composition of gap junctions in different tissues. Just as surprising as the finding that gap junction proteins are a multi-gene family is the finding that one connexin can be found in many different cell types and one cell type can express different connexins (see Table 1, page 10). For example, Cx43 is expressed in cardiac myocytes, astrocytes, endothelium, ependyma, fibroblasts and many other cell types, whereas cardiac myocytes can express Cx40, Cx45 as well as Cx43. Different connexins have also been located in the same gap junction plaque (Nichoson et al., 1987; Little et al., 1995). These observations raised the question whether these gap junctions are heterotypic or heteromeric gap junctions. A connexon formed by six identical connexins is termed a homomeric connexon, whereas a connexon formed by two or more different types of connexin is termed a heteromeric connexon. On the other hand, a gap junction formed by two identical homomeric or heteromeric connexons is a homotypic gap junction. A gap junction formed by two different homomeric or heteromeric connexons is a heterotypic gap junction. Now there is evidence to support the presence of both types of gap junctions. (Sosinsky, 1995; Jiang and Goodenough, 1996; Brink et al., 1997; Ochalski et al., 1997; Bevan et al., 1998; He et al., 1999; Nagy et al., 1999a).

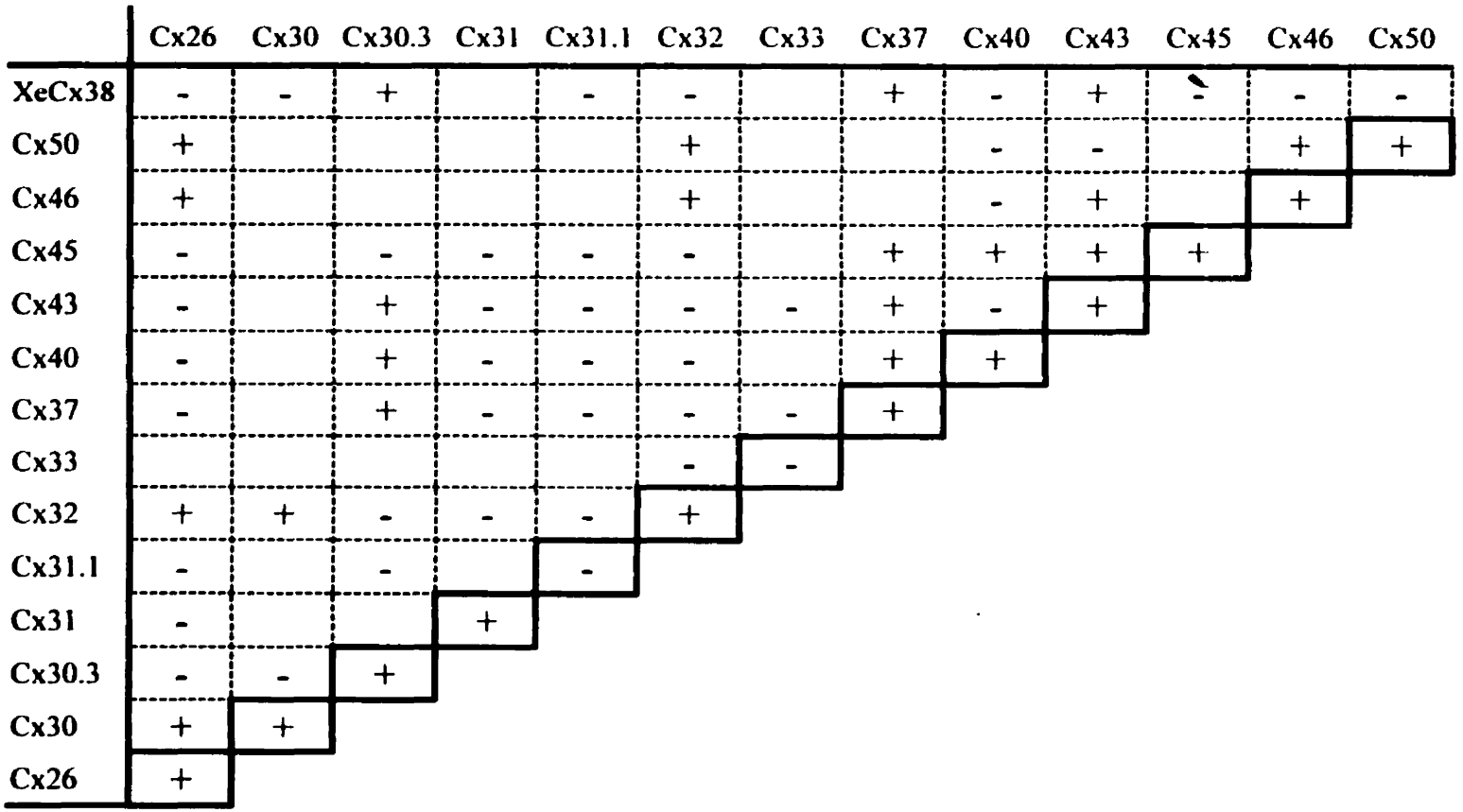

	Cx26	Cx30	Cx30.3	Cx31	Cx31.1	Cx32	Cx33	Cx37	Cx40	Cx43	Cx45	Cx46	Cx50
XeCx38	-	-	+		-	-		+	-	+	-	-	-
Cx50	+					+			-	-		+	+
Cx46	+					+			-	+		+	
Cx45	-		-	-	-	-		+	+	+	+		
Cx43	-		+	-	-	-	-	+	-	+			
Cx40	-		+	-	-	-		+	+				
Cx37	-		+	-	-	-	-	+					
Cx33						-	-						
Cx32	+	+	-	-	-	+							
Cx31.1	-		-		-								
Cx31	-			+									
Cx30.3	-	-	+										
Cx30	+	+											
Cx26	+												

Fig. 3. Diagram showing the compatibility of connexins in forming homotypic and heterotypic gap junctions. This figure is primarily based on experimental data from Drs. B. J. Nicholson, D. L. Paul and K. Willecke's laboratories. +, compatible; -, incompatible; blank, undetermined.

The presence of heterotypic gap junctions indicates that connexons formed by some connexins can interact with connexons formed by other connexins and constitute functional intercellular channels. Is this a property shared by all connexins or is there any selectivity forinteractions between connexins? Using Xenopus oocyte or Hela cell expression systems, investigators from several laboratories have demonstrated that many connexins can form homotypic as well as heterotypic gap junctions, while some other connexins can only form homotypic gap junctions. In rare cases, some connexins, such as Cx33 and Cx31.1, may not even form homotypic gap junctions (Elfgang et al., 1995; White et al., 1995b; Bruzzone et al., 1996). The capability of specific connexins to form heterotypic or heteromeric gap junctions has been shown to be the property of extracellular loops (Bruzzone et al., 1993; White et al., 1994). Chimeras constructed by replacing the extracellular domains of heterotypic gap junction-incompetent connexins with those of heterotypic gap junction-competent connexins increase their capacity to form heterotypic gap junctions (White et al., 1994). These studies confirmed that both extracellular loops are essential for channel formation. However, the intracellular domains were also found to be important in determination of the incompatibility of Cx40 and Cx43 to form heterotypic gap junctions (Haubrich et al., 1996). The available data on connexin compatibility, although not exhaustive, is shown in Figure 3 (page 15).

II.1.6. Functional significance of heterotypic and heteromeric gap junctions

Since gap junctions formed by a specific type of connexin appear to have distinct channel properties, the presence of different connexins in the same gap junctions may contribute to unique channel properties such as permeability and rectification. For example, homomeric connexons made of Cx32 are permeable to both cAMP and cGMP, whereas heteromeric connexons composed of Cx32 and Cx26 may lose permeability to cAMP, but not to cGMP (Bevans et al., 1998). Expression of specific connexins in a particular tissue may indicate that there is a special requirement of GJIC in this tissue. Inability of some connexins to form heterotypic gap junctions may contribute to the compartmentalization of GJIC observed

during embryo development (Guthrie and Gilula, 1989; Lo, 1996). On the other hand, the selectivity of some connexins in forming heterotypic gap junctions may provide guidance in identifying connexins expressed in specific gap junctions. For example, Cx43 is extensively expressed in astrocytes, while Cx32 is localized in oligodendrocytes in the central nervous system (CNS). These connexins are not believed to be mutually compatible in the formation of heterotypic gap junctions. Although astrocytic Cx43 -oligodendrocytic heterotypic gap junctions are frequently seen, these gap junctions are likely formed between Cx43 in astrocytes and connexins other than Cx32 in oligodendrocytes. The molecular selectivity of specific gap junctions remains to be determined.

II.2. Other gap junction proteins

II.2.1. MP26

MP26, also called MIP 26, is expressed in abundance in lens fibers (Beyer, 1993). Its identity as a gap junction protein has been under debate. This protein was detected at junctional and non-junctional membranes by some investigators but only at non-junctional membranes by others (Beyer, 1993). When purified MP26 was reconstituted into lipid bilayers, it was able to form sucrose-permeable channels (Girsch and Peracchia, 1985). More recent studies suggest that MP26 may not be a constituent protein of gap junctions. For instance, liposome membrane permeability in the presence of MP26 does not appear to be greatly different from that in the presence of other junctional and non-junctional proteins (Jarvis and Louis, 1992), suggesting that increased liposome membrane permeability induced by MP26 was probably nonspecific. This study also indicates that this model may not be the most suitable for testing gap junction properties. Moreover, MP26 reconstitution leads to the formation of tetragonal arrays instead of typical gap junctional hexagonal structures (Hasler et al., 1998). Since MP26 cDNA does not display obvious sequence homology to connexins, MP26 is unlikely a member of the connexin family. The primary structure of MP26 indicates that it may cross the lipid bilayer six times (Gorin et al., 1984) in contrast to connexins having four transmembrane domains (Fig. 2, page 13). Expression

of MP26 RNA in Xenopus oocytes failed to produce any detectable increase in intercellular conductance (Swenson et al., 1989). Most recently, using the sodium dodecyl sulphate polyacrylamide (SDS) -fracture immunolabeling technique, Dunia et al (1998) demonstrated that MP26 immunoreactivity was co-localized with Cx46 and Cx50 in small clusters or linear arrays, which are presumably newly formed gap junctions. In large junction plaques, however, MP26 was primarily found in the periphery. Considering the observation that the association of MP26 with lens gap junctions was rather transient (Gruijters, 1989), MP26 may not be an integral part of lens gap junctions, but rather may play a regulatory role in gap junction formation in lens fibers.

II.2.2. Ductin

Ductin is an integral membrane protein and has a molecular weight of 16-18 kDa. Lines of evidence suggest that ductin is a gap junction associated protein (Finbow and Pitts, 1993; Finbow et al., 1995). Ductin molecules have four hydrophobic regions indicating that ductin can transverse plasma membranes in a similar fashion to that of connexins (Mandel et al., 1988). Ductin was found in connexin-free liver gap junctions. Anti-ductin antibodies labeled isolated gap junctions and gap junctional regions in tissue sections. Intracellular injection of anti-ductin antibodies inhibits junctional communication. Reconstitution of ductin into lipid bilayers produces channels permeable to hydrogen ions and small molecules (Finbow and Pitts, 1993; Finbow et al., 1995). Using atomic force microscopy, John et al. (1997) demonstrated that gap junctions containing ductin have similar ultrastructure to that formed by connexins. However, no homology was found between ductin and connexins, suggesting that ductin may be a junctional protein different from connexins. Moreover, ductin cDNA is similar to a vacuolar H+-ATPase (Mandel et al., 1988), suggesting ductin may be a component of the hydrogen pump, which may be associated in some way with gap junctions.

II.2.3. Innexin

Innexins are members of a multiple-gene family of gap junction proteins in invertebrate organisms (Phelan et al., 1998). They were formerly known as the OPUS protein family (White and Paul, 1999). So far, two and 24 innexin genes have been cloned in Drosophila and Caenorhabditis genome, respectively (Phelan et al., 1998). The cDNA sequence of innexins predicts that these proteins may also have four transmembrane domains, analogous to the vertebrate connexins, although no evident homology has been found between innexin and connexin sequences (Starich et al., 1996; Barnes and Hekimi, 1997; White and Paul, 1999). There is evidence that innexins are invertebrate gap junction proteins. Some mutant phenotypes are well reconciled with the known functions of intercellular channels, and in vitro expression of some innexin genes results in formation of intercellular channels (White and Paul, 1999).

III. Functions of Gap Junctions and Connexins

GJIC is believed to be important for tissue homeostasis, signal transduction, cell growth and differentiation, and development. However, our understanding of the biological functions of GJIC is sometimes based on correlative observations. There are inherent shortcomings in the experimental approaches used in these observations. For instance, one approach to study GJIC function is to examine biological consequences following blockade of GJIC by application of gap junction blockers. Since gap junction blockers often have nonspecific effects, experimental results should be interpreted with caution. Recently, insight into biological functions of GJIC has been aided by chromosome mapping and connexin gene manipulations. These studies have provided valuable information on the role of GJIC in development and function of specific organs.

III.1. Contributions of GJIC to cellular activity

III.1.1. Facilitation of action potential conduction

The first physiological role proposed for gap junctions was based on the finding that these channels provide low resistance passage for intercellular flow of ions (Weidmann, 1952;

Furshpan and Potter, 1959). It is believed that gap junctions facilitate the propagation of action potentials in excitable cells (Bennett and Goodenough, 1978; Sotelo and Korn, 1978; Loewenstein, 1981; Bennett et al., 1991; Dermietzel and Spray, 1993). For example, GJIC was believed to be important for the rapid action potential conduction in cardiac tissue and in pregnant uterus to enable synchronized muscle contraction (Guerrero et al., 1997; Ou et al., 1997; Thomas et al., 1998). Heterologus Cx43 knockout mice display retarded atrial and ventricular conduction (Guerrero et al., 1997; Thomas et al., 1998). The role of neuronal gap junctions will be discussed in V.3.

III.1.2. Ionic and metabolic homeostasis

The size of gap junction channels suggests that gap junctions are highly permeable to ions. Intercellular flow of K^+ and Na^+ via gap junctions has been suggested in many cell types and is believed to participate in buffering $[K^+]_e$ and $[Na^+]_i$ and thereby contribute to ionic homeostasis (Newman, 1985; Walz, 1989; Rose and Ransom, 1997). Gap junctions may also provide passage for the intercellular flow of metabolites such as glucose, lactate, amino acids and nucleotides, and therefore may play an important role in the regulation of cellular metabolism.

III.1.3. Calcium signaling

Permeability of gap junctions to secondary messengers allows propagation of signals evoked by stimuli applied to localized cells (Saez et al., 1989a). For instance, mechanical or chemical stimulation of a cell can evoke an increase in $[Ca^{2+}]_i$. This cellular response to external stimuli can propagate to distant cells in vitro and in situ (Cornell-Bell et al., 1990; Finkbeiner, 1992; Newman and Zahs, 1997). During this process, diffusion of 1,4,5-inositol triphosphate and Ca^{2+} across gap junctions is believed to be important for the speed and amplitude of this long-distance calcium signaling (Leybaert et al., 1998), although an extracellular pathway may also be involved (Osipchuk and Cahalan, 1992; Cotrina et al., 1998b; Guthrie et al., 1999) (see more details in VIII.4). Gap junction-mediated intercellular

signaling may contribute to important cell functions such as regulation of hormonal secretion (Meda, 1996).

III.1.4. Cell growth and tumorgenesis

The role of GJIC in the regulation of cell proliferation and differentiation has been controversial. Evidence supporting this role is as follows: 1) tumor cells are usually not junctionally coupled (Yamasaki et al., 1999); 2) application of tumor promoters or transformation of normal cells by viral oncogenes leads to inhibition of GJIC (Crow et al., 1990; Swenson et al., 1990); 3) introduction of Cx43 into communication-deficient, glioma cells resulted in restoration of GJIC and inhibition of cell growth (Zhu et al., 1991) and 4) animals depleted of Cx32, a major liver gap junction protein, display higher probability of hepatocarcinogenesis (Temme et al., 1997; Moennikes et al., 1999).

However, contradictory evidence also exists. Some tumor cells retain a significant amount of GJIC (Yamasaki et al., 1999). On the other hand, cells with reduced GJIC by connexin deletion often do not appear to have higher growth rate or altered cell differentiation (Naus et al., 1997; Charollais et al., 1999). In a recent study, it was found that transfection of the Cx26 gene, but not Cx43 and Cx40 genes, suppressed the tumorigenic phenotype of HeLa cells both in vitro and in vivo, although expression of all these connexins increased gap junctional coupling in these cells. When the C-terminal tail of Cx43 was deleted, transfection of the truncated genes could inhibit cell growth (Omori and Yamasaki., 1999). These results suggest that connexin genes or connexin molecules, rather than GJIC, are involved in the regulation of carcinogenesis and cell growth.

III.1.5. Development

Embryonic cells are known to possess gap junctions. The coupled cells are gradually differentiated and segregated into different embryo compartments. Dye-coupling between cells in different compartments was minimal compared with cells in the same compartment (Guthrie and Gilula, 1989; Lo, 1996). More direct evidence supporting a role of GJIC in

development was from experiments involving blockade of gap junctional communication in embryonic cells by intracellular injection of antibodies against gap junction proteins. In these animals, developmental defects were manifested (Warner, 1999). In the nervous system, the neuronal domain in the developmental cerebral cortex was found to be coupled by gap junctions as assayed by intercellular transfer of neurobiotin (Yuste et al., 1995), suggesting that GJIC is involved in determining the fate of neurons. More recent molecular studies involving null mutations of a number of connexins provide further evidence supporting an important role of GJIC in the development of specific tissue or organs (Table 3, page 24). For example, Cx43 knockout mice display defects in the right ventricle outflow tract and die shortly after birth (Reaume et al., 1995). These defects have been proposed to be due to malfunctions of cardiac neural crest cells (Huang et al., 1998).

III.2. Gap junctions in disease

III.2.1. Human diseases associated with connexin mutations

So far, mutations of a number of connexin genes have been associated with several human genetic diseases (Table 2, page 23). For example, a variety of point mutations of Cx32 gene have been found in patients with X-linked Charcot-Marie-Tooth disease, a peripheral neuropathy (Bergoffen et al., 1993). Mutations of different connexins may be associated with similar disorders. For example, mutations of Cx26, Cx31 and Cx30 genes have been associated with several different types of hearing loss (Kelsell et al., 1997; Xia et al., 1998; Grifa et al., 1999). Mutations of Cx50 and Cx46 may cause congenital cataracts (Shiels et al., 1998; Berry et al., 1999; Mackay et al., 1999). These observations suggest that connexins expressed in a specific tissue may work collaboratively in fine-tuning GJIC to accommodate specific need of GJIC in this tissue for proper functioning. On the other hand, mutations of one connexin gene may be responsible for several different diseases. For instance, mutations in Cx31 are associated with hyperkeratosis as well as deafness (Richard et al., 1998; Xia et al., 1998), suggesting the essential role of a specific connexin type in multiple tissues. Nevertheless, the symptoms associated with connexin mutations are rather

Table 2 Connexin Gene Mutation and Human Diseases

Connexin	Human chromosome location	Associated human diseases	Selected References
Cx26	13q11-q13	Sensorineural deafness	Mignon et al., 1996; Kelsell et al., 1997
Cx30	13q12	Deafnes	Grifa et al., 1999
Cx31	1p34-p35	Erythrokeratodermia variabilis; deafness	Richard et al., 1998; Xia et al., 1998
Cx32	Xq13	X-linked Charcot-Marie-Tooth disease	Hsieh et al., 1991; Bergoffen et al., 1993
Cx36	15q14	n/a	Belluardo et al., 1999
Cx37	1p35.1	n/a	Van Camp et al., 1995
Cx40	1q21	n/a	Gelb et al., 1997
Cx43	6p21.1-q24.1	Heart malformation	Hsieh et al., 1991; Britz-Cunningham et al., 1995
Cx46	13q	Congenital cataract	Mackay et al., 1999
Cx50	1q21.1	Zonular pulverulent cataract	Shiels et al., 1998; Berry et al., 1999

Table 3 Mouse Connexin Gene Null Mutation and Phenotypes

Connexin	Mouse deficits	References
Cx26	Lethality at embryonic due to placental glucose transport defect	Gabriel et al., 1998
Cx32	Deficiency in glycogen mobilization; increased hepatocarcinogenesis; demyelination	Nelles et al., 1996; Temme et al., 1997; Anzini et al., 1997
Cx37	Female infertility due to defects in ovarian development	Simon et al., 1997
Cx40	Slowed atrioventricular and intraventricular conduction	Simon et al., 1998; Kirchhoff et al., 1998
Cx43	Early postnatal lethality due to conotruncal defect; slowed ventricular conduction; defect germ cells	Reaume et al., 1995; Guerrero et al., 1997; Juneja et al., 1999
Cx46	Nuclear cataract probably due to crystallin proteolysis	Gong et al., 1997
Cx50	Cataract	White et al., 1998
Cx32 + Cx43	Early postnatal lethality due to heart malformation	Houghton et al., 1999

restricted considering the widespread tissue expression of most connexins and universality of gap junctional communication.

III.2.2. Defects in connexin knockout mice

To date, mice with null mutation of Cx26, Cx43, Cx32, Cx37, Cx40, Cx46 or Cx50 have been generated. The phenotypes of these connexin knockout mice are listed in Table 3 (page 24). In Cx26 and Cx43 knockout animals, homozygous mice died before and soon after birth (Reaume et al., 1995; Gabriel et al., 1998). These results provide strong support for the essential role of GJIC in development. However, the premature death of these animals precludes the examination of other functions of target connexins in later stages of development. For these studies, animals with temporal and/or spatial inducible mutations of target connexins may be especially useful. On the other hand, Cx32, Cx37 and Cx40 knockout mice do survive, but the phenotypes are often restricted (Nelles et al., 1996; Simon et al., 1997, 1998; Kirchhoff et al., 1998), like the human counterpart with connexin gene mutations. This might be due to the compensatory up-regulation of GJIC by other connexins in the affected tissues given the fact that most tissues express multiple connexin types. Therefore, examination of GJIC contributed by other connexins in these animals should provide some insight into this possibility. Cx32 knockout mice only display minor abnormalities in myelination of peripheral nerve (Anzini et al., 1997), in contrast to the severe peripheral nerve demyelination in human counterparts with mutant Cx32 genes. This discrepancy is not well understood.

IV. Cx43 Phosphorylation and Regulation of GJIC

GJIC can be affected by various factors such as changes in $[Ca^{2+}]_i$, $[pH]_i$, transjunctional voltage, some anesthetics and lipophilic substances, growth factors and transforming oncogenes. The mechanisms that mediate changes in gap junctional coupling are not well defined. Alterations in GJIC can be induced by activation of some protein kinases and

alterations in connexin phosphorylation state (Saez et al., 1990; Swenson et al., 1990; Warn-Cramer et al., 1998). Most connexins are believed to be phosphoproteins (Goodenough et al., 1996). Among these connexins, regulation of Cx43 GJIC by connexin phosphorylation and dephosphorylation has been most extensively studied. Therefore, the following discussion is focused on the regulation of Cx43 GJIC by Cx43 phosphorylation and dephosphorylation.

IV.1. Cx43 phosphorylation and mobility in Western blots

Cx43 is characterized by a long carboxyl tail that contains multiple consensus sequences for a variety of protein kinases, suggesting that this protein can be multiply phosphorylated. Phosphorylation of Cx43 was demonstrated almost simultaneously in fibroblasts, lens and in cardiac myocytes by three independent groups (Crow et al., 1990; Musil et al, 1990; Larid and Revel, 1990). Cx43 in normal cell homogenates was resolved into three bands by sodium dodecyl sulphate polyacrylamide gel electrophoresis (SDS-PAGE) and Western blotting. The fastest migrating band is generally found at 41 kDa, which was demonstrated to be non-phosphorylated Cx43 and thus termed the P0 form. The other two bands migrate slower on SDS-PAGE and the reduced mobility was found solely due to differential phosphorylation as determined by in vitro dephosphorylation assays. Thus, the lower of these two bands was termed P1 and the upper band termed P2. Phosphoamino acid analysis revealed that phosphorylation of Cx43 in these cells was primarily at serine residues. Minimal phosphorylation was also found at threonine residues, but tyrosine phosphorylation was not detected. However, transformation of fibroblasts with Rous sarcoma virus induced tyrosine phosphorylation of Cx43, which lead to the appearance of new Cx43 bands at higher molecular weight (Crow et al., 1990), suggesting that Cx43 mobility can also be altered by tyrosine phosphorylation. Following these initial studies, investigators found that up to five different forms of Cx43 can be induced by treatments such as protein kinase C (PKC) activator 12-O-tetradecanoylphorbol-13-acetate (TPA), epidermal growth factor (EGF) and phosphatase inhibitors (Berthoud et al., 1992, 1993; Lampe, 1994; Lau et al.,

1996; Mikalsen et al., 1997). Appearance of new Cx43 forms was due to increased Cx43 phosphorylation at serine, threonine and tyrosine residues. These observations suggest that Cx43 phosphorylation occurs only at some of the phosphorylation sites in normal cells and that a stable phosphorylation state is due to the collective effects of protein kinases and protein phosphatases. Nevertheless, there is a consensus that the fastest migrating form is comprised of non-phosphorylated Cx43 and that alteration of Cx43 mobility is a valid indicator of protein phosphorylation state. In particular, increases in the slower migrating forms are believed to be due to stimulated Cx43 phosphorylation, whereas concurrent reduction of the P2 form and increase of the P0 form is believed to be the result of Cx43 dephosphorylation.

IV.2. Cx43 phosphorylation and gap junction formation

Taking advantage of the detergent-resistant property of gap junctions, Musil et al. (Musil et al., 1990; Musil and Goodenough, 1991) demonstrated that Cx43 in isolated gap junction plaques is primarily the P2 phosphorylated form, whereas intracellular soluble Cx43 is mostly the non-phosphorylated P0 form along with a small amount of the partially phosphorylated P1 form. A gap junction incompetent cell line does express Cx43, but proper phosphorylation of Cx43 does not occur in these cells. Transfection with a cDNA encoding the cell-cell adhesion molecule L-CAM induced GJIC and the P2 form of Cx43 in these cells. On the other hand, blockade of GJIC in gap junction-competent cells with octanol inhibited the formation of the P2 form of Cx43. These results suggested that appropriate or basal Cx43 phosphorylation is important for the formation of functional gap junctions. Cx43 oligomerization begins in the endoplasmic reticulum (ER) and continues during protein trafficking (Evans et al., 1999). On cell membranes, Cx43 may exist as floating connexons. Biotinylation experiments demonstrated that non-phosphorylated Cx43 can be transported to the cell membrane, suggesting that Cx43 phosphorylation is not required for protein trafficking (Musil and Goodenough, 1991). Therefore, the majority of Cx43 phosphorylation occurs either in the late stage of protein trafficking and/or prior to gap junction assembly at

cell membranes, and may be stimulated by cell-cell contact mediated by cell adhesion molecules. Phosphorylation and gap junction assembly may be completed within a few minutes since GJIC can be established shortly after cell contact (Loewenstein, 1981; Peracchia, 1980).

Currently, we do not know what protein kinases are responsible for the basal Cx43 phosphorylation required for gap junction assembly. However, mitogen-activated protein (MAP) kinase is not likely to play a major role in this process because deletion of all three serine residues believed to be MAP kinase phosphorylation sites did not prevent Cx43 gap junction formation (Warn-Cramer et al., 1998). Moreover, basal phosphorylation of Cx43 correlates with gap junction assembly and increase of GJIC, whereas Cx43 phosphorylation by MAP kinase is related to drastic reduction of GJIC. Activation of PKC is often achieved by application of the phorbol ester TPA. The most prominent effects of TPA treatment are Cx43 hyperphosphorylation, inhibition of Cx43 gap junction formation and reduction of GJIC (Berthoud et al., 1992; Lampe, 1994). Hence, PKC may not play a significant role in promoting gap junction assembly. Human Cx43 does not contain cGMP-dependent protein kinase (PKG) phosphorylation sites, which suggests Cx43 phosphorylation is not directly catalyzed by PKG (Kwak et al., 1995a). Tyrosine kinase can also be excluded, as Cx43 is not tyrosine phosphorylated in all normal cells examined so far.

Activation of cAMP-dependent protein kinase (PKA) is known to up-regulate GJIC. Unlike TPA treatment, phosphorylation induced by cAMP is frequently associated with increased junctional permeability and increased total numbers of gap junctions (Saez et al., 1986; Bennett et al., 1991; Atkinson et al., 1995). In a tumor cell line, 8-bromo-cAMP treatment produced increases in the level of detergent-insoluble phosphorylated Cx43 (P2), in the number of gap junctional plaques and in GJIC. Since Cx43 mRNA transcription and protein synthesis were not increased, 8-bromo-cAMP may have activated PKA, which subsequently stimulated Cx43 phosphorylation and gap junction assembly (Atkinson et al., 1995). In another study, the PKC and PKA inhibitor staurosporine caused a decrease in Cx43 immunolabeling between cultured MDCK kidney cells. This effect was not inhibited

by co-application of TPA, indicating that removal of Cx43 gap junctions after staurosporine treatment was due to inhibition of PKA activity (Berthoud et al., 1992). However, Cx43 does not contain the consensus sequence for PKA (Beyer et al., 1987; Kennelly and Krebs, 1991). Thus, PKA may not directly phosphorylate Cx43, but may instead phosphorylate and activate other serine/threonine protein kinase(s) that subsequently phosphorylate Cx43 at cell membranes. Currently, the property of this kinase is not defined. The candidates may include Ca^{2+}/calmodulin-dependent protein kinase II (CaMKII), $p34^{cdc2}$, casein kinase I and glycogen synthase kinase 3 for which consensus sequences have been found in Cx43 (Kennelly and Krebs, 1991).

Connexin phosphorylation may not be required for gap junction formation by other connexins. For example, Cx26 was found in gap junctions in many tissues (Table, 1). This gap junction protein does not contain consensus sequences for any known protein kinases, nor is there any evidence suggesting that Cx26 is phosphorylated. Apparently, connexin phosphorylation is not a prerequisite for the assembly of functional Cx26 gap junctions. Moreover, it has been shown that cleavage of the carboxy tail of Cx43 does not prevent the formation of functional gap junctions (Fishman et al., 1991). However, we can not rule out the possible contribution of endogenous connexins including Cx43 to the formation of gap junctions in these cells. Alternatively, cleaved Cx43 may behave like Cx26 (George et al., 1999) and no longer needs to be phosphorylated in the aggregation process on cell membranes.

IV.3. Cx43 phosphorylation and channel gating

Regulation of GJIC by protein phosphorylation was first suggested by an observation of Cx32 gap junctions in hepatocytes by Saez et al. in 1986. These investigators demonstrated that Cx32 can be phosphorylated by PKA, PKC and Ca^{2+}/calmodulin-dependent protein kinase II. Phosphorylation of Cx32 by PKA is related to increased gap junction conductance (Saez et al., 1986, 1990).

IV.3.1. Cx43 phosphorylation by tyrosine kinases

It has almost been two decades since Atkinson et al. (1981) first observed the rapid disruptive effects on gap junctional coupling in fibroblasts after Rous sarcoma virus transformation. Over-expression of Src protein can also reduce GJIC (Azarnia et al., 1988). Since these cells express high levels of Cx43, the effect of v-src on Cx43 phosphorylation was examined by transformation of Rous sarcoma virus and v-src oncogene (Crow et al., 1990; Filson et al., 1990). Fibroblast v-src transformation did not cause any evident inhibition of Cx43 expression. However, the reduction of GJIC was accompanied by a rapid increase in tyrosine phosphorylation of Cx43, indicating a role of Cx43 tyrosine phosphorylation in reduced GJIC. In Xenopus oocytes. v-src cRNAs were co-injected with either wildtype or mutated Cx43. Paired oocytes injected with wildtype Cx43 and v-src cRNAs were poorly coupled and accompanied by Cx43 tyrosine phosphorylation. However, when tyr265 of Cx43 was replaced by phenylalanine, the effect of v-src on tyrosine phosphorylation of Cx43 and GJIC was completely abolished (Swenson et al., 1990), suggesting that phosphorylation tyr265 on Cx43 mediates the inhibitory effect of v-src on GJIC. In vitro phosphorylation assay further demonstrated that Cx43 is a direct substrate of activated Src kinase (Loo et al., 1995). More tyrosine phosphorylation sites in Cx43 were later found, indicating that phosphorylation at other tyrosine residues such as tyr247 may also contribute to v-src-induced reduction of GJIC in fibroblasts (Atkinson et al., 1981; Loo et al., 1995; Lau et al., 1996). Thus, these results suggested that v-Src directly phosphorylates Cx43 at tyrosine residues and results in reduction of GJIC (Lau et al., 1996).

This notion was challenged recently by Zhou et al. (1999). These investigators tested the transformation of v-src in paired Xenopus oocytes transfected with different forms of Cx43 cDNA. v-src transformation virtually abolished dye-transfer between paired oocytes transfected with wildtype Cx43 but did not affect GJIC in cells transfected with C-terminal truncated Cx43, which is consistent with previous reports (Swenson et al., 1990). However, the v-src inhibition of GJIC still persisted when tyr265 and tyr247 were deleted. Although the binding of v-Src to proline-rich domains on Cx43 seemed to be essential for Src

inhibition of GJIC, deletion of serine residues in these regions reduced Src inhibition of GJIC to a greater degree than deletion of proline residues, suggesting that serine phosphorylation is more directly involved in the inhibition GJIC in v-src transformed cells than tyrosine phosphorylation. These regions contain multiple MAP kinase phosphorylation sites that have been related to inhibition of GJIC (Warn-Cramer et al., 1996, 1998). Therefore, stimulated serine phosphorylation by MAP kinase in v-src transformed oocytes may be key event leading to inhibition of GJIC in these cells. This is consistent with increased serine phosphorylation of Cx43 in addition to tyrosine phosphorylation (Crow et al., 1990; Filson et al., 1990; Swenson et al., 1990). In the same study, these investigators also demonstrated that inhibition of MAP kinase correlates with attenuated inhibition of Cx43 GJIC by v-src (Zhou et al., 1999).

IV.3.2. Cx43 phosphorylation by PKC

In addition to the inhibitory effect on Cx43 gap junction assembly (Lampe, 1994), phosphorylation of Cx43 by PKC may also inhibit channel conductance. In a rat liver epithelial cell line, application of TPA for 15 to 30 min induced two new Cx43 forms migrating at higher molecular weight positions on SDS-PAGE than normal Cx43 forms. Treatment of cell homogenate with alkaline phosphatase reduced all forms to the P0 form, suggesting that TPA caused hyperphosphorylation of Cx43. Phosphoamino acid analysis demonstrated that Cx43 was primarily phosphorylated at serine residues. Addition of PKC inhibitors blocked the effect of TPA on Cx43 phosphorylation state, suggesting that PKC was involved in increased Cx43 phosphorylation. Measurement of junctional conductance revealed over 90% reduction in TPA treated cells. Recording of unitary channel conductance in these cells indicated a dramatic reduction in the open probability of Cx43 channels. These results suggested that Cx43 hyperphosphorylation by PKC is associated with reduced GJIC in these cells (Berthoud et al., 1993). However, it is not clear whether PKC directly phosphorylates Cx43 and whether Cx43 phosphorylation is directly responsible for reduced GJIC. Saez et al. (1997) found that TPA also stimulated Cx43 phosphorylation and inhibited

GJIC in cultured cardiac myocytes. Peptide sequencing of a recombinant Cx43 C-terminal polypeptide phosphorylated by PKC demonstrated that Ser368 and Ser372 were phosphorylated. However, tryptic phosphopeptides of phosphorylated Cx43 from cardiac myocytes did not co-migrate with tryptic phosphopeptides of phosphorylated Cx43 C-terminal polypeptide, suggesting that Cx43 may not be directly phosphorylated by PKC in vivo (Saez et al., 1997). In a separate study, Lau et al. (1996) found that Ser368 phosphorylation occurred in vitro in the presence of PKC and in cells after TPA treatment. Taken together, these results suggest that Cx43 can be phosphorylated by PKC at residues including Ser368 in vivo. Protein conformation change induced by phosphorylation might have altered the ability of trypsin to cleave Cx43 at normal proteolytic cleavage sites, resulting in different phosphopeptide migrating patterns seen by Saez et al. (1997).

IV.3.3. Cx43 phosphorylation by MAP kinase

Growth factors, lysophosphatidic acid, TPA and v-src transformation have all been shown to activate MAP kinase (Gupta et al., 1992; Kumagai et al., 1993; Tournier et al., 1994) and inhibit GJIC (Swenson et al., 1990; Berthoud et al., 1992, 1993; Hill et al., 1994; Lau et al., 1992). The stimulatory effect of these bioactive substances on cell growth and proliferation has intrigued a number of investigators, leading to the study of the relationship between activation of MAP kinase and down-regulation of GJIC (Lau et al., 1996; Hossain et al., 1998, 1999a,b). The first observation indicating the regulation of Cx43 phosphorylation and GJIC by MAP kinase appeared in 1992 when Lau et al found that EGF stimulated Cx43 phosphorylation and also caused a rapid inhibition of GJIC in an epithelial cell line. The loss of GJIC correlated temporally with the increase in Cx43 phosphorylation, which was found exclusively on serine residues (Lau et al., 1992). These results suggested that activated EGF receptor tyrosine kinase may affect Cx43 GJIC by activating other serine kinases. Both PKC and MAP kinase can be activated by EGF receptor kinase and may thus constitute the downstream signaling pathway in down-regulation of Cx43 GJIC in these cells. PKC was subsequently excluded by the observation that desensitization of PKC did not affect the

EGF-induced reduction of GJIC and up-regulation of Cx43 phosphorylation state (Kanemitsu and Lau, 1993). On the other hand, involvement of MAP kinase was supported by the localization of consensus sequence in Cx43, the ability of MAP kinase to phosphorylate Cx43 in vitro and the co-migration of phosphopeptides from phosphorylated Cx43 in vivo and in vitro (Kanemitsu and Lau, 1993). Following these observations, three serine residues at Ser255, Ser279 and Ser282 of Cx43 were identified to be the phosphorylation sites for MAP kinase by in vitro Cx43 peptide phosphorylation, two-dimension gel electrophoresis, peptide sequencing and site-directed mutagenesis (Warn-Cramer et al., 1996). A MAP kinase inhibitor PD98059 was able to block the EGF- and lysophosphatidic acid-induced Cx43 phosphorylation and loss of GJIC. Removal of these phosphorylation sites from Cx43 abolished the inhibitory effect of EGF on GJIC (Warn-Cramer et al., 1998). Surprisingly, removal of these serine residues did not prevent EGF-stimulated Cx43 phosphorylation as shown by banding patterns on Western blots (Warn-Cramer et al., 1998). One possible explanation is that phosphorylation at these residues does not significantly contribute to changes in Cx43 mobility on SDS-PAGE. Furthermore, these results also indicate that Cx43 mobility is preferentially affected by phosphorylation at other serine residues. Nevertheless, these results strongly suggest that phosphorylation at Ser255, Ser279 and Ser282, as a result of MAP kinase activation, mediates EGF inhibition of Cx43 GJIC. It is likely that MAP kinase also activates other unknown protein kinases which as least mediate part of the Cx43 phosphorylation during EGF treatment. In other words, it is not clear whether MAP kinase directly phosphorylates these serine residues in vivo. What also remains to be addressed is whether each of these three phosphoserines makes a similar contribution to the reduction of GJIC.

MAP kinase may be a convergence point of multiple signaling pathways. For example, Zhou et al. (1999) found that v-src transformation may cause disruption of GJIC in Cx43 transfected Xenopus oocytes via activation of MAP kinase (see above). Activation of MAP kinase was also seen after application of platelet-derived growth factor (PDGF) (Hossain et al., 1998, 1999a,b). PDGF can also increase Cx43 phosphorylation and reduce GJIC.

However, activation of MAP kinase was not always associated with increased Cx43 phosphorylation and loss of GJIC, indicating the involvement of different signaling pathway(s) in the regulation of GJIC by PDGF (Hossain et al., 1999a). These researchers also found that disruption of GJIC by PDGF was not always accompanied by alteration in Cx43 mobility on SDS-PAGE (Hossain et al., 1999b). These observations prompt the suggestion that other signaling pathways may mediate the inhibitory effect of PDGF on Cx43 GJIC (Hossain et al., 1999b). A PKC- and MAP kinase-independent signaling pathway has been indicated by a recent study (Postma et al., 1998). The role of MAP kinase in PDGF-induced down-regulation of Cx43 GJIC still remains to be clarified.

IV.3.4. Regulation of Cx43 GJIC by other protein kinases

Activation of PKA has been shown to increase Cx32 gap junction channel conductance (Saez et al., 1986). However, application of activators and inhibitors of PKA did not cause any detectable change in channel conductance of SKHep1 cells transfected with rat Cx43 cDNA (Kwak et al., 1995b). Taken together with the absence of PKA consensus sequence in Cx43, these results suggest that PKA is not involved in the channel gating of Cx43 gap junctions. On the contrary, activators of PKG reduced dye-coupling between SKHep1 cells transfected with *rat* Cx43. The single channel conductance was also shifted from 61 and 89 pS to 31 pS. These alterations in *rat* Cx43 gap junction permeability were blocked by PKG antagonist (Kwak et al., 1995b). Interestingly, addition of PKG activators did not cause any change in junction channel conductance in SKHep1 cells transfected with *human* Cx43 (Kwak et al., 1995a). Metabolic labeling revealed increased incorporation of [^{32}P] in *rat* Cx43 at the P2 position, but not in *human* Cx43 (Kwak et al., 1995b). Comparison of the amino acid sequences of human and rat Cx43 displayed differences in only nine amino acids. Among these amino acid residues, Ser257 of rat Cx43 is replaced by alanine in human Cx43, which precludes phosphorylation at this position. Thus, Kwak et al. (1995a) suggested that Ser257 of rCx43 may be the phosphorylation site for PKG and that phosphorylation of this residue results in reduced GJIC.

$P34^{cdc2}$ kinase has been shown to stimulate Cx43 phosphorylation in vivo (Lampe et al., 1998) and directly phosphorylates Cx43 in vitro (Kanemitsu et al., 1998; Lampe et al., 1998). In vitro phosphorylation of Cx43 may occur at Ser255 (Lampe et al., 1998). However, the Cx43 phosphopeptides obtained from in vivo phosphorylation are different from those in vitro, suggesting that $p34^{cdc2}$ may activate other protein kinases to phosphorylate Cx43 in vivo (Lampe et al., 1998). Since $p34^{cdc2}$ plays an important role in regulating cell entry into mitosis, phosphorylation of Cx43 may be associated with the relocation of Cx43 to intracellular compartment during mitosis (Xie et al., 1997). CaMKII has been shown to increase GJIC in neurons (Pereda et al., 1998), indicting that calmodulin-dependent connexin phosphorylation may also be involved in the regulation of GJIC.

IV.4. Cx43 dephosphorylation and junctional coupling

IV.4.1. Protein phosphatases

Like protein kinases, protein phosphatases can be separated into two groups. Protein phosphatases removing phosphates from tyrosine residues are termed tyrosine phosphatases and those acting on phosphoserine and phosphothreonine are Ser/Thr phosphatases. Ser/Thr phosphatases are further categorized into type-1 (PP-1) and type-2 (PP-2). PP-1 can specifically dephosphorylate the β subunit of phosphorylase kinase, while PP-2 preferentially dephosphorylates the α subunit of phosphorylase kinase (Cohen, 1989). Additional criterion for separating PP-1 and PP-2 is that only the former can be inhibited by two small inhibitor proteins originally extracted from liver and muscle. (Cohen, 1989; Wera and Hemmings, 1995). PP-2 can be subclassified into PP-2A, PP-2B and PP-2C. Phosphatase activity of PP-2A does not depend on divalent cations. PP-2B is also termed calcineurin because of its preferential expression in neural tissue. The phosphatase activity of calcineurin depends on the presence of Ca^{2+} and calmodulin. On the other hand, the presence of Mg^{2+} is absolutely required for the phosphatase activity of PP-2C (Cohen, 1989; Wera and Hemmings, 1995).

Unlike protein kinases, consensus amino acid sequences for protein phosphatases are poorly defined (Kennelly and Krebs, 1991). This is likely due to the relatively nonselective nature of protein phosphatases. One phosphatase may remove phosphate groups from residues phosphorylated by different kinases. Identification of a specific type of protein phosphatases is often achieved by the blockade of phosphatase activity by specific inhibitors and by in vitro phosphatase assays. For example, PP-1 and PP-2A can be inhibited by okadaic acid and calyculin A (Cohen, 1989; Wera and Hemmings, 1995). Calcineurin can be inhibited by two immunosuppressors, FK506 and cyclosporin A (Snyder et al., 1998, Morioka et al., 1999). PP-2C can be distinguished from other phosphatases by its dependence on Mg^{2+}. In vitro phosphatase assays are often conducted to verify the targeted protein phosphatases.

IV.4.2. Cx43 dephosphorylation and GJIC

Protein phosphorylation states reflect the collective effects of protein kinases and protein phosphatases. If Cx43 GJIC can be regulated by protein kinases, dephosphorylation of Cx43 by protein phosphatases should equally contribute to the dynamic regulation of GJIC. However, in contrast to the large body of data on the regulation of GJIC by Cx43 phosphorylation, the role of Cx43 dephosphorylation has received less attention. So far, there is no evidence suggesting that Cx43 dephosphorylation is involved in the regulation of gap junction assembly. The effect of Cx43 dephosphorylation on GJIC is only supported by circumstantial evidence (Godwin et al., 1993; Moreno et al., 1994; Guan et al., 1996; Verrecchia and Herve, 1997; Verrecchia et al., 1999).. Even less understood are the properties of protein phosphatases involved in the maintenance of the basal Cx43 phosphorylation state in normal cells.

Currently, a consensus on the effect of Cx43 dephosphorylation on GJIC has not been reached. Studies involving the characterization of the relationship between Cx43 dephosphorylation and GJIC can be separated into two categories. In the first category, conclusions were drown based on presumptive effects of reagents on protein

phosphorylation states without direct visualization of Cx43 dephosphorylation (Takens-Kwak and Jongsma, 1992; Godwin et al., 1993; Moreno et al., 1994; Kwak et al., 1995b). The results of these observations have been controversial. In the second category, demonstration of Cx43 dephosphorylation was consistently related or associated with a reduction of GJIC (Oelze et al., 1995; Guan et al., 1996; Cotrina et al., 1998a). However, these studies did not address the identity of protein phosphatases involved in Cx43 dephosphorylation, even though PP-1 and PP-2A have been indicated in Cx43 dephosphorylation induced by a gap junction blocker (Guan et al., 1996).

IV.5. Cx43 phosphorylation and gap junction degradation

Like other connexins, Cx43 in cultured cells has a rapid turnover rate and a half-life time of 1.5-3.5 h (Laird, 1996). This suggests that Cx43 must be constantly synthesized and degraded. It is thought that gap junctions are first internalized into one of the apposing cells and form annular gap junctions or multivesicular structures before degradation (Bennett et al., 1991; Laird, 1996; Wolburg and Rohlmann, 1995). Subsequently, the gap junction proteins such as Cx43 are believed to be ubiquitinized for proteasomal degradation or transported to lysosomes for degradation (Laing and Beyer, 1995; Laing et al., 1998). Little is known about the role of Cx43 phosphorylation or dephosphorylation in Cx43 degradation.

A relationship between connexin phosphorylation and gap junction degradation was first suggested by the inhibition of Cx32 proteolytic degradation after increased phosphorylation by PKC (Elvira et al., 1993, 1994). However, similar effects of PKC were not seen on Cx43 gap junction degradation. In contrast, TPA treatment induced depletion of gap junctions from cell membranes (Berthoud et al., 1992) either by inhibiting gap junction assembly (Lampe, 1994) or by promoting gap junction degradation. The observation made by Guan et al. (1996) indicates that Cx43 dephosphorylation may promote gap junction degradation since inhibition of Cx43 dephosphorylation by okadaic acid prevented gap junction disassembly induced by a gap junction blocker. In a recent study, deletion of serine rich regions in the C-terminus of Cx45 led to increased turnover of Cx45 in transfected Hela

cells (Hertlein et al., 1998). These studies indicate that basal levels of connexin phosphorylation may play a role in maintaining the stability of gap junctions. In any case, the regulation of gap junction degradation by connexin phosphorylation or dephosphorylation is not expected to be a ubiquitous mechanism for all gap junctions since Cx26 is not believed to be phosphorylated at all.

V. Neuronal Gap Junctions in Mammalian CNS

V.1. Localization

Ever since the discovery of low resistance intercellular channels in cardiac tissue (Weidman, 1952) and neural tissue (Furshpan and Potter, 1959), signal transmission in the nervous system has been believed to take place at two specialized cell-cell junctions: chemical and electrical synapses. However, electrical synaptic transmission was believed to be restricted in phylogenetically primitive forms and did not receive much attention. Spearheaded by electrophysiologists, a large number of studies have been conducted in the last three decades and the presence of gap junctions between neuronal elements is well recognized in many structures in the nervous system of vertebrates including mammals (Sotelo and Korn, 1978; Llinas, 1985). In these studies, neurons were believed to possess gap junctions when they are found to be electronically or dye-coupled, or to possess unique pentalamina structures by conventional transmission EM or polygonal particles by freeze/fracture EM. To date, gap junctions have been found in neuronal structures including the cerebral cortex, hypothalamus, inferior olivary nucleus, hippocampus, olfactory bulb, the striatum, substantia nigra, cerebellum, lateral vestibular nucleus, trigeminal mesencephalic nucleus, inferior olive, anterior cochlear nucleus, the spinal cord and the retina. Moreover, gap junctions have been located between neuronal perikarya, dendrites, axon terminals and perikaryon and primary afferent fibers by EM (See reviews by Sotelo and Korn, 1978; Llinas, 1985; Wolburg and Rohlmann, 1995; Nagy and Dermietzel, 2000). Neuronal gap junctions can exist by themselves or can be co-localized with a chemical synapse, a structure termed a mixed synapse. Mixed synapses have been found in rat inferior vestibular nucleus,

lateral vestibular nucleus and spinal cord (Sotelo and Korn, 1978; Bennett and Goodenough, 1978; Llinas, 1985; Rash et al., 1996). Until recently, mixed synapses were rarely seen. Using "grid-mapped freeze fracture", Rash et al. (1996) found that most motoneurons in the spinal cord have 300-600 mixed synapses which may constitute 3-12% of the somatic and proximal dendritic synapses of these cells. Taking into account the location, the number and the nature of these electrical synapses, mixed synapses may make a significant contributions to the excitatory post-synaptic potentials in some motoneurons (Rash et al., 1996). The small size of these neuronal gap junctions may cause them to be easily overlooked by conventional transmission EM. Therefore, the population of neurons coupled by gap junctions may be larger than we think taking this factor into account as well as the fact that coupling assays utilizing LY may produce false negative results (Kandler and Katz, 1995).

V.2. Connexins

The study of neuronal gap junctions has been accelerated by recent successes in connexin cloning and the introduction of new tracers to assay gap junctional coupling. Using antibody against Cx32, Dermietzel et al. (1989) stained 20% of the cells in the basal ganglia and the thalamus. The Cx32 immunoreactivity (ir) was co-localized with immunolabeling by antibodies against neuron-specific enolase or neurofilament protein, suggesting neurons in these structures express Cx32. However, they did not detect any Cx32 immunolabeling in neurons at other locations known to possess gap junctions, such as hippocampus. Apparently, the majority of CNS neurons express connexins other than Cx32. Recently, immunohistochemical examination of Cx32 expression in the CNS with a panel of anti-Cx32 antibodies failed to locate Cx32 in neurons (Scherer et al., 1995; Li et al., 1997). These studies, in conjunction with others (Yamamoto et al., 1990c, 1991; Li et al., 1995), suggest that earlier reports of Cx32 in neurons may be due to cross-reaction with a Cx32-related protein. In an in situ hybridization study, Wachym et al. (1991) found that Cx43 mRNA was expressed in rat vestibular nuclei. However, the cell identity was not defined. In serial LM and EM studies, investigators found that Cx43 antibodies produced

immunolabeling at neuronal and glial gap junctions (Yamamoto et al., 1989b; Shiosaka., 1989). The subsequent studies demonstrate that neurons do not express detectable amounts of Cx43 (Yamamoto et al., 1990a,b).

One of the greatest findings in the study of neuronal GJIC is the cloning of connexin36 (Cx36) (Condorelli et al., 1998). The Cx36 transcript was found in brain regions expressing neuronal gap junctions, but not in non-neuronal tissues including liver and spleen (Condorelli et al., 1998). Therefore, Cx36 may represent the first identified neuronal connexin among at least 15 mammalian connexin members. Sequence analysis demonstrates that the predicted Cx36 amino acid sequence is 93% identical to that of the skate Cx35 (O'brian et al., 1996), suggesting that they are homologous proteins. The human Cx36 gene was recently assigned to chromosomal band 15q14 and makes it a possible candidate gene for a form of familial epilepsy previously linked to the same band (Belluardo et al., 1999). A unique feature was also found with Cx36 gene structure. The coding region of Cx36 is separated by an intron in contrast to other known connexins which all have an uninterrupted coding region. Therefore, Cx36 may also represent the first member of a different group of connexins. With the identification of this neuronal connexin, the research of neuronal GJIC now enters into a new stage.

V.3. Functions

The functional significance of neuronal gap junctions is poorly understood. This is partially due to a lack of tools to manipulate specifically the permeability of gap junctions, extensive gap junctional coupling in glial cells and the intimate physical as well as biochemical relationship between neurons and glial cells in the nervous system. Identification of neuronal Cx36 will allow genetic manipulation of neuronal GJIC and provide some insights into the specific role of neuronal GJIC in the CNS. Nevertheless, as in other tissues, neuronal GJIC may have several functions based on general gap junction properties. Permeability to ions would allow fast synaptic transmission aided by the short synaptic delay at electrical synapses. The presence of mixed synapses suggests that chemical and electrical synapses

may interact, which may contribute to synaptic plasticity at pre- and post-synaptic loci. The first step to confirm this would be the demonstration that these mixed synapses in mammalian CNS are functional (Loewenstein, 1981; Peusner and Giaume, 1994). Permeability to second messengers such Ca^{2+} and cAMP would allow the coordination of cellular activity and metabolism of junctionally coupled neurons. The participation of GJIC in calcium wave propagation may imply a novel system of neural transmission, which may differ from conventional synaptic transmission in mediators involved and in rate of transmission (Dermietzel and Spray, 1993; Zahs and Newman, 1997).

VI. Gap Junctions between Oligodendrocytes

VI.1. Localization and coupling states

Oligodendrocytes are a major type of macroglia in the CNS and are responsible for making and maintaining myelin wrapping around axons. Convincing morphological and electrophysiological evidence is available to support the presence of gap junctions between oligodendrocytes in vivo and in vitro (Kettenmann et al., 1983; Mass and Mugnaini, 1985; Mugnaini, 1986; Kettenmann and Ransom, 1988; Robinson et al., 1993; Li et al., 1997; Rash et al., 1997). In general, the coupling strength between oligodendrocytes is usually less than between astrocytes. Oligodendrocyte progenitor cells may not be coupled by gap junctions. Immature oligodendrocytes appear to be electrically coupled, but not dye coupled (Ransom, 1995). Mature cells are both electrically and dye-coupled in culture, but dye-coupling is usually limited to only a few neighboring cells (Kettenmann and Ransom, 1988; Butt and Ransom, 1993; Robinson et al., 1993, Ransom, 1995; Vanance et al., 1995a). These observations suggest that GJIC in cells of the oligodendrocyte lineage increases with cell maturity. Unitary junctional conductance of cultured oligodendrocytes can be separated into two groups, 20-30 pS and 100-120 pS, which may represent junctions formed by different connexins or different opening states (Dermietzel et al., 1997). Since the unitary conductance of cultured astrocytes is about 50-60 (Dermietzel et al., 1991; Giaume et al., 1991), the presence of dye-coupling in astrocytes but not in many oligodendrocytes may

indicate either that fewer gap junctions are formed between oligodendrocytes or that most oligodendrocytic gap junctions have only low conductance. Recently, Pastor et al. (1998) found that only oligodendrocytes in gray matter are dye-coupled, whereas those in white matter are not. These observations may indicate heterogeneity in Cx32 expression in these regions or environmental influence of oligodendrocytic GJIC.

VI.2. Connexins

Several groups have examined connexin expression in oligodendrocytes (Dermietzel et al., 1989, 1997; Scherer et al., 1995; Li et al., 1997; Pastor et al., 1998). The first connexin found in oligodendrocytes was Cx32 by using antibodies against basic myelin protein and Cx32 (Dermietzel et al., 1989). Extensive examination of Cx32 expression in CNS with a panel of anti-Cx32 antibodies demonstrated that Cx32 is expressed in many brain regions and gray matter in the spinal cord. In contrast, only sparse Cx32 immunolabeling was found in spinal cord white matter. Cx32-ir was located in oligodendrocyte cell bodies and processes, and along selective populations of myelinated fibers (Scherer et al., 1995; Li et al., 1997). EM examination demonstrated that Cx32-ir is present at gap junctions between oligodendrocytes and at the oligodendrocytic half of gap junctions between oligodendrocytic and presumptive astrocytic components (Li et al., 1997). In peripheral nerve, Cx32 is found in the paranodal myelin loops and incisures of myelinating Schwann cells, the peripheral nervous system counterpart of oligodendrocytes (Scherer et al., 1995). In their efforts to search for other connexins in oligodendrocytes, Dermietzel et al. (1997) demonstrated that Cx45 is the second type of connexin expressed by oligodendrocytes in vitro and in vivo (Dermietzel., et al., 1997; Kunzelmann et al., 1997).

VII. Gap Junctions between Astrocytes

VII.1. Classifications of astrocytes

Astrocytes are the other major type of macroglia in the CNS, and they form a physical barrier between neuronal components and the vascular system. Mature astrocytes in situ are

generally classified into two types, fibrous astrocytes in white matter and protoplasmic astrocytes in gray matter. A different classification is primarily based on studies of cultured optic nerve astrocytes which were termed type-1 and type-2 astrocytes (Raff, 1989). The first classification is used when referring to astrocytes in situ and the second is used when referring to astrocytes in culture or optic nerve. It is believed that all astrocytes express glial fibrillary acidic protein (GFAP) in the intermediate filaments. This protein is used as an astrocyte marker (Eng and Ghirnikar, 1994).

VII.2. Coupling states

Gap junctional coupling between presumptive astrocytes was first reported by Kuffler and Potter (1964) in their study of leech CNS. Morphological studies demonstrated that each astrocyte can be connected to adjacent cells by over 10,000 gap junctions mostly at their processes (Mass and Mugnaini, 1985; Mugnaini, 1986; Yamamoto et al., 1990a,b; Wolburg and Rohlmann, 1995; Wolff et al., 1998). In cultured type-1 astrocytes, the unitary channel conductance is about 50-60 pS (Dermietzel et al., 1991; Giaume et al., 1991). The average junctional conductance between cell pairs dissociated from these cultures was about 13 nS (Dermietzel et al., 1991). Thus, there are about 235 functional gap junction channels between each pair of these cultured astrocytes. Numerous astrocytic gap junction channels allow rapid diffusion of LY to neighboring cells, which results in the detection of dozens of dye-coupled astrocytes in situ and in vitro (Dermietzel et al., 1991; Giaume et al., 1991; Ransom, 1995). Surprisingly, type-2 astrocytes, although coupled in situ, appear not coupled to each other or to type-1 astrocytes in culture (Sontheimer et al., 1990; Belliveau and Naus, 1994; Ransom, 1995). Taken together, these results demonstrate that most astrocytes are strongly coupled by gap junctions in situ.

VII.3. Connexins

Astrocytes are currently known to express two connexins, Cx43 and Cx30. Antibodies against these connexins have been generated and recognize specific protein bands

corresponding to the predicted molecular weights in Western blots (Nagy et al., 1992; Hossain et al., 1994a,b,c). Immunostaining of CNS tissue sections by these antibodies is located in astrocytic processes, gap junctions between astrocytes and the astrocytic halves of gap junctions formed between astrocytic and oligodendrocytic elements (Yamamoto et al., 1990a,b; Ochalski et al., 1995; 1997; Nagy et al., 1997a, 1999). Astrocytes cultured from neonatal brain also express significant but various amounts of Cx43 at different culture periods. Cx30 was detected immunohistochemically in astrocytes after 5 weeks in vitro (Dermietzel et al., 1991; Giaume et al., 1991; Kunzelmann et al., 1999). In addition to Cx43 and Cx30, mRNAs (but not proteins) of a few other connexins have been detected in cultured astrocytes. Moreover, some cultured astrocytes were labeled with an antibody against Cx31.1 (Naus et al., 1997). However, it is not clear whether this was a result of specific recognition of Cx31.1. Among sixteen cloned connexins, only Cx43 and Cx30 are believed to be expressed by astrocytes (Nagy and Dermietzel, 2000).

VII.4. Localization

Identification of connexins expressed by astrocytes greatly facilitated the study of distribution, localization and regulation of astrocytic gap junctions in vivo. In their extensive studies, Yamamoto et al. (1990a,b) found that there is a significant heterogeneity in astrocytic Cx43 expression in different CNS regions. In brain, Cx43-ir was mostly located at astrocytic gap junctions or astrocytic processes adjacent to Cx43 immunoreactive gap junctions. High density of astrocytic gap junctions was found between astrocytic processes surrounding synaptic glomeruli (Yamamoto et al., 1990b). In the spinal cord, however, Cx43-ir was also found in astrocytic processes that were not directly associated with gap junctions. Heterotypic gap junctions between Cx43 immunostained astrocytic processes and unstained oligodendrocytic elements were frequently encountered in spinal cord (Ochalski et al., 1997). The differences in the intensity and pattern of Cx43 immunostaining in different CNS regions suggest different strengths of astrocytic GJIC and may indicate the formation of astrocytic communication compartments in the CNS (Yamamoto et al., 1990a,b).

Moreover, there is evidence that astrocytic GJIC can be regulated by neuronal activity (see details in XI.4)

VII.5. Astrocytic GJIC under pathological conditions

Astrocytes may also respond to tissue injury by altering the efficacy of GJIC. A variety of animal models have been used to study astrocytic responses to tissue injuries. Typically, morphological changes such as cell swelling were among the first astrocytic reactions to be seen within one hour before massive neuronal damages (Chen et al., 1993; Garcia et al., 1993). In 24 to 48 hours, astrocytes in the vicinity of the injury may migrate towards the lesion center and, in the meantime, may also resume mitotic activity and proliferation (Janeczko, 1991; Eddleston and Mucke, 1993; Eng and Ghirnikar, 1994). These astrocytes are termed reactive astrocytes to distinguish from the astrocytes in normal tissue and are characterized by enlarged cell bodies and processes due to progressive swelling, increase in GFAP immunostaining and sometimes, reappearance of another cytoskeleton protein, vimentin (Chen et al., 1993; Garcia et al., 1993; Janeczko, 1993). The coupling state of astrocytes at various stages of this progression is not well elucidated. For example, astrocyte swelling can be rapidly induced in vitro by increase of $[K^+]$, excitatory amino acid and hypo-osmolar solutions (Walz, 1989). However, treatment of cultured astrocytes with glutamate and increased $[K^+]$ increases junctional coupling (Enkvist and McCarthy, 1994) whereas hypo-osmolar solution reduces cell-cell electrical coupling (Kimelberg and Kettenmann, 1990). Longer-term changes in astrocytic GJIC after injury are also poorly defined. Treatments that induce reactive states of astrocytes in vivo were shown to cause cell uncoupling in cultured astrocytes (Anders et al., 1990). However, when astrocytes were cultured for 72 hours in the presence of dead and injured neurons, these cells displayed an increase in junctional coupling, suggesting that neuronal injury may affect astrocytic GJIC in vitro and perhaps also in vivo (Anders and Moolery, 1992). Previous studies from our laboratory suggested that regulation of astrocytic GJIC after tissue injury is a complicated

process and may differ at different stages of response to tissue injury (Vukelic et al., 1991; Hossain et al., 1994a,b; Ochalski et al., 1995; Sawchuk et al., 1995; see details in XI.1 and XI.3). Elucidation of this process requires comprehensive characterization of the synthesis, post-translational modifications and degradation of astrocytic gap junction proteins in conjunction with assays of junctional coupling.

VIII. Gap Junctions Formed by Other Cells in the CNS

Ependymal cells are also coupled by gap junctions. Leptomeninges in pia mater lie on the outer surface of CNS parenchyma. Ependymal cells delineate brain ventricular cavities and the spinal cord central canal. These cells may express Cx43 and Cx26 (Dermietzel et al., 1989; Spray et al., 1991). Since Cx26 is apparently incompatible with Cx43 in forming heterotypic gap junctions, gap junctions in these tissues apparently consist of primarily homotypic gap junctions. Basal lamina lies between CNS parenchyma and the pia mater or ependymal cells and may prevent the formation of gap junctions between cells in these tissues and in CNS parenchyma.

The progenitors of microglia are different from those of other cells in the CNS parenchyma. Thus, microglial cells are not considered glial cells by most investigators. There is no report of the presence of gap junctions on the membrane of these cells.

IX. Gap Junctions between Astrocytes and Oligodendrocytes

IX.1. Asymmetrical GJIC

Neural cells are traditionally separated into neurons and glial cells. Although it was recently shown that cultured astrocytes may be coupled to the co-cultured neurons in the first 4 days-in-vitro (Froes et al., 1999), a large body of evidence indicates that these two major categories of neural cells are not coupled to each other by gap junctions in vivo. Heterotypic gap junctions have frequently been seen between two major glial cell types, astrocytes and oligodendrocytes by EM examination of tissue sections and cultures (Massa and Mugnaini, 1982, 1985; Mugnaini, 1986; Li et al., 1997; Ochalski et al., 1997; Nagy et al., 1999b).

These heterotypic gap junctions were more numerous than gap junctions formed between oligodendrocytes (Mugnaini, 1986). These heterotypic gap junctions occur not only between cell bodies and processes, but also between astrocytic processes in contact with the outer turn of the myelin sheath (Massa and Mugnaini, 1982, 1985; Mugnaini, 1986; Butt and Ransom, 1993; Ochalski et al., 1997; Rash et al., 1997; Nagy and Dermietzel, 2000). Electrical coupling between these cells has been demonstrated in cultures and in vivo (Robinson et al., 1993; Venance et al., 1995a; Ransom, 1995; Zahs and Newman, 1997). However, it is still controversial as to whether there is dye-coupling through these heterotypic gap junctions. In rat retina, dye transfer was found to be unidirectional and occurs only from astrocytes to oligodendrocyte, but not from oligodendrocytes to astrocytes (Robinson et al., 1993; Zahs and Newman, 1997). However, in cultures containing astrocytes and oligodendrocytes, dye-coupling was found to be bi-directional between these two cell types (Venance et al., 1995a). Also in cultured cells, Ransom and Kettenmann found only electrical coupling between these cells (Ransom and Kettenmann, 1990). Nevertheless, at least some of the gap junction channels formed between astrocytes and oligodendrocytes appear to be asymmetrical channels that probably allow only bi-directional electrical, but not metabolic coupling. The unidirectional LY transfer from astrocytes to oligodendrocytes in retina also indicates the presence of specific intracellular channel gating mechanism in oligodendrocytes, which prohibits the entry, but not the exit of this dye from these rectifier channels.

IX.2. Heterotypic gap junctions

Identification of connexins expressed in these glial cells provides a biochemical basis for the asymmetrical nature of these heterotypic channels. Astrocytes express Cx43 and Cx30 whereas oligodendrocytes express Cx32 and Cx45 (Dermietzel et al., 1989, 1991, 1997; Yamamoto et al., 1990a,b, 1992; Nagy et al., 1992, 1997a, 1999). It is believed that Cx43 can form heterotypic gap junctions with Cx45, but not with Cx32 (Elfgang et al., 1995). The presence of heterotypic gap junctions between astrocytes (Cx43) and oligodendrocytes

suggests that Cx45 rather than Cx32 in oligodendrocytes contribute to this type of heterotypic gap junctions (Ochalski et al., 1997). Further, Cx30 instead of Cx43 may constitute the astrocytic hemichannels apposing Cx32 hemichannels in oligodendrocytes at heterotypic gap junctions between these cells. The presence of multiple connexins in each cell type may also explain the lack of significant CNS developmental deficits in Cx43 or Cx32 deficient mice (Giaume et al., 1995; Nelles et al., 1996; Naus et al., 1997; Scherer et al., 1998). In these mice, the function of Cx43 and Cx32 may be compensated or replaced by Cx30 and Cx45 respectively.

X. Functions of GJIC in Glial Cells

X.1. Panglial syncytium

If neurons have the dominant role in signal transmission and integration in the nervous system, glial cells may be required to keep the neurons functioning in a well-regulated environment. In the past decade, numerous observations suggest that glial cells function well beyond the traditional supporting role. Intercellular communication is deemed to be important for coordinating the activities of these neural cells. However, glia are not equipped with chemical synapses and thus they can not rapidly communicate in a similar manner as neurons. Thus, GJIC may play an important role in coordinating the metabolism and functions of these cells. Localization of gap junctions between oligodendrocytes, between oligodendrocytes and astrocytes and between astrocytes has led to the extension of the idea of an astrocytic syncytium to a pan-glial syncytium (Mugnaini, 1986; Ochalski et al., 1997; Rash et al., 1997; Nagy and Rash, 1999). Compared with the strength of astrocytic gap junctions, coupling between oligodendrocytes and between oligodendrocytes and astrocytes is relatively weaker. Thus, astrocytes are likely to participate more vigorously than oligodendrocytes in most of the functions of the pan-glial syncytium. Moreover, a gradual increase of coupling capacity from oligodendrocytes to astrocytes also makes astrocytes the ideal candidate for interfacing with the vascular system, which would greatly facilitate substance exchange between CNS parenchyma and the circulation system.

X.2. Potassium spatial buffering

One of the functions proposed for glial cells is potassium buffering. Depolarization of glial cells was seen when adjacent neurons were active, which is likely due to uptake of the K^+ released from discharging neurons. This may help to maintain the K^+ concentration in the vicinity of active neurons, a process termed potassium spatial buffering (Orkand et al., 1966). Gap junctions between glial cells may provide passage for the flow of K^+ down its concentration gradient to a quiescent region or into a perivascular compartment and overcome the obstacles of the narrow interstitial space in the CNS (Newman, 1985; Orkand, 1986; Walz, 1989). On the other hand, gap junctions may also connect a large group of astrocytes and increase the volume of the buffer sink (Dermietzel and Spray, 1993).

X.3. Metabolic homeostasis

Extensive dye-coupling between astrocytes indicates that these cells are metabolically coupled. This is further supported by the demonstration of inter-astrocyte diffusion of metabolic compounds (Giaume et al., 1997). This is especially noteworthy since astrocytes have the largest store of energy substrate in the form of glycogen in the CNS. When the glucose supply is reduced, increased glycolytic activity is seen in astrocytes (Wiesinger et al., 1997). Degradation of glycogen in astrocytes may provide lactate to neurons and thus support the function and survival of neurons, especially when the blood supply is reduced during ischemia (Schoushoe, et al., 1997; Tsacopoulos and Magistretti, 1996). Gap junctions are well positioned for the exchange of glucose and metabolites between adjacent cells and between the astrocytic syncytium and circulatory system. Moreover, regulation of astrocytic GJIC has recently been associated with alterations in glucose uptake by these cells (Giaume et al., 1997; Lavado et al., 1997).

X.4. Calcium wave

Permeability of gap junctions to second messengers allows the intercellular diffusion of signal molecules and may help in coordination of cellular activity and function (Saez et al., 1989a). One focus of recent studies is the role of gap junctions in the propagation of increases in cytosolic free calcium (Cornell-Bell et al., 1990, Charles et al., 1992). The role of gap junctions in the calcium wave propagation in astrocytes is supported by a number of observations. 1. Calcium waves can be greatly reduced by gap junction blockers (Enkvist and McCarthy, 1992; Finkbeiner, 1992; Venance et al., 1995b). 2. Glioma cells overexpressing Cx43 exhibit increased speed and distance of calcium propagation (Charles et al., 1992). 3. Deletion of Cx43 reduced the amplitude of calcium increase and efficacy of wave spread (Naus et al., 1997; Scemes et al., 1998). However, GJIC is unlikely the only mediator of calcium wave since calcium increase can pass through a cell-free area (Hassinger et al., 1996; Charles, 1998), and blockade of purinergic extracellular signaling also reduces the speed and amplitude of the calcium wave (Cotrina et al., 1998b; Guthrie et al., 1999). The functional significance of astrocytic calcium waves may reside in the interaction with neurons. It was found that the calcium level of neurons co-cultured with astrocytes was increased upon the arrival of an astrocytic calcium wave (Nedergaard, 1994; Parpura et al., 1994; Hassinger et al., 1995). The effect of astrocytic calcium waves on the activity of neurons was further demonstrated in cultured brain slices (Dani et al., 1992) and in isolated rat retina (Newman and Zahs, 1998). These observations point to the possibility that astrocytes may actively participate in the processing of neural signals.

X.5. Functional implications from Cx43 and Cx32 knockout mice

Mice with Cx43 null mutation died within hours after birth from obstruction of right ventricle outflow tract. No abnormalities were found in the nervous system at this developmental stage (Reaume et al., 1995). Astrocytes and neurons cultured from Cx43 knockout mice brain have normal appearance. The electrical properties of Cx43 deficient astrocytes are indistinguishable from wildtype astrocytes (Perez Velazquez et al., 1996; Naus et al., 1997). However, the density of astrocytes from Cx43 knockout mice is slightly

lower than that of wildtype astrocytes. Most significantly, Cx43 deficient astrocytes are not dye-coupled, although electrical coupling remains (Naus et al., 1997). Moreover, the amplitude and efficacy of calcium wave spread in cultured astrocytes deficient of Cx43 are reduced by 15% and 14%, respectively, compared with those in wildtype cells (Scemes et al., 1998). However, early death precludes further examination of the potential roles of astrocytic GJIC in the late stages of CNS development and in the functions of the nervous system.

Similar to astrocytic gap junctions, gap junctions between oligodendrocytic processes at internodal regions of myelin may also participate in the maintenance of ionic and metabolic homeostasis in the vicinity of axons. Oligodendrocytes may uptake K^+ released in the paranodal loops from discharging axons. The gap junctions between oligodendrocytes and between oligodendrocytes and astrocytes provide a venue for the dispersion of K^+ to adjacent glial cells. However, no significant differences were found in the structure of central myelin between wildtype and Cx32 deficient mice (Anzini et al., 1997). Nevertheless, minor defects were found in peripheral myelin. Moreover, progressive demyelinating peripheral neuropathy began to develop three months after birth, suggesting that Cx32 has an important role in the functions of Schwann cells (Anzini et al., 1997; Scherer et al., 1998). This is consistent with the finding of numerous mutations of Cx32 in patients suffering from the X-linked Charcot-Marie-Tooth disease (Bergoffen et al., 1993).

XI. Specific Objectives

Although GJIC is believed to be essential for astrocytes in these proposed roles in the CNS, the significance of GJIC has not been well established. We adopted an indirect way to approach this issue by investigating the functional state of astrocytic GJIC under physiological and pathological conditions, and the underlying mechanisms. Knowledge obtained from such studies may pave the way to design interventions of astrocytic GJIC and ultimately clarify the roles of GJIC in astrocytic functions in the CNS.

XI.1. Expression of Cx43 in human Alzheimer's disease (AD) brain

Senile plaques in human AD brain are the regions with high density of reactive astrocytes and their processes, suggesting that astrocytes respond to degenerative neuronal injury in human brain (Duffy et al., 1980; Mandybur and Chuirazzi, 1990; Hatten et al., 1991). A question arising from this observation is whether reactive astrocytes also regulate their gap junction network in regions of degenerative neurons. Gap junctions and Cx43 have been found between elements of reactive astrocytes in rat brain (Alonso and Privat, 1993; Lafarga et al., 1993; Hossain et al., 1994b,c; Ochalski et al., 1995). Astrocytes subjected to treatments that can induce reactive astrocytes in vivo are dye-coupled, suggesting that gap junctions between reactive astrocytes are functional (Anders et al., 1990; Anders and Woolery, 1992). Moreover, reactive astrocytes cultured from human epileptic brain display a higher level of junctional coupling (Lee et al., 1995; Bordey and Sontheimer, 1998). Thus, reactive astrocytes in human may react to neural tissue injury by up-regulation of GJIC.

One of the specific aims in this study is to investigate whether human reactive astrocytes also express Cx43 gap junctions, which is the first step toward the ultimate clarification of the role astrocytic GJIC in AD. Another aim is to investigate whether neurons in human AD brain express Cx43. This is stimulated by the observation that transfection of a neuronal cell line with β/A4 C-terminal peptide of the amyloid precursor protein induced Cx43 expression in PC12 cells (Nagy et al., 1995, Nagy, 1996a). This observation indicates that β/A4 may induce neuronal expression of Cx43 that was never seen in normal mature neurons.

XI.2. Characterization of a commercial anti-Cx43 antibody

Antibodies against Cx43 have greatly aided in studies of various aspects of Cx43 GJIC. A well-characterized commercial antibody is a very useful tool for a great number of investigators in this field. In this study, we successfully characterized a monoclonal anti-Cx43 antibody that specifically and selectively recognizes the non-phosphorylated form of Cx43 in several cultured peripheral cell types and in heart tissue.

XI.3. Cx43 and astrocytic gap junctions in rat brain after focal ischemia

Astrocytic responses are different at different phases of tissue injury (see above). Astrocytic GJIC also appears to be in different states apparently associated with the severity of tissue injury. When rat brain was subjected to mild global ischemia, Cx43 immunostaining with an anti-Cx43 antibody designated 18A was evidently increased in the striatum at two days after ischemia. Moderate ischemia induced an even stronger increase of 18A-ir. When animals were subjected to severe ischemia, however, a decrease in 18A-ir was seen (Hossain et al., 1994a), a phenomenon similar to what we have seen after intra-cerebral injection of kainic acid (Vukelic et al., 1991; Hossain et al., 1994b). Western blots of ischemic tissues did not reveal any alteration of Cx43 protein level (Hossain et al., 1994a). Apparently, ischemia treatment caused alteration of Cx43 immunorecognition by 18A rather than protein expression, and this alteration of Cx43 immunostaining is associated with severity of ischemia injury. In a comprehensive study of Cx43 immunorecognition using a panel of Cx43 antibodies, Hossain et al. (1994b) found that areas with massive neuron loss induced by kainic acid was devoid of 18A-ir, but was intensely stained with another anti-Cx43 antibody (16A), whereas in the area surrounding the lesioned tissue, 18A-ir was increased presumably in reactive astrocytes. Similarly, no alteration of protein level was found. Thus, kainic acid treatment caused masking of Cx43 epitopes recognized by 18A and unmasking of those recognized by 16A in the lesioned area. In contrast to numerous gap junctions in normal tissue, EM examination of the lesioned area failed to find any gap junctions. The intense 16A-ir was located at intracellular multivesicular structures believed to be internalized gap junctions (Larsen and Tung, 1978; Wert and Larsen, 1990; Ochalski et al., 1995). Thus, increased 16A-ir in the lesioned area corresponded to Cx43 internalization and removal of astrocytic gap junctions. Similar results were seen in striatum after injection of N-methy-D-aspartate (NMDA) (Ochalski et al., 1995) and in the spinal cord after compression lesion (Theriault et al., 1997). Since astrocytes do not express detectable NMDA receptors (Hosli and Hosli, 1993; Kimelberg, 1995), the alterations in Cx43

immunostaining and reorganization of astrocytic gap junctions are likely related to severe neuronal injury seen in these tissues (Vukelic et al., 1991; Hossain et al., 1994b; Ochalski et al., 1995). These observations also indicated that 16A-ir in injured tissues is a useful indicator of Cx43 internalization and removal of gap junctions, which is suggestive of the total shutdown of astrocytic GJIC. Increased 18A-ir in the region peripheral to the lesioned area may reflect the up-regulation of GJIC in reactive astrocytes. Moreover, these studies demonstrated that astrocytes in different regions of the CNS regulate Cx43 and gap junctions in a similar manner in response to different modes of tissue injury.

However, these observations were made at least 5 h after the onset of various treatments. Astrocytes can quickly respond to early neural tissue injury (Garcia et al., 1993; Laskawi et al., 1997; Aldskogius and Kozlova, 1998). The coupling state of astrocytes may be especially important at early stage of neural injury if astrocytic GJIC is involved in maintaining CNS homeostasis (Walz, 1989; Aldskogius and Kozlova, 1998). Moreover, since Cx43 phosphorylation and dephosphorylation can occur in a matter of minutes (Crow et al., 1990; Goldberg and Lau, 1993), the absence of Cx43 phosphorylation state in these lesioned tissues (Hossain et al., 1994b,c) does not preclude the possibility that alterations in Cx43 phosphorylation state may occur at early stages of tissue injury and may lead to changes of astrocytic GJIC. Indeed, Cx43 dephosphorylation has been shown in ischemic heart tissue within 1 h after ischemia, which has been associated with a reduction in GJIC (Huang et al., 1999). Alterations of Cx43 phosphorylation states have frequently been related to alterations in gap junction assembly and channel conductance (Musil et al., 1990; Lampe, 1994; Moreno et al., 1994; Oleze et al., 1995; Kwak and Jongsma, 1996). Thus, the potential changes in the phosphorylation state of Cx43 in astrocytes may have important implications to the functional state of astrocytic GJIC. On the other hand, the studies described above have detailed long-term alterations of Cx43 and astrocytic gap junctions in relatively healthy tissue and in lesioned tissue. GJIC in astrocytes adjacent to endangered neurons is not known since experimental models previously used do not have such a well-defined region. These neurons may be rescued if the deleterious stimuli are removed before

irreversible cell injury occurs. Thus, it is especially interesting to examine the functional state of astrocytic GJIC in these regions. Rat brain subjected to focal ischemia contains a well-defined region, termed the penumbra, that contains high density of such endangered neurons (Siesjo, 1992) and thus make it an ideal model for the study the state of astrocytic GJIC in this area. The availability of an anti-Cx43 antibody (13-8300) that specifically and selectively recognizes dephosphorylated Cx43 greatly facilitated the characterization of Cx43 phosphorylation state in various regions of ischemic rat brain.

Therefore, our specific objectives in this study are to determine 1) the selective and specific recognition of non-phosphorylated Cx43 by antibody 13-8300 in astrocytes; 2) the immunostaining patterns and phosphorylation states of Cx43 at early stages of ischemic injury; 3) the morphology and organization of astrocytic gap junctions in ischemic brain; 4) the immunorecognition, phosphorylation and localization of Cx43 in ischemic penumbra; 5) the similarity of the sequential alterations in Cx43 immunostaining patterns between ischemic brain tissue and other CNS tissue after various injuries; 6) the possible functional significance of alterations of Cx43 immunostaining.

XI.4. Immunorecognition and phosphorylation state of astrocytic Cx43 after increased neuronal activity

Astrocytic GJIC is believed to be under the regulation of neuronal activity. Gap junction coupling in cultured astrocytes can be altered by extracellular $[K^+]$ and a number of neurotransmitters such as glutamate, kainic acid, norepinephrine, anandamide (Giaume and McCarthy, 1996; Giaume et al., 1997). More direct evidence was obtained from a study of isolated optic nerve. Increased neuronal activity evoked by electrical stimulation of the optic nerve increases junctional coupling in astrocytes (Marrero and Orkand, 1996). However, it is not known whether astrocytic GJIC in vivo was also similarly affected by neuronal activity. Like peripheral cells, astrocytic GJIC may also be affected by $[pH]_i$, $[Ca^{2+}]_i$, lipophilic molecules, growth factors and gap junction blockers in addition to $[K^+]_o$ and neurotransmitters (Anders, 1988; Giaume and McCarthy, 1996; Giaume et al., 1997; Guan

et al., 1997; Lavado et al., 1997; Reuss and Unsicker, 1998). However, the mechanisms underlying these effects are not clear. One mechanism may be the regulation of Cx43 phosphorylation state which has been shown in a number of studies of peripheral cell types (Goodenough et al., 1996; Lau et al., 1996; Warn-Cramer et al., 1996; Unger, 1999). Applicability of similar mechanisms in astrocytes is indicated by observations that substances known to activate PKC and MAP kinase in astrocytes (Kasuya et al., 1994; Chisamore et al., 1996; Lazarini et al., 1996) also alters astrocytic GJIC (Konietzko and Muller, 1994; Enkvist and McCarthy, 1992; Lazarini et al, 1996). On the other hand, we have seen reversible Cx43 dephosphorylation in astrocytes, which are not likely to be severely injured after mild focal ischemia (Part III). Mild ischemia and increased neuronal activity may induce some similar changes in neural environment such as increase in extracellular concentrations of K+, neurotransmitter, and metabolites (Walz et al., 1989; Nedergarrd, 1995; Martin et al., 1994). This raised the possibility that alterations in Cx43 immunostaining patterns, such as decreased 18A-ir and increased 13-8300-ir and Cx43 dephosphorylation after mild ischemia, may also occur in astrocytes after increased neuronal activity. Also important is whether increased neuronal activity can induce widespread internalization of Cx43 and reorganization of astrocytic gap junctions, phenomena seen in severely injured tissues (Vukelic et al., 1991; Hossain et al., 1994b, Ochalski et al., 1995). In other words, whether dramatic increase of 16A-ir and characteristic Cx43 internalization are specific to injured tissue still needs further examination. This study was designed to address these questions.

XI.5. Cx43 dephosphorylation and coupling states in hypoxic astrocytes

Cx43 dephosphorylation has been indicated in the regulation of GJIC in peripheral cell types. However, the subsequent alterations of GJIC have been controversial. In ovarian granulosa cells, Godwin et al. (1993) found that intracellular injection of an exogenous nonspecific alkaline phosphatase led to transient decrease of dye-coupling. However, in SKHep1 cells, intracellular injection of alkaline phosphatase caused a downshift of unitary

junction conductance (Moreno et al., 1994). However, these studies did not directly demonstrate the dephosphorylation of Cx43 by these treatments. Dephosphorylation of Cx43 can also be induced by transfection of a viral protein (Oelze et al., 1995) or a gap junction blocker (Guan et al., 1996). In these cases, Cx43 dephosphorylation was related to a reduction of GJIC and degradation of gap junctions (Oelze et al., 1995; Guan et al., 1996). Cx43 dephosphorylation was also found in ischemic heart tissue and was accompanied by reduced GJIC (Huang et al., 1999). Thus, Cx43 dephosphorylation may be related to the alteration, likely reduction, of GJIC. However, this conclusion is weakened by the expression of multiple connexins in these tissues (Table 1). Recently, Cotrina et al. (Cotrina et al., 1998a) found that treatment of cultured astrocytes with chemical hypoxia for 1.5 h induced an increase of non-phosphorylated form of Cx43, which was believed to be the dephosphorylation product of phosphorylated forms of Cx43. Similar to reports in peripheral cells (Flagg-Newton and Loewenstein, 1979), chemical hypoxia also induced a reduction of GJIC in astrocytes (Cotrina et al., 1998a). Although these authors proposed a relationship between Cx43 dephosphorylation and reduction in astrocytic GJIC, three potential problems in this study cast some doubt to this suggestion. First, increase in the non-phosphorylated Cx43 at 1.5 h after hypoxia may be due to Cx43 dephosphorylation as well as increased protein synthesis considering that Cx43 is known short-lived protein with a half-life time of 1.5-3 h in vitro (Musil et al, 1990; Laird et al., 1990, 1995; Beardslee et al., 1998). Second, Cx43 consists of intracellular components and membrane components, with the latter directly associated with functional gap junctions. Dephosphorylation of intracellular Cx43 may not have direct effect on GJIC. Finally, since reduction of GJIC occurred prior to the increase of non-phosphorylated Cx43, an initial reduction of GJIC is apparent not due to Cx43 dephosphorylation. Whether Cx43 dephosphorylation contributes to further reduction of GJIC in hypoxic astrocytes requires further experimental manipulation to dissociate or associate these two events. Thus, a relationship between Cx43 dephosphorylation and GJIC in astrocytes remains to be clarified. To address this issue, we re-examined the Cx43 dephosphorylation and GJIC in hypoxic astrocytes. In this study, Cx43 dephosphorylation at

gap junctions was confirmed by experiments involving faster induction, resistance to protein synthesis inhibition and membrane localization by using the newly tested anti-Cx43 antibody 13-8300 that selectively recognizes non-phosphorylated form of Cx43 (Part II). Relationships between Cx43 dephosphorylation and GJIC were studied by inhibition of Cx43 dephosphorylation in conjunction with assays of GJIC in hypoxic astrocytes. The specific objectives were to confirm the occurrence of Cx43 dephosphorylation in hypoxic astrocytes and to determine 1) whether alterations associated with Cx43 dephosphorylation seen in vivo also occur in vitro; 2) protein phosphatases responsible for Cx43 dephosphorylation in normal and hypoxic astrocytes and 3) the relationship between Cx43 dephosphorylation and GJIC in these cells.

Part I

Elevated Connexin43 Immunoreactivity at Sites of Amyloid Plaques in Alzheimer's Disease

Nagy, J. I., Li, W., Hertzberg, E. L. and Marotta, C. A.

Brain Research, 717 (1996) 173-178

Abstract

The distribution of the astrocytic gap junctional protein, connexin43 (Cx43) was compared immunohistochemically with that of amyloid plaques in Alzheimer's Disease (AD) brain. By light microscopy (LM), cortical areas containing numerous β/A4 amyloid plaques exhibited increased immunostaining density for Cx43 and some plaques corresponded exactly to sites of intensified Cx43 immunoreactivity. By electron microscopy, Cx43 was localized to astrocytic gap junctions in AD brain. Increased Cx43 expression in AD may represent an attempt to maintain tissue homeostasis by augmented intercellular communication via gap junction formation between astrocytic processes that invest senile plaques, or alternatively, an aberrant induction of astrocytic Cx43 expression which may further compromise homeostasis and exacerbate pathological conditions in the microenvironment of amyloid plaques.

Introduction

Astrocytes in normal brain are extensively coupled by gap junctions composed of the gap junctional protein Cx43 (Yamamoto et al., 1990a,b; Nagy and Dermietzel, 2000). These junctions are considered to contribute to local metabolic homeostasis (Walz, 1989) by allowing direct intercellular movement of ions and small molecules. After induction of brain injury leading to reactive gliosis, we have observed complex responses of astrocytic junctions including increases in Cx43 or loss of junctions with or without a persistence of Cx43 (Hossain et al., 1994a,b; Ochalski et al., 1995). We have also found an induction of Cx43 in PC12 cells overexpressing the β/A4 C-terminal peptide of the amyloid precursor protein (Nagy et al., 1995, 1996a). A characteristic feature in AD brain is the presence of reactive astrocytes in the vicinity of senile or amyloid plaques and an accumulation of their processes around and within the plaques (Duffy et al., 1980; Mandybur and Chuirazzi, 1990; Hatten et al., 1991). β/A4 is the major protein component of senile plaques and amyloid-laden blood vessels in AD and β/A4 deposition is a neuropathological feature in AD brain (Glenner and Wong, 1984; Masters et al., 1985), although numerous factors may contribute to the micropathology of the disorder. The present study was undertaken to assess the relationship between gap junctions and the occurrence of senile plaques and to determine whether alterations in Cx43 accompany either the gliotic response in AD or the accumulation β/A4 peptide as seen in PC12 cells. Thus, the distribution of Cx43 in AD cortical samples was immunohistochemically compared with that of senile plaques.

Materials and methods

Two well characterized anti-Cx43 antibodies (designated 18A-8 and 16A-8) to different regions of the Cx43 sequence (Beyer et al., 1987) were used (Yamamoto et al., 1990a,b; Hossain et al., 1994a,b,c). Preadsorptions of anti-Cx43 antibody with synthetic peptides were performed as previously described (Yamamoto et al., 1990a,b; Hossain et al., 1994a). Human tissues were processed with an anti-β/A4 monoclonal antibody designated 10H3

(Majocha et al., 1988; Friedland et al., 1994), which was raised against a 28 residue synthetic polypeptide containing the first 28 amino acids of β/A4 (Masters et al., 1985; Majocha et al., 1992a) and reacts with high sensitivity and selectively with senile plaques of AD brains and AD brain blood vessels with congophilic angiopathy (Majocha et al., 1988, 1992b; Honda and Marotta, 1992). Immunostaining of normal control human brains with 10H3 was shown to produce only light background staining (Majocha et al., 1988, 1992b).

Blocks of temporal cortex from 3 clinically confirmed cases of AD (post-mortem interval no more than 20 hr) and 3 matched controls were used for LM. An AD temporal cortex with post-mortem interval of 2.5 hr was used for EM. Brains were fixed in 10% formalin and stored at -70 ^{o}C after equilibration in 10% formalin/25% sucrose. Samples were sectioned at a thickness of either 15 or 20 μm on a sliding microtome, collected free-floating in phosphate buffered saline (PBS) with, in some cases, consecutive sections in separate wells for comparison of staining profiles in adjacent sections. They were then washed at 4 ^{o}C for 12 to 18 hr in PBS and taken for either peroxidase anti-peroxidase (PAP) or immunofluorescence staining for Cx43 and β/A4. Sections processed by PAP method were first treated with 0.3 % hydrogen peroxide in PBS for 30 min to eliminate endogenous peroxidase activity, washed for 30 min in PBS, and then incubated for 72 hr at 4 ^{o}C with either anti-Cx43 antibody diluted 1:1000 or a monoclonal antibody against β/A4 diluted 1:500 in PBS containing 0.3% Triton X-100 (PBST) and 2% normal serum derived from same animal species as the secondary antibody. Sections were further processed with secondary antibodies followed by rabbit PAP (Sternberger) for Cx43 or mouse clono-PAP (Sternberger) for β/A4, reacted in 0.02% 3,3-diaminobenzidine (DAB) and 0.005% hydrogen peroxide and mounted onto slides as previously described (Yamamoto et al., 1990a,b; Hossain et al., 1994a).

For double immunofluorescence staining, sections were incubated for 72 hr at 4 ^{o}C simultaneously with both the anti-Cx43 and anti-β/A4 antibodies diluted as above. They

were then washed for 1 hr in PBST, incubated for 1.5 hr at room temperature with a mixture of biotin-conjugated horse anti-mouse antibody (Vector) diluted 1:100 and Cy3-conjugated sheep anti-rabbit antibody (Sigma) diluted 1:250. They were then washed for 20 min in PBST and for 40 min in PBS and incubated with fluorescein isothiocyanates (FITC)-conjugated streptavidin (Amersham) diluted 1:100 in PBS. After washing for 20 min in PBS and 20 min in 50 mM Tris-HCl buffer, pH 7.4, sections were mounted onto slides and coverslipped. Control procedures for immunostaining specificity in the above two processing methods included omission of primary antibodies with sections stained by the PAP method, and omission of one or the other of the two primary antibodies in sections processed by immunofluorescence. In addition, sections were processed with anti-Cx43 antibody preadsorbed with the peptide against which it was directed. The results of these controls indicated lack of cross reaction of the combination of immunoreagents used for double immunofluorescence staining and an absence of immunostaining with preadsorbed anti-Cx43 antibody.

Western blots of Cx43 in rat or human brain were performed in order to demonstrate the specificity of the Cx43 antibodies used in localization of Cx43 in human brain. Frozen cerebral cortical tissues were homogenized and 10 μg of homogenate was loaded onto polyacrylamide gels and processed with anti-Cx43 antibody 18A-8 or 16A-8 as previously described (Hossain et al., 1994b,c). For EM examination of Cx43 in human brain, sections were collected and processed by the PAP method as described above except for the absence of Triton-X100 in the incubation and wash solutions. Sections were embedded and areas of interest were excised and glued onto resin blocks. Ultrathin sections were stained with lead citrate for 1-2 min.

Results

In sections of temporal lobe from 3 normal brains processed for Cx43 localization with the 18A-8 antibody by the PAP method, Cx43 was relatively uniformly distributed with a

slightly greater density of staining in cortical gray than in white matter (Fig. 1A). In sections of similar temporal lobe areas from 3 confirmed cases of AD, immunostaining density was discernibly increased throughout cortical gray matter and in immediately underlying white matter, but less so in regions of deep white matter (Fig. 1B). In addition to an overall rise in diffuse staining, two features of Cx43 distribution on a finer scale were noteworthy. First, Cx43 labeling around blood vessels was generally greater than in control material. Second, a higher density of staining was localized to round patches ranging from 20 to 150 μm in diameter (Fig. 1B).

The same field of a section adjacent to that shown in Fig. 1B was processed for localization of β/A4 with the anti-β/A4 antibody 10H3. Numerous faint to densely labeled β/A4-immunoreactive plaques (Fig. 1C) were seen in cortical areas corresponding to regions of increased Cx43 staining. Very few plaques were seen in white matter. The plaques had highly variable diameters (4 to 120 μm) similar to that of the Cx43-positive patches. Labeling within Cx43 patches consisted largely of punctate immunoreactivity (Fig. 1D). As shown by staining for β/A4 in the same field of a section adjacent to that in 1D, some patches of Cx43 corresponded exactly to sites of amyloid plaque deposition (Fig. 1E). Control procedures showed an absence of labeling in sections processed after omission of anti-Cx43 antibody (Fig. 1F) or anti-β/A4 antibody (Fig. 1G). Labeling was also absent in sections processed with preimmune serum (not shown). These controls indicate that labeling was not due to endogenous peroxidase activity or to non-specific binding of secondary antibodies. Preadsorption of anti-Cx43 with the peptide against which it was raised reduced immunostaining (not shown) to the level seen after primary omission. Finally, staining patterns for Cx43 seen with the 18A-8 and 16A-8 anti-Cx43 antibodies were similar.

In sections processed by immunofluorescence (Fig. 2), Cx43 immunoreactivity in cortical regions of normal brain consisted of puncta and some light labeling of what appeared to be astrocyte cell bodies and their proximal processes (Fig. 2A), which labeled poorly for glial fibrillary acidic protein (GFAP) (not shown). In sections of AD brain (Fig.

2B), puncta tended to be concentrated, in part, in patches similar to those seen in sections processed by the PAP method. As shown in sections double-labeled for Cx43 (Fig. 2B) and GFAP (Fig. 2C), immunostaining of the latter accompanied the elevated punctate labeling of Cx43. Increased staining for Cx43 was also found in astrocytes which were positive for GFAP and had relatively short, thick processes and enlarged cell bodies characteristic of reactive astrocytes. Often, GFAP-labeled somata were located outside the patches of Cx43-positive puncta and these patches were more associated with astrocytic processes that appeared either to stream toward, concentrate within or surround the patches. Just as seen in adjacent sections processed by the PAP method, double-labeling for Cx43 and β/A4 confirmed that some of these Cx43-positive patches (Fig. 2D) were co-localized with β/A4-immunoreactive plaques (Fig. 2E). Although subject to uncertainties regarding efficiency of immunolabeling in post-mortem human brain, counts of clear overlap in 30 different fields containing a total of 219 β/A4-positive plaques yielded a value of 80% co-localization with Cx43-positive patches. Only a low level of background fluorescence was seen in sections from AD brain processed with omission of monoclonal primary antibody for either GFAP or β/A4 (Fig. 2F). A similar level of background staining and an absence of β/A4-positive plaques was seen in sections of normal human brain processed with anti-β/A4 antibody (not shown).

EM was conducted on AD brain to confirm antibody detection of gap junctions. Areas corresponding to the plaques seen by LM exhibited dystrophic neuronal processes that contained multilammelar dense bodies (Fig. 3A,B) and often abundant filaments (Fig. 3D) which frequently took the form of paired helicies with interhelical periodicity of 30 to 60 nm (Fig. 3E). Extracellular fibular material, astrocytic processes and blood vessels with thickened, reduplicated basal laminae were additional features of tissue within plaques (not shown). Cx43 immunoreactivity was restricted to astrocytic gap junctions (Fig. 3A,D), which were seen throughout the tissue both within and outside (not shown) plaque-containing regions (3 A-D). No quantitation of junctions was performed. Western blots

conducted with samples of human cerebral cortical tissue indicated Cx43 antibody detection of a major band (Fig. 3F, lane 1) which co-migrated with that of Cx43 derived from extracts of rat brain (Fig. 3F, lane 2), indicating cross-reaction of this antibody against a sequence in rat Cx43 with the corresponding connexin in human brain.

Discussion

The anatomical correspondence between amyloid plaques and elevated immunolabeling for Cx43 in AD brains together with the association of reactive astrocytes with plaques is consistent with dramatic alterations we have observed in astrocytic Cx43 levels and cellular localization accompanying CNS insult and the ensuing reactive gliosis (Hossain et al., 1994b,c; Ochalski et al., 1995). Thus, increased Cx43 in amyloid plaques may reflect infiltration of these plaques by astrocytic processes and thereby an elevated local concentration of their attendant gap junctions. Alternatively, the observed elevation of Cx43 in amyloid plaques may suggest a possible relationship between some aspect of gap junction-mediated intercellular interactions and the apparently diverse roles so far attributed to amyloid precursor protein. More specifically, as seen with Cx43 induction in transfected PC12 cells (Nagy et al., 1995, 1996a), β/A4 amyloid may pathologically augment Cx43 expression independently of local metabolic requirements for gap junctions between astrocytic elements. Should an increase in astrocytic Cx43 represent greater gap junctional coupling and, for example, an increase in spatial buffering of K^+ or neurotransmitter uptake and dispersal by astrocytes, alterations in efficacy of neuronal transmission might well take place.

Figure legends

Fig. 1. Immunoperoxidase localization of Cx43 and β/A4 in human brain. A,B: Immunolabeling for Cx43 in normal brain (A) and increased labeling in AD brain (B). C: Labeling for β/A4 in an adjacent section and the same field as that shown in B. Numerous β/A4-positive plaques occur in areas of elevated Cx43 staining. D,E: Magnifications of the same field in adjacent sections stained for Cx43 (D) and β/A4 (E). Some patches of Cx43 labeling (arrows in D) overlap with β/A4-positive plaques (arrows in E). F,G: No immunolabeling is seen in AD brain processed with omission of anti-Cx43 (F) or anti-β/A4 antibodies (G). Magnifications: A-C, F,G, x18; D,E, x60.

Fig. 2. Immunofluorescence micrographs of Cx43, GFAP and β/A4 labeling in human brain. A: Punctate (arrows) and faint astrocytic somal (arrowheads) Cx43 labeling is seen in normal brain. B,C: The same field in a section of AD brain double-labeled for Cx43 (B) and GFAP (C). Patches of Cx43 puncta (arrows in B) appear associated with GFAP-labeled processes (corresponding arrows in C). Cx43-positive somata (arrowheads in B) are also GFAP-positive (arrowheads in C). D,E: The same field in a section of AD brain double-labeled for Cx43 (D) and β/A4 (E). Some patches of Cx43 (arrows in D) co-localize with β/A4-immunoreactive plaques (corresponding arrows on E) and somal astrocytic labeling for Cx43 (arrowheads in D) is evident. F: Section from AD brain showing only background staining after primary antibody omission. Magnifications: A-C, x200; D-F, x100.

Fig. 3. Electron micrographs of Cx43 immunoreactive gap junctions in AD human brain. A: Labeled gap junctions (arrows) between glial processes are seen near dystrophic neurites (n). B,C: Labeled junction shown in A and, for comparison, a gap junction from a non-immunostained section of the same brain. D,E: Gap junctions (arrows) in neuropil near processes displaying paired helical filaments (asterisks), shown in E from a field where their helical morphology is more evident (arrowheads). F: Western blot showing anti-Cx43

antibody recognition of human brain Cx43 (lane 1) which migrates similarly to Cx43 from rat brain (lane 2). Numbers indicate Mr (kDa). Magnifications: A, x17,000; B,C, x105,000; D, x16,000; E, x92,000.

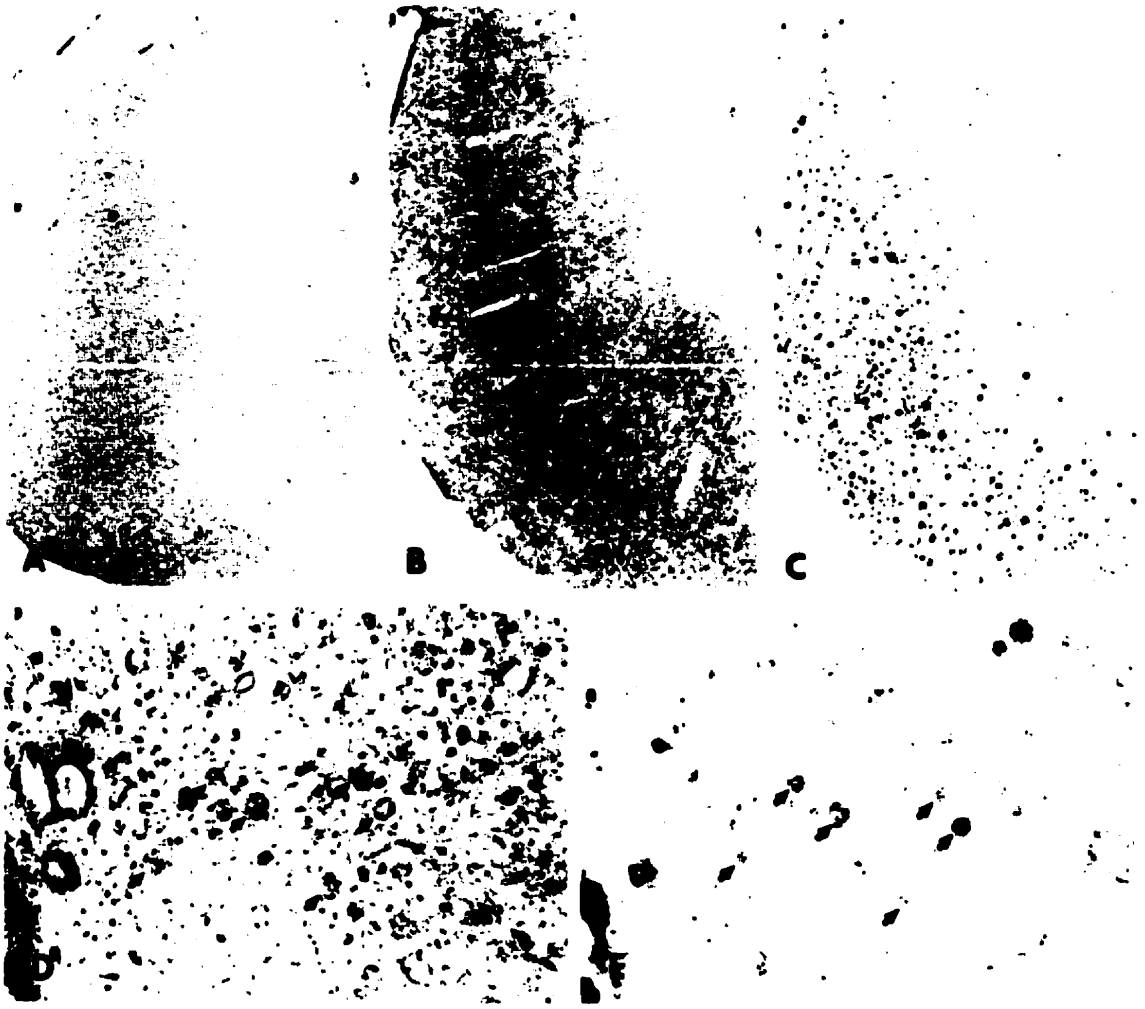

Fig. 1

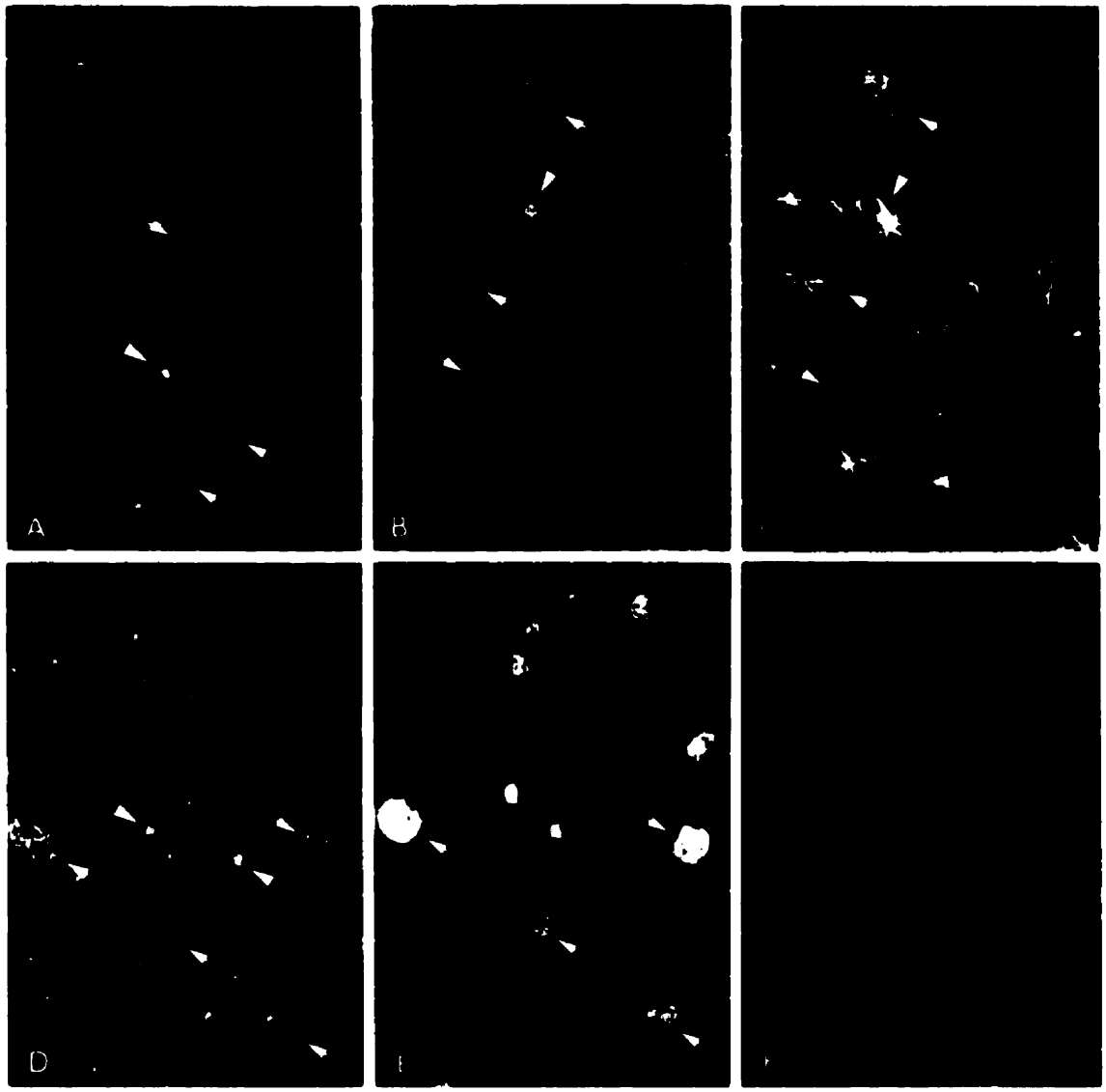

Fig. 2

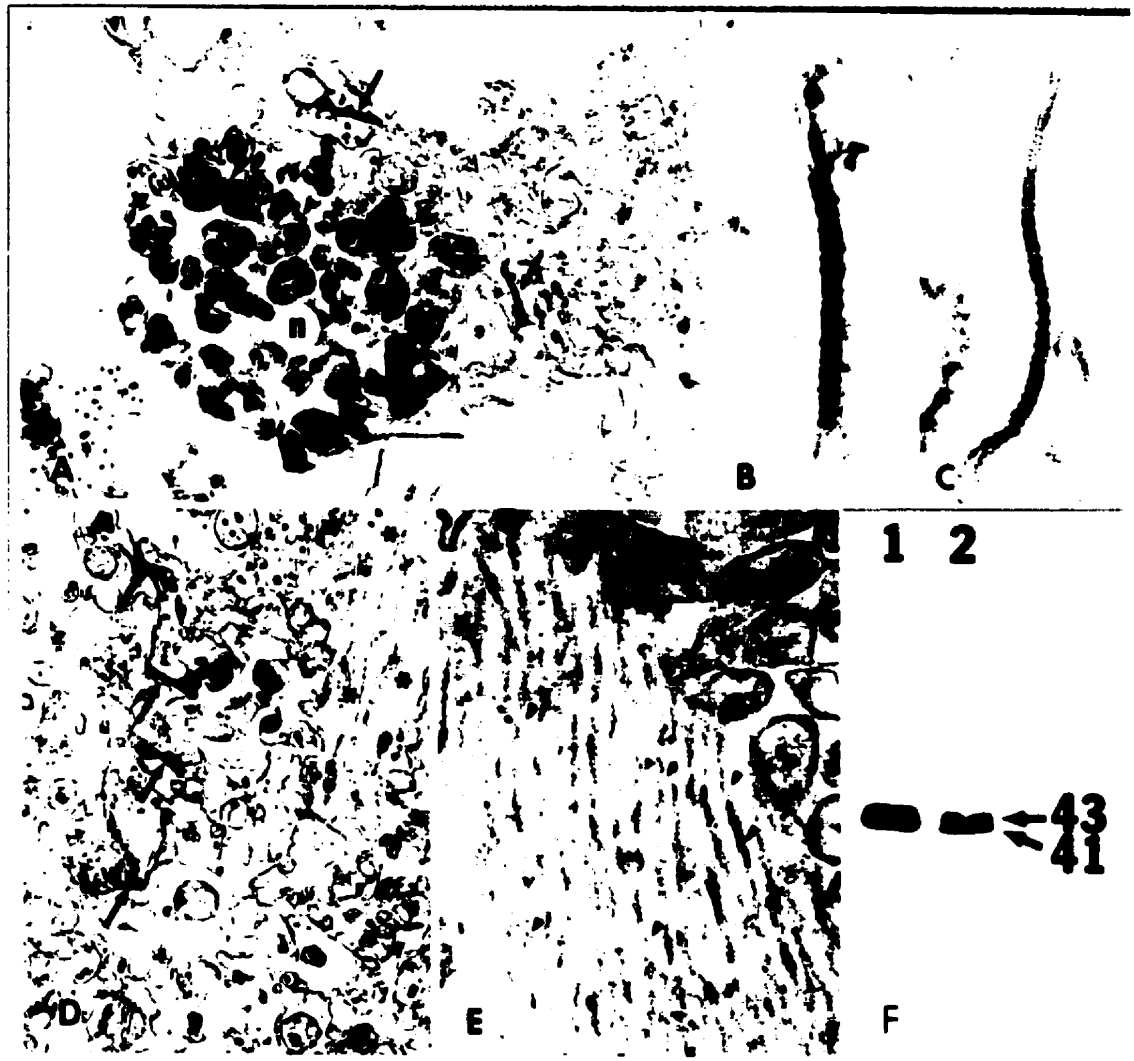

Fig. 3

Part II

Selective Monoclonal Antibody Recognition and Cellular Localization of an Unphosphorylated Form of Connexin43

Nagy, J. I., Li, W. E. I., Roy, C., Doble, B. W., Gilchrist, J. S., Kardami, E. and Hertzberg, E. L.

Experimental Cell Research, 236 (1997) 127-136

Abstract

A sequence-specific monoclonal antibody directed against the gap junction protein connexin43 (Cx43) is shown here to be specific for the unphosphorylated form of this protein. In tissues and cultured cells containing different phosphorylated and unphosphorylated forms of Cx43, the antibody detected only the latter as shown by Western blotting of native and alkaline phosphatase-treated samples. Immunohistochemically, this monoclonal antibody did not recognize gap junctions in the vast majority of cultured cardiac myocytes, where nearly all detectable Cx43 is phosphorylated. In contrast, it was able to detect some intracellular Cx43 in tracheal smooth muscle cells and an epithelial cell line (Cl-9 cells), producing patterns of labeling consistent with those seen using a polyclonal antibody that recognizes both phosphorylated and unphosphorylated forms of Cx43. Immunostaining of gap junctions in the cultured cells indicates that both phosphorylated and unphosphorylated Cx43 are present in some assembled gap junctions, suggesting that assembled junctions do not contain exclusively the phosphorylated form of the protein. Annular gap junctions, believed to form as part of the pathway for internalization and degradation of gap junctions, were only occasionally and sparsely labeled by the monoclonal antibody, indicating that complete protein dephosphorylation is not required for uptake and degradation of gap junctions. Furthermore, the ability of this antibody to recognize only unphosphorylated Cx43, and not any of the phosphorylated forms present in the tissues and cell types examined, suggests that a unique phosphorylation site, perhaps present in the epitope recognized by this antibody, must be phosphorylated prior to phosphorylation of Cx43 at other sites.

Introduction

The gap junction protein, Cx43, originally identified in rodent heart (Beyer et al., 1987), has been the focus of a now extensive literature. Studies characterizing its phosphorylated forms, especially as they might relate to regulation of assembly and functional properties have been particularly well-developed (for review see Saez et al., 1993). Among these, several studies have correlated phosphorylation state of Cx43 with its residence in particular subcellular compartments (Atkinson et al., 1981; Musil and Goodenough, 1991, 1993; Revel et al., 1992; Puranam et al., 1993; Lampe, 1994; Laird et al., 1995). The more phosphorylated forms, which are relatively insoluble to detergent extraction, are usually assembled into gap junctions (Musil and Goodenough, 1991). Other studies suggest that phosphorylation correlates with inhibition or stimulation of channel function, or with alteration of single channel properties (Godwin et al., 1993; Kwak et al., 1995a,b,c; Kwak and Jongsma, 1996; Moreno et al., 1994). Various studies have identified specific seryl residues phosphorylated by MAP kinase (Warn-Cramer et al., 1996) and PKC (Sáez et al., 1997), as well as a specific tyrosine phosphorylation that correlates with channel closure upon activation of src kinase (Swenson et al., 1990).

Like other connexins thus far analyzed, Cx43 appears to turn over quite rapidly, with a half-life on the order of about 2 h in cultured cardiomyocytes (Laird et al., 1991; Darrow et al., 1995) as well as several cell lines (Musil and Goodenough, 1991; Laird et al., 1995). The turnover of ^{32}P-labeled Cx43 appears to be of about the same in most systems examined (Musil and Goodenough, 1991; Laird et al., 1995), suggesting that bulk phosphorylation is a constant and relatively uniform process over time. The possibility remains, however, that dynamic cycles of phosphorylation and dephosphorylation of one or a few specific sites might be obscured by a static rate of phosphorylation of a larger number of amino acids. One mechanism by which gap junction turnover occurs is thought to involve their internalization as annular structures that might enter a lysosomal compartment for degradation (Larsen and Tung, 1978). However, molecular features of turnover of connexins remain obscure. For example, a recent report has implicated a ubiquitin-based proteosomal

degradation pathway for Cx43 (Laing and Beyer, 1995), although it has not yet been established if all Cx43 is degraded by this pathway or if it is only a minor contributor to turnover, perhaps degrading Cx43 misfolded during its biosynthesis as suggested for other proteins (Peters, 1994; Jennissen, 1995).

The availability of antibodies specific for unphosphorylated and phosphorylated forms of connexins would, in principle, be useful immunohistochemical markers for analysis of their distribution in various cellular compartments under physiological conditions as well as for identifying and localizing connexins in various phosphorylated forms following treatments that alter properties of gap junctions. Using cells and tissues that were chosen for their differential expression of Cx43 phosphorylation states as well as cellular localization of Cx43, we characterize in this study a commercially available monoclonal antibody and show it to be specific for unphosphorylated Cx43. Evidence presented indicates that unphosphorylated Cx43 is present in assembled gap junctions in some, but not all cell types and that internalized annular gap junctional structures are only partially labeled by this antibody. Furthermore, the fact that this monoclonal antibody identifies only unphosphorylated Cx43 implies that phosphorylation of Cx43 may be a sequential process requiring phosphorylation of one or more specific sites prior to phosphorylation at other sites.

Materials and methods

Antibodies

Two different anti-Cx43 antibodies were used in this study. A rabbit polyclonal antibody (designated 18A) that was generated against amino acids 346-363 of the Cx43 sequence (Beyer et al., 1987) has been used extensively by us and demonstrated to exhibit high Cx43 specificity based on peptide adsorption controls in Western blots and immunohistochemistry of brain and heart tissue (Yamamoto et al., 1990a,b; Nagy et al., 1992). A mouse monoclonal antibody (designated 13-8300, clone CX-1B1), generated against amino acids 360-376 of the Cx43 sequence Beyer et al., 1987), was obtained from Zymed Laboratories

(South San Francisco, CA). The epitope recognized by antibody 13-8300 is a cytoplasmically-located sequence present at the C-terminus of the protein.

Cell culture

Canine tracheal smooth muscle (TSM) cells were cultured as previously described (Halayko et al., 1996). Briefly, trachealis muscle was removed from adult mongrel dogs and minced in antibiotic-containing Hanks' balanced salt solution (HBSS) followed by incubation in HBSS containing collagenase, type IV elastase and Nagarse protease. After trituration at 37°C and passage through a 70 μm nylon mesh, cells were washed in HBSS, suspended in culture medium consisting a mixture of Dulbecco's modified essential medium and F12 nutrient (DMEM/F12) (Gibco, Burlington, Ontario) containing 10% fetal bovine serum (FBS) and antibiotics, then plated on 100 mm plastic culture dishes and maintained in a humidified 5% CO_2 atmosphere at 37°C. Confluent cultures were washed with HBSS, incubated at 37°C with trypsin-containing HBSS, centrifuged, resuspended in culture medium for replating and used at 70-90% confluence. Cardiomyocyte cell cultures were prepared from ventricles of neonatal Sprague-Dawley rats 1-2 days of age. Tissue was dissociated with trypsin, passed through a Percoll gradient to isolate pure cardiomyocytes as previously described (Shubeita et al., 1992) and cells were plated on collagen-coated culture dishes or coverslips. Cells were maintained for 6-7 days in 0.5% FBS in DMEM/F12 medium supplemented with 20 nM selenium, 0.2% bovine serum albumin (BSA), 10 μg/ml of insulin, 10 μg/ml transferrin and 20 μg/ml ascorbic acid. A rat liver epithelial cell line, clone 9 (Cl-9) was cultured in DMEM supplemented with 10% fetal bovine serum as previously described (Berthoud et al., 1993).

Tissue preparation and Western blot analysis

Membrane fractions enriched in gap junctions and purified sarcolemma (SL) membrane were prepared from rat heart as previously described (Pitts, 1979; Kardami et al, 1991; Mesaeli et al., 1992). Cardiac sarcoplasmic reticulum (SR) membranes, including heavy

(HSR) and light (LSR) fractions, were prepared as reported (Gilchrist et al., 1992) with some modifications. Briefly, rat hearts were powdered in liquid nitrogen and homogenized in ice-cold Buffer A containing 300 mM sucrose, 400 mM KCl, 20 mM imidazole (pH 7.4), 0.5 mM Mg/ATP, 0.5 mM EGTA, 1 mM dithiothreitol (DTT), 1 mM phenylmethanesulfonyl fluoride (PMSF), 10 μM antipain, 28 μM TPCK, 28 μM TLCK, 10 μM pepstatin, and 2 μM leupeptin. SR-enriched cardiac microsomes were obtained by pelleting homogenate at 16,000 g, resuspending and pelleting at 43,500 g for 10 min. After resuspending in Buffer A, microsomes were layered onto 25-45% linear sucrose gradients in Buffer A, centrifuged overnight and HSR consisting of terminal cisternae were harvested at the 40-42% sucrose region. A band of protein at 34-36% sucrose contained the LSR. Both fractions were diluted 3-fold with buffer containing 400 mM KCl, 5 mM imidazole (pH 7.4), 1 mM DTT and protease inhibitors, stirred on ice for 1 h, pelleted and resuspended in 300 mM sucrose containing 20 mM imidazole (pH 7.4), 1 mM DTT, 1 mM PMSF and 2 μM leupeptin. Fractions were taken for alkaline phosphatase treatment and SDS/PAGE as described below.

Cultured cardiomyocyte extracts were prepared by lysis for 30 min in modified RIPA buffer (150 mM NaCl, 1% NP-40, 0.25% deoxycholic acid, 0.1% SDS, 1 mM EGTA, 1 mM EDTA, 50 mM Tris, pH 8.0; supplemented with 1 mM PMSF and 20 μg/ml each of leupeptin, pepstatin and aprotinin). Cells were scraped, sonicated and centrifuged at 10,000 g for 10 min at 4°C. In some experiments, 10 μg of lysate protein was treated with 8 units of calf intestine alkaline phosphatase (Boehringer Mannheim, Germany) for 30 min at 37°C. Samples (1-5 μg protein) were resolved by SDS-PAGE (9.5% acrylamide), transferred to Immobilon-P membrane (Millipore) and probed with antibody 13-8300 diluted 1:500 or antibody 18A diluted 1:20,000.

Extraction of cultured TSM cells was conducted either by detergent lysis in buffer containing the phosphatase inhibitors NaF and sodium orthovanadate (method 1) or by microwave heating prior to detergent lysis in buffer lacking phosphatase inhibitors (method

2). We previously reported that microwave heating was effective in preventing Cx43 dephosphorylation during tissue preparation (Hossain et al., 1994). In order to be sure that Cx43 dephosphorylation did not occur during lysis of cells, we used the two methods for preparation of tracheal cells where preliminary results indicated the presence of dephosphorylated Cx43. In method 1, cultures were washed with 50 mM sodium phosphate buffer, pH 7.4, containing 0.9% saline (PBS) and extracted with 1 ml of lysis buffer (40 mM Tris buffer, pH 7.4, 1% NP-40, 1 mM PMSF, 20 μg/ml each of leupeptin and pepstatin, 10 mM NaF and 1 mM sodium orthovanadate). The extract was centrifuged at 5,000 g for 10 min at 4°C and the supernatant taken for Western blotting. In method 2, cultures were washed with PBS and, with 1 ml of fresh PBS added, were heated to 90°C for 17 seconds in a microwave oven and then extracted as in method 1. Samples were prepared for Western blotting with primary antibody detection by chemiluminescence (Amersham) as previously described Hossain et al., 1994). Protein concentration was determined by either the bicinchoninic acid method (Sigma, Oakville, Ontario) or by a BIO-RAD DC protein assay (Bio-Rad).

Immunohistochemistry

For double immunofluorescence staining of cardiac myocytes and TSM cells, coverslips with attached cells were rinsed in PBS, fixed for 15 min in ice-cold PBS containing 1% paraformaldehyde and washed in PBS. After treatment for 15 min at 4°C in PBS containing 0.1% Triton X-100, cultures were sequentially processed with antibodies diluted in PBS. They were first incubated for 24 h at 4°C with antibody 13-8300 diluted 1:500, washed and then incubated with Cy3-conjugated donkey anti-mouse IgG diluted 1:200. Cultures were then washed, incubated with antibody 18A (diluted 1:1,000) for 24 h at 4°C, washed, incubated with FITC-conjugated donkey anti-rabbit IgG diluted 1:50, washed in 50 mM Tris-HCl buffer, pH 7.4, and coverslipped with anti-fade medium. Omission of one or the other of the primary antibodies resulted in a total absence of staining with fluorochrome

corresponding to the primary antibody omitted, indicating absence of inappropriate antibody reactions. Sections were viewed with a Leitz Dialux 20 microscope using filter cubes L3 and N2 for FITC and Cy3, respectively.

Electron microscopy

TSM cultures taken for EM were fixed as above and processed for Cx43 detection by the peroxidase anti-peroxidase method. Cells were incubated for 24-48 h with either antibody 18A or 13-8300 each diluted 1:500 in PBS containing 0.1% Photo-Flo (Kodak) (PBSF) and 2% normal serum. Following a 1 h wash in PBSF, they were incubated for 1.5 h with appropriate secondary antibody diluted in PBSF (either goat anti-rabbit IgG, 1:100 or horse anti-mouse IgG, 1:50), washed for 1 h in PBSF, incubated in appropriate tertiary antibody (either rabbit PAP or clonoPAP each diluted in 1:500 in PBSF), washed and incubated with 3,3-diaminobenzidine (DAB)/H_2O_2 as described Ochalski et al., 1995). After rinsing in PBS, cells were osmicated for 2 h in 2% osmium tetroxide in PB, rinsed, dehydrated in ethanol and embedded in TAAB 812 (Marivac). Ultrathin sections of excised areas were counterstained for 1-2 min with lead citrate.

Cl-9 cells grown on glass coverslips were rinsed with Dulbecco's phosphate-buffered saline, pH 7.4 (D-PBS), fixed on ice for 10 min with 4% formaldehyde in D-PBS, rinsed and permeabilized with 0.08% Triton X-100 in D-PBS for 3 min and blocked with 0.1% bovine serum albumin (essentially globulin free), 5% normal goat serum and 5% sheep serum in D-PBS. Cultures were incubated overnight at 4°C with either antibodies 18A (affinity purified, diluted 1:500) or 13-8300 (diluted 1:25) in D-PBS. For control purposes, mouse IgG, normal rabbit serum, and D-PBS were substituted for antibodies. After washing in D-PBS, goat anti-mouse IgG(Fc) 5 nm gold particles (Amersham) or goat anti-rabbit IgG(H+L) 10 nm gold particles (Amersham) diluted in D-PBS were applied for 2 h at room temperature for detection of monoclonal or polyclonal primary antibodies, respectively. Cultures were washed in D-PBS, fixed with 0.5% glutaraldehyde in 0.175 M cacodylate buffer, pH 7.4 for 1 h on ice, rinsed, dehydrated and embedded with LR White resin. Ultrathin sections were stained with uranyl

acetate or with Reynold's lead citrate. For double labeling, ultrathin sections labeled as above with antibody 13-8300 using 5 nm gold particles were treated with 0.1 M glycine in 0.1 M phosphate buffer pH 7.4 (PB), blocked at 37°C with PB containing 0.5% gelatin, 0.01 M glycine, 0.1 % non-fat dry milk and 1.0% normal goat serum and rinsed with 0.1 M glycine in PB. They were then incubated overnight with antibody 18A diluted in PB, washed in PB, incubated with goat anti-rabbit IgG(H+L)-conjugated-10 nm gold particles for 1.5 h at room temperature, washed, fixed briefly with 2% glutaraldehyde in PB and counterstained as above.

Results

Western blots of cardiac gap junctional membranes probed with antibody 18A, which detects both the phosphorylated (slower-migrating ca. 43 kDa band) and unphosphorylated (faster-migrating ca. 41 kDa band) forms of Cx43, indicated that cardiac gap junctions contain primarily the phosphorylated 43 kDa form (Fig. 1A, lane 1). This 43 kDa form was not detected with antibody 13-8300 as shown in an adjacent lane loaded with the same homogenate (Fig. 1A, lane 2). Similar results were obtained with membrane fractions of cultured cardiac myocytes where only the 43 kDa form was detected with antibody 18A (Fig. 1B, lane 1) and no recognition of this form was evident with antibody 13-8300 (Fig. 1B, lane 3). Treatment of cardiomyocyte membranes with alkaline phosphatase shifted the mobility of Cx43 to 41 kDa confirming that the differential migration of Cx43 is due to its phosphorylation state and that antibody 18A detects the 41 kDa form as well (Fig. 1B, lane 2). The 41 kDa form is readily detected by antibody 13-8300 in phosphatase-treated samples (Fig. 1B, lane 4).

Migration patterns of Cx43 in cardiac SL and SR membranes are shown in Fig. 1C,D. Without alkaline phosphatase treatment, antibody 18A indicated that SR fractions contained both the 43 and 41 kDa forms of Cx43 (Fig. 1C, lane 2 and 4). In contrast, SL membrane contained only the 43 kDa form (Fig. 1C, lane 1). Treatment with alkaline phosphatase increased the 41 kDa and decreased the 43 kDa form in both SR fractions (Fig. 1C, lanes 3 and 5). An identical blot was analyzed using antibody 13-8300 which detected only the 41

kDa band in all SR samples (Fig. 1D, lanes 2-5). The 41 kDa form appeared to be present at higher levels in the LSR than the HSR fraction. Curiously, alkaline phosphatase treatment of SL membranes had no affect on the mobility of the 43 kDa form in these membranes as detected by antibody 18A (not shown) and did not result in the appearance of the 41 kDa form (Fig. 1D, lane 1).

In cultures of confluent cardiac myocytes (Fig. 2A), immunofluorescence with antibody 18A was localized in perinuclear regions and at puncta around cells (Fig. 2B). In contrast and consistent with the prevalence of the phosphorylated form of Cx43 in cultured cardiac myocytes, very little labeling was seen with antibody 13-8300 (Fig. 2C). Although not readily evident, the vast majority of puncta seen with 13-8300 were superimposable with puncta at the periphery of cells in the same field labeled with antibody 18A. Occasionally, a very small percentage of cells (< 1%) did exhibit more densely distributed punctate labeling around their periphery with both antibodies (Fig. 2D,E). Due to their small number, it was not determined whether these were myocytes or a contaminating cell type such as fibroblasts.

Cultured canine TSM cells harvested in the absence of phosphatase inhibitors contained both the 41 and 43 kDa forms of Cx43. As shown in Fig. 3, cells lysed in the presence of phosphatase inhibitors (lanes 1 and 3) displayed slower migrating bands with antibody 18A (lane 1) similar to those seen in heart. However, despite phosphatase inhibition, antibody 18A also detected an intense lower band (lane 1) migrating at 41 kDa. Only the lower of these bands was detected with antibody 13-8300 (lane 3). Similar results were obtained with TSM cells heated by microwave treatment and then lysed in the absence of phosphatase inhibitors (lanes 2 and 4). The upper doublet of bands detected in cells prepared with phosphatase inhibitors (lane 1) show a slight mobility difference relative to their counterparts in cells lysed in the absence of these inhibitors after microwave treatment (lane 2). Although it is unclear whether the inhibitors interact in some manner with Cx43 to generate these mobility differences, a comparison of the two treatments is included here to illustrate that a clearer separation of the various Cx43 forms can be obtained after

microwave heat treatment. Apart from this point, little difference is seen in the relative proportions of 41 and 43 kDa forms of Cx43 in TSM cells prepared with or without phosphatase inhibition. Similar Western blot profiles were obtained for Cl-9 cells (Berthoud et al., 1993).

In confluent cultures of TSM cells (Fig. 4A), Cx43 immunofluorescence was seen intracellularly in most cells with antibodies 18A and 13-8300 (Fig. 4B,C). Labeling was found throughout the cytoplasmic compartment and often had the appearance of distinct globular profiles. A small proportion of cells (10-15%) also exhibited punctate labeling along plasma membranes with antibody 18A (Fig. 4B). These puncta were not detectable with antibody 13-8300 (Fig. 4C) as shown in the same field double-labeled with the two antibodies (Fig. 4B,C).

Previous studies of cultured TSM cells have addressed the issue of contamination by other cell types (Avner et al., 1981; Tom-Moy et al., 1987), however, cultures prepared here were shown by TSM cell-specific markers to comprise >95% TSM cells (Halayko et al., 1996). Ultrastructurally, these cells were identified by established criteria including pronounced cytoplasmic electron density and presence of ordered pinocytotic vesicles along lateral margins of cells as well as small electron-dense structures (termed "dense bodies") among filament bundles at the cell periphery. By LM, labeling by the PAP method with both antibody 18A and 13-8300 was similar to that seen by immunofluorescence (not shown). Both antibodies labeled rough endoplasmic reticulum (RER) (Fig. 5A) as well as cytoplasmic inclusions (Fig. 5B) that had the appearance of secondary lysosomes. Antibody 18A labeled all gap junctions between TSM cells (Fig. 5C) producing a dense DAB reaction product on the cytoplasmic surface of junctional membranes (Fig. 5D). In contrast, gap junctions were characteristically unstained with antibody 13-8300 (Fig. 5E,F), although relatively light staining was seen at a few junctions (Fig. 5G). Intracellular annular gap junctions were commonly seen in TSM cells (Fig. 5H-J). Labeling of these structures by antibody 13-8300 was generally light and intermittent, and some annular junctions were

unlabeled (Fig. 5I). In contrast, labeling of annular junctions was more robust and consistently observed with antibody 18A (Fig. 5J).

In Cl-9 cells, Cx43 immunofluorescence with antibody 18A was localized at perinuclear and appositional membranes as reported previously (Berthoud et al., 1993). Staining with antibody 13-8300 was only rarely observed and localized to small puncta in the cytoplasm and at points of cell-cell contact (not shown). Immunogold labeling for Cx43 in Cl-9 cells using different size gold particles in conjunction with antibodies 18A (5 nm) and 13-8300 (10 nm) is shown in Fig. 6. In these studies, antibody 13-8300 and secondary antibodies were applied to cells subsequent to fixation and permeabilization. Antibody 18A and secondary antibodies were then applied to sections after embedding. A representative image (Fig. 6A) demonstrates that while labeling of a gap junction is sparse, specificity is similar to that observed in TSM cells using immunoperoxidase techniques. As in the case of TSM cells, not all gap junctions at points of cell-cell contact were labeled with antibody 13-8300 in Cl-9 cells (not shown), but were with antibody 18A.

Double immunogold labeling of a gap junction at appositional membranes between Cl-9 cells indicates that both 18A and 13-8300 antibodies can bind to the same gap junction (Fig. 6B). Such double-labeling of junctional structures invariably occurred when any labeling with 13-8300 was observed. When antibody 13-8300 was localized to annular gap junctions, staining was present only on the cytoplasmic surface, suggesting that the permeabilization protocol utilized did not permit access of the antibody to the lumenal surface of the annular junction. When antibody 18A alone was used post-fixation on sections, it generally stained both surfaces of annular gap junctions (not shown) as was reported for its staining of annular gap junctions in corporal smooth muscle (Campos de Carvalho et al., 1993). In double immunogold labeling of annular gap junctions, antibody 18A exhibited lumenal localization (Fig. 6C) and variable labeling at the cytoplasmic surface. In what may be an extreme case, little or no binding of antibody 18A at the cytoplasmic surface of annular gap junctions was observed when high levels of antibody 13-8300 labeling was present (Fig. 6C). Rather than reflecting the presence of dephosphorylated Cx43 at the cytoplasmic surface of annular gap

junctions, this apparent asymmetric immunolabeling is likely due to sequential application of antibody 13-8300 to permeabilized and lightly-fixed cells followed by antibody 18A to post-fixed, embedded and sectioned cells. As a consequence, binding of antibody 13-8300 may occlude sites on Cx43 normally recognized by antibody 18A, although more detailed analysis will be necessary to establish this point. That immunostaining was observed on both cytoplasmic and lumenal surfaces of the vesicular structure in Fig. 6C is, in any case, consistent with its being an annular gap junction because the domains of Cx43 to which these antibodies bind are exposed both cytoplasmically and lumenally, whereas only one surface would be labeled in a single-membrane structure derived from a gap junction. Further, serial sectioning of immunolabeled structures inferred to be annular gap junctions in Cl-9 cells confirmed that these were not continuous the plasma membrane (not shown). Fixation conditions utilized here for immunogold studies did not adequately preserve intracellular membranes to permit identification of immunogold labeled structures other than annular and appositional gap junctions.

Discussion

In heart, numerous studies have demonstrated punctate labeling for Cx43 at intercalated discs and the lateral margins of cells similar to that we have observed with antibody 18A (Yamamoto et al., 1990a,b; Kardami et al., 1991), but no such labeling was evident with antibody 13-8300 (not shown). Western blot analyses indicating that 13-8300 recognizes only the unphosphorylated 41 kDa form of Cx43, together with the predominance of the phosphorylated 43 kDa form at cardiac gap junctions (Crow et al., 1990; Musil et al., 1990; Laird et al., 1991; Lau et al., 1991) is consistent with the lack of Cx43 detection at heart gap junctions by 13-8300. The selectivity of this antibody is further indicated by its recognition of dephosphorylated Cx43 in alkaline phosphatase-treated extracts of cultured cardiomyocytes and SR membranes. Reasons for the lack of alkaline phosphatase action on Cx43 in SL membranes remain unclear. As regards Cx43 in cardiac SR, unphosphorylated Cx43 is likely to be present in RER, a potential contaminant of our SR preparations.

Alternatively, newly synthesized Cx43 may be deposited into the SR which then contributes to transport of Cx43 to and from the plasma membrane. The two SR fractions obtained here appear to represent distinct internal cardiac membrane systems based on different protein composition (unpublished observations). The HSR fraction may contain junctional SR located in the vicinity of T-tubules and the sarcolemma, while the LSR is likely composed of the remaining SR, located at a distance from T tubules. Further characterization is required to delineate intracellular trafficking of Cx43 in association with SR in cardiac tissue.

Our analysis of TSM cells, cardiomyocytes and Cl-9 rat liver epithelial cells demonstrated several different immunostaining patterns. Both abundance and subcellular localization of unphosphorylated Cx43 varies with cell type; levels were low in Cl-9 cells and at gap junctions in cardiomyocytes, but high in RER of TSM cells, low at their annular gap junctions, and very low at their cell-cell gap junctions. In cardiomyocytes, both phosphorylated Cx43 and unphosphorylated Cx43 were found at membrane appositions suggestive of gap junctions. Antibody 18A labeled all typical gap junctions in TSM cells, but did not distinguish between the phosphorylation states of Cx43. However, the paucity of gap junctions labeled with antibody 13-8300 suggests that junctions between these cells generally contain little unphosphorylated Cx43. EM labeling of PER in TSM cells by antibodies 13-8300 and 18A was similar to staining of RER in other cell types and likely reflects sites of Cx43 synthesis (Ochalski et al., 1995), which is consistent with the presence of unphosphorylated Cx43 non-junctional pools (Musil and Goodenough, 1991). Intracellular Cx43 in TSM cell structures having the appearance of secondary lysosomes were also observed in corporal smooth muscle cells (Campos de Carvalho et al., 1993). Vacuolar structures displaying acid phosphatase activity and having a similar morphology to the Cx43-positive lysosomal profiles described here were thought to play a role in degrading gap junctional plaques in rabbit granulosa cells, where turnover of these junctions is high (Larsen and Tung, 1978). Similarly, the prominence of these lysosomal elements may indicate a high turnover rate of Cx43 in TSM cells, which is consistent with rapid Cx43

turnover in other cells (Musil et al., 1990; Musil and Goodenough, 1991; Laird et al., 1991, 1995; Gilchrist et al., 1992).

The annular gap junctional profiles occasionally seen in cultured TSM cells may result from gap junctional plaques spanning the circumference of small caliber processes that interdigitate and form junctions with other larger processes. However, these annular structures lacked organelles (e.g. mitochondria, ER, ribosomes) or cytoplasmic ground substance that can be identified in annular cell-cell gap junctions and more likely correspond to gap junctions internalized prior to their degradation during turnover (Wert and Larsen, 1990). In both TSM and Cl-9 cells, all annular profiles were immunostained with antibody 18A, but some were devoid of staining or stained only intermittently with antibody 13-8300 in a proportion of cells. While annular profiles stained with antibody 13-8300 might reflect internalization of gap junctions containing some unphosphorylated Cx43, the sparse labeling of such profiles with this antibody raises the possibility that Cx43 dephosphorylation is not a strict requirement for its uptake into annular structures. It should be noted that immunostaining with 13-8300 is unlikely to be due to artifactual dephosphorylation of Cx43 during tissue processing, which did not occur in, for example, TSM cells harvested for Western blots in the absence of phosphatase inhibition and is even less likely to occur during rapid paraformaldehyde fixation of monolayer cell cultures.

Several studies have suggested that Cx43 post-translational phosphorylation may represent a mechanism involved in trafficking and assembly into gap junctions (Musil et al., 1990; Musil and Goodenough, 1991, 1993; Puranam et al., 1993; Laird et al., 1995), although at least one connexin, Cx26, is not phosphorylated (Traub et al., 1989; Saez et al., 1990). Others have implicated connexin phosphorylation in aspects of gap junction turnover (Musil et al., 1990; Musil and Goodenough, 1991, 1993; Puranam et al., 1993; Lampe, 1994; Laird et al., 1995) and regulation of channel properties (Godwin et al., 1993; Kwak et al., 1995a,b,c; Kwak and Jongsma, 1996; Moreno et al., 1994; Oh et al., 1991). An ability to immunolocalize Cx43 with an antibody specific for its unphosphorylated form in situ provides an opportunity to address issues relating to connexin phosphorylation by

microscopy in a manner complementary to biochemical approaches. Thus, antibody 13-8300 should permit analysis of cells in which communication patterns are influenced by agents leading to altered Cx43 phosphorylation state. Given that a monoclonal antibody recognizes but a single epitope in a protein, the inability of this antibody to recognize any phosphorylated form of Cx43 suggests that this epitope may be phosphorylated itself, obliterating antibody binding, or that the epitope is conformationally sensitive to phosphorylation at other sites. The former is more likely and suggests that Cx43 is phosphorylated sequentially beginning with a site contained in the epitope recognized by antibody 13-8300. The sequence used to raise this antibody (amino acids 360-376 of Cx43) includes ser-368 and ser-372 that have recently been shown to be phosphorylated in vitro by protein kinase C (PKC) using as substrate a polypeptide fragment of Cx43 (Sáez et al., 1997). It remains to be determined whether phosphorylation at these sites or at another seryl residue in this sequence blocks binding of antibody 13-8300.

Treatments stimulating Cx43 phosphorylation by PKC lead to several different effects on gap junction assembly and channels properties. For most cell types, brief stimulation of PKC by TPA leads to inhibition of junctional coupling (Saez et al., 1993) that can be followed by down-regulation of Cx43 expression (Oh et al., 1991). In cardiac myocytes, stimulation of dye-coupling occurs after brief treatment with TPA if the cells are pretreated with a PKC inhibitor (Sáez et al., 1997). TPA-induced phosphorylation of Cx43 has also been shown to block its assembly into gap junctions (Lampe, 1994). Assuming that initial phosphorylation at seryl residues within the 13-8300 epitope serves a permissive function in assembly and formation of gap junctions, our data suggest that the PKC-dependent phosphorylation of Cx43 analyzed in these other studies involves phosphorylation either at other sites in the protein or at a site within residues 360-376 distinct from that recognized by antibody 13-8300. We anticipate that molecular definition of these events will be provided by studies that focus on the seryl residues present in amino acids 360-376 of Cx43.

Figure Legends

Fig. 1. Western blots showing selective recognition of the 41 kDa dephosphorylated form of Cx43 by monoclonal anti-Cx43 antibody 13-8300 in heart tissues and cells. (A) Blots of heart gap junction membrane preparation showing prevalence of the phosphorylated 43 kDa form of Cx43 as revealed by antibody 18A (lane 1) and lack of detection of this form with monoclonal antibody 13-8300 (lane 2). (B) Samples of cultured cardiomyocyte membrane fraction probed with antibody 18A (lanes 1 and 2) or monoclonal antibody 13-8300 (lanes 3 and 4) before (lanes 1 and 3) or after (lanes 2 and 4) treatment with alkaline phosphatase. (C,D) Duplicate blots loaded with subcellular fractions of heart were analyzed using antibody 18A (C) or 13-8300 (D). Lanes 1, Cardiac sarcolemma; lane 2, cardiac LSR; lane 3, cardiac LSR treated with alkaline phosphatase; lane 4, cardiac HSR; lane 5, cardiac HSR treated with alkaline phosphatase. Migration of molecular weight markers is indicated in kDa.

Fig. 2. Immunofluorescence labeling for Cx43 in cultures of cardiac myocytes. (A) Representative phase contrast (different from B,C) showing myocyte cultures at confluence. (B,C) The same field in a culture double-labeled with polyclonal antibody 18A (B) and monoclonal antibody 13-8300 (C). Intense staining for Cx43 obtained with polyclonal antibody appears as puncta distributed along cell-cell contacts (B, arrowheads) or is localized intracellularly in perinuclear regions (B, arrows). Cx43 detection with monoclonal antibody is restricted to only a few puncta (C). (D,E) In the same field double-labeled with both antibodies, detection of Cx43 puncta at the periphery of some cells with polyclonal antibody (D, arrows) is occasionally accompanied by detection with monoclonal antibody (E, arrows). Scale bar: A, 50 μm; B,C, 45 μm; D,E, 22 μm.

Fig. 3. Western blots showing selective recognition of the 41 kDa dephosphorylated form of Cx43 by monoclonal anti-Cx43 antibody 13-8300 in extracts of cultured canine tracheal

smooth muscle cells (TSM). Samples of TSM cell cultures (20 μg/lane) harvested in the presence of phosphatase inhibitors (10 mM sodium fluoride and 1 mM sodium orthovanadate) (lane 1 and 3) or microwaved prior to extraction in the absence of phosphatase inhibitors (lanes 2 and 4) were probed with either antibody 18A (lanes 1 and 2) or monoclonal antibody 13-8300 (lanes 3 and 4).

Fig. 4. Immunofluorescence labeling for Cx43 in cultures of tracheal smooth muscle cells. (A) Representative phase contrast (different form B,C) showing the appearance of confluent tracheal myocytes. (B,C) The same field in a culture double-labeled with polyclonal antibody 18A (B) and monoclonal antibody 13-8300 (C). Both antibodies exhibit labeling of corresponding intracellular structures having a dispersed annular appearance (arrows). Polyclonal antibody also occasionally reveals a punctate distribution of Cx43 at the periphery of cells (B, arrowheads), which remains undetectable with monoclonal antibody (C, arrowheads). Scale bar: A, 30 μm; B,C, 18 μm.

Fig. 5. Immunoelectron microscopy of cultured smooth muscle cells labeled with anti-Cx43 antibodies 18A (A,C,D,J) and 13-8300 (B,E-I). (A,B) Labeling is seen associated with the ER (A, arrows) and within cytoplasmic inclusions (B, arrowheads). (C,D) Labeling with antibody 18A is present at typical gap junctions (arrows) between adjacent smooth muscle cell bodies (smc) and processes (p). (E-G) Labeling with antibody 13-8300 is absent at a gap junction (E, arrow, magnified in F) between adjacent cell bodies (smc), but is present at a gap junction (G, arrow) between two processes (p). (H) Annular gap junctional profiles (H, arrows) display staining (H, arrowheads) with antibody 13-8300. (I) At higher magnification, the junctional profiles from (H) can be seen to display intermittent staining (arrows), uniform labeling (arrowheads) or no immunoreaction (small arrow). (J) An annular gap junction (arrows) exhibits immunostaining with antibody 18A. Scale bar: A-C,H, 500 nm; D, 90 nm; E, 840 nm; F, 60 nm; G, 80 nm; I, 120 nm; J, 120 nm.

Fig. 6. Immunogold labeling of Cx43 at gap junctions in Cl-9 cells with rabbit polyclonal antibody 18A and mouse monoclonal antibody 13-8300. (A) Plasma membrane gap junction labeled by pre-embedding method with monoclonal anti-Cx43 antibody 13-8300 and goat anti-mouse IgG(Fc) 5 nm gold particles. (B) Plasma membrane gap junction labeled by pre-embedding methods with monoclonal antibody 13-8300 and goat anti-mouse IgG(Fc) 5 nm gold particles and followed by post-embedding methods with rabbit affinity-purified anti-Cx43 18A antibody and goat anti-rabbit.

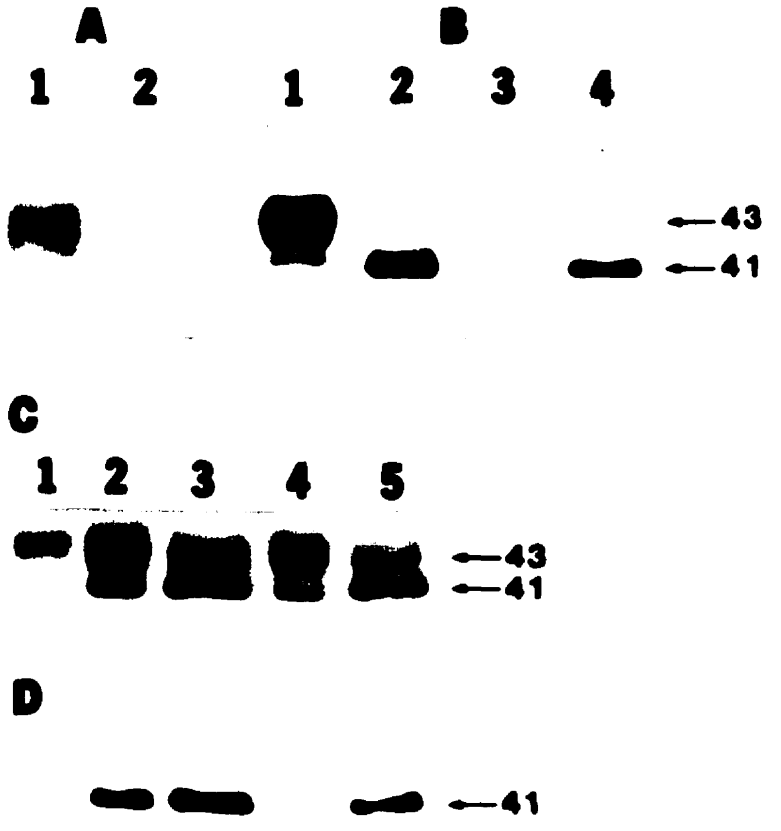

Fig. 1

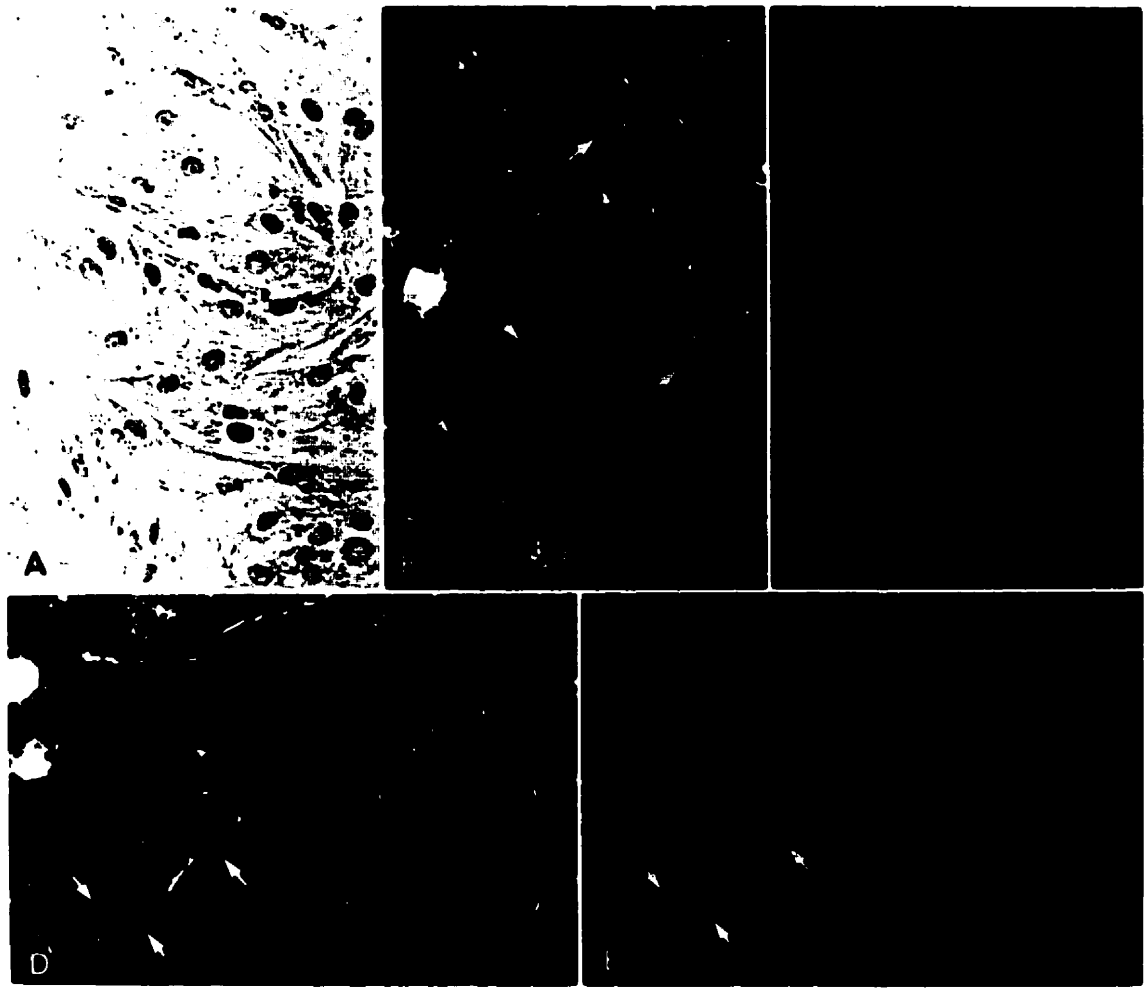

Fig. 2

Fig. 3

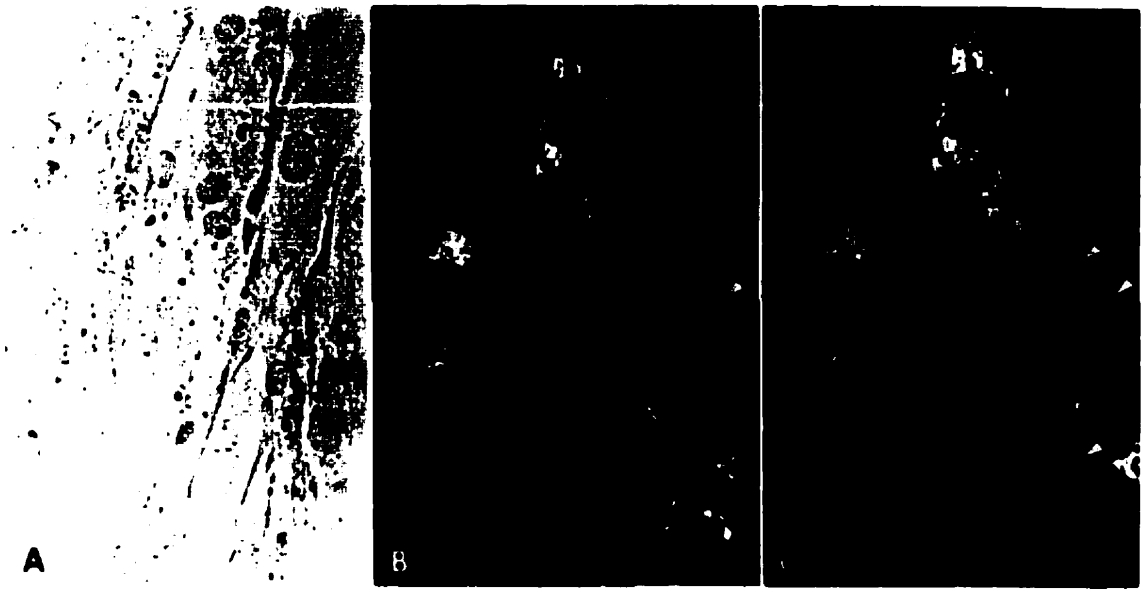

Fig. 4

Fig. 5

Fig. 6

Part III

Immunorecognition, Ultrastructure and Phosphorylation Status of Astrocytic Gap Junctions and Connexin43 in Rat Brain After Cerebral Focal Ischemia

Li, W. E. I., Ochalski, P. A. Y., Hertzberg, E. L. and Nagy, J. I.

European Journal of Neuroscience, 10 (1998) 2444-2463

Abstract

Gap junctions between astrocytes support a functional syncytium that is thought to play an important role in neural homeostasis. In order to investigate regulation of this syncytium and of connexin43 (Cx43), a principal astrocytic gap junction protein, we determined the sequelae of gap junction and Cx43 disposition in a rat cerebral focal ischemia model with various ischemia/reperfusion times using sequence-specific anti-Cx43 antibodies (designated 13-8300, 18A, 16A and 71-0700) that exhibit differential recognition of Cx43, perhaps reflecting functional aspects of gap junctions. Antibody 13-8300 specifically detects only an unphosphorylated form of Cx43 in both Western blots and tissue sections. In hypothalamus after brief (15 min) ischemic injury, Cx43 at intact gap junctions undergoes dephosphorylation, accompanied by reduced epitope recognition by antibodies 16A and 71-0700. Tissue examined 24 hr after reperfusion showed that these effects were reversible. Astrocytic gap junction internalization occurring 1 hr after ischemia was accompanied by decreased immunodetection with 13-8300. At this time, gap junctions were absent in the ischemic core, coinciding with a loss of Cx43 recognition with 18A and 13-8300, but elevated labeling of internalized Cx43 with 16A and 71-0700. Unphosphorylated Cx43 persisted at intact gap junctions confined to a thin corridor at the ischemic penumbra which contained presumptive apoptotic cell profiles. Similar results were obtained in ischemic striatum and cerebral cortex, though with a delayed time course that depended on the severity of the ischemic insult. These results demonstrate that astrocytic Cx43 epitope masking, dephosphorylation and cellular redistribution occur after ischemic brain injury, proceed as a temporally and spatially ordered sequence of events and culminate in differential patterns of Cx43 modification and sequestration at the lesion center and periphery. These observations suggest an attempt by astrocytes in the vicinity of injury to remodel the junctional syncytium according to altered tissue homeostatic requirements.

Introduction

Gap junctions are assemblies of intercellular channels formed by hemichannels (connexons) from each of two apposing cell membranes. A connexon consists of a hexamer of gap junction proteins termed connexins, of which more than a dozen family members have been identified. Far from being passive conduits for the intercellular movement of substances, gap junction channels are functionally responsive to diverse regulatory stimuli (White et al., 1995a; Wolburg and Rohlmann, 1995; Bruzzone et al., 1996). Connexin phosphorylation is one mechanism whereby regulatory control is exerted at a variety of levels in what appears to be kinase-, connexin-, and in some cases, cell-specific manner (Bruzzone et al., 1996; Goodenough et al., 1996). For example, numerous studies indicate that phosphorylation of connexin43 (Cx43) affects such key processes as gap junction assembly and regulation of channel permeability (Musil et al., 1990; Musil and Goodenough, 1991; Moreno et al., 1994; Kwak et al., 1995a; Laird, 1996). Several serine residues in Cx43 have been identified as substrates or potential substrates for various protein kinases (Saez et al., 1993, 1997; Lau et al., 1996; Warn-Cramer et al., 1996) and tyrosine phosphorylation of Cx43 leads to disruption of gap junctional communication in src-transfected cells (Lau et al., 1996). Further, changes in Cx43 phosphorylation status may accompany Cx43 internalization and degradation (Oh et al., 1991; Hu et al., 1995; Guan et al., 1996; Guan and Ruch, 1996).

Astrocytes in the central nervous system (CNS) are extensively coupled via gap junctions containing high levels of Cx43 (Yamamoto et al., 1990a,b; Wolburg and Rohlmann, 1995; Giaume and McCarthy, 1996; Ochalski et al., 1997). We have shown recently that the newest member of the connexin family to be identified, namely connexin30 (Cx30) (Dahl et al., 1996), is also expressed by astrocytes and is co-localized with Cx43 at astrocytic gap junctions (Nagy et al., 1997a). The ubiquity of interastrocytic gap junctions, and the spatial heterogeneity of their distribution and of Cx43 expression in the CNS, support the idea that a functional syncytium of glial cells permeates parenchymal tissue, selectively linking or compartmentalizing various brain regions with respect to flow of ions and small molecules (Mugnaini, 1986). The role of this glial syncytium, however, has been most discussed in

terms of K^+ spatial buffering, wherein gap junctions are thought to provide pathways for dispersal of K^+ accumulated by astrocytes during increased neuronal activity (Orkand et al., 1966; Newman, 1985; Walz, 1989). That this syncytium is regulated, in part, by neuronal/glial interactions is suggested by in vitro studies demonstrating that astrocytic gap junctional communication can be altered by substances released by neurons including K^+, noradrenaline and glutamate, and by increased neuronal activity (Giaume et al., 1991b; Enkvist and McCarthy, 1994; Marrero and Orkand, 1996; Muller et al., 1996).

Characterization of Cx43 expression and localization in response to chemically or surgically induced neuronal injury in vivo has also revealed morphologic alterations in the organization of astrocytic gap junctions (Alonso and Privat, 1993; Rohlmann et al., 1993, 1994; Laskawi et al., 1997; Wolburg and Rohlmann, 1995). We have shown, for example, that astrocytes in brain and spinal cord respond to kainic acid-, NMDA- or trauma-induced neuronal damage by internalizing and degrading their gap junctions with sequestration of Cx43 in multivesicular clusters of putative autophagic origin (Vukelic et al., 1991; Hossain et al., 1994b; Ochalski et al., 1995; Sawchuk et al.,1995; Theriault et al., 1997). We have also reported that striatal and hippocampal astrocytes respond to global ischemia by redistributing Cx43 in a manner apparently dependent upon the severity of neuronal damage or loss (Hossain et al., 1994a). These responses were accompanied by masking and unmasking of certain Cx43 epitopes reflected by altered Cx43 detectability with various antibodies (Hossain et al., 1994a,b; Ochalski et al., 1995). The role of Cx43 phosphorylation in these events and in relation to junctional coupling within the glial syncytium has received little attention. However, Cx43 is multiply phosphorylated in brain (Hossain et al., 1994c), and activation of various kinase pathways that could potentially act on Cx43, as in peripheral systems, has been demonstrated in astrocytes after various treatments (Kasuya et al., 1994; Bhat et al., 1995; Chisamore et al., 1996).

The present investigation was undertaken to further understanding of the way in which gap junctional communication contributes to astrocytic-dependent homeostatic mechanisms in normal and damaged CNS. To this end, we utilized a focal ischemia model employing

various ischemia and reperfusion times in conjunction with light and electron microscopical immunohistochemistry using a panel of anti-Cx43 antibodies. The focal ischemia model allowed observations of progressive modification of Cx43 and astrocytic gap junctions over a reproducible gradual transition from massive cellular damage at the lesion center to relatively less or undamaged tissue at penumbral regions and beyond. In addition, an anti-Cx43 antibody that recognizes exclusively an unphosphorylated form of Cx43 (Nagy et al., 1997a) was utilized to address Cx43 phosphorylation state in the ischemia model. Some of the present results have been reported in abstract form (Li et al., 1996; Nagy et al., 1996b).

Materials and methods

Antibodies

Four anti-Cx43 antibodies were used in this study. Two rabbit polyclonal antibodies, designated 18A and 16A, were generated against peptides corresponding to amino acids 346-363 and 241-260 of the Cx43 sequence, respectively (Beyer et al., 1987). We have used these antibodies extensively in previous studies where their Cx43 specificity in immunohistochemical and Western blotting protocols of normal and lesioned brain as well as in normal heart tissue has been well documented (Yamamoto et al., 1990a,b; Nagy et al., 1992; Hossain et al., 1994a,b,c; Ochalski et, al., 1995, 1997). Two commercially available (Zymed Laboratories Inc.) anti-Cx43 antibodies used included a rabbit polyclonal anti-peptide antibody designated 71-0700 and a mouse monoclonal antibody designated 13-8300. The specificity of these antibodies for Cx43 has been demonstrated by the manufacturer as well as in the present study. The region of Cx43 recognized by each antibody, with respect to the proposed topological arrangement of the protein, is shown in Fig. 1.

Focal cerebral ischemia

A total of 99 male Sprague Dawley rats weighing 280-330 g were used in this study. Ninety animals were subjected to focal cerebral ischemia and an additional 9 served as normal, sham-surgery or anesthesia controls at various survival times (0 hr, 48 hr, 7 days). Cerebral

ischemia was induced by transient occlusion of the middle cerebral artery (MCA) with a 3-0 surgical nylon monofilament suture advanced to the level of the MCA after insertion into the internal carotid artery (Koizumi et al., 1986; Longa et al. 1989). Anesthesia was induced with 5% halothane, and maintained intratracheally with 1-2% halothane in 70% oxygen/30% nitrous oxide. Cranial temperature was monitored with a thermocouple microprobe and maintained at 37.5 °C. The tail artery was cannulated for monitoring blood pressure and for measurement of blood pH, pO2, and pCO2 during surgery and induction of ischemia. Blood pressure was maintained at 65 mmHg and blood glucose levels at less than 8 mM during ischemia induction. In some experiments, the MCA was occluded for 15 min followed by no reperfusion recovery or by recovery periods of 1 or 24 hr. In others, the MCA was occluded for 1 hr followed by no reperfusion recovery or by reperfusion survival times of 1, 6, 12, 24 or 48 hr, and 7, 14 or 21 days. Each of these time parameters included at least three rats. Animals at short survival times (15 min, 1 hr) were perfused with tissue fixative as described below while they were still under halothane anesthesia. Those at longer survival times were given chloral hydrate anesthesia prior to perfuion. Animals exhibiting evidence of ischemia-induced brain hemorrhage at the time of dissection were excluded from analysis.

Cranial microwave irradiation

We have previously shown that Cx43 in brain is largely phosphorylated and undergoes rapid post-mortem dephosphorylation within minutes of tissue dissection (Hossain et al., 1994c). Our studies of its phosphorylation state in CNS thus required procedures that effectively eliminated this artifactual dephosphorylation and preserved resident forms of Cx43 in normal as well as ischemic brain. As in studies elsewhere (Hossain et al., 1994c), this was accomplished in experiments where adult male Sprague-Dawley rats weighing 270-320 g were killed by focused cranial microwave irradiation using a Cober Metabolic Vivostat (model S6B) equipped with a 10-kW power upgrade. Brains from these rats were designated

"microwaved tissue". To control for possible effects of microwave exposure and consequent rapid heating of tissue, some animals carcasses were subjected to focused cranial microwave irradiation 15 min post-mortem. Brains from these animals, where Cx43 is allowed to undergo endogenous dephosphorylation, were designated "control tissue". The microwave procedure has been approved by the Canada Council on Animal Care and has been endorsed by the American Veterinary Medical Association. All animals in the present study were obtained from the local Central Animal Care Services and utilized according to approved protocols by the local Animal Care Committee with minimization of stress to, and numbers of, animals used.

Western Blots

For biochemical studies, control and microwaved brains were excised and hypothalamus, striatum and temporal cerebral cortex from both the ischemic and contralateral sides removed and immediately frozen. Some animals were injected in the tail artery with 1.0 ml of 0.5% Evan's blue dye in order to locate ischemic areas when damage at short survival times was not evident; ischemic areas are stained blue due to blood-brain barrier disruption. Tissue was homogenized in 1 mM bicarbonate buffer (pH 7.4) containing 1 mM phenylmethylsulfonyl fluoride and 1 μg/ml each of leupeptin and pepstatin. In some experiments, homogenization buffer also contained the phosphatase inhibitors sodium fluoride and sodium orthovanadate at concentrations of 10 mM and 1 mM, respectively. Total homogenate protein was determined using a BIO-RAD assay kit. As previously described, samples for Western blotting, were heated in loading buffer for 3.5 min in boiling water (Hossain et al., 1994c), separated by sodium dodecyl sulfate polyacrylamide gel (9%) electrophoresis (SDS-PAGE) and electrophoretically transferred onto polyvinylinene difluoride membranes in buffer consisting of 25 mM Tris, 192 mM glycine, 0.05% SDS and 20% (v/v) methanol. Membranes were blocked for 2 hr at room temperature in TBS (20 mM Tris, pH 7.4 and 150 mM NaCl) containing 0.2% Tween 20 (TBS-T) and 5% skim milk

powder then incubated for 3 hr at room temperature in TBS-T containing 1% skim milk powder and one of the following anti-Cx43 antibodies: 18A diluted 1:200,000; 71-0700 diluted 1:1,000; 13-8300 diluted 1:750. Membranes were washed 4 x 10 min in TBS-T then incubated for 1 hr at room temperature in TBS-T containing 1% skim milk powder and one of the following secondary antisera (Sigma): horseradish peroxidase-conjugated goat anti-rabbit IgG diluted 1:5,000 for detection of 18A and 17-0700 or horseradish peroxidase-conjugated goat anti-mouse IgG diluted 1:3,000 for detection of 13-8300. Membranes were washed as above and immunoreactive bands detected by enhanced chemiluminescence (Amersham).

Immunohistochemistry

Animals were perfused transcardially with 0.9% saline containing 0.05 M sodium phosphate, 1 unit/ml heparin and 0.1% sodium nitrite, then with 0.1 M sodium phosphate buffer (PB, pH 7.4) containing 4% paraformaldehyde, which was delivered according to a pH change protocol involving perfusion of fixative at pH 7.5, followed by the same fixative at pH 9.0 as previously described (Nagy et al., 1992). Brains were removed, post-fixed for 12 to 16 hr, then either cryoprotected in 0.05 M sodium phosphate (pH 7.4) containing 25% sucrose and 10% glycerol for sectioning on a sliding microtome in LM studies or stored in PB prior to sectioning on a vibrating microtome for EM studies. Microwaved brains were immersion-fixed overnight in PB containing 4% paraformaldehyde, cryoprotected as above and sectioned on a sliding microtome. Sections were cut at a thickness of 20-30 μm and collected free floating in PB containing 0.9% saline (PBS). For peroxidase-anti-peroxidase (PAP) labeling, sections were treated for 30 to 60 min with 0.5% hydrogen peroxide in PBS to eliminate endogenous peroxidase activity and then incubated for 24-48 hr with antibody 18A, 16A, 71-0700 or 13-8300 diluted 1:2,000, 1:1,000, 1:500 or 1:500, respectively, in PBS containing 0.3% Triton X-100 (PBST) and 2% normal serum. Following a 1 hr wash in PBST, sections were incubated for 1.5 hr with appropriate secondary antibody diluted in

PBST (goat anti-rabbit IgG, 1:100; horse anti-mouse IgG, 1:50), washed for 1 hr in PBST, incubated in appropriate tertiary antibody (rabbit PAP or clonoPAP each diluted 1:500 in PBST), washed as above and incubated with 0.00005% H_2O_2 and 0.02% 3,3-diaminobenzidine (DAB) in 50 mM Tris-HCl buffer, pH 7.4, for 8 to 15 min. Sections were mounted onto slides from a gelatin/alcohol solution, dehydrated in alcohol, cleared in Histoclear and coverslipped with Lipshaw mounting medium. Some sections were separately stained by hematoxylin and eosin (H&E) and some sections processed by the PAP method were counterstained by H&E.

In order to compare Cx43 localization with antibodies 18A, 16A and 13-8300 in ischemic tissues, some sections through ischemic hypothalamus were taken for triple immunostaining with these antibodies. Immunolabeling with 16A by the PAP method was conducted as described above. Sections were then sequentially processed for immunofluorescence by incubation, first with 18A followed by detection with Cy2-conjugated goat anti-rabbit secondary antibody and then by incubation with 13-8300, followed by detection with Cy3-conjugated donkey anti-mouse secondary antibody. Sections were washed in 50 mM Tris-HCl buffer, pH 7.4, mounted onto slides from the same buffer and coverslipped with antifade medium.

For EM, 30 μm vibratome sections were processed by the PAP method described above, except that Triton X-100 was replaced with 0.1% Photo-Flo 200 (Kodak) for all incubations and washes. Following the DAB reaction, sections were rinsed in PBS, osmicated, dehydrated and embedded as described (Yamamoto et al., 1990a,b). Areas of interest were excised, glued onto resin blocks and ultrathin sections were collected on 400 mesh copper grids, counterstained for 1-2 min with lead citrate and photographed on a Philips 201 electron microscope.

Results

Selective antibody recognition of dephosphorylated Cx43

In order to demonstrate selective antibody recognition of non-phosphorylated Cx43, Western blots of samples were prepared from control brains in which Cx43 undergoes rapid post-mortem dephosphorylation (Hossain et al., 1994c), and compared with those from brains in which dephosphorylation was prevented by microwave irradiation. The occurrence of post-mortem dephosphorylation and the differing mobilities of phosphorylated and dephosphorylated forms of Cx43 is illustrated in Fig. 2. Homogenates of microwaved (lane 1, Fig. 2A, B) and control (lane 2, Fig. 2A, B) brain were probed with antibodies (18A and 71-0700) that detect all forms of Cx43. After microwave treatment, there is a prevalence of the phosphorylated forms (lane 1), migrating at a relative molecular weight (Mr) of about 43 kDa, while only the faster migrating 41 kDa form is detectable in controls brains (lane 2). At varying protein levels loaded (1-20 μg), antibody 71-0700 detects the 41 kDa form at the lowest level of protein examined (Fig. 2A, lane 3) and begins to detect phosphorylated forms at 3 μg (Fig. 2B, lane 4). No phosphorylated forms were detected by this antibody at a protein loading of up to 20 μg from control brains (Fig. 2A, lane 6), and very little dephosphorylated Cx43 was evident in microwaved brain loaded with this amount (Fig. 2B, lane 6). The same samples were used to determine the relative sensitivity and selectivity of detection of the two Cx43 forms by monoclonal antibody 13-8300. In lanes loaded with homogenates of control brain containing largely the 41 kDa form (Fig. 2A, lanes 7-11), antibody 13-8300 detection of this form was not seen at 0.1 μg protein loading (lane 7), evident at 0.3 μg (lane 8), and robust at 1.0 μg (lane 9). In contrast, antibody 13-8300 failed to bind to the 43 kDa phosphorylated form of Cx43 which was present in abundance in homogenates from microwaved brain (Fig. 2B, lanes 7-10), even at 20 μg of protein loading (lane 10). This antibody did detect minor levels of the 41 kDa unphosphorylated form of Cx43 that was present (lanes 9 and 10), as did the polyclonal antibodies (Fig. 2B, lanes 1, 5 and 6).

The above results were confirmed in Western blots of heart homogenates where 13-8300 only recognized the 41 kDa form of Cx43 (Nagy et al., 1997b), despite the much greater

abundance of the phosphorylated 43 kDa species in this tissue. Furthermore, treatment of cardiac gap junction membrane fractions with alkaline phosphatase was found to shift the mobility of Cx43 from 43 kDa to the 41 kDa form recognized by antibody 13-8300, confirming that differential migration of Cx43 is due to its phosphorylation state and that 13-8300 binds only to unphosphorylated Cx43.

Sections of brain and heart were processed for immunostaining by the PAP method to determine whether antibody 13-8300 exhibited the same selectivity for unphosphorylated Cx43 as it did on Western blots. Under post-mortem conditions where Cx43 in brain undergoes rapid dephosphorylation, 13-8300 produced punctate immunostaining in most brain areas including cerebral cortex (Fig. 3A, B). This staining was typical of the patterns and relative densities seen with antibodies 18A (Yamamoto et al., 1990a) as well as 71-0700 (not shown) and serves as a positive control for 13-8300 detection of dephosphorylated Cx43 in paraformaldehyde-fixed tissue. After prevention of dephosphorylation by microwave irradiation, as confirmed by Western blot analysis, immunostaining for Cx43 with antibody 13-8300 was virtually absent in sections of brain, as shown in cerebral cortex (Fig. 3C). In heart, antibody 71-0700 labeled intercalated discs and the lateral margins of cells giving rise to puncta (Fig. 3D) similar to those observed with antibody 18A (Yamamoto et al., 1990b; Kardami et al., 1991). Consistent with the predominance of phosphorylated Cx43 in heart and the inability of antibody 13-8300 to recognize this form in Western blots, no Cx43 detection was observed with this antibody in cardiac tissue (Fig. 3E).

Western blots of Cx43 after focal cerebral ischemia

Western blots were conducted to determine the phosphorylation state of Cx43 in ischemic compared with control brain regions. Blots were probed with 18A for detection of both phosphorylated and dephosphorylated forms or with 13-8300 for selective detection of the latter. Six animals subject to unilateral focal ischemia were killed by microwave treatment in order to prevent artifactual post-mortem Cx43 dephosphorylation, followed by dissection of

ischemic and contralateral control regions of brain. As shown in Figure 4, contralateral control tissues dissected after 15 min (Fig. 4A) and 1 hr (Fig. 4B) of MCA occlusion and probed with antibody 18A contained only 43 kDa phosphorylated forms of Cx43. These included hypothalamus (A, B, lane 1), striatum (A, B, lane 3) and cerebral cortex (A, B, lane 5). In contrast, ischemic hypothalamus (A, B, lane 2), striatum (A, B, lane 4) and cerebral cortex (A, B, lane 6) contained both phosphorylated as well as the faster migrating dephosphorylated 41 kDa form of Cx43, although the latter was barely detectable in hypothalamus after 1 hr MCA occlusion. These observations were confirmed in blots of the same tissues probed with antibody 13-8300 and, for Cx43 mobility comparisons, included with lanes of non-microwaved (Fig. 4C, D, lane 1) and microwaved (Fig. 4C, D, lane 2) non-ischemic brains probed with antibody 18A. Thus, 15 min (Fig. 4C) and 1 hr (Fig. 4D) after MCA occlusion, ischemic hypothalamus (C, D, lane 4), striatum (C, D, lane 6) and cerebral cortex (C, D, lane 8) all contained the dephosphorylated form of Cx43. None of the same control brain regions exhibited this form (lanes 3, 5 and 7, respectively), nor were the phosphorylated forms in any of these samples recognized by antibody 13-8300. Comparisons of Cx43 detection with antibody 13-8300 in 15 min and 1 hr ischemic tissue show a reduction of the 41 kDa form in hypothalamus and an increase of this form in the cerebral cortex after longer MCA occlusion.

LM immunohistochemistry of Cx43 after focal cerebral ischemia

Histological features of ischemic tissue assessed in H&E and glial fibrillary acidic protein stained sections (not shown) were similar to those previously reported (Chen et al., 1993; Garcia et al., 1993). In particular, the onset of identifiable ischemic damage after focal ischemia occurred first in the hypothalamus, then in striatum followed by cerebral cortex. This temporal sequence paralleled changes in Cx43-ir which were qualitatively similar in the three areas. Longer periods of ischemia (3 hr of MCA occlusion) produced a greater severity of injury with more rapid onset in the striatum and cortex, but had similar effects on Cx43-ir as seen after 1 hr occlusion. Following 15 min of MCA occlusion with no survival,

no damage was evident in H&E stained sections. The development of ischemic injury in hypothalamus and cortex was analyzed in animals surviving for different reperfusion periods after 1 hr MCA occlusion, up to a survival time of 48 hr.

Our initial immunohistochemical tests of antibody 13-8300 labeling in microwaved ischemic brain confirmed that similar results can be obtained using perfusion-fixed ischemic tissue, allowing use of the latter in anatomical investigations. In brain sections from ischemic animals, antibodies 18A (Fig. 5A) and 16A (Fig. 5B) produced Cx43-ir on the control non-ischemic side similar to that reported in normal rat brain. This consisted of fine puncta, more robustly stained with the former than latter antibody (Yamamoto et al., 1990b, Hossain et al., 1994a). After 15 min MCA occlusion without survival, 18A-ir (Fig. 5A) and 16A-ir (Fig. 5B) were uniformly reduced in ischemic hypothalamus, though less so around vascular elements (not shown). 13-8300-ir was faint in normal brain and in control sides of all ischemic brains as shown in hypothalamus (Fig. 5C, F; left side). In contrast, 13-8300-ir was greatly elevated (Fig. 5C) in the ischemic hypothalamic area. In control (Fig. 5G) and ischemic sides (Fig. 5H), 13-8300-ir was punctate like that seen in normal tissue with other antibodies. It should be noted that the presence of some minor Cx43-ir with antibody 13-8300 in control hypothalamus (Fig. 5G), compared with its total absence in microwaved brains (e.g. Fig. 3C), indicates that perfusion fixation largely prevents, but does not totally eliminate, the occurrence of post-mortem Cx43 dephosphorylation. Cx43-ir in hypothalamus appeared normal in animals subjected to 15 min ischemia followed by 24 hr survival (not shown).

After 1 hr MCA occlusion without survival, 18A-ir was further reduced or absent in large areas of the hypothalamus compared to that seen after 15 min of ischemia, and was slightly increased outside the ischemic periphery (Fig. 5D). Staining that remained in central ischemic areas was localized mostly to astrocyte cell bodies. Such somal staining with this antibody was never seen in control brain regions. Patches of intense, punctate 16A-ir were distributed in central ischemic areas (Fig. 5E) corresponding to those displaying 18A-ir. These patches were surrounded by areas devoid of staining with antibody 16A. In contrast to

results after 15 min of ischemia, 13-8300-ir was absent in the ischemic center and reduced in the surrounding area (Fig. 5F) after 1 hr of ischemia.

After 1 hr MCA occlusion followed by 6 hr survival, 18A-ir in hypothalamus was virtually absent in the ischemic center and clearly elevated beyond the lesion periphery (Fig. 6A). 16A-ir was elevated in the ischemic center (Fig. 6B), as was staining with antibody 71-0700 (Fig. 6C); no staining with 13-8300 was evident in this area. However, a rim surrounding the ischemic core, corresponding to the borders outlined by 18A-depleted and 16A-intensified staining, was labeled with 13-8300 (Fig. 6D). After 1 hr MCA occlusion followed by 12 hr reperfusion survival, Cx43-ir in hypothalamus was much the same as at 6 hr reperfusion, except that regions of intensified 16A-ir (Fig. 6F) occasionally overlapped those with intensified 18A-ir (Fig. 6E). This was seen at earlier survival times, but most prominently at 12 hr.

Details of Cx43-ir at 6-24 hr survival are shown in Figure 7. Four distinct zones of labeling were evident with 18A. i) Increased 18A-ir consisting of fine puncta in neuropil and surrounding neuronal cell bodies occurred just outside the ischemic region in what appeared to be relatively normal tissue (Fig. 7A, left side). ii) Adjacent to this was a zone of reduced staining with sparsely distributed puncta. iii) Occasionally sandwiched between this zone and the ischemic center or extending further into the center were dense patches of coarse puncta (Fig. 7A). iv) The ischemic center was largely devoid of 18A-ir (Fig. 7A, right side). In contrast, all areas of reduced, coarse or depleted 18A-ir contained dense 16A-ir (Fig. 7B) and 71-0700-ir (Fig. 7C), indicating the persistence of Cx43 in these regions. Comparisons of alternate sections suggested that staining with 13-8300 at the ischemic rim (Fig. 7D) was located adjacent to 18A-ir circumscribing the lesion and overlapped the zone of reduced 18A-ir (Fig. 7A). This zone contained numerous cells with segmented nuclei (Fig. 7E, F) suggestive of apoptosis. Such cells were less frequently encountered within the ischemic center where neuron loss was almost complete and any remaining cells appeared to be necrotic.

The relative distribution of staining with the various Cx43 antibodies in hypothalamus after 1 hr MCA occlusion and 1 hr survival was confirmed in sections triple-labeled by immuno-fluorescence and PAP (Fig. 8). The shell of reduced 18A-ir between peripheral staining and the ischemic unlabelled ischemic core (Fig. 8A) corresponded very nearly to the band of intense 13-8300-ir circumscribing the ischemic center (Fig. 8B). Dense labeling with 16A was localized inside the ischemic core and extended to, but did not overlap, the band of 13-8300-ir (Fig. 8C). Interference of labeling by 16A with either of the other two antibodies was not a concern since neither 18A or 13-8300 produced labeling in the ischemic center when used alone. Control experiments involving reversal of the sequence of labeling with 18A and 13-8300 did, however, indicate reduced labeling with whichever was applied last. Thus, it became clear that 13-8300-ir could occur in regions where some staining with 18A was still evident, rather than exclusively in regions where it was absent.

Cx43-ir in normal cerebral cortex was punctate similar to that seen in the hypothalamus. In temporal cortex, 15 min MCA occlusion with no survival produced only a light increase in 13-8300-ir. After 1 hr ischemia followed by 1 hr survival, 18A-ir was diminished in patches (Fig. 9B) compared with the more uniform staining it produced on the contralateral control side (Fig. 9A). No visible alterations in cortical 16A-ir were seen in these animals (not shown). Compared with the absence of 13-8300-ir in microwaved control brains (Fig. 3C), this antibody produced patches of fine punctate labeling in ischemic cortex of animals killed by cranial microwave irradiation (Fig. 9C). This microwave treatment was used as an extra measure to prevent post-mortem Cx43 dephosphorylation, but was found to be unnecessary since normal cerebral cortex (Fig. 9G), like the control side of hypothalamus (Fig. 5F, G), was devoid of 13-8300-ir after perfusion fixation. After 1 hr MCA occlusion followed by 24 hr survival, 18A-ir was prominent in central ischemic areas and often conspicuously absent at the periphery (Fig. 9D). In contrast, 16A-ir was distributed in the whole of the ischemic area (Fig. 9E), while regions surrounding, as well as portions within, this area exhibited 13-8300-ir (Fig. 9F). Preadsorption of 13-8300 with peptide antigen eliminated the immunostaining seen in cortex after 1 hr ischemia (Fig. 9H).

EM immunohistochemistry of Cx43 after focal cerebral ischemia

In normal hypothalamus, 18A labeled astrocytic gap junctions as well as non-junctional membranes and some cytoplasmic elements near stained junctions (Fig. 10A), as previously described (Yamamoto et. al.,1990a,b). After 15 min ischemia without survival, swelling of astrocyte processes was evident in ischemic regions, coincident with an overall reduction of 18A-ir that included diminished labeling intensity of astrocytic gap junctions (Fig. 10B). After 1 hr MCA occlusion with 1 hr survival, ischemic tissues displayed increased swelling and disruption of astrocytic elements at the lesion center, as well as a general absence of 18A-ir (Fig. 10C), except in patches corresponding to those seen by LM. Labeling in these patches was localized to multivesicular clusters, plasma membrane surrounding edematous astrocytic processes and cytoplasmic elements within these processes (Fig. 10D). Tissue disruption increased with increasing post-ischemic survival times (12 and 24 hr). 18A-ir was rarely seen within the ischemic area at 12 hr survival and was virtually absent at 24 hr survival (not shown). No labeled or unlabelled astrocytic gap junctions were seen in the ischemic core following 1 hr MCA occlusion, at any survival time. At 1, 12 and 24 hr post-ischemia, regions that circumscribed the ischemic area contained unlabelled and asymmetrically-labeled gap junctions between what appear to be astrocytic processes (Fig. 10E), as well as stained annular gap junctional structures (Fig. 10F). These structures were never observed in normal brain. Such labeled annular profiles have been observed at excitotoxic lesion sites in rat brain and may represent internalized gap junctions as previously discussed (Ochalski et al., 1995). The unlabelled and asymmetrically-labeled junctions may indicate the occurrence of some degree of epitope masking with antibody 18A outside the ischemic area, such as seen with this antibody by LM in the ischemic area at shorter survival times.

The low level of 13-8300-ir, seen by LM in control hypothalamus of perfusion-fixed brain, corresponded by EM to sparse labeling of astrocytic processes and their gap junctions. Asymmetrically labeled and unlabelled gap junctions were also seen in this material (Fig.

11A, B), but never in normal material processed with antibodies 18A, 16A or 71-0700. After 15 min MCA occlusion without survival, 13-8300-ir in ischemic hypothalamus was found at all astrocytic gap junctions observed within the ischemic site (Fig. 11C), although labeling intensity was variable, even between gap junctions located in close proximity to each other (Fig. 11D). After 1 hr MCA occlusion, the ischemic area was devoid of 13-8300-ir at survival times of 1 hr (not shown), 12 hr (Fig. 11E) and 24 hr (not shown). At these times, 13-8300-immunoreactive astrocytic gap junctions were observed around the ischemic periphery (Fig. 11F), and 13-8300-ir was occasionally seen in portions of multivesicular clusters in this area (Fig. 11G).

While staining seen in normal hypothalamus with antibodies 16A (not shown) and 71-0700 (Fig 12A) were similar, the latter produced robust cytoplasmic labeling of astrocyte cell bodies (Fig. 12B) uncharacteristic of the former. Staining with both antibodies comprised predominantly astrocytic gap junctions (Fig. 12A, C) and cytoplasmic elements near labeled junctions (Fig. 12C). In 1 hr ischemic hypothalamus, 16A-ir and 71-0700-ir was similar at survival times of 1, 12 and 24 hr, although there was progressive deterioration of ultrastructure at the lesion center. Neither labeled nor unlabelled astrocytic gap junctions were seen within the ischemic core at any survival time and immunoreactivity with both antibodies was confined to multivesicular structures (Fig. 12D) that contained labeled cytoplasmic components, vacuolar elements and membranes that resembled disrupted gap junctions (Fig. 12E).

In cerebral cortex, EM localization of Cx43-ir with all antibodies in normal and ischemic tissue was similar to that seen in hypothalamus. EM observations of 18A-ir and 13-8300-ir after 1 hr MCA occlusion and 24 hr survival are shown in Figure 13. No recognizable astrocytic processes or cell bodies were found at the ischemic center, which was occupied by large regions of electron lucent vacuolar spaces. 18A-ir was seen in a corridor immediately adjacent to the central depleted region and was localized to membranes lining what appear to be astrocytic processes (Fig. 13A, B) and multivesicular clusters (Fig. 13C). These membranes were always non-junctional and were usually relatively intact (Fig. 13B), often

surrounding electron-lucent vacuolar spaces that sometimes contained mitochondria, immunoreactive segments of membrane or small vacuoles (Fig. 13A, B). Membrane-lined vacuolar spaces containing numerous labeled vacuoles formed multivesicular structures which were often seen in apposition to blood vessels (Fig. 13C). Very little 13-8300-ir was detected in the cortical ischemic core at 24 hr after 1 hr MCA occlusion (not shown). Immediately adjacent to regions devoid of staining, numerous edematous processes in neuropil (Fig. 13D) exhibited 13-8300-ir at degenerating (Fig. 13E) or intact (Fig. 13F) gap junctions and along membranes segments contiguous with gap junctions.

Technical considerations

Halothane anesthesia is widely used in animal models of cerebral focal ischemia and was chosen in the present study to allow correlations of our findings with the large body of information available on ischemic damage in these models. Halothane has been shown to influence gap junctional communication in cultured cells (Johnston et al., 1980; Mantz et al., 1993) and we cannot exclude the possibility the this agent, by virtue of its actions on gap junctions, may influence ischemic outcome when administered during ischemia induction. This would be best tested in stroke models utilizing conscious animals during MCA occlusion. It should be noted, however, that halothane anesthesia alone followed by various survival times (0 and 48 hr, 7 days) had no effects on any of the Cx43 parameters we examined; results in these animals were similar to those obtained on the control side of ischemic brains. Further, the rapid Cx43 responses occurring in hours in the hypothalamus were similar to those seen after 1 to 2 days in striatum and cerebral cortex. This tends to dissociate a role of halothane from processes giving rise to neural degeneration and Cx43 related events at these two widely separated survival times.

Discussion

Cx43 phosphorylation state in normal CNS

Connexin phosphorylation is thought to play a significant role in assembly of gap junctions (Musil et al., 1990; 1991; Laird, 1996) and the regulation of the biophysical properties of the cell-cell channels (Moreno et al., 1994; Kwak et al., 1995a). Earlier studies of connexin43, abundant in astrocytic (Yamamoto et al., 1990a,b) and myocardial (Beyer et al., 1987) gap junctions, demonstrated both rapid turnover, with a half-life of about 2-4 hours (Crow et al., 1990; Laird et al., 1991; Musil et al., 1990), as well as differences in the mobility of different phosphorylated forms on SDS-PAGE and Western blots (Musil et al., 1990; Laird et al., 1991; Lau et al., 1992; Hossain et al., 1994c; Moreno et al., 1994). The ability to resolve unphosphorylated Cx43 as the most-rapidly migrating form of Cx43 on SDS-PAGE and Western blots provided a useful assay for demonstration that Cx43 phosphorylation occurs after its biosynthesis, perhaps in the Golgi apparatus (Puranam et al., 1993) or in a compartment associated with insertion of connexon hemichannels into the plasma membrane (Musil et al. 1990; Musil and Goodenough, 1991). An initially puzzling interpretation of Western blots of various tissues was that unphosphorylated Cx43 predominated in some tissues, including brain, while it was mostly phosphorylated in others, such as heart (Kadle et al., 1991). The presence of unphosphorylated Cx43 was demonstrated to occur post-mortem (Hossain et al., 1994c) during brain removal, presumably due to activation of an astrocytic phosphatase, and can be largely eliminated by heat treatment following rapid brain excision, by focused microwave irradiation in situ (Hossain et al., 1994c), or by appropriate tissue fixation as shown in the present study.

This dephosphorylation phenomenon and its preventability, along with available data demonstrating that the form of Cx43 with fastest mobility on SDS-PAGE (Mr $\approx$ 41 kDa) is the unphosphorylated form (Musil et al., 1990; Laird et al., 1991; Lau et al., 1992; Hossain et al., 1994c; Moreno et al., 1994), allowed demonstration of specific and sensitive detection of exclusively the 41 kDa dephosphorylated form of astrocytic Cx43 by antibody 13-8300. We have obtained similar selective Cx43 detection in various cell lines and have shown that lack of phosphorylated Cx43 recognition in heart and brain homogenates can be overcome

by alkaline phosphatase treatment (Nagy et al., 1997b). The utility of antibody 13-8300 for immunohistochemical applications is evident from our demonstration of its LM and EM immunolabeling patterns in paraformaldehyde-fixed tissue sections where corresponding Western blots showed the presence of dephosphorylated Cx43 or only the phosphorylated form.

Lack of 13-8300 recognition of phosphorylated forms under normal conditions may well be due to epitope blockade by phosphate groups on residues within the 13-8300 epitope itself, rather than to conformational blockade resulting from protein folding. Indeed, peptide studies have suggested two protein kinase C phosphorylation sites (Ser368 and Ser372) in the sequence of the 13-8300 epitope (aa's 360-376 of Cx43) (Saez et al., 1993, 1997), although it remains to be determined whether these residues are phosphorylated in native Cx43 in situ and, if so, whether kinase C participates in this process. In any case, it is noteworthy that under no conditions in tissues or cultured cells so far examined did 13-8300 detect other than the unphosphorylated 41 kDa form of Cx43, supporting the suggestion that the 13-8300 epitope is an early, if not the first, phosphorylation site of Cx43 during its biogenesis (Nagy et al., 1997b). This is consistent with the absence of astrocytic Cx43 immunolabeling by 13-8300 at sites of synthesis and trafficking such as endoplasmic reticulum and Golgi apparatus, although we cannot exclude the possibility that Cx43 levels at these locations may be below the limits of detection.

Focal ischemia, Cx43 and structural correlates

This study revealed astrocytic responses to ischemic brain injury which include dephosphorylation and serial Cx43 epitope masking, unmasking and removal of gap junctions from cell membranes. The occurrence of similar events in different brain regions suggests that astrocytes respond stereotypically to ischemia in a sequential, programmatic manner. This is supported by our observations that Cx43 staining patterns seen by LM correlated reliably with labeling of particular structures by the various antibodies at the EM level, which in turn correlated well with underlying ultrastructural indicators of progressive

ischemic pathology. The decline of punctate 18A-ir observed by LM after brief ischemia consistently occurred in parallel with the appearance, by EM, of unlabelled and lightly labeled gap junctions. The concomitant dramatic rise in punctate 13-8300-ir invariably corresponded to labeling exclusively of gap junctions. Thus, masking of the 18A and exposure of the unphosphorylated 13-8300 epitopes take place together at intact astrocytic gap junctions when ultrastructural disruption is mild or limited. These events did not necessarily portend internalization or disruption of the affected gap junctions since they were reversible as indicated by a return to normal Cx43 immunostaining patterns at longer survival times. Moreover, there was a temporal dissociation between these events, which occurred within minutes of ischemia in all three brain regions examined, and the varied times of onset of clear ischemic damage in these regions as observed by us here and by others (Chen et al., 1993; Garcia et al., 1993).

The general decline of Cx43-ir with antibodies 18A and 13-8300 at the center of more severe (1 hr MCA occlusion) ischemic lesions corresponds to the disappearance of most resident astrocytic elements and their gap junctions. This was coincident with a shift of the Cx43-ir LM staining pattern from punctate to diffuse, reflecting Cx43 redistribution to a predominantly cytoplasmic localization in some astrocyte somata destined for elimination. Patches of coarse Cx43-ir remaining in areas of severely damaged tissue after ischemia and other forms of CNS injury (Ochalski et al., 1995; Theriault et al., 1997) has consistently corresponded to the emergence of Cx43-ir multivesicular structures intensely labeled with 16A and 71-0700. Thus, in the later stages of severe ischemic pathology before the disappearance of astrocytic elements, intense labeling with antibodies 16A and 71-0700 appears to be indicative, indeed predictive, of Cx43 localization in membranes of multivesicular structures. These structures of autophagic origin constitute a lysosomal pathway for Cx43 degradation in other cells (Naus et al., 1993; Guan and Ruch, 1996; Laird, 1996) and may contribute to this process in astrocytes as previously discussed (Ochalski et al., 1995), although we cannot exclude the additional involvement of a ubiquitin-proteosomal pathway described in other cells (Laing and Beyer, 1995).

Our results indicating differential astrocytic gap junctional responses at the ischemic center and periphery can perhaps be best considered in terms of reports showing necrosis in the ischemic core, in contrast to apoptotic cell death in the ischemic penumbra, which appears to be a prominent feature of infarct expansion (Li et al., 1995a,b). Persistent 18A masking and 13-8300-ir at intact gap junctions in the ischemic penumbra correlated with the presence of presumptive apoptotic profiles, in contrast to intense Cx43 labeling with 18A and 16A in central necrotic areas. In a spinal cord trauma model, we also found that severely damaged or necrotic areas proximal to a compression site displayed intense staining with both antibodies, whereas in distal regions exhibiting a milder degree of injury, Cx43 resequestration was accompanied by 18A masking (Theriault et al., 1997). This suggests, as in the spinal cord model, that specific Cx43 regulatory processes may be operative in areas containing cells undergoing a particular mode of cell death in the ischemic periphery or center.

Alteration of Cx43 epitope recognition and Cx43 dephosphorylation after ischemia

After brief ischemia, Western blot and anatomical results both demonstrate Cx43 dephosphorylation. We found no changes in total Cx43 protein levels or lower Mr fragments of Cx43 species, indicating the absence of bulk Cx43 degradation or epitope pruning by proteases. This is consistent with our conclusion that absence of immunostaining with 18A and presence with 13-8300 in identical tissue areas results from Cx43 masking and unmasking. Epitope pruning is further excluded by the more carboxy-terminal location of the 13-8300 epitope in Cx43 than the 18A epitope, so that pruning of the latter requires loss of the former. After more severe ischemia, the loss of 13-8300-ir at the ischemic center may be due to modifications in other regions of Cx43 in association with its cellular redistribution and internalization, rather than re-phosphorylation of the 13-8300 epitope for which no Western blot evidence was found. The concomitant further reduction of 18A-ir is likely due to epitope blockade by altered Cx43 conformation or protein-protein interactions, rather than phosphate groups since the 18A epitope contains no known phosphorylation

sites. As previously discussed, masking of the 18A epitope is robust and reproducible, is unlikely a fixation artifact since it occurs after in situ transblotting of Cx43 from fresh tissue sections and is eliminated under denaturing Western blot conditions (Hossain et al., 1994a; Sawchuk et al., 1995; Ochalski et al., 1995).

The epitopes recognized by antibodies 16A and 71-0700 (aa's 241-260 and 252-270, respectively) are likely to both contain serine and/or tyrosine phosphorylation sites. Ser255 as well as s279 and s282 downstream to these epitopes may include sites for phosphorylation by mitogen-activated protein kinase (MAP kinase) (Lau et al., 1996; Warn-Cramer et al., 1996). Phosphorylation of one or more of these sites or limited epitope exposure could give rise to the generally weak immunostaining produced by these antibodies in normal tissue. Progressive alterations in Cx43 phosphorylation state at these or nearby epitopes may be responsible for the sequentially reduced staining after brief ischemia and the subsequent intense staining after severe ischemia. While hyperphosphorylation of Cx43 prior to its internalization and/or degradation, followed by its dephosphorylation during gap junction disassembly, has been observed in other systems (Oh et al., 1991; Hu et al., 1995; Guan et al., 1996), we found no evidence for Cx43 hyperphosphorylation during astrocytic gap junction disposal at ischemic sites.

Astrocyte coupling status and turnover of Cx43 after ischemia

Numerous reports indicate that processes or treatments compromising cell viability or homeostasis cause gap junctional uncoupling (Dermietzel et al., 1987; Kleber et al., 1987; Dekker et al., 1996). In the case of astrocytes, the most prominent pathology after mild ischemia is cell body swelling (Chen et al., 1993; Garcia et al., 1993), which can lead to gap junctional uncoupling (Kimelberg and Kettenmann, 1990). By contrast, concentrations of extracellular K^+ and glutamate are elevated at the ischemic site (Walz and Hertz, 1983; Choi and Rothman, 1990) and these agents increase astrocytic coupling, at least in vitro (Enkvist and McCarthy, 1994). Such alterations in coupling may result from changes in Cx43 phosphorylation which clearly affect junctional communication-competence (Bruzzone et

al., 1996; Goodenough et al., 1996; Lau et al., 1996), although the role of phosphorylation at any particular serine residue in the regulation of coupling, and the likelihood of tissue- and cell-type specificity, have not yet been established. Cx43 dephosphorylation increased average single channel conductance and prevented reduction of unitary conductance by 8-bromo-cGMP in cardiomyocytes, but transiently abolished junctional communication in ovarian granulosa cells (Takens-Kwak and Jongsma, 1992; Godwin et al., 1993; Moreno et al., 1994; Kwak et al., 1995a).

Dephosphorylation of Cx43 and increased 13-8300 labeling at astrocytic gap junctions occurs in spinal cord after moderate sciatic nerve stimulation (Nagy et al., 1996b), and may well imply enhanced junctional coupling to facilitate spatial buffering. Similar transient and reversible Cx43 dephosphorylation after brief ischemia suggests that this is not simply a response to pathological conditions, but may be a sensitive indicator of compensatory homeostatic processes, including increased junctional coupling, that are invoked in relatively normal tissue. After more severe ischemia, a well coupled astrocytic syncytium in the penumbra, where Cx43 dephosphorylation persists, may contribute to dissipation of potentially damaging substances thereby reducing secondary damage and expansion of the lesion. Alternatively, if the initial Cx43 dephosphorylation throughout ischemic areas and their persistence at the ischemic rim reflect junctional uncoupling, then this could serve to limit the spread of damage by isolating severely affected areas as previously suggested (Hossain et al., 1994a,b; Ochalski et al., 1995). While these two alternatives remain, the present results may provide a physiological relevant basis for further analyses of astrocytic Cx43 regulation in vitro.

In addition to providing yet another set of data that call for better elucidation of the role(s) of connexin phosphorylation, these observations of the alteration and remodeling of gap junctions over a period of days *in vivo* subsequent to ischemia, or to challenges with excitatory amino acids (Ochalski et al., 1995) are not readily reconciled with available data suggesting rapid turnover of Cx43 *in vitro* (Crow et al., 1990; Laird et al., 1991; Musil et al., 1990). Initial observations indicating rapid turnover of gap junctions arose during analysis of

the loss of gap junctional communication and identifiable gap junctions during a period of 18-24 hours after partial hepatectomy (Yee and Revel, 1978; Yancey et al. 1981; Meyer et al., 1981; Traub et al., 1983). Subsequent studies of primary cultures of hepatocytes demonstrated a similar kinetics of loss of gap junctional coupling with nearly complete loss of the liver gap junction proteins now termed Cx32 and Cx26 (Fujita et al., 1986; Traub et al., 1989; Saez et al., 1989b). These data were also broadly consistent with rapid turnover of liver gap junction proteins measured *in vivo* (Fallon and Goodenough, 1981; Yancey et al., 1981).

The subsequent finding of similarly rapid turnover of Cx43 in primary cell cultures (Laird et al., 1991) or cell lines (Crow et al., 1990; Musil et al., 1990) reinforced the emerging dogma that connexins have short half-lives *in vivo*. While we cannot yet explain functional aspects of dephosphorylation of Cx43, and but speculate on the role of gap junction loss or remodeling in astrocytes, it seems that our data are inconsistent with rapid turnover of Cx43 in astrocytes. The interpretation of these data within the context of a normally rapid turnover of Cx43 would require either a pathophysiological slowing down of turnover of Cx43 in this and other model systems of cerebral insult, or rapid turnover with newly-synthesized Cx43 being directed, as described above, to structures and cytoplasmic locales other than gap junctions in appositional membranes. While these latter events are possible, our results are equally consistent with slow turnover of Cx43, at least in astrocytes, *in vivo*. Experiments directly addressing the turnover of Cx43 *in vivo* would be required to reveal gap junction dynamics in this ischemia model system. Within the more general context of astrocytic gap junctional coupling, such studies should be extended to include analysis of Cx30 (Dahl et al., 1996), which we have recently shown to be and additional connexin expressed in astrocytes (Nagy et al., 1997a, 1999).

Figure legends

Fig. 1. Diagram showing the deduced topological arrangement of Cx43 in the cell membrane in relation to the locations of sequences against which the antibodies used in this study were directed. Antibody 18A, aa 346-363; antibody 16A, aa 241-260; antibody 71-0700; antibody 13-8300; 360-376. Also indicated are putative or identified phosphorylation sites by protein kinase C (*), MAP kinase (#) and tyrosine kinase (+).

Fig. 2. Western blots showing selective recognition of dephosphorylated Cx43 (41 kDa) by monoclonal anti-Cx43 antibody 13-8300. (A, B) Control brains in which post-mortem Cx43 dephosphorylation occurs and microwaved brains in which dephosphorylation is prevented were homogenized in the absence of phosphatase inhibitors, loaded onto lanes at the protein levels indicated (μg) and separated on 9% polyacrylamide gels. Tissue probed in (A) were: lane 1, microwaved brain; lane 2-11, control brain. Tissues probed in (B) were: lane 1 and 3-10, microwaved brain; lane 2, control brain. Lanes in both (A) and (B) were probed with anti-Cx43 antibodies as follows: lanes 1-2, polyclonal antibody 18A; lanes 3-6, polyclonal antibody 71-0700; lanes 7-11, monoclonal antibody 13-8300.

Fig. 3. Selective immunohistochemical detection of Cx43 by monoclonal antibody 13-8300 in sections of rat brain and heart. (A-C) Sections of cerebral cortex from a control brain in which in vivo Cx43 dephosphorylation was allowed to occur exhibit a typical punctate immunolabeling pattern for Cx43 with antibody 13-8300 (A) (shown at higher magnification in B). Cortical section of a brain in which dephosphorylation was prevented by microwave irradiation is totally devoid of labeling with this antibody (C). (D, E) Sections of rat heart processed with polyclonal antibody 71-0700 show a typical distribution of Cx43 at intercalated discs (D, arrows) and along lateral cell margins (D, arrowheads). No labeling is evident in sections of heart processed with antibody 13-8300 (E). Scale bar: A, C, 200 μm; B, 25 μm; D, E, 50 μm.

Fig. 4. Western blots of Cx43 in homogenates of microwaved rat brain after 15 min and 1 hr of MCA occlusion. (A, B) Blots of hypothalamus (lanes 1 and 2), striatum (lanes 3 and 4) and cerebral cortex (lanes 5 and 6) from the ischemic (lanes 2, 4 and 6) and contralateral control side (lane 1, 3 and 5) of brains dissected after 15 min (A) and 1 hr (B) of MCA occlusion and probed with antibody 18A. Tissues from the control side exhibit only the 43 kDa forms of Cx43 (lanes 1, 3 and 5), while most ischemic tissues contain these as well as the 41 kDa form (lanes 2, 4 and 6). (C, D) Blots of control (lane 1) and microwaved brain (lane 2) probed with antibody 18A are compared with antibody 13-8300 detection of Cx43 in blots of hypothalamus (lane 3 and 4), striatum (lane 5 and 6) and cerebral cortex (lane 7 and 8) from the ischemic (lane 4, 6 and 8) and contralateral control side (lane 3, 5 and 7) of brains dissected after 15 min (C) and 1 hr (D) MCA occlusion. All ischemic (lanes 4, 6 and 8), but not control (lanes 3, 5 and 7), tissues contain 41 kDa dephosphorylated Cx43, and no reaction is evident with the phosphorylated forms.

Fig. 5. Cx43-ir in rat hypothalamus demonstrated with antibodies 18A (A, D), 16A (B, E) and 13-8300 (C, F) after 15 min and 1 hr of MCA occlusion without reperfusion survival. In each section, the control hypothalamic side is on the left and ischemic side on the right. After 15 min of MCA occlusion (A-C), reduced 18A-ir (A, asterisk) and 16A-ir (B, asterisk) on the ischemic side coincides with an elevated 13-8300-ir (C, arrows) in the same area. After 1 hr MCA occlusion (D-F), 18A-ir and 16A-ir are absent in large areas of ischemic hypothalamus (D, E asterisks), and 18A-ir is sparse in patches (D, arrows) that coincide with areas of elevated 16A-ir (E, arrows). 13-8300-ir is absent in the lesion center (F, asterisk) but remains in surrounding areas. (G, H) Higher magnifications of 13-8300-ir in control (G) and ischemic (H) hypothalamus after 15 min of MCA occlusion. Scale bar: A-F, 500 μm; G, H, 50 μm.

Fig. 6. Cx43-ir in rat hypothalamus shown with four different anti-Cx43 antibodies after 1 hr of MCA occlusion followed by 6 and 12 hr reperfusion survival. (A, B) At 6 hr post-ischemia, 18A-ir is absent in the ischemic area (A, asterisk) and increased in the periphery (A, arrows). 16A-ir is increased throughout the ischemic region (B, arrows) and comparable staining is seen with antibody 71-0700 in the same area (C, arrows). (D) A rim of 13-8300-ir (D, arrows) circumscribes the ischemic area (asterisk). (E, F) At 12 hr post-ischemia, areas are seen with depleted (E, asterisk) as well as increased 18A-ir (E, arrows), while most of the ischemic region contains 16A-ir (F, arrows). Scale bar: A-F, 350 μm.

Fig. 7. Cx43-ir in hypothalamus after 1 hr of MCA occlusion followed by 6 hr (A-D) and 24 hr (E-F) reperfusion survival. (A) A region encompassing ischemic periphery and center (left to right) shows elevated 18A-ir at the periphery (arrows), reduction in a zone surrounding the ischemic center (asterisks) and dense patches of coarse puncta (arrowheads) within the largely depleted central area (star). (B, C) Sections showing similarity of 71-0700-ir (B) and 16A-ir (C) in normal areas of tissue (asterisks) and within the adjacent ischemic region (arrows). (D) A band of punctate 13-8300-ir is localized between the intensified periphery and depleted center (arrows). (E, F) Sections stained with antibody 18A and counterstained with H&E. At the ischemic periphery (E, asterisks; shown at higher magnification in F), densely hematoxylin-stained nuclei suggestive of cells undergoing apoptosis (F, arrows) are concentrated in the region indicated by asterisks in (A). Scale bar: A, D, 60 μm; B, C, 80 μm; E, 125 μm; F, 25 μm.

Fig. 8. Cx43-ir in hypothalamus after 1 hr of MCA occlusion and 1 hr reperfusion survival. (A-C) Photomicrographs show the same field at the border between normal and ischemic tissue triple-labeled with antibodies 18A (A) and 13-8300 (B) by immunofluorescence, and 16A by PAP (C). Labeling with antibody 18A outside ischemic tissue (A, stars) surrounds an absence of staining in the ischemic core (A, asterisk) and a shell of reduced staining (A,

arrows) which corresponds to a band of intense immunofluorescence with antibody 13-8300 (B, arrows). Dense labeling with 16A (C, arrows) occurs inside the ischemic core extending immediately adjacent to the band of 13-8300-ir. Scale bar: 80 μm.

Fig. 9. Cx43-ir in the cerebral cortex after 1 hr of MCA occlusion. (A-D) Temporal cortex after a survival time of 1 hr showing normal 18A-ir on the control side (A) and a patchy reduction on the ischemic side (B). 13-8300-ir is seen on the ischemic side in a microwaved brain 1 hr after MCA occlusion (C), while it is absent in a microwaved control brain (compare with Fig. 3C) and barely evident in the control side after perfusion fixation (G). Temporal cortex after a survival time of 24 hr. 18A-ir is elevated in the ischemic core (D, arrows) and eliminated in a zone around this core (D, arrowheads). 16A-ir is increased throughout the ischemic area (E, arrows). 13-8300-ir is seen partially within as well as around the periphery (F, arrows) of the ischemic area. (H) Monoclonal 13-8300 peptide adsorption. Scale bar: A-D, 400 μm.

Fig. 10. EM of Cx43-ir structures in normal and ischemic hypothalamus stained with antibody 18A. (A, B) Distribution of labeled gap junctions in normal neuropil (A, arrows) and after 15 min ischemia without survival (B, arrows). Gap junctions from (A) and (B) are shown magnified in corresponding insets. (C, D) After 1 hr ischemic insult and 1 hr survival, tissue disruption with translucent areas is evident in regions corresponding to LM zones lacking 18A-ir (asterisks) and patches of elevated labeling in these zones is localized to swollen processes (D, arrows). (E, F) After 1 hr ischemia and 12 hr survival, structures atypical of control tissue, but evident in the region of increased 18A-ir that circumscribes the lesion center include asymmetrically labeled (E, arrows) or unlabelled (E, arrowheads) putative astrocytic gap junctions and stained annular gap junctional profiles (F). Scale bar: A, B, 800 nm (inset in A, 170 nm; inset in B, 100 nm); C, 1.4 μm; D, 1 μm; E, 160 nm; F, 150 nm.

Fig. 11. EM of Cx43-ir with antibody 13-8300 in normal and ischemic hypothalamus. (A, B) Area in normal hypothalamus showing an unlabelled gap junction (A, arrow; magnified in inset) near an immunoreactive process (A, arrowhead, magnified in B) making an asymmetrically-labeled gap junction (B, arrow) with an unstained process. (C, D) Following a 15 min ischemic insult without survival, labeled gap junctions (C, arrows; magnified in D) are commonly seen within the ischemic site. (E-G) After 1 hr MCA occlusion and 12 hr survival, 13-8300-ir is absent within the ischemic area (E), but labeled gap junctions (F, arrows; magnified in inset) and very few sparsely labeled multivesicular clusters (G) are seen at the ischemic periphery. Scale bar: A, 320 nm (inset 100 nm); B, D, 100 nm; C, E, F, 650 nm (inset in F, 120 nm); G, 320 nm.

Fig. 12. EM of Cx43-ir with antibodies 71-0700 and 16A in normal and ischemic hypothalamus. (A-C) In normal tissue, 71-0700-ir is localized in astrocyte processes (A, arrows), somatic cytoplasm (B) and at astrocytic gap junctions (A, arrowheads; magnified in C). (D, E) After 1 hr MCA occlusion and 1 hr survival, 16A-ir (D, arrows; magnified in E) and 71-0700-ir (not shown) is seen in multivesicular clusters where it is particularly dense along vesicular membranes (E, arrows). i, intermediate filaments. Scale bar: A, 840 nm; B, 220 nm; C, E, 100 nm; D, 1.3 μm.

Fig. 13. EM of Cx43-ir with antibodies 18A and 13-8300 in cerebral cortex after 1 hr MCA occlusion and 24 hr survival. (A-C) 18A-ir in a labeled area adjacent to the depleted lesion center is localized to non-junctional membranes of swollen vacuolar structures (A, arrows; magnified in B) and multivesicular clusters (C, arrows). (D-F) 13-8300-ir at the rim around the depleted lesion center is associated with degenerating gap junctional profiles and contiguous non-junctional membranes (D, arrows; magnified in E) and with relatively intact

gap junctions (D, arrowheads; magnified in F). Scale bar: A, 1.3 μm; B, 340 nm; C, 1.2 μm; D, 850 nm; E, 85 nm; F, 100 nm.

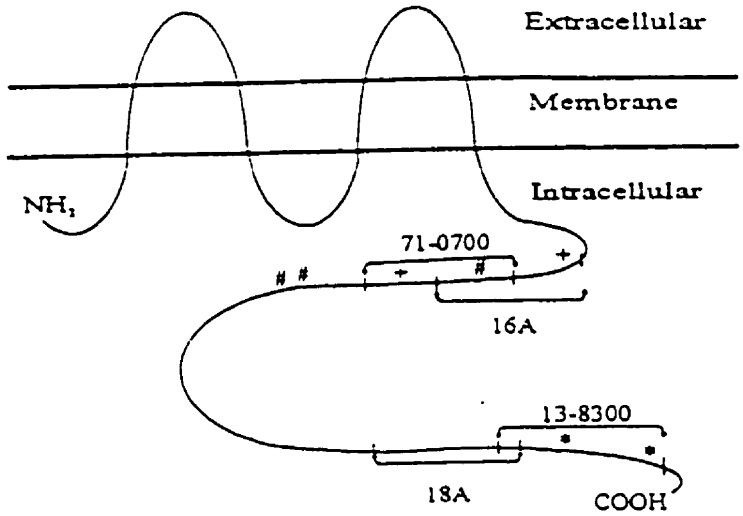
Extracellular
Membrane
Intracellular
NH2
71-0700
16A
13-8300
18A
COOH

Fig. 1

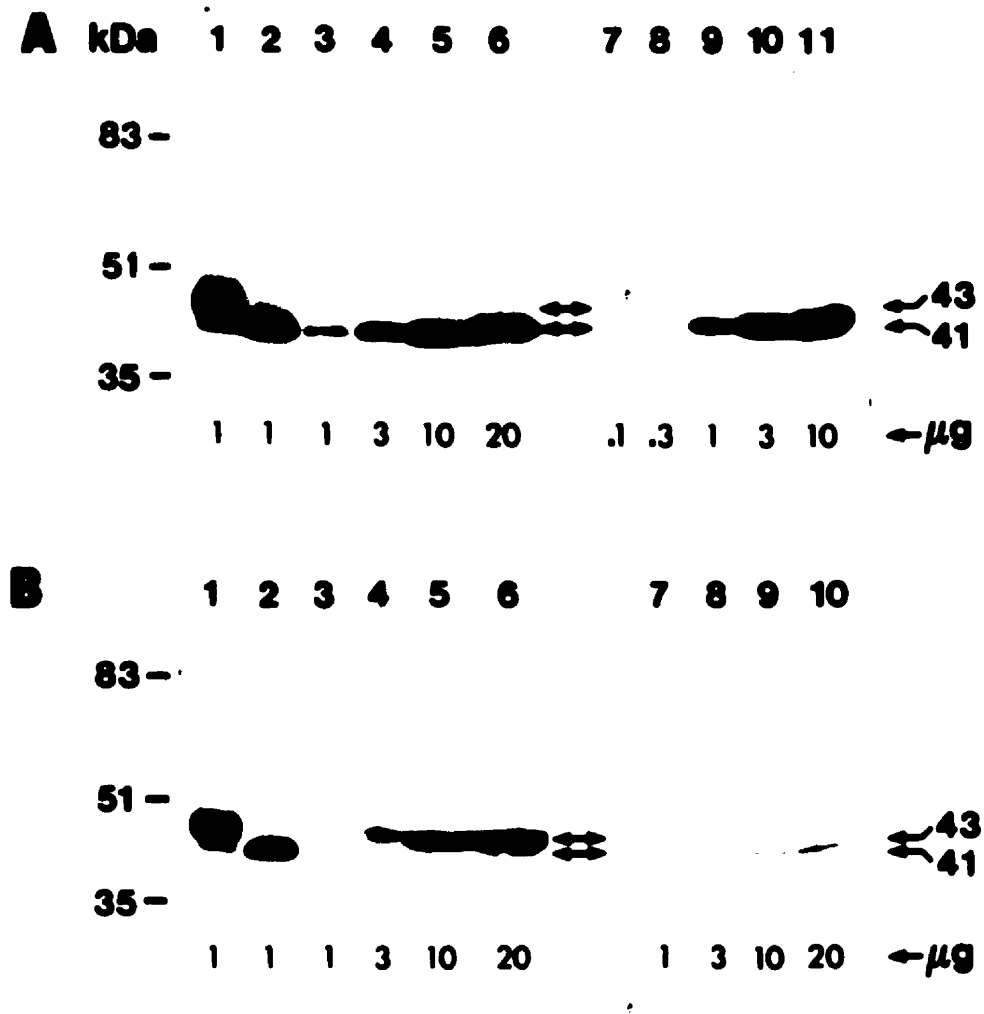
A
kDa
1 2 3 4 5 6 7 8 9 10 11
83-
51-
35-
43
41
1 1 1 3 10 20 .1 .3 1 3 10 μg
B
1 2 3 4 5 6 7 8 9 10
83-
51-
35-
43
41
1 1 1 3 10 20 1 3 10 20 μg

Fig. 2

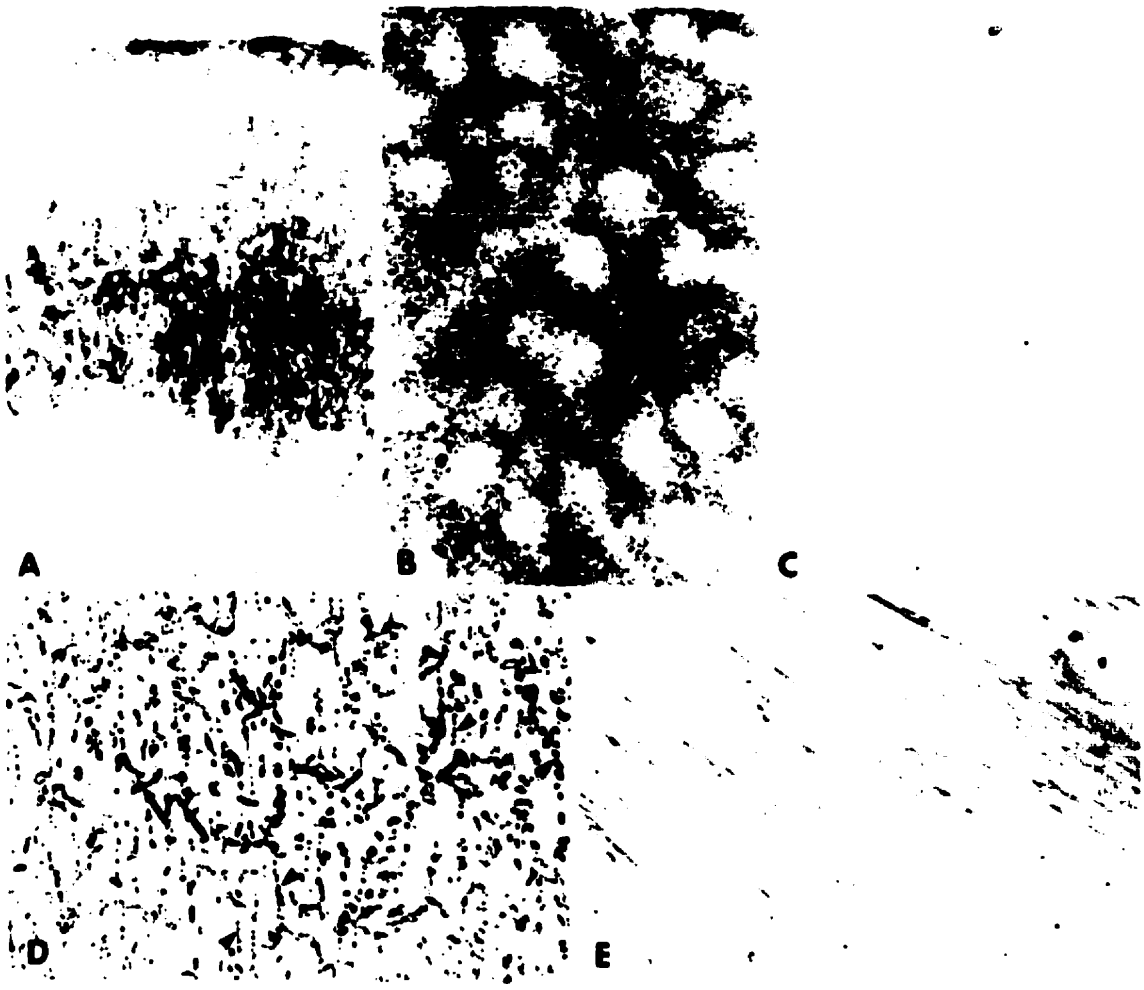

Fig. 3

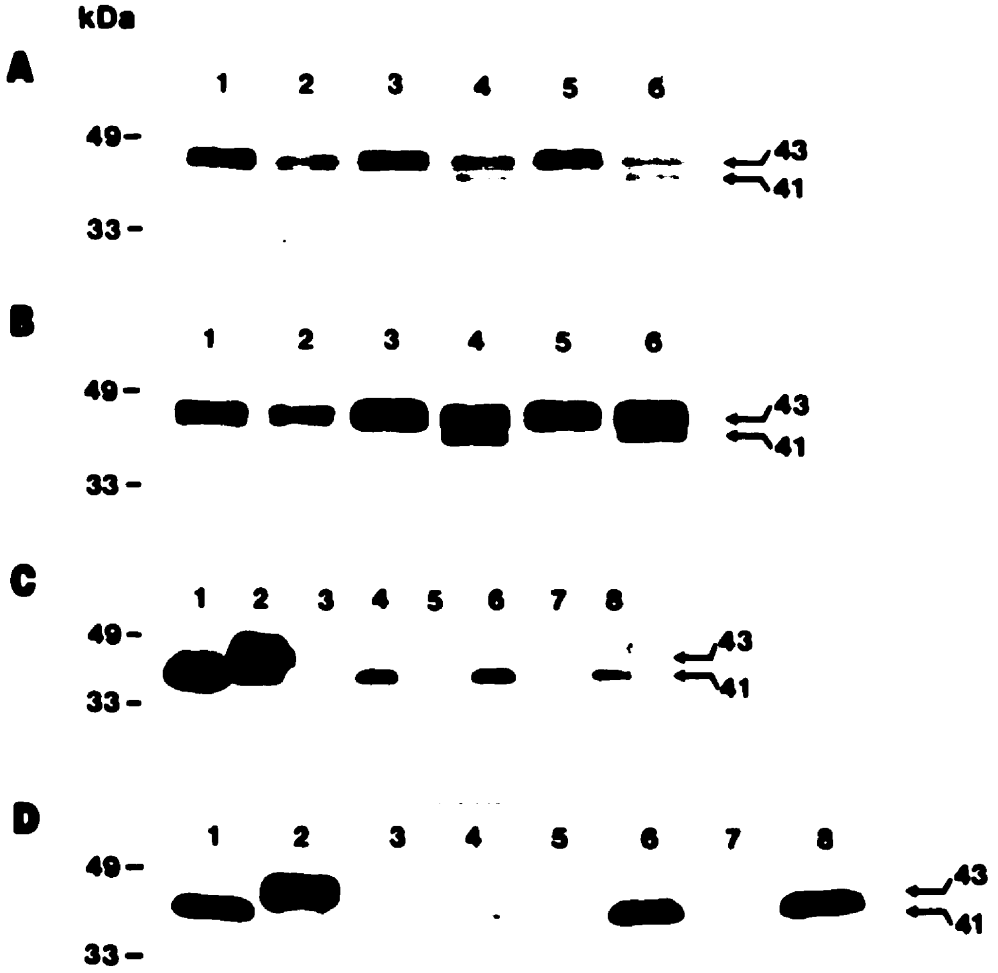
kDa
A
1 2 3 4 5 6
49-
33-
43
41
B
1 2 3 4 5 6
49-
33-
43
41
C
1 2 3 4 5 6 7 8
49-
33-
43
41
D
1 2 3 4 5 6 7 8
49-
33-
43
41

Fig. 4

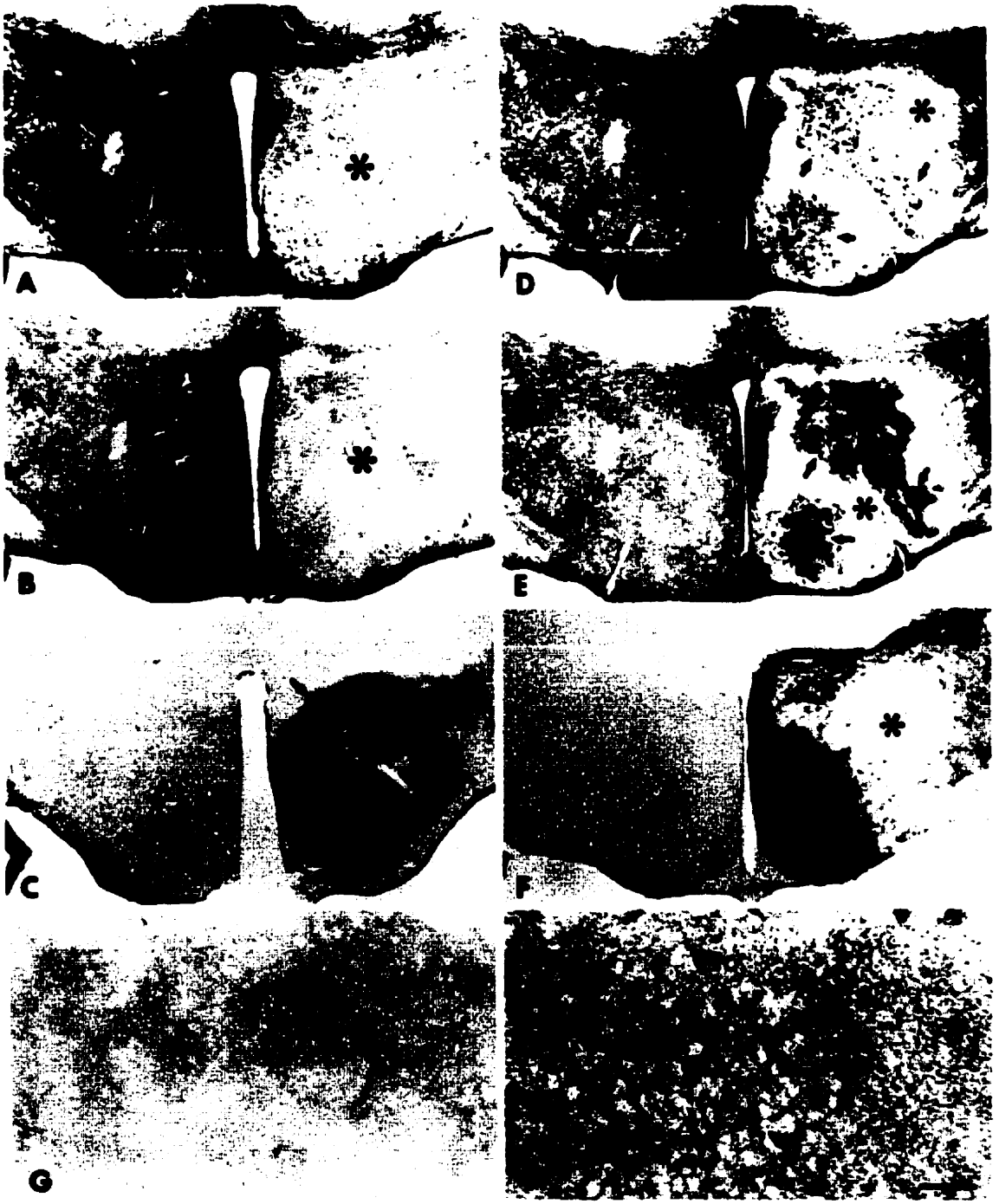

Fig. 5

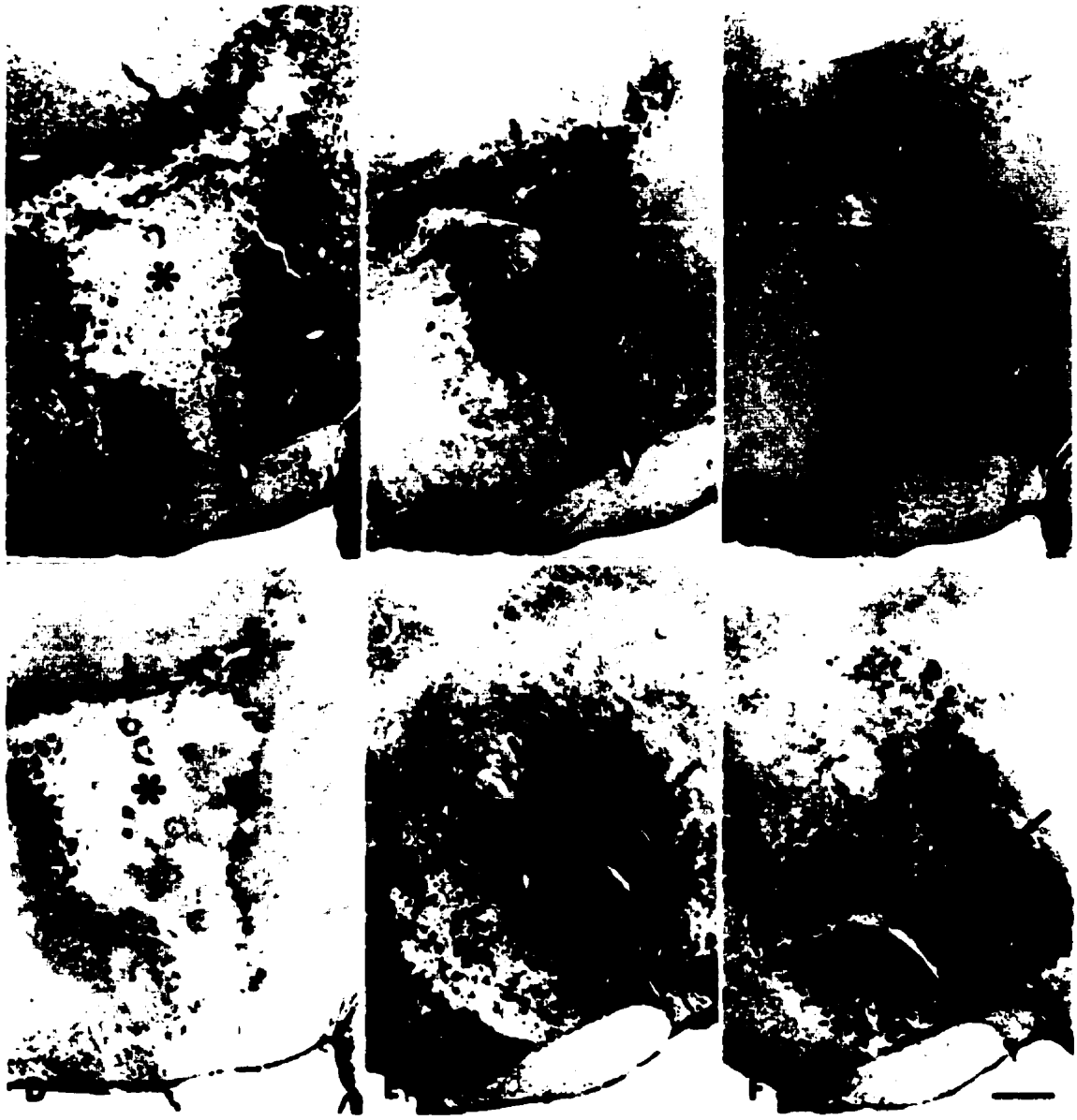

Fig. 6

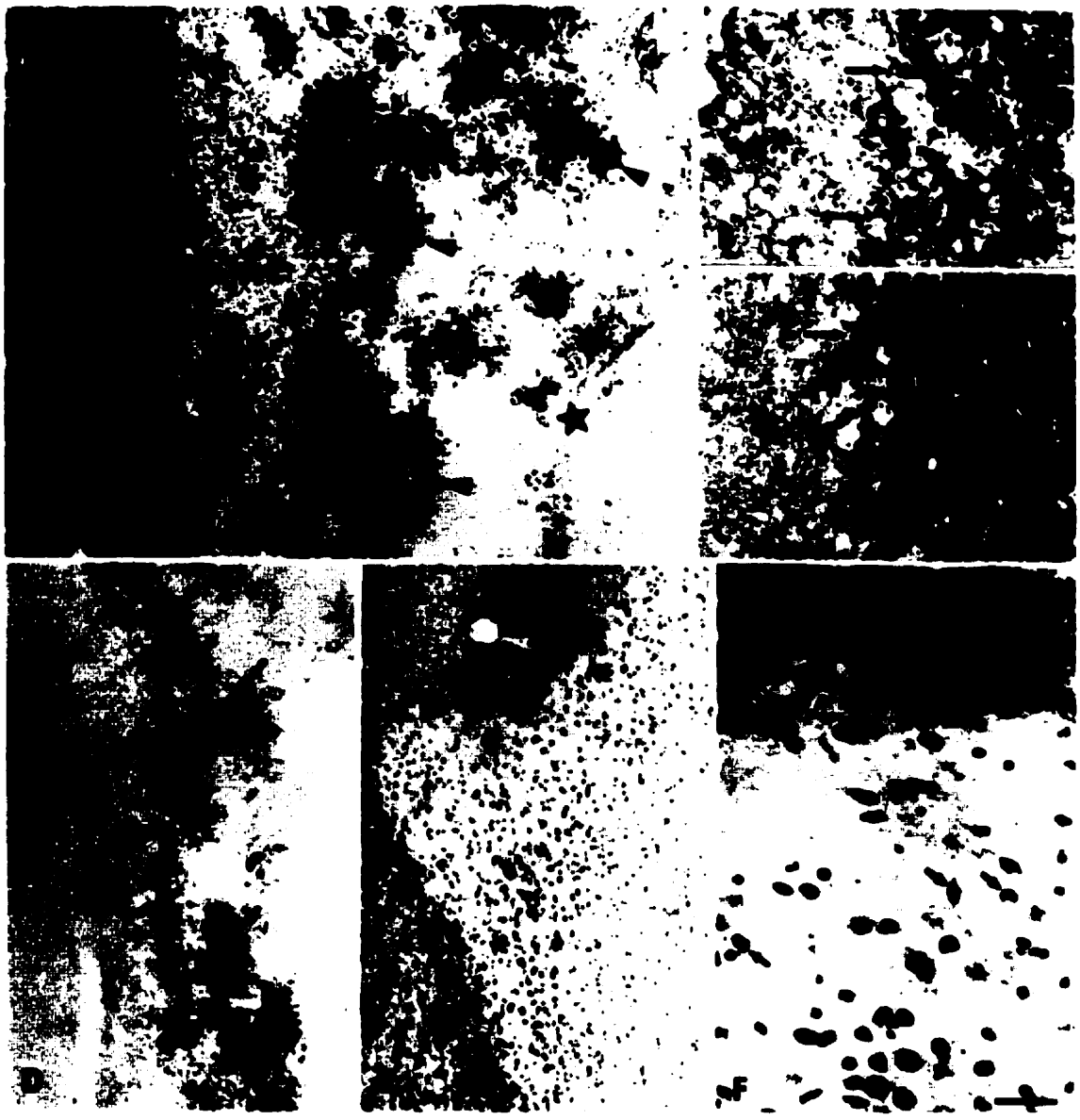

Fig. 7

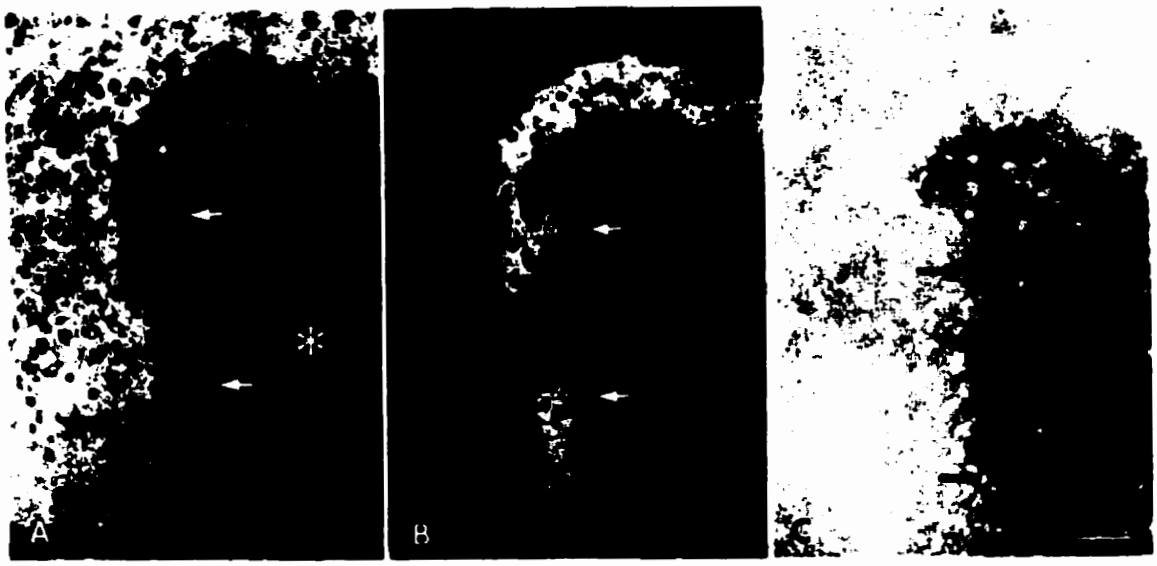

Fig. 8

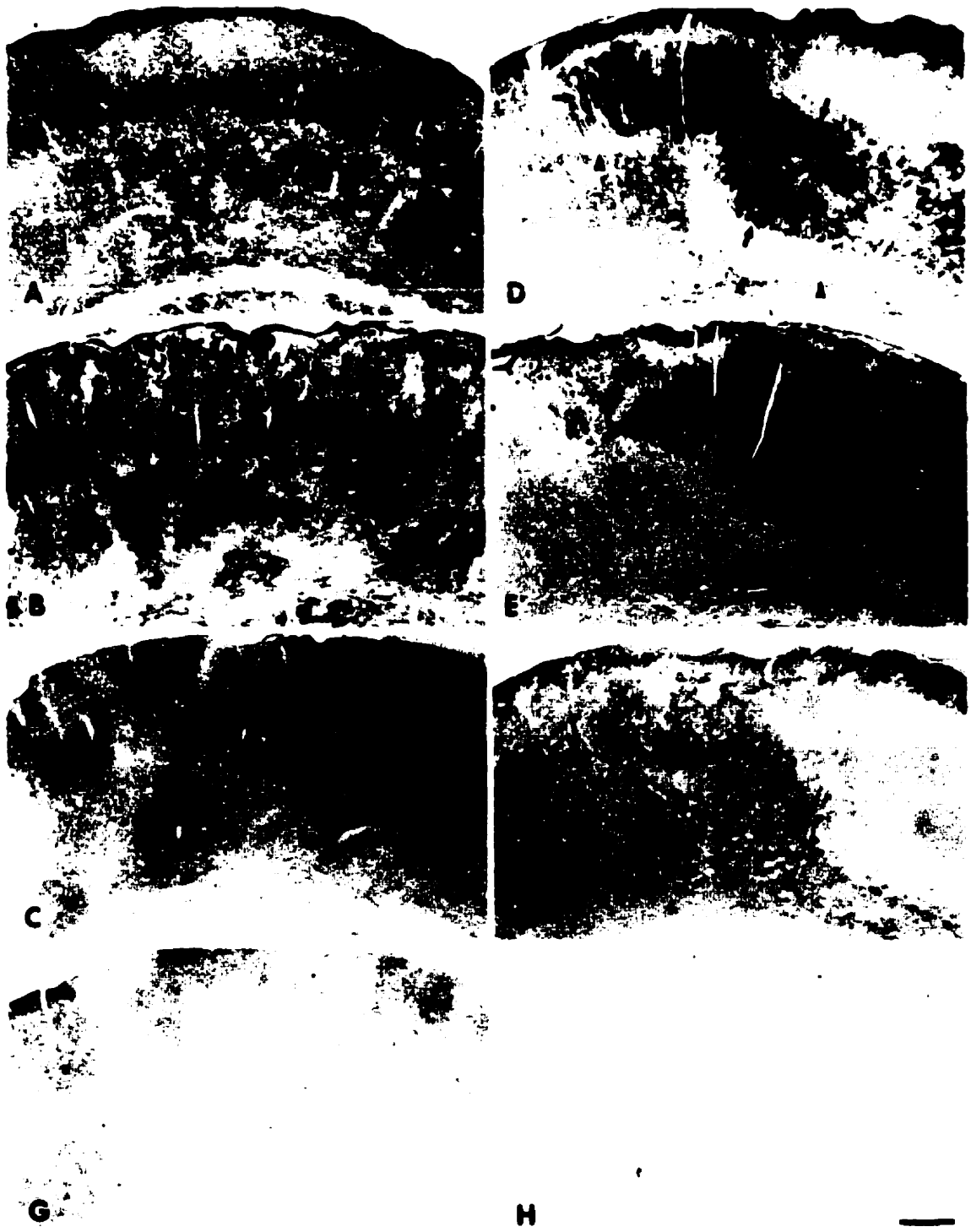

Fig. 9

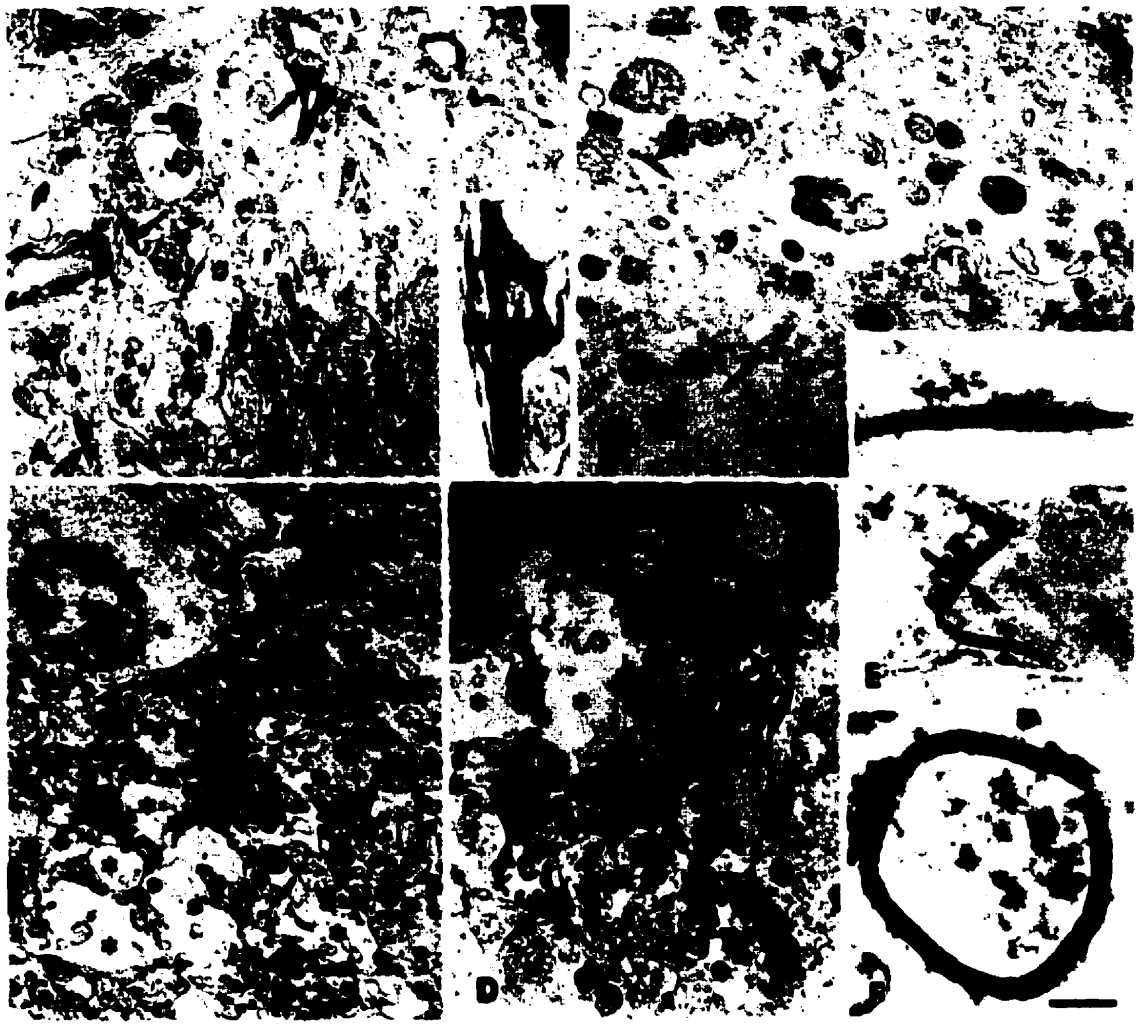

Fig. 10

Fig. 11

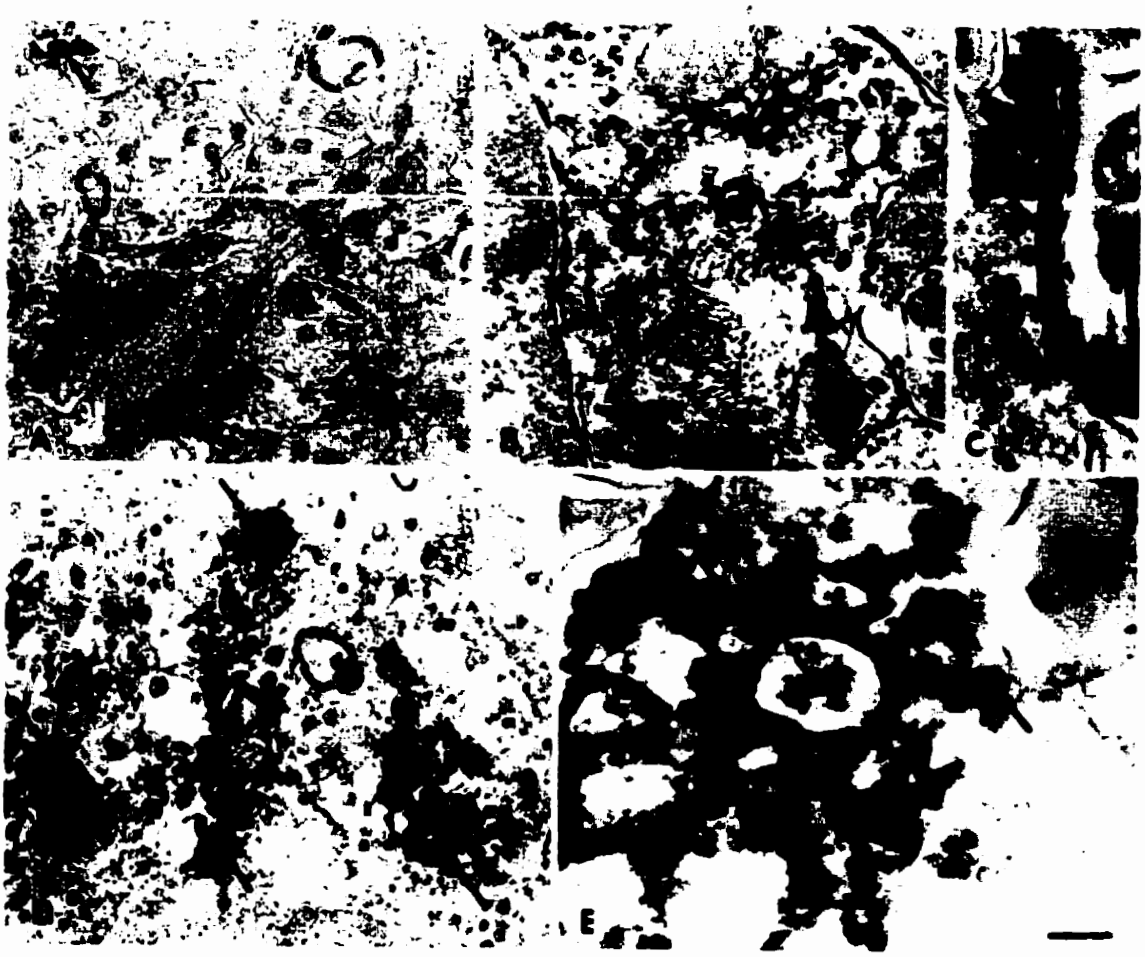

Fig. 12

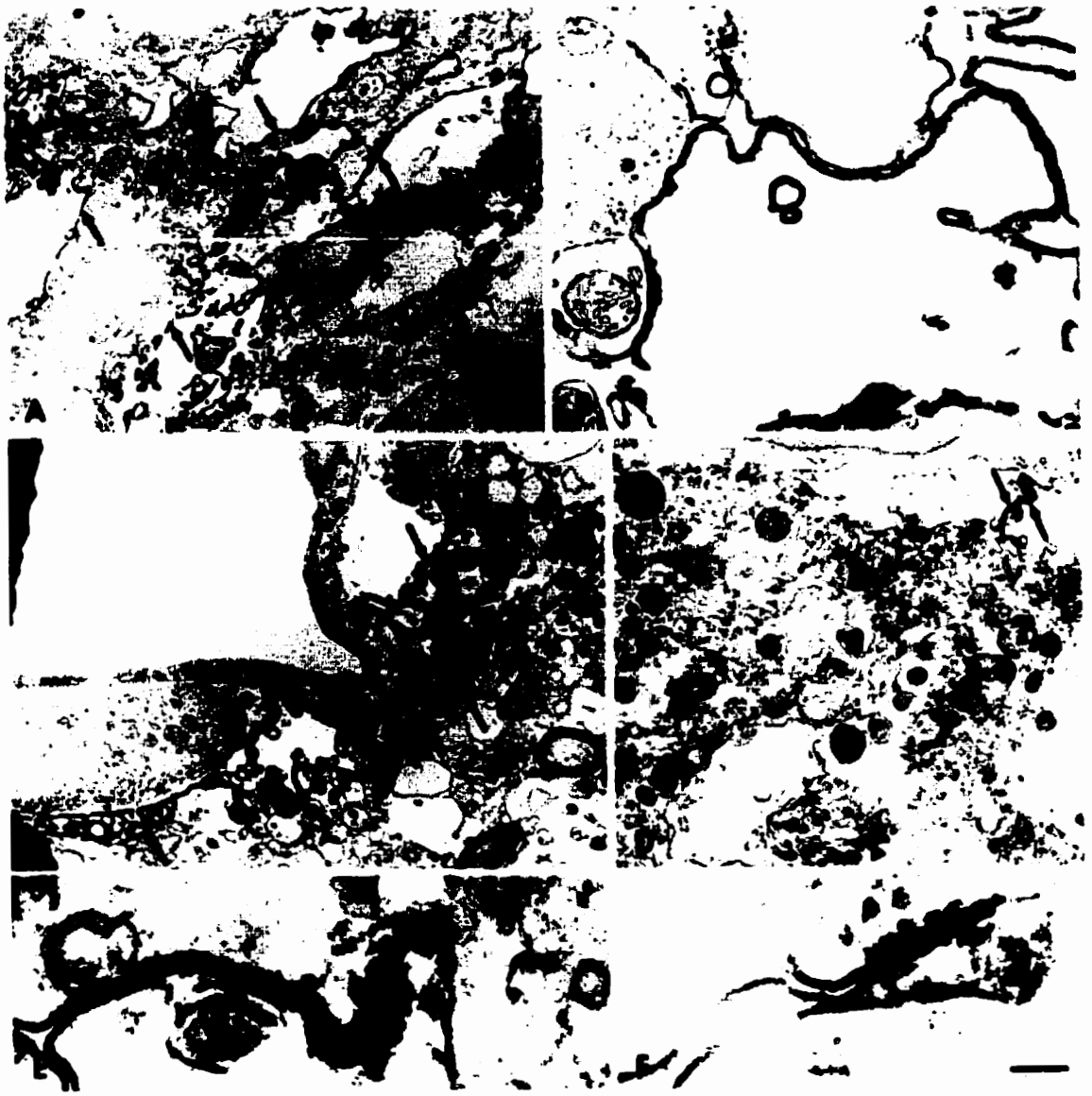

Fig. 13

Part IV

Activation of Fibers in Rat Sciatic Nerve Alters Phosphorylation State of Connexin43 at Astrocytic Gap Junctions in Spinal Cord: Evidence for Junction Regulation by Neuronal-Glial Interactions

Li, W. E. I. and Nagy, J. I.

Neuroscience, in press

Abstract

Intercellular communication via gap junction channels composed of connexin43 is known to be regulated by phosphorylation of this protein. We investigated whether connexin43 at astrocytic gap junctions is similarly regulated in response to neural activation. The effect of peripheral nerve stimulation on connexin43 phosphorylation state in the spinal cord of rats was examined with a monoclonal antibody (designated 13-8300) previously shown to recognize selectively a dephosphorylated form of connexin43. Immunolabeling with 13-8300 was absent in the lumbar spinal cord in control animals, but was induced in the dorsal horn ipsilateral to sciatic nerve electrical stimulation for 15 min or 1 h at a frequency of 1 or 100 Hz. Immuno-recognition of connexin43 by a polyclonal anti-connexin43 antibody, previously shown to undergo epitope masking under various conditions, was reduced in dorsal horn on the stimulated side. These responses were abolished by local anesthetic or tetrodotoxin application proximal to the site of nerve stimulation. Selective electrical stimulation of A-fibers or activation of cutaneous C-fibers by capsaicin evoked labeling with 13-8300 in deep and superficial laminae of the dorsal horn, respectively. Nerve stimulation increased the number of 13-8300-positive astrocytic gap junctions as well as the levels of dephosphorylated connexin43 in the dorsal horn on the stimulated side. Sciatic nerve transection produced results similar to that seen after C-fiber activation with capsaicin.

Thus, peripheral nerve stimulation evokes astrocytic connexin43 dephosphorylation in the spinal cord dorsal horn, suggesting that gap junctional coupling between astrocytes in vivo is subject to regulation by neuronal-glial interactions following neural activation.

Introduction

Gap junctions occur at apposing plasma membranes of many cell types and are thought to contribute to local metabolic homeostasis and synchronization of cellular activities by allowing direct intercellular movement of ions, metabolites and second messengers. These junctions are composed of clustered hemichannels, termed connexons, that form aqueous conduits linking the intracellular compartments of junctionally coupled cells. Each connexon consists of a hexameric arrangement of gap junction proteins termed connexins (Bruzzone et al., 1996; Goodenough et al., 1996; Kumar and Gilula, 1996). Gap junctional intercellular communication (GJIC) or channel conductance is regulated by a variety factors including pH, $[Ca^{+2}]$, transjunctional voltage and signaling mechanisms (Bruzzone et al., 1996; Giaume and McCarthy, 1996; Goodenough et al., 1996). Numerous studies of cells coupled via gap junctions composed of connexin43 (Cx43), one member of the multigene connexin family (Bruzzone et al., 1996), indicate that channel gating is also regulated by connexin phosphorylation (Bruzzone et al., 1996; Lau et al., 1996). A number of serine phosphorylation sites have been identified within the Cx43 sequence (Unger et al., 1999), and induction of Cx43 dephosphorylation by various methods has been correlated with either a reduction of GJIC (Godwin et al., 1993; Oelze et al., 1995; Cotrina et al., 1998a), or an increase in unitary channel conductance (Moreno et al., 1994).

In the central nervous system (CNS), it is well established that astrocytes in vivo express Cx43 and connexin30 (Cx30) (Yamamoto et al., 1990a,b; Ochalski et al., 1997; Nagy et al., 1997a,b, 1999; Nagy and Dermietzel, 2000;), and that these cells are extensively coupled (Mugnaini, 1986; Giaume and McCarthy, 1996; Rash et al., 1997; Nagy and Rash, 1999) with as many as 30,000 gap junctions per astrocyte (Wolburg and Rohlmann, 1995). Although the functional purpose for this high level of coupling is not yet clear, it has been suggested that astrocytic GJIC serves a role in K^+ spatial buffering (Walz, 1989) and intercellular exchange of Na^+ (Rose and Ransom, 1997). There is now reason to consider that the conductance state of astrocytic junctional channels may be dynamically regulated by neuronal-glial interactions. In isolated optic nerve, for example, dye-coupling between

astrocytes is increased by electrical stimulation of the nerve (Marrero and Orkand, 1996). Further, GJIC between astrocytes in vitro can be rapidly altered by elevated K^+ as well as by a variety of neuronally released substances, including ATP, glutamate, noradrenaline, endothelin and anandamide (Giaume and McCarthy, 1996). As in peripheral tissue, Cx43 in the CNS exists as a phosphoprotein (Hossain et al., 1994c; Li et al., 1998) and control of its phosphorylation state by kinase- and phosphatase-associated signaling pathways may be one mechanism whereby astrocytic GJIC is regulated by these substances. Indeed, agents known to alter coupling between astrocytes can also influence the activity of, for example, protein kinase C (PKC) and mitogen-activated protein kinases in these cells (Kasuya et al. 1994; Chisamore et al., 1996; Lazarini et al., 1996), and it is known that activation of PKC reduces astrocytic GJIC (Enkvist and McCarthy, 1992; Konietzko and Muller, 1994).

To date, most studies of astrocytic GJIC and Cx43 phosphorylation state have been conducted using cultured astrocytes or CNS tissues subjected to various lesions (Hossain et al., 1994b; Giaume and McCarthy, 1996; Hofer et al., 1996; Campos de Carvalho et al., 1998; Cotrina et al., 1998a; Li et al., 1998; Martinez and Saez, 1999; Nagy and Rash, 1999; Nagy and Dermietzel, 2000). Thus, it is not clear whether Cx43 phosphorylation mechanisms potentially contribute to astrocytic GJIC regulation under normal physiological conditions. To address this as well as to examine the possible role of neuronal-glial interactions in GJIC regulation between astrocytes in vivo, we investigated the phosphorylation status of astrocytic Cx43 in the spinal cord after electrical stimulation of sciatic nerve or topical capsaicin application to skin, which selectively activates unmyelinated C-fibers (Kenins, 1982; Szolcsanyi, 1987; Lynn et al., 1992). Spinal cord tissues were analyzed immunohistochemically and by Western blotting with various anti-Cx43 antibodies including one that we previously characterized as selectively recognizing a dephosphorylated form of Cx43 in at least neural tissues and some cell lines (Nagy et al., 1997b; Li et al., 1998).

Materials and methods

Antibodies

Two rabbit polyclonal anti-Cx43 antibodies designated 18A and 71-0700, and one monoclonal Cx43 antibody designated 13-8300 were used in this study. The latter two antibodies were obtained from Zymed Laboratories (South San Francisco, CA). Anti-Cx43 18A and 13-8300 were produced against peptides corresponding to amino acids 346-363 and 360-376, respectively, in the carboxy-terminal sequence of Cx43 (Beyer et al., 1987). The Cx43 sequence recognized by antibody 71-0700 is proprietary, but does not correspond to sequences recognized by either 18A or 13-8300 (Li et al., 1998). All three antibodies have been extensively characterized for specific detection of Cx43 by immunohistochemical, Western blotting and immunoprecipitation methods as well as by antibody preadsorption with synthetic peptide in a variety of tissues including normal and lesioned CNS, cardiac myocytes and cultured cells (Yamamoto et al., 1990a,b; Hossain et al., 1994a,b; Nagy et al., 1992, 1997a, Ochalski et al., 1995, 1997; Theriault et al., 1997; Li et al., 1998). Selective detection of a dephosphorylated form of Cx43 by antibody 13-8300 in some tissues has also been previously described by us (Nagy et al., 1997a; Li et al., 1998). Synthetic peptide preadsorption of 13-8300 in control experiments performed in the present studies was conducted as previously described (Li et al., 1998). Selective immunohistochemical recognition of dephosphorylated Cx43 by 13-8300 is supported by the consistent presence or absence of immunostaining with this antibody in tissues that contain or lack, respectively, dephosphorylated Cx43 as seen by Western blotting (Nagy et al., 1997a; Li et al., 1998). Specificity of 13-8300 for Cx43 in spinal cord is further indicated by the similar appearance of 18A labeling before and 13-8300 labeling after sciatic nerve stimulation as seen in the present study, the localization of 13-8300 immunoreactivity at astrocytic gap junctions and the elimination of 13-8300 immunolabeling by peptide preadsorption.

Animal preparation

Sixty-five male Sprague-Dawley rats weighing 280-330 g were used in this study. A minimum of 3 animals were used for each treatment condition and six animals served as

sham-operated controls. All animals were obtained from the local Central Animal Care Services (CACS) at the University of Manitoba and utilized according to approved protocols by the CACS Care Committee with minimization of stress to, and the numbers of, animals used. Anesthesia was induced with 5% halothane and maintained with 1-2% halothane in 70% O_2 and 30% N_2O using a tracheal catheter by a resperator. Animals were immobilized with gallamine triethiodide (40 mg/kg, i.v.) in order to avoid muscle activation and limb movement during sciatic nerve stimulation. To enable control of anesthesia during surgery and stimulation, the tail artery was cannulated for measurement of blood gases (pH, pO_2, pCO_2) and for monitoring blood pressure, which was maintained between 70-100 mmHg in all experiments. Body temperature was monitored and maintained at 37.5°C.

The left and right sciatic nerves were exposed and carefully freed of connective tissue along a length of 2-3 cm. The sciatic nerve of one side was subjected to electrical stimulation, while the other side served as control for nerve exposure and manipulation. With the sciatic nerve resting in warm mineral oil, nerve stimulation was achieved with bipolar silver electrodes linked to a Grass SD9 electrical stimulator, which was set to generate 1 ms electrical pulses of either 1 or 100 Hz. Stimulation intensity was varied from 20 μA to 2 mA to allow selection of current that produced excitation of both large and small diameter fibers or only A-fibers. Additional electrodes, placed proximal to the site of stimulation, were used to monitor compound action potentials allowing selection of appropriate current strength for nerve activation. Nerves were stimulated for a duration of either 15 min or 1 h. In some experiments, cotton soaked with either 0.25% bupivacaine hydrochloride or 1 μM tetrodotoxin was applied to the sciatic nerve proximal to the stimulating electrodes in order to block impulse conduction to the spinal cord, with verification of blockade by more proximally placed electrodes. In separate animals, selective C-fiber activation in animals anesthetized with equithesin was attained by topical application of a 1% capsaicin solution to the left hind limb. Capsaicin was dissolved in 48% ethanol, 25% propylene glycol, 25% distilled water and 2% methyl laurate to facilitate maximum C-

fiber excitation (Lynn et al., 1992). The solvent alone was applied to the right hind limb. In another group of animals, the sciatic nerve was unilaterally ligated with surgical thread and cut distal to the ligation.

Immunohistochemistry

Immediately after nerve stimulation, or 1 h after either capsaicin application or nerve transection, animals were given an overdose of nembutol and perfused transcardially with cold 4% formaldehyde dissolved in 0.1 M sodium phosphate buffer at pH 7.4 (PB). The L4 to S1 segment of spinal cord was removed, post-fixed for 2 h at 4°C in the same fixative and cryoprotected in PB containing 25% sucrose and 10% glycerol. Sections were cut transversely at a thickness of 20 μm on a sliding microtome and collected free-floating in PB containing 0.9% saline (PBS). For electron microscopy, spinal cords were stored in PBS and cut at 30 μm with a vibratome. Sections for light microscopy were incubated for 48 h with either antibody 18A diluted 1:2,000, antibody 71-0700 diluted 1:500, or antibody 13-8300 diluted 1:500 in PBS containing 0.3% Triton X-100 (PBST). Sections were then processed for labeling with peroxidase anti-peroxidase (PAP) as previously described (Ochalski et al., 1995, 1997; Li et al., 1998). Briefly, goat anti-rabbit or goat anti-mouse IgG were used as secondary antibodies at 1:100 dilution in PBST and rabbit PAP or mouse clonoPAP (Sternberger Monoclonals) were used at 1:500 dilution in PBST. Secondary and tertiary antibody incubations were conducted for 1.5 h. Sections were washed with PBST for at least 60 min between antibody incubations. Final enzyme reaction was conducted for 10-15 min in 50 mM Tris-HCl buffer, pH 7.4, containing 0.00005% H_2O_2 and 0.02% diaminobenzidine. The immunostained sections were mounted onto slides, dehydrated in alcohol, cleared in Histoclear and coverslipped with Lipshaw mounting medium. Sections were similarly processed for electron microscopy except that 0.2% Photo-Flo 200 (Kodak) instead of Triton X-100 was included in the PBS for all the incubation and wash steps.

Sections were plastic embedded and counterstained as previously described (Ochalski et al., 1995, 1997; Li et al., 1998).

Western blotting

After 1 h of nerve stimulation and laminectomy at a lumbar level, spinal cord segments containing L4-S1 were rapidly removed and dorsal horns from control and stimulated sides were separately dissected and stored at -70°C. Tissue was homogenized in 1 mM bicarbonate buffer (pH 7.4) containing 1 mM phenylmethylsulfonyl fluoride and 1 mg/ml each of leupeptin and pepstatin. The phosphatase inhibitors sodium fluoride and sodium orthovanadate at concentrations of 10 mM and 1 mM, respectively, were also included in the homogenization buffer to inhibit Cx43 dephosphorylation during tissue processing. The total protein in homogenates was assayed with a BIO-RAD protein assay kit. Sodium dodecylsulphate polyacrylamide gel electrophoresis and Western blotting were performed as previously described (Hossain et al., 1994a,b,c; Nagy et al., 1997a; Li et al., 1998) using antibodies 18A and 13-8300 at 1:200,000 and 1:750 dilution, respectively.

Results

LM of Cx43 immunolabeling in dorsal horn

In sham-operated animals and in the control unstimulated side of spinal cords from animals given unilateral electrical stimulation of the sciatic nerve, immunoreactivity (ir) with antibody 18A (Fig. 1A,C) was similar to patterns that we previously described in normal unoperated rats (Ochalski et al., 1997). This was also true of animals treated unilaterally with topical capsaicin or nerve transection, indicating that none of these treatments had an effect on the appearance of labeling contralateral to the side of treatment. Labeling consisted primarily of punctate profiles in gray matter and was localized to puncta or fibrous astrocytic elements in white matter. Immunostaining was distributed throughout dorsal and ventral gray matter, but was most intense in the superficial layers of the dorsal horn and around the central canal. Antibody 71-0700 produced qualitatively similar, but a lower

intensity of immunostaining in control spinal cord (not shown). Monoclonal anti-Cx43 antibody 13-8300 gave a near total absence of labeling in spinal cords of normal or sham-operated animals (not shown), and 13-8300-ir was also virtually absent in the spinal cord contralateral to the various treatments (Fig. 1B,D).

The effect of sciatic nerve electrical stimulation on 18A-ir and 13-8300-ir in the spinal cord is shown in Figure 1. Stimulation for 1 h at 1 Hz with a current strength of 2 mA, leading to the activation of both myelinated and unmyelinated fibers as judged from observation of proximal compound action potentials, resulted in a consistent reduction of 18A-ir in the L4 to S1 segment of dorsal horn ipsilateral to the stimulation (Fig 1A). In adjacent sections processed with antibody 13-8300, immunoreactivity was induced on the stimulated side in an area of dorsal horn (Fig 1B) corresponding closely to the region of 18A reduction, which was demarcated ventrally at the level of lamina VI-VII. Nerve stimulation also induced 13-8300-ir in the dorsal portion of the dorsolateral funiculus (Fig 1B). Cx43 remained undetectable by antibody 13-8300 in all other areas of spinal cord and no alterations in either 18A-ir or 13-8300-ir were evident in dorsal column nuclei or thalamus of animals receiving nerve stimulation (not shown). As well, nerve activation had no discernable effect on Cx43 detection by antibody 71-0700 in spinal cord or the more rostral regions examined (not shown). Nerve stimulation for 1 h at a frequency of 100 Hz gave results similar to that seen after stimulation at 1 Hz for 1 h (not shown). Reduction of the stimulation time to 15 min at 1 Hz diminished the loss of 18A-ir (Fig. 1C) and reduced the expanse of dorsal horn exhibiting intense 13-8300-ir on the stimulated side (Fig 1D). Although already evident from sham-operated controls that these changes in Cx43 detection were not due to surgery alone, a relationship to nerve activation was further tested by blockade of impulse conduction with bupivacaine or tetrodotoxin application to the sciatic nerve proximal to the site of stimulation. Both agents abolished the alterations in 18A-ir and 13-8300-ir seen after nerve stimulation for 1 h at 1 Hz (not shown).

We next determined whether alterations in Cx43 detection by antibodies occurs only after activation of all fibers in sciatic nerve or whether this could be elicited by activation of

A-fibers or C-fibers alone. Selective activation of A-fibers was achieved by sciatic nerve stimulation at a reduced intensity of about 100 μA, at which C-fiber potentials recorded from a proximal electrode were not evident. After 1 h stimulation at 1 Hz, 18A-ir was only minimally reduced in deep and medial superficial dorsal horn laminae on the stimulated (Fig. 2B) compared with the contralateral control side (Fig. 2A). Immunoreactivity with antibody 13-8300 was induced in most areas of the dorsal horn, although not as prominently as seen after stimulation of both A- and C-fibers, and lateral regions of laminae I, II and III remained unlabelled (Fig. 2C). After selective C-fiber activation by topical application of capsaicin unilaterally to the hind leg for 1 h, 18A-ir was unaltered (not shown) and 13-8300-ir was increased robustly in the lateral half of dorsal horn regions encompassing laminae I, II and III (Fig 2E). As shown in the case of capsaicin-induced labeling with 13-8300 (Fig. 2F), 13-8300-ir was punctate, and whenever present after nerve activation, had an appearance similar to that seen in normal tissue stained with antibody 18A. Further, as shown in the case of A-fiber stimulation, specificity of Cx43 detection by antibody 13-8300 is indicated by abolition of immunolabeling after preadsorption of 13-8300 with synthetic peptide antigen (Fig 2D).

In the dorsal horn of animals receiving sciatic nerve transection followed by a survival time of 1 h, 18A-ir was reduced slightly in the superficial half of laminae II on the transected (Fig 3B) compared with the control side (Fig. 3A) and 13-8300-ir was consistently induced in lateral regions of laminae I, II and III (Fig 3D), which corresponded closely to areas of induced 13-8300-ir seen after capsaicin treatment. Nerve transection did not elicit Cx43 detection with antibody 13-8300 in the ventral horn on the transected side (not shown) or in the dorsal (Fig. 3C) or ventral horn on the non-transected side. Sciatic nerve transection produced no alterations in immunolabeling for Cx43 with antibody 71-0700 (not shown).

EM of Cx43 immunolabeling in dorsal horn

Ultrastructural immunolabeling patterns obtained with antibody 18A in dorsal horn of unstimulated spinal cord were similar to those we previously reported (Ochalski et al., 1997). This consisted of an exclusively astrocytic localization where label was either diffuse and dispersed throughout the cytoplasm of fine astrocyte processes, particularly those ensheathing glomeruli, axons and dendrites, or was concentrated at gap junctions between these processes (Fig. 4A). After sciatic nerve stimulation at 1 Hz for 1 h at a strength activating both A- and C-fibers, 18A-ir (Fig. 4B,C) was largely comparable qualitatively with that in normal dorsal horn. Some gap junctions, however, tended to exhibit lighter labeling of their inner membranes (Fig. 4C) than seen in control tissue and unlabelled astrocytic gap junctions were observed in the vicinity of labeled processes (Fig.4D), indicating that lack of labeling was not simply due to failure of antibody penetration into sections. In dorsal horn of the non-stimulated side, such unlabelled astrocytic gap junctions were never observed in tissue processed with antibody 18A.

In representative dorsal horn areas of sections processed with antibody 13-8300, very little labeling was seen on the side contralateral to nerve stimulation (Fig. 5). Astrocyte processes were almost entirely devoid of 13-8300-ir (Fig. 5A) and the majority of astrocytic gap junctions examined were unlabelled (Fig. 5B). However, lightly or partially labeled gap junctions were seen (Fig. 5C) and the occurrence of these in the vicinity of unlabelled junctions (Fig. 5D) again indicated that lack of labeling, in this case with antibody 13-8300, was not due to failure of antibody penetration to the depth of section analyzed by EM.

After stimulation of both A- and C-fibers in sciatic nerve at 1 Hz for 1 h, 13-8300-ir of *gap junctions* in the dorsal horn on the stimulated side was similar to the labeling of junctions with 18A in normal dorsal horn and in dorsal horn contralateral to the side of stimulation. Labeling of astrocytic gap junctions was intense (Fig. 6A,B) and junctions characteristically displayed dense, uniform immunoreaction product deposited along each side of their inner membranes (Fig. 6C), resulting in a symmetric appearance of labeling at the majority of junctions. Occasionally, however, labeling was asymmetric such that one side of a junction formed by an immunoreactive process was labeled, while the other side

along with the contributing process was unstained (Fig. 6D). Labeling within astrocytic processes with 13-8300 was less widely distributed than seen with 18A in control animals, and was mostly seen near labeled gap junctions where it may have arisen by diffusion of immunoreaction product.

A survey of labeled and unlabelled gap junctions in the dorsal horns of animals receiving sciatic nerve stimulation as described above in tissues examined by EM is given in Table 1. In control dorsal horn, the number of junctions unlabelled with 13-8300 was about twice that of labeled junctions. After nerve stimulation, 13-8300 immunoreactive gap junctions on the stimulated side was significantly increased to 98% of junctions counted compared with 35% on the control side. A similar analysis was attempted in material stained with antibody 18A, but the presence of numerous very lightly stained junctions often made it difficult to designate these unequivocally as stained or unstained.

Western blotting of Cx43 after nerve stimulation

Western blotting of Cx43 was conducted to determine the relative levels of phosphorylated and non-phosphorylated forms of this protein in the spinal cord dorsal horn after nerve stimulation. Phosphorylation status is typically deduced from the progressively slower mobility of Cx43 in gels as it becomes phosphorylated at multiple sites. Comparable to results in rat brain probed with antibody 18A (Hossain et al., 1994c; Li et al., 1998), which detects all phosphorylated forms of Cx43, a higher proportion of astrocytic Cx43 in control dorsal horn was found to migrate at a slower Mr of 43 kDa compared with the non-phosphorylated 41 kDa form (Fig. 7A, lane 1). Following activation of C-fibers by topical capsaicin application as in the anatomical studies above, a small increase in the non-phosphorylated 41 kDa form was evident (Fig. 7A, lane 2), although resolution of bands was poor due to necessary inclusion of phosphatase inhibitors, which inexplicably deteriorates band separation as previously noted (Mikalsen et al., 1997; Nagy et al., 1997a). Also consistent with results obtained using brain tissue (Nagy et al., 1997a; Li et al., 1998), antibody 13-8300 was found to detect only a dephosphorylated 41 kDa form of Cx43 in

control dorsal horn (Fig. 7B, lanes 1 and 2). After activation of C-fibers with topical capsaicin, blots probed with antibody 13-8300 showed an increased level of the 41 kDa form of Cx43 in the dorsal horn on the side of capsaicin application (Fig 7B, lane 4) compared with the control side (Fig. 7B, lane 3). This increase was not likely due to surgical or dissection artifact since no such differences were seen between the left and right sides of animals receiving topical application of capsaicin vehicle (Fig. 7B, Lane 1 and 2). Similar results were seen in spinal cord dorsal horns from animals given electrical stimulation of sciatic nerve (not shown).

Discussion

We show that Cx43 in spinal cord is largely phosphorylated and that the response to sciatic nerve input is dephosphorylation of a specific pool of Cx43 located at astrocytic gap junctions. These results demonstrate that remote activation of primary fibers in the sciatic nerve can influence the phosphorylation state of astrocytic Cx43 in the dorsal horn of the spinal cord and provide indirect evidence for the involvement of neuronal-glial interactions in the regulation of astrocytic GJIC under physiological conditions in vivo.

Immunorecognition of Cx43 by 13-8300

The above conclusions rely on the proposition that antibody 13-8300 selectively detects a dephosphorylated form of Cx43 in our spinal cord preparations. As demonstrated in brain tissue, cardiac tissue and cultured cells (Nagy et al., 1997a; Li et al., 1998), this antibody also fails to recognize the slower migrating, phosphorylated 43 kDa forms of Cx43 in spinal cord, but does react with a faster migrating 41 kDa form, which corresponds to dephosphorylated Cx43 (Crow et al., 1990; Musil et al., 1990; Laird et al., 1991; Saez et al., 1997). We have suggested that the lack of 13-8300 reaction with slower mobility forms of Cx43 is likely due to epitope blockade by phosphate groups (Li et al., 1998). This is supported by the presence of PKC phosphorylation sites (Ser368 and Ser372) within the Cx43 sequence (amino acids 360-376) against which 13-8300 was generated (Saez et al.,

1993, 1997) and by results showing that phosphorylated forms of Cx43 ordinarily undetectable by 13-8300 are detected following Cx43 dephosphorylation with alkaline phosphatase (Li et al., 1998).

It should be noted that Cx43 phosphorylation within the 13-8300 epitope remains to be demonstrated specifically in astrocytes. Further, although Cx43 is known to be multiply phosphorylated (Musil et al., 1990; Goldberg and Lau, 1993), it is not clear which sites containing phosphate groups cause a slower mobility on Western blots. There is evidence, however, that the form with the fastest mobility is entirely non-phosphorylated (Crow et al., 1990; Musil et al., 1990; Laird et al., 1991; Saez et al., 1997) and it is this form that appears to be detected by 13-8300. Thus, for tissues we have examined so far, now including spinal cord, we suggested that dephosphorylation at the 13-8300 epitope may be accompanied by dephosphorylation at other, if not all other, sites in the molecule. We did not, however, exclude the possibility that 13-8300 detection of phosphorylated forms of Cx43 having slower mobility on Western blots could occur in other systems where phosphate removal at the 13-8300 epitope may not be accompanied by dephosphorylation at other sites. Evidence for this has, in fact, recently been reported in cultured fibroblasts (Cruciani and Mikalsen, 1999).

Immunorecognition of astrocytic Cx43 by 18A

In several CNS lesion preparations, antibody 18A consistently exhibits loss of Cx43 immunorecognition in tissue sections, which cannot be accounted for by reduced levels or degradation of Cx43 (Vukelic et al., 1991; Hossain et al., 1994b, Ochalski et al., 1995; Sawchuk et al., 1995; Theriault et al., 1997; Li et al., 1998). We now show that this epitope masking also occurs in normal spinal cord following nerve stimulation and that it often coincides spatially and temporally with Cx43 dephosphorylation, suggesting a relationship between the two processes. The molecular basis for this masking is as yet unclear, but is not likely due to phosphorylation of the 18A epitope (amino acids 346-363 of Cx43), which does not appear to contain any known phosphorylation sites (Unger et al., 1999). The nearby

carboxy-terminus of Cx43, however, has been reported to contain a PDZ interaction domain that is able to bind to a PDZ domain in the tight junction protein zona occludens-1 (ZO-1) (Giepmans and Moolenaar, 1998; Toyofuku et al., 1998). As well, myotonic dystrophy protein kinase was reported to be co-localized with Cx43 at gap junctions in cardiac tissue (Mussini et al., 1999). Thus, we speculate that the 18A epitope of Cx43 in astrocytes may undergo blockade of antibody recognition following association of an as yet unidentified protein with possibly the PDZ interaction domain of Cx43. Since epitope masking and Cx43 dephosphorylation almost always occur concomitantly, we further speculate that Cx43 association with a protein that blocks the 18A epitope may be promoted by dephosphorylation at the 13-8300 epitope.

LM and EM immunolabeling in spinal cord

We have previously demonstrated that Cx43 in both brain and spinal cord is localized exclusively to astrocytes (Yamamoto et al., 1990a,b; Ochalski et al., 1997). A striking difference, however, was that labeling with 18A in brain was localized largely at or near astrocytic gap junctions, while in spinal cord it was present at junctions, along non-junctional membranes and intracellularly within astrocytic processes (Ochalski et al., 1997). This is noteworthy for two reasons. First, our EM counts indicate some light and partial labeling of gap junctions with 13-8300 in normal dorsal horn, consistent with Western blot detection of some dephosphorylated Cx43 in this tissue. This may represent a normal complement of dephosphorylated gap junctional Cx43, or it may be due to rapid postmortem Cx43 dephosphorylation, which we have characterized in brain (Hossain et al., 1994c). This low level of labeling appears to be below the sensitivity of LM detection since no 13-8300-ir was seen by LM in normal tissue. It is perhaps curious that little cytoplasmic labeling is found with 13-8300 in control tissue, suggesting that a cytoplasmic pool of Cx43 detectable with 18A in cord remains largely phosphorylated.

Second, nerve stimulation increased the number and immuno-reaction density of gap junctions labeled with 13-8300, but produced a less striking enhancement of cytoplasmic

Cx43-ir. Given the rapid appearance of dephosphorylated Cx43 after nerve stimulation, together with its presence almost exclusively at gap junctions, it is unlikely that induction of labeling with 13-8300 was due to de novo synthesis of Cx43. This is further supported by the lack of any changes in Cx43 labeling with antibody 71-0700, which was generated against an epitope in the molecule different from those recognized by either 18A or 13-8300. Thus, conditions in spinal cord that cause Cx43 dephosphorylation may activate a phosphatase that appears to act selectively on Cx43 localized at gap junctions. Lack of action on the cytoplasmic pool may explain the large proportion of Cx43 that remains phosphorylated after nerve stimulation as seen by Western blotting with antibody 18A.

Neuronal activity and Cx43 dephosphorylation

Neurons in the dorsal horn are mostly quiescent in resting animals and display burst discharges upon peripheral nerve stimulation. Activation of either myelinated fibers by low intensity electrical stimulation or unmyelinated C-fibers increases neuronal discharge in widespread areas of dorsal horn, despite the largely superficial and deep dorsal horn termination areas of unmyelinated and myelinated primary afferent fibers, respectively (Woolf and Fitzgerald, 1983; Woolf and King, 1987; Laird and Bennett, 1993). Thus, our observation that Cx43 dephosphorylation occurs in superficial or deep laminae corresponding to the termination area of the fiber types activated suggests that this response is perhaps more related to the activity of primary afferents than that of dorsal horn neurons. In any event, the nature of neuronal-glial interactions leading to astrocytic Cx43 dephosphorylation remains to be elucidated. Transmitter substances released from primary afferents or dorsal horn neurons may mediate such interactions via a direct action on astrocytes, which are endowed with a host of neurotransmitter receptors linked to intracellular signaling cascades (Hosli and Hosli, 1993; Kimelberg, 1995). Alternatively, such interactions may be mediated by changes in ionic milieu, particularly elevation of extracellular K^+ in the dorsal horn by even low levels of sciatic nerve stimulation (Kriz et al., 1974; Walz, 1989). This is less likely, however, since extracellular $[K^+]$ in the ventral

horn can be increased to levels similar to those observed in the dorsal horn following antidromic activation of motor axons at frequencies similar to those used here (Vyklicky et al., 1972; Kriz et al., 1974), yet no Cx43 dephosphorylation was observed in the ventral horn.

Astrocytic Cx43 after sciatic nerve transection

Facial nerve transection was reported by Rohlmann et al. (Rohlmann et al., 1993, 1994) to cause a rapid increase (within 45 min) in Cx43 immunostaining in the facial nucleus. Using 13-8300, which was generated against a similar Cx43 sequence as the antibody employed by Rohlmann et al. (Rohlmann et al., 1993, 1994), we observed no changes in Cx43 labeling in the ventral horn after sciatic nerve transection. These differing results may be due to differences in the properties of astrocytes in the facial nucleus compared with those in spinal cord motor nuclei. Sciatic nerve transection did, however, elicit a pattern of superficial dorsal horn 13-8300 labeling similar to that seen after skin application of capsaicin, suggesting that Cx43 dephosphorylation following nerve transection is due to activation of C-fibers. This is consistent with findings that sciatic nerve transection induces prolonged unmyelinated fiber discharge comparable in duration and frequency to that evoked in C-fibers by capsaicin (Wall et al., 1974; Blenk et al., 1996).

Regulation of astrocyte coupling

Relationships between Cx43 phosphorylation state and GJIC have been examined in a few studies, but has yet to be fully clarified. In cells lines and peripheral tissues, both increases and decreases in GJIC have been seen following Cx43 dephosphorylation (Godwin et al., 1993; Moreno et al., 1994; Oelze et al., 1995). In cultured astrocytes subjected to hypoxia, Cx43 dephosphorylation occurred after reduced dye-coupling (Cotrina et al., 1998a). We have found that hypoxia-induced Cx43 dephosphorylation is accompanied by reduced GJIC in cultured astrocytes and that both of these events can be partially reversed by inhibitors of protein phosphatase (Li and Nagy, 2000b). Thus, it may be tentatively concluded that Cx43

dephosphorylation in astrocytes in vitro and perhaps in vivo results in reduced GJIC. Astrocytes are thought to be essential for maintaining neuronal excitability by accumulating extracellular K^+ (Orkand et al., 1966; Newman, 1985; Walz, 1989) and possibly by providing neurons with energy substrate in the form of lactate (Tsacopoulos and Magistretti, 1996). These processes are likely facilitated by gap junction-mediated intercellular flow of ions and metabolites between astrocytes distributed among active and inactive neurons. What purpose could then be served by the counterintuitive process of channel closure at junctions composed of Cx43 within the astrocytic syncytium if such closure indeed occurs under physiological conditions? As discussed in detail elsewhere (Nagy and Dermietzel, 2000), this may be related to the dynamic creation of open and closed junctional pathways for routing substances between astrocytes according to neuronal needs. In addition, transiently reduced coupling may be important for maintenance of normal metabolism since it has been observed (Tabernero et al., 1996; Giaume et al., 1997) that glucose uptake and glycolysis within astrocytes is linked to their state of gap junctional coupling such that the former is increased when astrocytic GJIC is reduced. Further studies of these issues will need to take into consideration the additional presence of Cx30 at astrocytic junctions and the regulatory responses of this connexin to neuronal activity.

Figure legends

Fig. 1. Photomicrographs showing Cx43 detection with antibody 18A and 13-8300 in rat spinal cord dorsal horn after unilateral sciatic nerve stimulation on the right side compared with control unstimulated left side. In all sections, labeling on the control side is dense with antibody 18A and virtually absent with 13-8300. **A,B:** After 1 h of nerve stimulation, 18A-ir is reduced in the dorsal horn (A, arrows), while 13-8300-ir is induced in the corresponding area of an adjacent section (B, arrows). **C,D:** After 15 min of sciatic nerve stimulation, 18A-ir is slightly reduced in deeper laminae (C, arrows) and 13-8300-ir is induced in the superficial half of the dorsal horn (D, arrows). Magnifications: A-D, x50.

Fig. 2. Photomicrographs showing Cx43 detection with antibody 18A and 13-8300 in spinal cord dorsal horn after 1 h electrical stimulation of A-fibers in the sciatic nerve or C-fiber activation by topical capsaicin applied to the left hind skin. **A-C:** A-fiber stimulation slightly reduced 18A-ir in the dorsal horn on the stimulated (B, arrows) compared with control unstimulated (A) side, and induced 13-8300-ir in dorsal horn laminae subjacent to the substantia gelatinosa (C, arrows). **D:** The 13-8300-ir seen in C is eliminated in an adjacent section after preadsorption of 13-8300 with peptide antigen. **E:** After cutaneous C-fiber activation, dense 13-8300-ir is seen in superficial laminae on the side (left, arrows) corresponding to that of capsaicin application, while no labeling is seen on the control side or elsewhere in the spinal cord. **F:** Higher magnification of 13-8300-ir in E shows the punctate appearance of labeling. Magnifications: A,B, x110; C-E, x50; F, x330.

Fig. 3. Photomicrographs showing antibody detection of Cx43 in the spinal cord dorsal horn 1 h after unilateral sciatic nerve transection. **A,B:** A slight reduction in 18A-ir is seen in dorsal horn laminae I and II of the transected (B) compared with the control (A) side. **C,D:** 13-8300-ir is induced in superficial laminae ipsilateral to nerve transection (D, arrows), but remains undetected on the contralateral control side (C). Magnifications: A,B, x110; C,D, x90.

Fig. 4. Electron micrographs of immunolabeling for Cx43 with antibody 18A in spinal cord dorsal horn contralateral and ipsilateral to unilateral sciatic nerve electrical stimulation. **A:** In contralateral control areas, diffuse labeling is seen in astrocyte processes (arrows) and at gap junctions between these processes (arrowheads, magnified in inset). **B-D:** After stimulation of sciatic nerve for 1 h, labeling is seen in astrocyte processes (B, arrows), and astrocytic gap junctions are either densely stained (C, arrows), lightly stained (C, arrowhead) or unlabelled (D, arrowhead) despite the presence of cytoplasmic 18A-ir in nearby processes (D, arrows). Magnifications: A, x13,000; inset, x82,000; B, x20,000; C, x95,000; D, x46,000.

Fig. 5. Electron micrographs of immunolabeling for Cx43 with antibody 13-8300 in normal spinal cord dorsal horn. **A-C:** Cytoplasmic 13-8300-ir is very sparse and typical gap junctions distributed in neuropil are generally unlabelled (A,B, arrowheads) or occasionally lightly labeled (C, arrowheads). **D:** A partly labeled gap junction (arrow; magnified in lower inset) is seen in the same field as two unlabelled junctions (arrowheads; magnified in upper inset). Magnifications: A, x20,000; B, x140,000; C, x95,000; D, x32,000; upper inset, x87,000; lower inset, x76,000.

Fig. 6. Electron micrographs of immunolabeling for Cx43 with antibody 13-8300 in spinal cord dorsal horn after 1 h of sciatic nerve electrical stimulation. **A:** Labeling is seen dispersed in astrocyte processes (arrows) as well as at gap junctions between labeled processes (arrowheads). **B:** Two fibrous astrocyte processes containing intermediate filaments (if) are seen forming a densely labeled gap junction (arrowhead). **C,D:** Gap junctions display either an equal density of labeling on each side of the junctional membranes (C, arrowheads) or occasionally exhibit labeling on only one side (D, arrow) and not the other (D, arrowhead). Magnifications: A, x22,000; B, x35,000; C, x90,000; D, x124,000.

Fig. 7. Western blots showing Cx43 phosphorylation state in spinal cord dorsal horn after cutaneous C-fiber activation by capsaicin. **A:** Blot probed with antibody 18A shows detection of both phosphorylated and non-phosphorylated Cx43 migrating at Mr of 43 and 41 kDa, respectively, with the former predominating on both control (lane 1) and stimulated (lane 2) sides of the dorsal horn. **B:** Blot probed with antibody 13-8300 shows detection of only the non-phosphorylated form migrating at Mr 41 kDa. Control animals display an equal level of this form in the left (lane 1) and right (lane 2) dorsal horn. Topical capsaicin application to the right hind flank for 1 h induces an increase in the non-phosphorylated form in the ipsilateral (lane 4) compared with the contralateral control dorsal horn (lane 3).

Table 1. Comparison of the proportion of astrocytic gap junctions that are unlabelled and immunolabelled with antibody 13-8300 in control spinal cord dorsal horn and in dorsal horn after sciatic nerve electrical stimulation

	Control		SNS	
	Unlabelled	Labelled	Unlabelled	Labelled
Average	118 ± 10 (65%)	66 ± 9 (35%)	4 ± 1* (2%)	186 ± 7* (98%)
Total counted	353	197	11	558

Control, control side; SNS, sciatic nerve stimulated side. Values are means ± SEM of three animals. * $P < 0.01$. Values in parentheses indicate percentage of unlabelled and labelled junctions in control or stimulated animals. Total counted indicates the cumulative number of gap junctions counted in 3 animals.

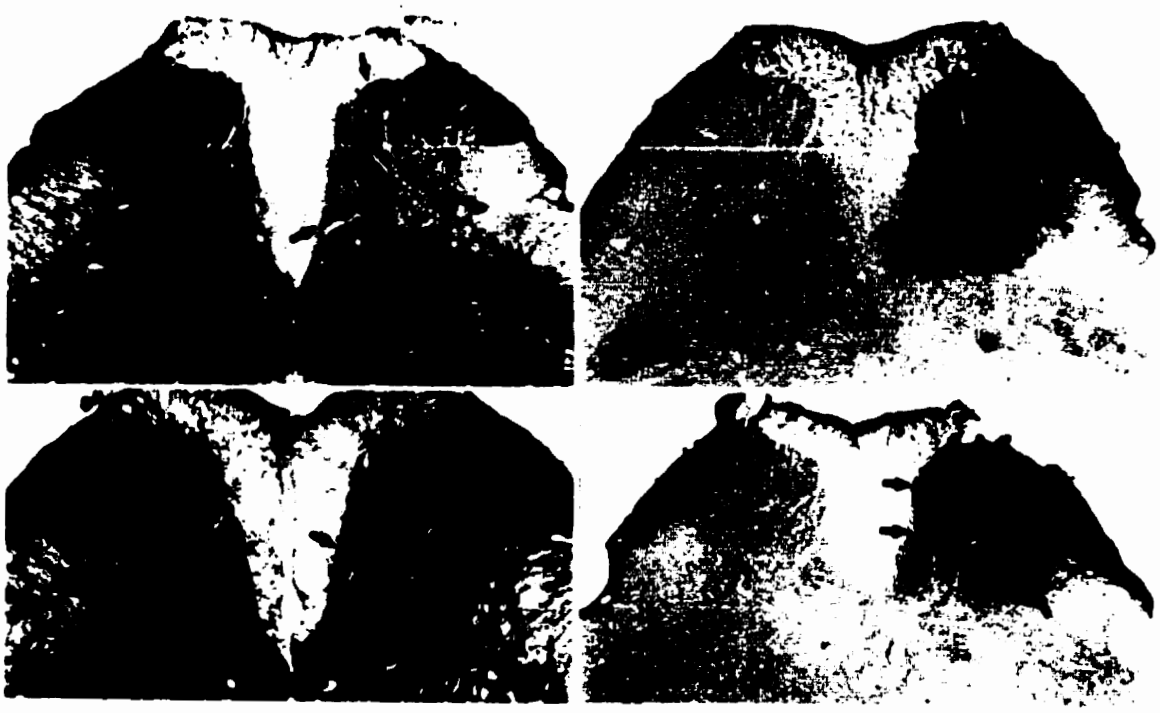

Fig. 1

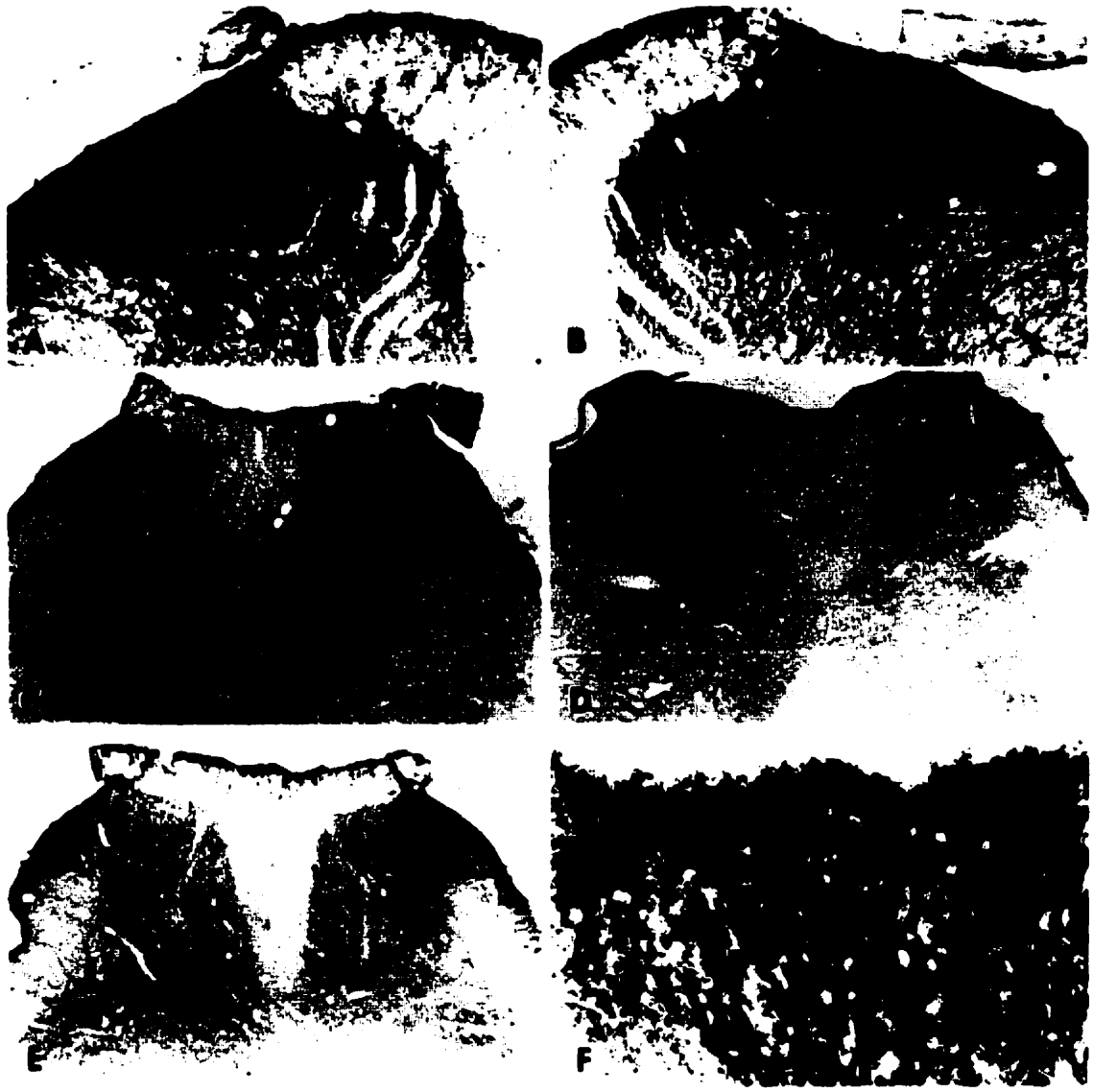

Fig. 2

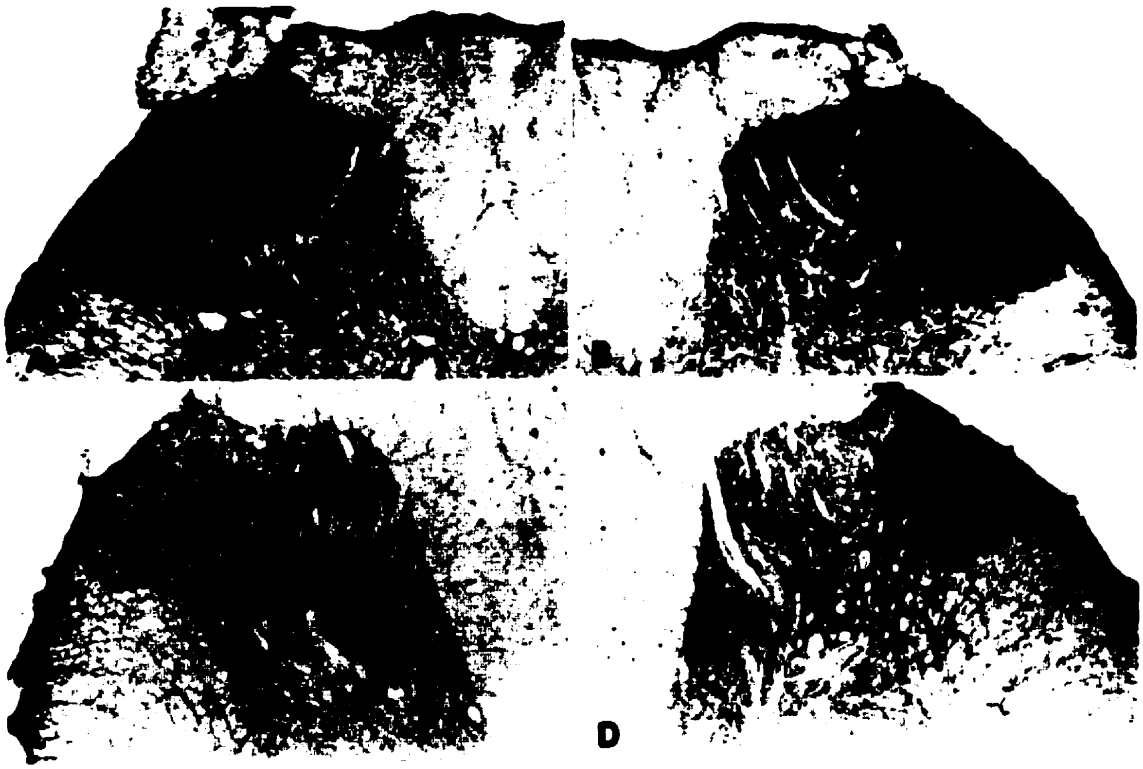

Fig. 3

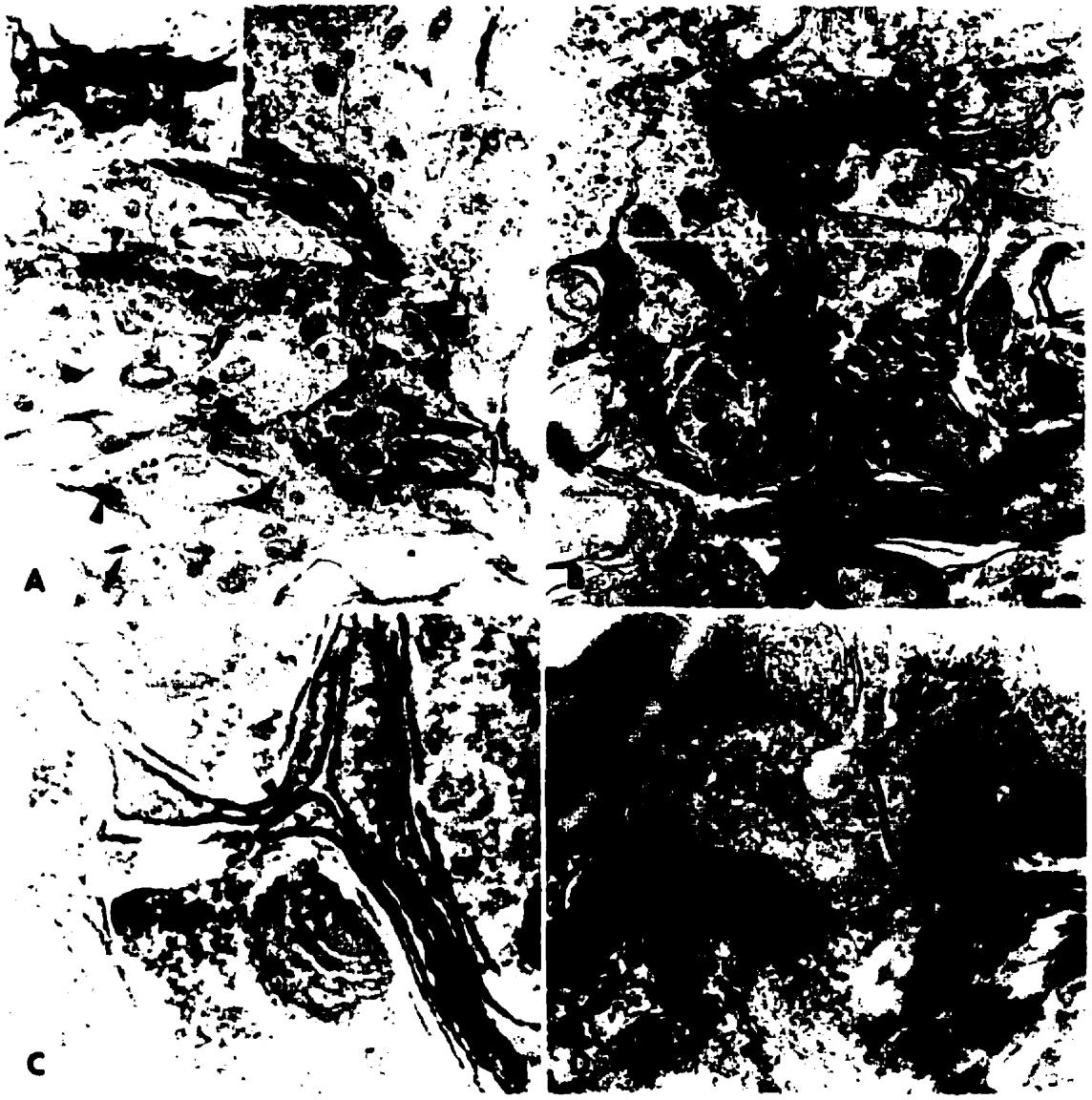

Fig. 4

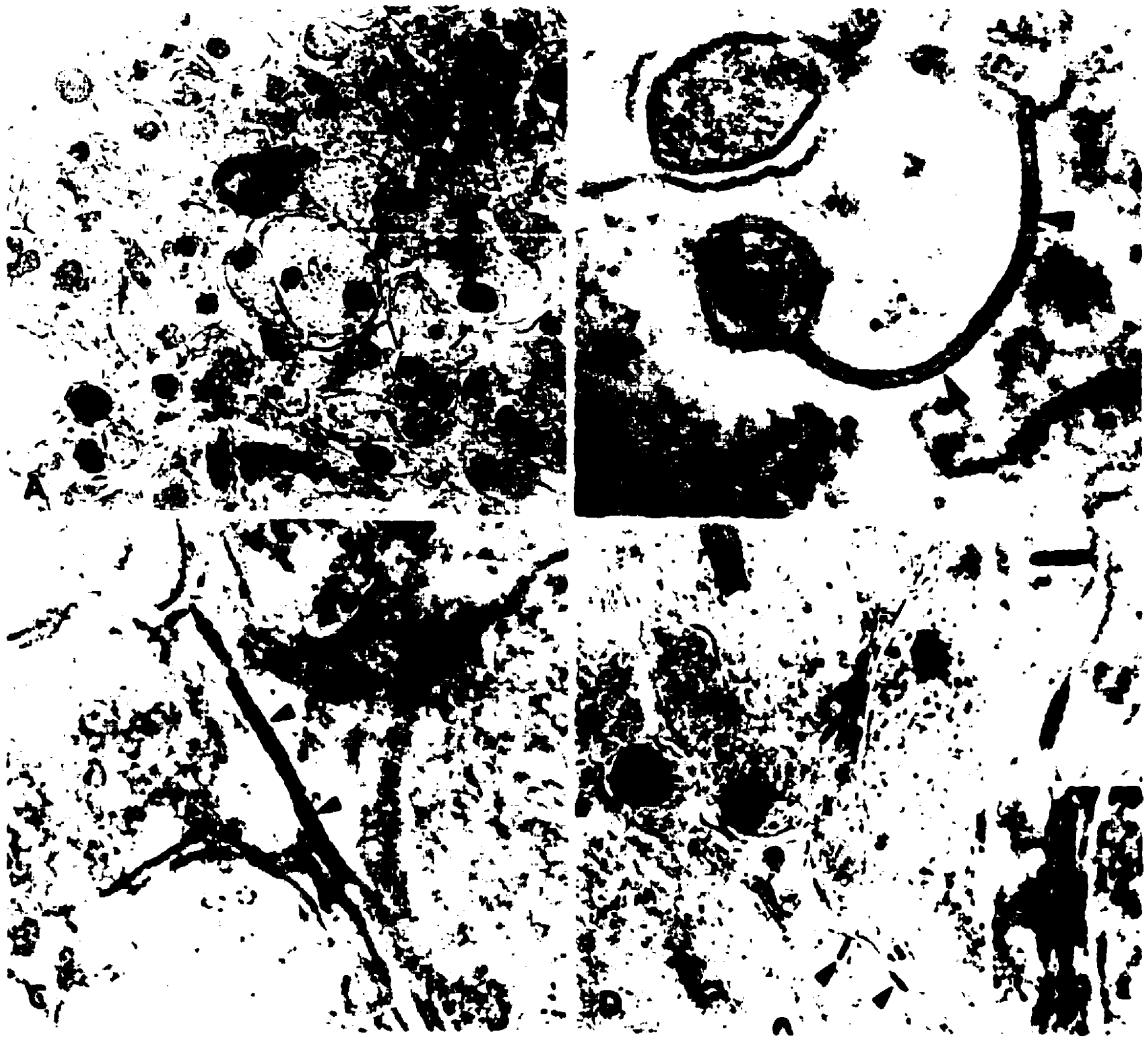

Fig. 5

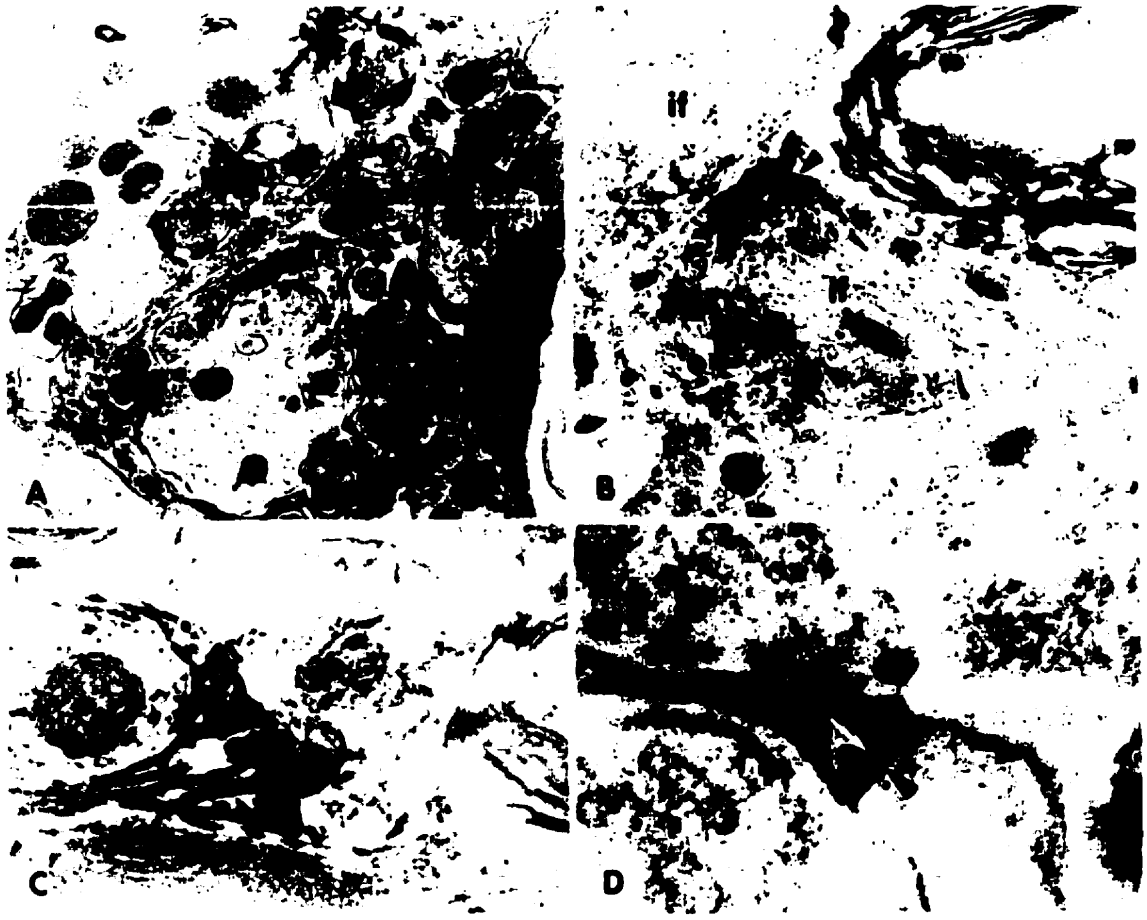

Fig. 6

Fig. 7

Part V

Connexin43 Phosphorylation State and Gap Junctional Intercellular Communication in Cultured Astrocytes Following Hypoxic Treatments and Inhibition of Protein Phosphatases

Li, W. E. I. and Nagy, J. I.

European Journal of Neuroscience, submitted

Abstract

The effects of hypoxia and phosphatase inhibitors on connexin43 (Cx43) phosphorylation state, gap junctional intercellular communication (GJIC) and immunolabeling with anti-Cx43 antibodies were investigated in cultured rat astrocytes. Astrocytes contained predominantly phosphorylated forms of Cx43, and these underwent dephosphorylation 30 min after hypoxia. This was preceded by a 77% reduction in GJIC 15 min after hypoxia, suggesting that this degree of reduced GJIC is not likely a direct result of massive Cx43 dephosphorylation. Hypoxia caused a reduction in punctate immunostaining (epitope masking) at cell-cell contacts with one anti-Cx43 antibody (18A), and increased labeling with another antibody (13-8300) that detects only a dephosphorylated form of Cx43 in astrocytes. Inhibition of type-1 protein phosphatases (PP-1) and type-2 protein phosphatases (PP-2A) with okadaic acid or calyculin A stimulated Cx43 phosphorylation in normal astrocytes, but only slightly inhibited hypoxia-induced Cx43 dephosphorylation. Inhibition of PP-2B (calcineurin) with cyclosporin A or FK506 had no effect in normal astrocytes, but reduced the degree of Cx43 dephosphorylation and junctional uncoupling seen after hypoxia. Co-application of calyculin A with calcineurin inhibitors completely prevented hypoxia-induced Cx43 dephosphorylation. These results demonstrate that responses of astrocytic Cx43 to hypoxia in vitro are similar to those seen after ischemia in vivo, suggesting that these responses can occur after direct injury to astrocytes. Further, inhibition of protein phosphatases may protect astrocytes from hypoxia-induced processes that lead to Cx43 dephosphorylation and junctional uncoupling. Alternatively, calcineurin in particular may play a direct role in the regulation of astrocytic GJIC and Cx43 phosphorylation state.

Introduction

Astrocytes in the central nervous system (CNS) express the two gap junctional proteins Cx43 and connexin30 (Cx30), and are extensively linked by gap junctions composed of these connexins (Mugnaini, 1986; Yamamoto et al., 1990a,b; Nagy et al., 1997a, 1999; Kunzelmann et al., 1999; Nagy and Rash, 1999; Nagy and Dermietzel, 2000). As in peripheral tissue where junctional channels allow cell-to-cell passage of ions and metabolites (Bruzzone et al., 1996; Goodenough et al., 1996; Kumar and Gilula, 1996), GJIC between astrocytes is thought to coordinate the activity of these cells and may be important for K^+ spatial buffering as well as dispersion of signaling molecules and energy substrates (Newman, 1985; Walz, 1989; Wolburg and Rohlmann, 1995; Giaume and McCarthy, 1996; Giaume et al., 1997; Rose and Ransom, 1997). In further analogy with other cell types, astrocytic GJIC may be a dynamic process subject to regulation by a variety of factors including pH, neuroactive substances and growth factors (Anders, 1988; Giaume and McCarthy, 1996; Reuss and Unsicker, 1998). One mechanism for regulation of events ranging from connexin trafficking to gap junction channel gating is connexin phosphorylation, which has been extensively studied in cells coupled by Cx43 (Bruzzone et al., 1996; Goodenough et al., 1996; Lau et al., 1996; Unger et al., 1999). Several protein kinases act on Cx43 (Loo et al., 1995; Warn-Cramer et al., 1996; Saez et al., 1997; Kanemitsu et al., 1998) and both tyrosine and a number of serine phosphorylation sites have been identified in this connexin (Lau et al., 1996; Saez et al., 1997). Cx43 phosphorylation is correlated with alterations in junctional coupling (Swenson et al., 1990; Warn-Cramer et al., 1998), and its dephosphorylation is correlated with either decreased GJIC (Godwin et al., 1993; Oelze et al., 1995) or, conversely, increased channel conductance (Moreno et al., 1994). In cultured astrocytes exposed to chemical hypoxia, Cx43 dephosphorylation occurred in conjunction with reduced GJIC (Cotrina et al., 1998a).

We have reported that the vast proportion of Cx43 in normal brain is phosphorylated in vivo and that it undergoes dephosphorylation during brain extraction or in response to ischemic injury (Hossain et al., 1994c; Li et al., 1998). Cx43 dephosphorylation also occurs

in normal spinal cord after peripheral nerve stimulation (Li and Nagy, 2000a). This dephosphorylation was often accompanied by altered recognition of Cx43 (epitope masking) by various antibodies (Li et al., 1998; Li and Nagy, 2000a). Relationships between astrocytic GJIC, Cx43 dephosphorylation and epitope masking following these manipulations in vivo are not yet clear, but may be important for understanding of how astrocytes regulate their junctional coupling during normal neural activity or after CNS injury. To address these issues in a reduced system, we investigated whether Cx43 in cultured astrocytes exhibits responses to injury similar to that seen in vivo and we examined the contribution of various phosphatases to hypoxia-induced alterations in Cx43 phosphorylation state and astrocytic gap junctional coupling status.

Materials and methods

Connexin antibodies

Two polyclonal anti-Cx43 antibodies (designated 18A and 71-0700), a monoclonal anti-anti-Cx43 (designated 13-8300) and a polyclonal anti-Cx30 (designated 71-2200) were used in this study. The latter three antibodies were obtained from Zymed Laboratories (South San Franscico, CA). These antibodies were generated against peptides corresponding to different sequences within the carboxy-terminus tail of Cx43 or Cx30 and have been extensively characterized for specific detection of these connexins by immunohistochemistry, Western blotting and antibody preadsorption with synthetic peptide in a variety of tissues (Yamamoto et al., 1990a,b; Hossain et al., 1994c; Ochalski et al., 1995,1997; Nagy et al., 1997b, 1999; Li et al., 1998; Li and Nagy, 2000a). Antibody 13-8300 was previously shown by us to detect selectively a dephosphorylated form of Cx43 in Western blots of several tissues and cultured cells (Nagy et al., 1997b; Li et al., 1998; Li and Nagy, 2000a).

Primary astrocyte culture

Astrocytes from cerebral cortices of 2 day old Sprague-Dawley rats were cultured in DMEM/F12 containing 10% FBS according to a previously described protocol with some

modifications (McCarthy and DeVellis, 1980). Briefly, tissue was minced after removing meninges, digested with trypsin in a divalent cation-free Hank's balanced salt solution (HBSS) for 30 min, triturated with a polished Pasteur pipette and plated in plastic culture flasks (Falcon) with medium for an initial period of about 7 days. Once cultures reached a confluency of about 80%, the flasks were shaken at 280 rpm on a rotary shaker for approximately 18 h. After removing culture medium, cells remaining attached were rinsed twice with HBSS free of divalent cations, detached by incubation with trypsin and replated on plastic cultured dishes (Falcon) or poly-L-lysine coated glass coverslips. The medium was changed every 3 days. Cultures contained large type-1-like astrocytes as judged from the appearance of cells under phase contrast microscopy and were about 98% pure as indicated by immunostaining for astrocytes-specific glial fibrillary acidic protein (GFAP) using a polyclonal antibody (DAKO). Just before use in all experiments, astrocyte cultures were transferred to HBSS. Studies involving hypoxia, Western blotting, immunohistochemistry and analysis of cell coupling were repeated using at least two separate preparations of astrocytes. With each preparation, these procedures were conducted either in duplicate or triplicate.

Induction of hypoxia

Hypoxia was mimiced in cultured astrocytes by standard chemical methods as previously described (Cotrina et al., 1998a), except that the concentrations of the agents used here to produce energy depletion were lower than those typically employed (Gramolini and Renaud, 1997; Frey et al., 1998). This involved the transfer of cultures to HBSS and bath application of 0.3 mM sodium iodoacetate (Sigma) and 1 mM potassium cyanide (Fisher) dissolved in HBSS. Cell viability was examined using a trypan blue exclusion assay in which the dye is taken up by dead cells, but excluded by live cells during a 5 min incubation with 0.4% trypan blue (Sigma). Cultured astrocytes maintained for up to 2 h in HBSS appeared healthy and were devoid of trypan blue staining. Cells subjected to longer incubation in HBSS had darkened cytoplasm suggestive of apoptosis. This limited use of these cultures to a

maximum of 2 h under these conditions. Astrocytes receiving hypoxic treatment for up to 1 h had an appearance similar to control astrocytes under phase contrast microscopy and were also devoid of trypan blue staining. However, uptake of dye in a small proportion of astrocytes began to appear 1 h after hypoxia and the number of dye-positive cells increased progressively thereafter. Hypoxic treatments were therefore limited to a maximum of 30 min, except for time-course analysis of junctional uncoupling and Cx43 dephosphorylation after hypoxia, which was examined over a period of 1 h.

Treatment of cultures with phosphatase inhibitors

Control and hypoxic astrocytes were treated with a panel of serine/threonine protein phosphatase inhibitors including the PP-1 and PP-2A inhibitors okadaic acid (Sigma) and calyculin A (Research Biochemicals Inc), and the PP-2B (calcineurin) inhibitors cyclosporin A (Sigma) and FK506 (generously provided by Fugisawa Pharmaceutical Co., Japan). Stock solutions of okadaic acid and calyculin A were prepared in dimethyl sulfoxide (DMSO) and diluted with HBSS to produce working concentrations of 1 μM and 10 nM, respectively. Stock solutions of cyclosporin A and FK506 were prepared in anhydrous ethanol and diluted in HBSS to yield working concentrations of 1 μM and 100 nM, respectively. These agents were applied 5 min before the initiation of hypoxia. Sister cultures of astrocytes on separate dishes or coverslips served as controls or were treated with either hypoxia, phosphatase inhibitors, or hypoxia plus phosphatase inhibitors. Control cultures were treated with vehicle concentrations of DMSO or ethanol after it had been determined that these agents alone had no effect on cell morphology, trypan blue staining, Cx43 immunolabeling or dye-coupling state compared with astrocytes incubated in HBSS alone or astrocytes maintained in normal culture medium. In preliminary studies, astrocytes incubated with 1% DMSO for over 3 h displayed increased immunolabeling with antibody 13-8300, indicating altered Cx43 expression and/or phosphorylation. These changes were eliminated when final

concentrations of DMSO in cultures were limited to less than 0.5% applied for less than 1 h in all subsequent experiments.

Western blotting

Astrocytes in culture dishes were harvested and homogenized in 40 mM Tris HCl buffer, pH 7.4, containing 1 mM phenylmethylsulphonyl fluoride, 5 μg/ml each of leupeptin, pepstatin and the phosphatase inhibitors sodium fluoride (10 mM) and sodium orthovanadate (1 mM). Total homogenate protein was determined using a Bio-Rad assay kit. Sodium dodecylsulphate polyacrylamide gel (9%) electrophoresis (SDS-PAGE) and Western blotting on polyvinylinene difluoride (PVDF) membranes were performed as previously described using antibodies 18A at a dilution of 1:400,000, 13-8300 at a dilution of 1:750 and 71-2200 at a dilution of 1:500 (Hossain et al., 1994c; Li et al., 1998; Nagy et al., 1999a; Li and Nagy, 2000a). Blots probed with 18A and 13-8300 were loaded with 1 and 10 μg of protein per lane, respectively, and blots probed with 71-2200 were loaded with 30 μg of protein per lane. Tissue homogenates from rat hippocampus and cerebral cortex were used as positive controls for antibody 71-2200 detection of Cx30.

Alkaline phosphatase digestion of immobilized protein

Alkaline phosphatase dephosphorylates proteins at phosphoserine and phosphotyrosine residues (Crow et al., 1990; Musil et al., 1990; Cahill and Perlman, 1991; Holmes et al., 1996) and was used here to dephosphorylate Cx43 immobilized on PVDF membranes. Protein samples from homogenates of brain tissue prepared as described (Hossain et al., 1994c; Li et al., 1998) were separated by SDS-PAGE and transblotted onto membranes. Blots of a phosphoprotein-enriched sample from epidermal growth factor (EGF)-stimulated A431 cells (Signal Transduction Laboratories) was included as a positive control for alkaline phosphatase activity. Prior to incubation with enzyme, membranes were blocked overnight at 4 °C and subsequently at room temperature for 3 h in 20 mM Tris-buffer, pH

7.4, containing 0.9% saline and 1% Tween-20. Membranes were then briefly washed in Tris-buffered saline and equilibrated in two changes of incubation buffer (0.1 M diethanolamine and 1 mM $MgCl_2$, pH 10). A region of membrane corresponding to the migratory position of Cx43 was excised, placed in sealed plastic containers containing 300 units/ml of activated alkaline phosphatase (Sigma) and incubated at 37 °C for 4 h. Control membranes were similarly treated except without alkaline phosphatase. Following incubation, membranes were washed for 20 min in 20 mM Tris-HCl buffer, pH 7.4, containing 0.9% saline and probed with anti-Cx43 antibodies.

Tyrosine phosphorylation of Cx43

The tyrosine phosphorylation state of Cx43 in cultured astrocytes was examined by immunoprecipitation of astrocyte lysate with a monoclonal phosphotyrosine antibody (4G10, Upstate Biotechnology) using a protocol provided by the manufacturer. As a positive control for this procedure, some astrocyte cultures were treated with the tyrosine phosphatase inhibitor pervanadate, which has been shown to induce tyrosine phosphorylation of Cx43 in several other cell types (Mikalsen et al., 1997, Cruciani and Mikalsen, 1999). Homogenates from control, hypoxic and pervanadate-treated astrocytes were analyzed by Western blotting with anti-Cx43 antibody 18A and 13-8300. Pervanadate was prepared as previously described (Mikalsen et al., 1997). Briefly, 30 mM sodium orthovanadate (Sigma) was activated by incubation in 60 mM H_2O_2 for 15 min and then diluted in HBSS for addition to cultures at a final concentration of 100 μM.

Immunohistochemistry

For immunofluorescence staining, cells were fixed for 30 min in a 0.1 M sodium phosphate buffer (PB, pH 7.4) containing 4% paraformaldehyde. Single and double immunofluorescence labeling with anti-Cx43 antibodies 18A and 13-8300 were performed as previously described with some modifications (Nagy et al., 1997b; Li et al., 1998). After

a 1 h wash in PB containing 0.9% saline and 0.3% Triton X-100 (PBST), cells were incubated for 30 min in PBST containing 1% skim milk. All subsequent incubations with primary and secondary antibodies, and all wash steps were conducted with PBST containing 0.1% skim milk. Primary antibodies 18A and 13-8300 were used at a dilution of 1:1,000 and 1:500 for single labeling, respectively. For simultaneous labeling with both antibodies, 18A was diluted 1:500. Cy3-conjugated donkey anti-mouse and Cy2-conjugated goat anti-rabbit IgG (Jackson Immunoresearch Laboratories) diluted 1:250 and 1:100 were used as secondary antibodies. Immunofluorescence for GFAP was conducted as we previously described (Nagy et al., 1996c). Immunolabeled cells were coverslipped with anti-fade medium and examined with a Leitz Dialux-20 microscope. Astrocytes grown on glass coverslips were more vulnerable to the deleterious actions of okadaic acid and calyculin A than those grown on plastic dishes. A 35 min incubation with either of these phosphatase inhibitors caused near total detachment of astrocytes from coverslips, thus precluding immunohistochemical and dye-coupling analysis following treatment with these inhibitors, which was typically conducted using cells on coverslips.

Dye-coupling in cultured astrocytes

Following a change to HBSS, gap junctional communication between confluent astrocytes grown on 12 mm glass coverslips placed in 35 mm cultures dishes was assessed by intercellular transfer of tracer loaded into single astrocyte either by intracellular microinjection of lucifer yellow (LY) (Sigma) or by single-cell-scrape-loading (SCSL) of biocytin (Sigma). For intracellular injection, a solution of 1% LY dissolved in 0.33 M lithium chloride was pressure injected into individual astrocyte over a duration of 2 min as we previously described (Hossain et al., 1995). Intercellular dye diffusion was allowed to take place for a further 1 min. Cells were subsequently fixed for 15 min in PB containing 4% paraformaldehyde, washed in 50 mM Tris-HCl, pH 7.4, coverslipped with anti-fade medium and viewed under a fluorescence microscope. The SCSL approach was essentially the standard scrape-loading method (el-Fouly et al., 1987) for measurements of GJIC, but

modified here for analysis at a single cell level. Astrocytes were briefly washed with HBSS free of divalent cations and incubated in this solution containing 0.2% biocytin. A single astrocyte within the monolayer was then identified by phase contrast microscopy, scraped open with a micropipette (3 μm tip diameter) attached to a micromanipulator and biocytin was allowed to diffuse to adjacent astrocytes for 3 min. The coverslips were then washed in normal HBSS and fixed as above for 30 min. After a 30 min wash in PBST, astrocytes were incubated at 4 °C for 1.5 h at room temperature with Cy3-conjugated streptavidin (Sigma) diluted 1:100. The cells were then washed for 20 min in PBST, further washed for 20 min in 50 mM Tris-HCl buffer, pH 7.4, and coverslipped with anti-fade medium. The number of LY- or Cy3-labelled astrocytes were counted and statistical analysis of differences between experimental treatment was conducted by Student's t-test. For control astrocyte cultures and those receiving various treatments, a total of 4 widely separated astrocytes per coverslip were injected or scraped for analysis of coupling. This was repeated using a minimum of three coverslips per treatment condition.

Results

Cx43 immunorecognition following alkaline phosphatase treatment

It has previously been shown that phosphorylated forms of astrocytic Cx43 migrating at 43 kDa on Western blots predominate in rat brain in vivo and that the protein undergoes rapid postmortem dephosphorylation to a form migrating at 41 kDa (Hossain et al., 1994c; Li et al., 1998). Further, we have reported that anti-Cx43 antibody 13-8300 detects only the fastest migrating 41 kDa form in some cell types, and suggested that lack of detection of phosphorylated forms may be due to epitope blockade by phosphate groups (Nagy et al., 1997b; Li et al., 1998). Our first aim here was to confirm that this possibility also applies to Cx43 in astrocytes, thereby extending utility of antibody 13-8300 in the present study. Western blotted PVDF membranes of brain homogenates containing largely the phosphorylated forms of Cx43 were incubated with alkaline phosphatase to dephosphorylate

phosphoproteins and were then probed with various anti-Cx43 antibodies. Control membranes received mock incubations without this enzyme. Antibodies 18A and 71-0700 recognize all forms of Cx43 in untreated blots (Fig. 1A, lanes 1 and 3, respectively), and alkaline phosphatase treatment had no effect on Cx43 recognition by either of these antibodies (Fig. 1A, lanes 2 and 4). Antibody 13-8300 detects only the fastest migrating 41 kDa form of Cx43 in untreated samples (Fig. 1A, lane 5), but reacts with the slower migrating forms after alkaline phosphatase treatment (Fig. 1A, lane 6).

As a positive control to show that phosphoproteins bound to PVDF membranes were susceptible to dephosphorylation by alkaline phosphatase, blots containing protein from EGF-stimulated A431 epithelial cells were treated with or without alkaline phosphatase and probed with a phosphotyrosine antibody. Numerous proteins were detected by this antibody in untreated samples (Fig. 1B, lane 1), while detection of these after alkaline phosphatase treatment was greatly reduced (Fig.1B, lane 2), indicating effective dephosphorylation of phosphoproteins by alkaline phosphatase at phosphotyrosine, serine and threonine residues as has previously been reported (Crow et al., 1990; Musil et al., 1990; Cahill and Perlman, 1991; Holmes et al., 1996). This together with reports that the faster migrating 41 kDa form of Cx43 and the slower migrating 43 kDa forms correspond, respectively, to non-phosphorylated and phosphorylated Cx43 (Crow et al., 1990; Musil et al., 1990; Laird et al., 1991; Saez et al., 1997) suggests that antibody 13-8300 detects only dephosphorylated Cx43 in astrocytes.

Astrocytic Cx43 dephosphorylation after hypoxia

We next examined the effect of chemical hypoxia on the phosphorylation state of Cx43 in cultured astrocytes. In control astrocytes, anti-Cx43 antibody 18A detected three bands, a single band at approximately 41 kDa and a more intense doublet of bands at about 43 kDa (Fig. 2A, lane 1). Antibody 13-8300 detected only a weak band at 41 kDa (Fig. 2B, lane 1). Cultured astrocytes thus contain both phosphorylated and non-phosphorylated forms of Cx43 with a preponderance of the former. Hypoxic treatments for 1 or 5 min did not alter

the relative proportions of these forms (Fig. 2A, lanes 2 and 3), and did not alter levels of the 41 kDa form detected by 13-8300 (Fig. 2B, lanes 2 and 3). Hypoxia for 15 min lead to only a slight increase in the 41 kDa forms (Fig. 2A,B, lane 4). As indicated by both antibody 18A and 13-8300, substantial dephosphorylation occurred only after 30 min of hypoxia (Fig. 2A,B, lane 5), and this was further increased after 1 h of hypoxia (Fig. 2A,B, lane 6). The concomitant disappearance of the 43 kDa forms and appearance of the 41 kDa forms, together with similar results obtained when hypoxia was induced in the presence of cycloheximide (not shown), suggest that the increased levels of the 41 kDa form was not due to de novo synthesis of the protein, but rather to Cx43 dephosphorylation.

Inhibition of hypoxia-induced Cx43 dephosphorylation

The phosphatases that may contribute to hypoxia-induced Cx43 dephosphorylation in cultured astrocytes were investigated by treatment of cultures with various phosphatase inhibitors added 5 min prior to the beginning of hypoxia exposure. Okadaic acid and calyculin A were used to inhibit PP-1 and PP-2A phosphatases, and cyclosporin A and FK506 were used to inhibit the phosphatase activity of calcineurin. During 35 min treatment of control cultures with okadaic acid or calyculin A, astrocytes retracted their processes, rounded up and dissociated from each other as well as from the culture dish. However, hypoxia appeared to protect against this response such that when induced within 5 min after addition of these agents, a sufficient proportion appeared normal and remained attached to allow analysis of Cx43 phosphorylation state. In contrast, cyclosporin A and FK506 did not alter astrocyte appearance when added to control cultures (not shown).

Compared with control astrocytes containing largely phosphorylated, but also non-phosphorylated forms of Cx43 (Fig. 3A, lane 1), addition of either 1 μM okadaic acid (Fig. 3A, lane 3) or 10 nM calyculin A (Fig. 3A, lane 5) to cultures without hypoxia increased the phosphorylated Cx43 kDa and eliminated non-phosphorylated 41 kDa forms of Cx43. Application of these agents at lower concentrations (0.1-0.5 μM and 1-5 nM, respectively)

reduced their stimulatory effect on Cx43 phosphorylation (not shown). Compared with hypoxic astrocytes containing only dephosphorylated Cx43 as seen with antibody 18A (Fig. 3A, lane 2) or 13-8300 (Fig. 3B, lane 2), addition of either okadaic acid (Fig. 3A,B, lane 4) or calyculin A (Fig. 3A,B, lane 6) only slightly reduced hypoxia-induced Cx43 dephosphorylation. No greater effect was seen after doubling the concentration of either agent or adding them in combination (not shown). Thus, inhibition of PP-1 and PP-2A evoked an increase in Cx43 phosphorylation in control astrocytes, but these phosphatases contribute minimally to Cx43 dephosphorylation in hypoxic astrocytes.

Shown in Figure 4 are the effects of calcineurin inhibition on Cx43 phosphorylation state in control and hypoxic astrocytes as revealed by antibody 18A (Fig. 4A,C) and 13-8300 (Fig. 4B,D). When applied without hypoxia, neither cyclosporin A (Fig. 4A,B) nor FK506 (Fig. 4C,D) altered the relative proportions of phosphorylated and non-phosphorylated forms of Cx43 (A-D, lane 2) compared with that seen in control cultures (A-D, lane 1). However, compared with the preponderance of dephosphorylated Cx43 in hypoxic astrocytes (Fig. 4A-D, lane 3), both cyclosporin A (Fig. 4A,B, lane 4) and FK506 (Fig. 4C,D, lane 4) partially inhibited hypoxia-induced Cx43 dephosphorylation. Co-application of calyculin A with either cyclosporin A (Fig. 4A,B, lane 5) or with FK506 (Fig. 4C,D, lane 5) completely blocked hypoxia-induced Cx43 dephosphorylation, as did co-application of okadaic acid with either of the calcineurin inhibitors (not shown).

Tyrosine phosphorylation of astrocytic Cx43

We next sought to determine whether hypoxia induces tyrosine phosphorylation of Cx43 in astrocytes by using a monoclonal phosphotyrosine antibody to immunoprecipitate phosphoproteins from lysates of control and hypoxic astrocytes. Blots of immunoprecipitated proteins probed with antibody 18A (Fig. 5A) or 13-8300 (Fig. 5B) failed to detect any Cx43 in control (A,B, lane 1) or hypoxic astrocytes (A,B, lane 2). As a positive control for immunoprecipitation of phosphotyrosine proteins, control astrocyte cultures were treated with pervanadate (Fig. 5A,B, lane 3), which has been shown to

stimulate tyrosine phosphorylation of Cx43 in other cell types (Mikalsen et al., 1997; Cruciani and Mikalsen, 1999). In immunoprecipitates from these cultures, antibody 18A detected novel forms of Cx43 migrating at 45 kDa (Fig. 5A, lane 3), while 13-8300 detected a band at about 42 kDa (Fig. 5B, lane 3). Blots of total lysates from pervanadate-treated astrocytes probed with antibody 18A also revealed a novel 45 kDa band accompanied by reduced intensity of the 41 kDa band (not shown). Thus, Cx43 tyrosine phosphorylation appears to be absent in control or hypoxic astrocytes, but can be induced by pervanadate resulting in the appearance of forms with novel migration profiles.

Immunohistochemical labeling of Cx43 in astrocytes

The appearance of Cx43 immunoreactivity (ir) in control and hypoxic astrocytes treated with phosphatase inhibitors was examined by immunohistochemistry using antibody 18A and 13-8300. In control astrocytes, 18A produced intense punctate labeling primarily at contacts between cells (Fig. 6A), while 13-8300 gave little or no labeling (Fig. 6B). After 30 min of hypoxia, there was a total loss of 18A-ir (Fig. 6C) and an increase in 13-8300-ir (Fig. 6D). These alterations in Cx43 immunostaining were minimal at 1, 5, and 15 min after hypoxia (not shown) and therefore paralleled the pattern of hypoxia-induced Cx43 dephosphorylation observed by Western blotting. Application of cyclosporin A or FK506 had no discernable effect on Cx43 immunostaining patterns or density with either antibody 18A or 13-8300 in control astrocytes (not shown). However, treatment of hypoxic astrocytes with cyclosporin A largely restored Cx43 immunolabeling with antibody 18A (Fig. 6E) and partially inhibited the increase in 13-8300-ir (Fig. 6F). Co-application of cyclosporin A with calyculin A completely reversed the hypoxia-induced changes in immunolabeling and produced patterns of Cx43 detection with 18A (Fig. 6G) and 13-8300 (Fig. 6H) seen in control cultures. Similar results were obtained with FK506 alone or with co-application of FK506 with calyculin A (not shown).

Intercellular dye-coupling between astrocytes

The effects of hypoxia and phosphatase inhibition on GJIC in cultured astrocytes were investigated by dye-transfer following intracellular microinjection of LY or by tracer-transfer after cell loading of biocytin. As shown by examples of images in Figure 7, numerous astrocytes were junctionally coupled in control cultures as revealed by intercellular transfer of LY (Fig. 7A) or biocytin (Fig. 7C). Consistent with reports by others (Hidaka et al., 1993; Teranishi and Negishi, 1994; Umino et al., 1994; Little et al., 1995), biocytin in combination with detection of this tracer with the highly fluorescent dye Cy3 allowed visualization of a greater number of coupled cells than seen with LY. After 30 min of hypoxia, the number of coupled astrocytes was dramatically reduced as determined by transfer of either LY (Fig. 7B) or biocytin (Fig. 7D). The time course of this hypoxia-induced uncoupling, examined using LY is shown in Figure 8. In control cultures, junctional coupling was only slightly diminished after 1 h of incubation in normal HBSS. After initiation of hypoxia, coupling was significantly reduced by 77% after 15 min, 92% after 30 min and 97% after 1 h. The effects of cyclosporin A or FK506 on junctional coupling, examined using biocytin, are summarized in Figure 9. These agents added to cultures without hypoxia had no significant effect on the number of coupled cells. However, in contrast to the 95% reduction in coupling observed after 30 min of hypoxia, addition of cyclosporin A to hypoxic astrocytes preserved coupling to a level of 34% of that seen in control astrocytes, (Fig. 7E, Fig. 9), while FK506 preserved coupling by only 9% (Fig. 9).

Cx30 in astrocytes in vitro and in vivo

Western blots were probed with anti-Cx30 antibody to determine the relative levels of Cx30 expression in the cultured astrocytes used in the above studies compared with the levels expressed in vivo. Antibody 71-2200 detected a 30 kDa band in blots of homogenates from rat hippocampus and cerebral cortex (Fig. 10, lane 1 and 2, respectively), which corresponds to Cx30 as we previously reported (Nagy et al., 1999). Cx30 was undetectable in astrocytes cultured for 14 or 21 days (Fig. 10, lane 3 and 4, respectively). Although protein detection on blots is certainly dependent on antibody sensitivity, non-detectability in this case may

well reflect negligible levels of Cx30 expression in cultured astrocytes since comparisons here were made with brain structures containing among the lowest levels of Cx30 (Nagy et al., 1999). Moreover, these were relatively pure cultures of astrocytes compared with multiple cell types and neural elements in brain, which would bias results towards an enrichment of Cx30 in astrocyte cultures.

Discussion

The present results demonstrate that Cx43 dephosphorylation and epitope masking previously observed in astrocytes shortly after ischemia in vivo also occur in hypoxic astrocytes in vitro, thus allowing the use of cultured astrocytes to study the molecular mechanisms underlying these events. Results showing that substantial astrocytic junctional uncoupling precedes massive Cx43 dephosphorylation during hypoxia suggest that bulk removal of phosphate groups from Cx43 is unlikely to be an immediate cause of uncoupling. The effects of phosphatase inhibitors indicate that the protein phosphatase calcineurin may be activated in hypoxic astrocytes and that it may directly or indirectly contribute to Cx43 dephosphorylation.

Connexin expression and phosphoprotein forms of Cx43 in cultured astrocytes

Astrocytes in vivo express both Cx43 and Cx30, whereas astrocytes in vitro express Cx43, but little or no Cx30 for up to five weeks in culture (Kunzelmann et al., 1999). Similarly, the cultured astrocytes used here lacked Cx30, which conveniently allows studies of astrocytic Cx43 independently of Cx30. Thus, alterations in junctional coupling after hypoxia or treatments with phosphatase inhibitors reflect responses of junctions composed of Cx43. However, regulation may differ at astrocytic junctions containing both rather than just one of these connexins. Moreover, astrocytes may form heterotypic (Cx43/Cx30) as well as homotypic (Cx43/Cx43; Cx30/Cx30) channels and the former may be subject to different modes of regulation than the latter. Thus, use of astrocytes with low levels of Cx30

expression warrant caution in extrapolating culture results to the in vivo condition where both connexins are expressed.

The presence of predominantly phosphorylated Cx43 in cultured astrocytes parallels the largely phosphorylated forms found in vivo (Hossain et al., 1994c). A further similarity between astrocytes in vitro and their counterparts in brain (Yamamoto et al., 1990a,b), though not in spinal cord (Ochalski et al., 1997), is the apparently very low intracellular levels of Cx43. These two observations are in contrast to findings in other cell types that contain an abundance of non-phosphorylated as well as intracellular Cx43 (Musil and Goodenough, 1991; Nagy et al., 1997b; Cruciani and Milalsen, 1999). This suggests rapid trafficking of phosphorylated Cx43 to plasma membranes in astrocytes as has been found in other systems (Crow et al., 1990; Berthoud et al., 1993; Laing and Beyer, 1995). Further, it appears that maintenance of a largely phosphorylated pool of Cx43 in cultured astrocytes does not require complex glial-neuronal interactions that occur in vivo.

Cx43 detection by antibody 13-8300

We previously reported that antibody 13-8300 selectively recognizes a dephosphorylated form of Cx43 in heart, cultured cardiac myocytes, tracheal smooth muscle cells and an epithelial cell line (Nagy et al., 1997b), and have presented evidence for this in brain and spinal cord (Li et al., 1998; Li and Nagy, 2000a). The present result from alkaline phosphatase treatment of brain tissue further confirms that 13-8300 recognizes only dephosphorylated Cx43 in astrocytes. Moreover, we demonstrate that Cx43 immunolabeling with 13-8300 is correlated with Cx43 dephosphorylation in cultured astrocytes, further suggesting this antibody to be a useful immunohistochemical indicator of Cx43 modification.

Antibody 13-8300 was recently found to react with a form of Cx43 exhibiting slightly slower migration on polyacrylamide gels (Cruciani and Mikalsen, 1999) than that corresponding to its well documented non-phosphorylated form (Crow et al., 1990; Musil et al., 1990; Laird et al., 1991; Saez et al., 1997). This minor form was absent in cultured

astrocytes, but was seen in other cells where it was considered to be either partially dephosphorylated or a degradation product (Musil et al., 1990; Laird et al., 1991). In any case, failure to detect phosphorylated Cx43 by 13-8300 may be due to blockade of epitope by phosphate groups (Nagy et al., 1997b; Li et al., 1998; Li and Nagy, 2000a), which does not exclude possible detection of phosphorylated forms lacking phosphate groups at the 13-8300 epitope. Notwithstanding results by others (Cruciani and Mikalsen, 1999), it remains curious that antibody 13-8300 often detects only the slowest migrating form of Cx43 corresponding to what is considered to be totally dephosphorylated. As discussed earlier (Nagy et al., 1997b), this suggests that Cx43 modification by phosphate addition or removal at the 13-8300 epitope in some systems may occur before phosphorylation or after dephosphorylation, respectively, at other sites in the molecule.

Masking of antibody 18A epitope

Cultured astrocytes are shown here to display the immunohistochemical epitope masking with 18A that frequently accompanies astrocytic Cx43 dephosphorylation in response to various treatments in vivo (Li et al., 1998; Li and Nagy, 2000a). This close relationship between masking and dephosphorylation is unlikely to be due to chemical modification of the 18A epitope (amino acids 346-363), which lacks phosphorylated residues (Unger et al., 1999). Rather, we have suggested (Li and Nagy, 2000a) that the recently identified PDZ interaction domain within the nearby carboxy-terminus of Cx43 may bind to a PDZ domain-containing protein following Cx43 dephosphorylation and thereby cause epitope masking. One mediator of this masking may be the tight junction protein zona occludens-1 (ZO-1), which contains PDZ domains, has been shown to interact with Cx43 via such a domain (Giepmans and Moolenaar, 1998; Toyofuku et al., 1998) and is expressed in astrocytes in vitro (Howarth et al., 1992). If such an interaction underlies Cx43 masking, then this would require association of Cx43 with some other PDZ domain-containing protein in vivo since astrocytes in the CNS do not express ZO-1 (Howarth et al., 1992; Petrov et al., 1994).

Lack of Cx43 tyrosine phosphorylation in cultured astrocytes

Cx43 phosphorylation in normal cells occurs on serine/threonine residues resulting in three Cx43 forms that are usually resolved in Western blots (Crow et al., 1990; Musil et al., 1990, Laird et al., 1991; Saez et al., 1997). However, treatments of cells with the tyrosine protein phosphatase inhibitor pervanadate often produce novel hyperphosphorylated forms displaying retarded mobility by SDS-PAGE. Some of these may correspond to Cx43 tyrosine phosphorylation, which has been observed under certain conditions in other cell types (Crow et al., 1990; Goldberg and Lau, 1993; Mikalsen et al., 1997). Pervanadate treatment of astrocytes here produced novel forms of Cx43 migrating at 45 and 42 kDa, which were never seen in our previous studies of Cx43 in the CNS (Nagy et al., 1992; Hossain et al., 1994b,c; Nagy et al., 1997b; Li et al., 1998; Li and Nagy, 2000a). Immunoprecipitation of these forms with a phosphotyrosine antibody suggests that Cx43 is either tyrosine phosphorylated or becomes associated with a tyrosine phosphoprotein after exposure of astrocytes to pervanadate. However, failure of Cx43 immunoprecipitation with phosphotyrosine antibodies in lysates of normal or hypoxic astrocytes suggests lack of involvement of Cx43 tyrosine phosphorylation or dephosphorylation in the responses of cultured astrocytes to hypoxia.

GJIC and Cx43 dephosphorylation in hypoxic astrocytes

Phosphorylation of Cx43 is important for gap junction assembly and channel gating, whereas dephosphorylation is often associated with reduced junctional coupling (Musil and Goodenough, 1991; Godwin et al., 1993; Oelze et al, 1995; Guan et al., 1996; Cotrina et al., 1998a; Verrecchia et al., 1999; see however Moreno et al., 1994). In this study, both of the methods used to assess junctional coupling gave a 90-95% reduction in GJIC 30 min after hypoxia, which has been observed by others (Harold and Walz, 1992). Use of biocytin compared to LY led to detection of a greater number of coupled astrocytes, which is consistent with the greater sensitivity of biocytin for assays of GJIC (Hidaka et al., 1993; Teranishi and Negishi, 1994; Umino et al., 1994; Little et al., 1995). The 77% reduction in

GJIC seen in astrocytes after 15 min of hypoxia and the subsequent massive Cx43 dephosphorylation seen at 30 min post-hypoxia suggest that factors other than near total Cx43 dephosphorylation to the 41 kDa form contribute to this initial level of hypoxia-induced uncoupling. Such factors may include reduced pH following ATP depletion, increased intracellular calcium levels and/or generation of free radicals following hypoxia (Bickler and Kelleher, 1992; Sun et al., 1993; Ogata et al., 1995; Wu et al., 1996), all of which reduce GJIC (Guo et al., 1993; Bruzzone et al., 1996; Giaume and McCarthy, 1996; Goodenough et al., 1996 Wolburg and Rohlmann, 1995; Kojima et al., 1996). In any event, our results are consistent with findings that junctional uncoupling precedes Cx43 dephosphorylation in hypoxic astrocytes (Cotrina et al., 1998a). This raises the possibility that uncoupling may be more a causal factor than a consequence of Cx43 dephosphorylation. Since Cx43 is multiply phosphorylated, this conclusion may apply only to what appears to be a totally dephosphorylated form of Cx43. It remains possible that the slight degree of Cx43 dephosphorylation seen at 15 min post-hypoxia is sufficient to promote uncoupling or that dephosphorylation may occur at some sites in Cx43 prior to 15 min of hypoxia, but do not lead to mobility shifts on Western blots and hence go undetected.

Contribution of phosphatases to regulation of astrocytic GJIC

Serine/threonine protein phosphatases are divided into type-1, -2A, -2B and -2C (Cohen, 1989). PP-1 and PP-2A have been implicated in the regulation of gap junctions in various peripheral cell types and their inhibition leads to increased Cx43 phosphorylation, increased GJIC and inhibition of gap junction disassembly (Guan et al., 1996; Tripuraneni et al., 1997; Verrecchia et al., 1999; but see Husoy et al., 1993). In astrocytes, PP-1 and PP-2A appear to regulate a variety of important functions (Pshenichkin and Wise, 1995; Randriamampita and Tsien, 1995; Vinade and Rodnight, 1996), but we were unable to examine their regulatory role in astrocytic GJIC due to the disruptive action of inhibitors of these phosphatases (okadaic acid or calyculin A) on astrocyte adhesion in culture, which has also been observed in other cell types (Boe et al., 1991; Hedman and Lundgren, 1992; Seminario et al., 1998).

Nevertheless, our findings that inhibition of PP-1 and PP-2A stimulated Cx43 phosphorylation in control astrocytes, but had minimal effect on hypoxia-induced Cx43 dephosphorylation indicate that these phosphatases contribute to processes that ultimately influence Cx43 phosphorylation state in astrocytes, but do not play a major role in hypoxia-induced Cx43 dephosphorylation.

Calcineurin and astrocytic Cx43 phosphorylation state

Several isoforms of the type 2B phosphatase calcineurin are expressed in astrocytes (Hashimoto et al., 1998; Matsuda et al., 1998) and may regulate processes that govern cell survival based on findings that the well established calcineurin inhibitors FK506 and cyclosporin A (Snyder et al., 1998; Morilka et al., 1999) are cytoprotective in vivo and in vitro (Matsuda et al., 1998; Morioka et al., 1999). In view of this, the effects of calcineurin inhibitors on dephosphorylation of particular proteins under investigation have two possible interpretations in most studies where dephosphorylation is evoked by manipulations that compromise cell viability leading ultimately to cell death. Thus, despite the absence of overt cell damage at the post-hypoxia time points examined in the present study, calcineurin inhibition may protect astrocytes from the initial stages of hypoxic injury via some as yet unclear mechanism, thereby indirectly reducing the degree of Cx43 dephosphorylation and cell uncoupling that occurs as a consequence of cell injury. Alternatively, reduction of hypoxia-induced Cx43 dephosphorylation by calcineurin inhibitors may suggest that Cx43 serves as one possible substrate of calcineurin under conditions of cell stress, but perhaps not in normal astrocyte cultures where calcineurin inhibitors had no effect on Cx43 phosphorylation state. This latter alternative would be consistent with suggestions that calcineurin activity may be regulated by peptidyl-prolyl isomerase, that this isomerase may be the target of PP-2B inhibitors (Gaymes et al., 1997), and that the isomerase may serve to promote Cx43 dephosphorylation (Cruciani et al., 1999). It would also be consistent with the dependence of calcineurin activation on calmodulin (Cohen, 1989; Snyder et al., 1998; Morioka et al., 1999) and numerous reports (Peracchia and Girsch, 1985; Cole and Garfield,

1988; Saez et al., 1990; Albright et al., 1991; Toyama et al., 1994; Jansen et al., 1996; Peracchia et al., 1996; Pereda et al., 1998) indicating that calmodulin-dependent signaling systems play a role in the regulation of GJIC in many cell types.

Figure legends

Fig. 1. Western blots showing the effect of alkaline phosphatase treatment on immuno-recognition of brain Cx43. (A) Following SDS-PAGE and transblotting of brain tissue homogenate, PVDF membranes were incubated with alkaline phosphatase and then probed with anti-Cx43 antibodies. Recognition of 43 and 41 kDa forms of Cx43 by 18A (lanes 1 and 2) and 71-0700 (lanes 3 and 4) was largely the same with (lanes 2 and 4) or without (lanes 1 and 3) phosphatase treatment. Antibody 13-8300 recognizes only the 41 kDa form of brain Cx43 without phosphatase treatment (lane 5), but detects all Cx43 forms after incubation of transblotted proteins with phosphatase (lane 8). (B) Positive control for alkaline phosphatase treatment of phosphoproteins on PVDF membranes. Detection of numerous phosphoproteins in lysates from EGF-stimulated A431 epithelial cells by a phosphotyrosine antibody (lane 1) is dramatically reduced after phosphatase treatment of PVDF membranes containing the same lysate (lane 2).

Fig. 2. Western blots of lysates from cultured astrocytes showing Cx43 dephosphorylation at various times after hypoxia. (A,B) Blots probed with antibody 18A (A) and 13-8300 (B). In control astrocytes, antibody 18A detected Cx43 migrating as a doublet of bands at about 43 kDa and a weaker band at 41 kDa (A, lane 1), while 13-8300 detected only the 41 kDa non-phosphorylated form. This pattern remained unchanged after 1 min (A,B, lane 2) and 5 min (A,B, lane 3) of hypoxia, and a slight increase in the 41 kDa band was evident after 15 min (A,B, lane 4). A marked decrease in the phosphorylated 43 kDa forms and an increase in the 41 kDa dephosphorylated form became evident only after 30 min of hypoxia (A,B, lane 5). After 60 min of hypoxia, the 41 kDa dephosphorylated form predominates (A,B, lane 6).

Fig. 3. Western blots of control and hypoxic astrocyte lysates showing Cx43 phosphorylation state after phosphatase PP-1 and PP-2A inhibition with okadaic acid and calyculin A. (A,B) Blots were probed with antibody 18A (A) and 13-8300 (B). Hypoxic treatments were for 30 min and phosphatase inhibitors were added 5 min prior to hypoxia.

After okadaic acid (A, lane 3) and calyculin A (A, lane 5) treatment, phosphorylated forms of Cx43 are increased and the non-phosphorylated 41 kDa form seen in control astrocytes (A, lane 1) is absent. As evident with both antibody 18A (A) and 13-8300 (B), treatment of hypoxic astrocytes with okadaic acid (lane 4) and calyculin A (lane 6) only slightly inhibited the degree of Cx43 dephosphorylation seen after hypoxia treatment alone (lane 2).

Fig. 4. Western blots showing Cx43 phosphorylation state in control and hypoxic astrocytes after inhibition of calcineurin. Hypoxia was induced for 30 min and phosphatase inhibitors were applied 5 min before hypoxia. (A,B) Blots probed with antibody 18A (A) and 13-8300 (B). Cyclosporin A had little effect on Cx43 phosphorylation state (lane 2) compared with that seen in control astrocytes (lane 1), but substantially reduced Cx43 dephosphorylation (lane 4) seen after hypoxia (lane 3), and together with calyculin A, completely blocked this hypoxia-induced dephosphorylation (lane 5). (C,D) Blots probed with antibody 18A (C) and 13-8300 (D). FK506 also had little effect on Cx43 phosphorylation state (lane 2) compared with that seen in control astrocytes (lane 1), and reduced Cx43 dephosphorylation (lane 4) seen in hypoxic astrocytes (lane 3). FK506 and calyculin A in combination abolished hypoxia-induced Cx43 dephosphorylation (lane 5).

Fig. 5. Western blots showing the absence of phosphorylation at tyrosine residues in Cx43 of control and hypoxic astrocytes. (A,B) Blots containing phosphotyrosine proteins immunoprecipitated with a phosphotyrosine antibody from control, hypoxic and pervanadate-treated astrocyte lysates were probed with antibody 18A (A) and 13-8300 (B). No detectable levels of Cx43 were immunoprecipitated from control (lane 1) or hypoxic (lane 2) astrocytes, while pervanadate treatment led to detection of novel phosphorylated forms of Cx43 migrating at 45 kDa (A, lane 3) and 42 kDa (B, lane 3).

Fig. 6. Double immunofluorescence of cultured astrocytes showing hypoxia-induced alterations in Cx43 immunorecognition and the effect of phosphatase inhibitors. (A,B)

Control astrocytes. Punctate labeling is seen with antibody 18A (A), while very little labeling is evident with 13-8300 (B). (C,D) Astrocytes after 30 min of hypoxia. Punctate labeling is lost with 18A (C), but appears with 13-8300 (D). (E,F) Astrocytes incubated with the calcineurin inhibitor cyclosporin A during 30 min of hypoxia. The inhibitor prevented the hypoxia-induced loss in 18A-ir (E) and reduced labeling density with 13-8300 (F) compared with that seen in D. (G,H) Astrocytes incubated with cyclosporin A and calyculin A during 30 min of hypoxia. The combination of inhibitors preserved labeling with 18A (G) and totally prevented labeling with 13-8300 (H). Scale bar, 30 μm.

Fig. 7. Photomicrographs showing the effects of hypoxia and calcineurin inhibition on gap junctional coupling between cultured astrocytes. (A,B) Intercellular transfer of LY seen after single cell injection (arrows) of the dye in control astrocytes (A) is reduced after 30 min of hypoxia (B). (C-E) Gap junctional transfer of biocytin seen after loading of single cells (arrows) with this agent in control astrocytes (C) is also reduced after hypoxia (D), and this hypoxia-induced uncoupling is partial prevented by inhibition of calcineurin by cyclosporin A (E). Though not evident at the gray scale shown, individual cells could be identified by microscopic examination of all areas containing labeled cells in C. Scale bars, 50 μm.

Fig. 8. Time course of hypoxia-induced gap junctional uncoupling between cultured astrocytes. Coupling was assessed by counting the total number of cells containing LY following injection of single cells with this dye. Values represent means ± S.E.M. of experiments repeated three times on separate astrocyte cultures (■, control; ▲, hypoxia-treated).

Fig. 9. Effect of hypoxia, calcineurin inhibitors (cyclosporin A, cycloA; FK506) and hypoxia in combination with calcineurin inhibitors on gap junctional coupling between cultured astrocytes. Coupling was assessed by intercellular transfer of biocytin. Values

represent percent of the number of cells coupled in control cultures, which was 141 $\pm$ 10. * $P \leq 0.001$ compared with control value. ** $P \leq 0.001$ and *** $P \leq 0.01$ compared with hypoxia value.

Fig. 10. Western blots showing relative levels of Cx30 in structures of rat brain compared with cultured astrocytes. Cx30 was detectable in homogenates of rat hippocampus (lane 1) and cerebral cortex (lane 2), but not in astrocytes cultured for 14 days (lane 3) or 21 days (lane 4). Similar results were obtained with cultured astrocytes prepared on three separate occasions.

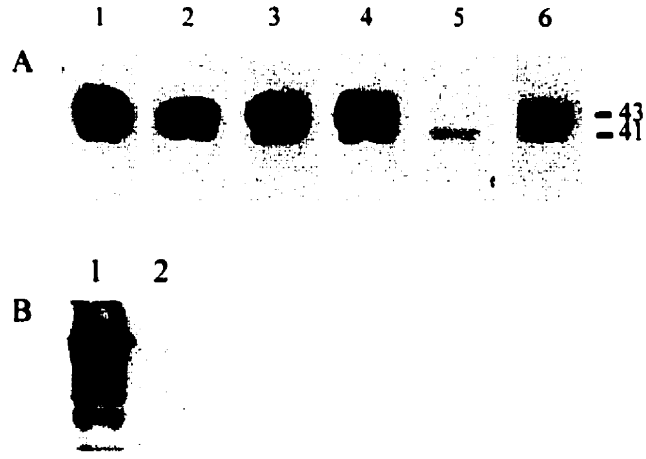

Fig. 1

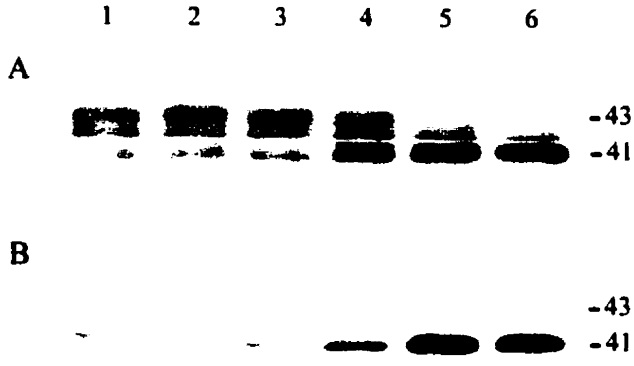

Fig. 2

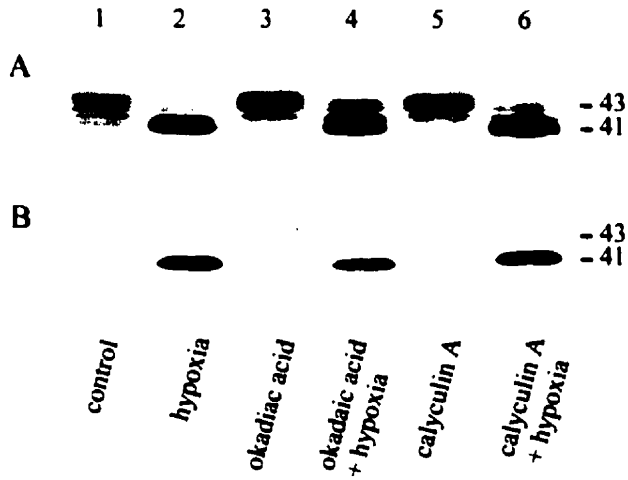
1
2
3
4
5
6
A
B
-43
-41
-43
-41
control
hypoxia
okadiac acid
okadaic acid + hypoxia
calyculin A
calyculin A + hypoxia

Fig 3

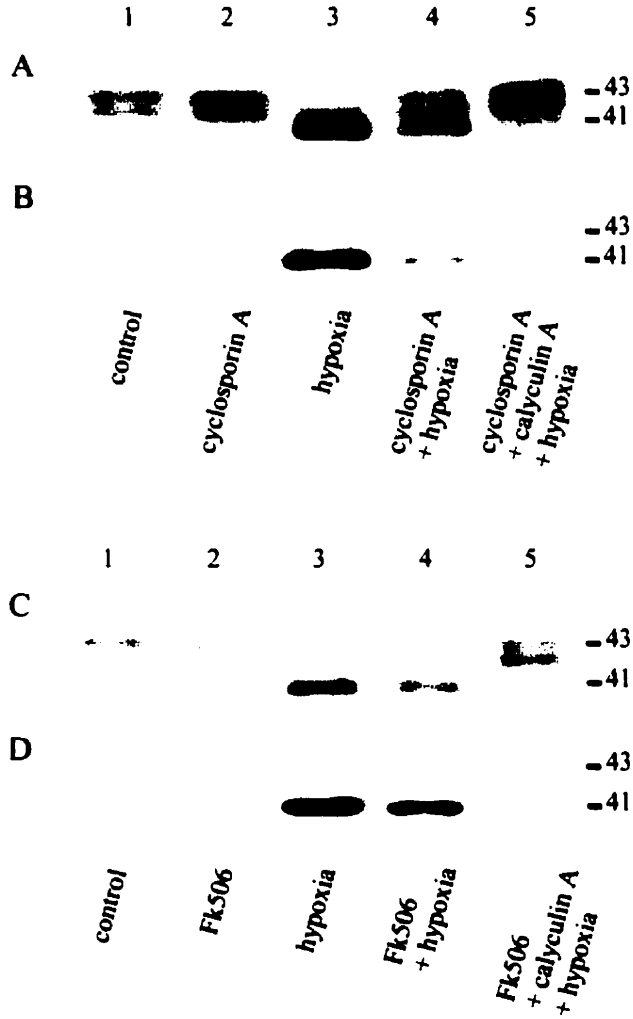
1
2
3
4
5
A
-43
-41
B
-43
-41
control
cyclosporin A
hypoxia
cyclosporin A + hypoxia
cyclosporin A + calyculin A + hypoxia
1
2
3
4
5
C
-43
-41
D
-43
-41
control
Fk506
hypoxia
Fk506 + hypoxia
Fk506 + calyculin A + hypoxia

Fig. 4

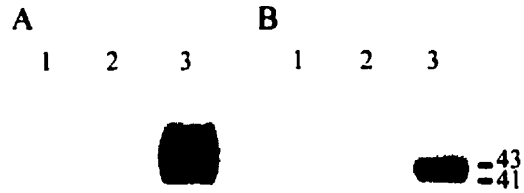

Fig. 5

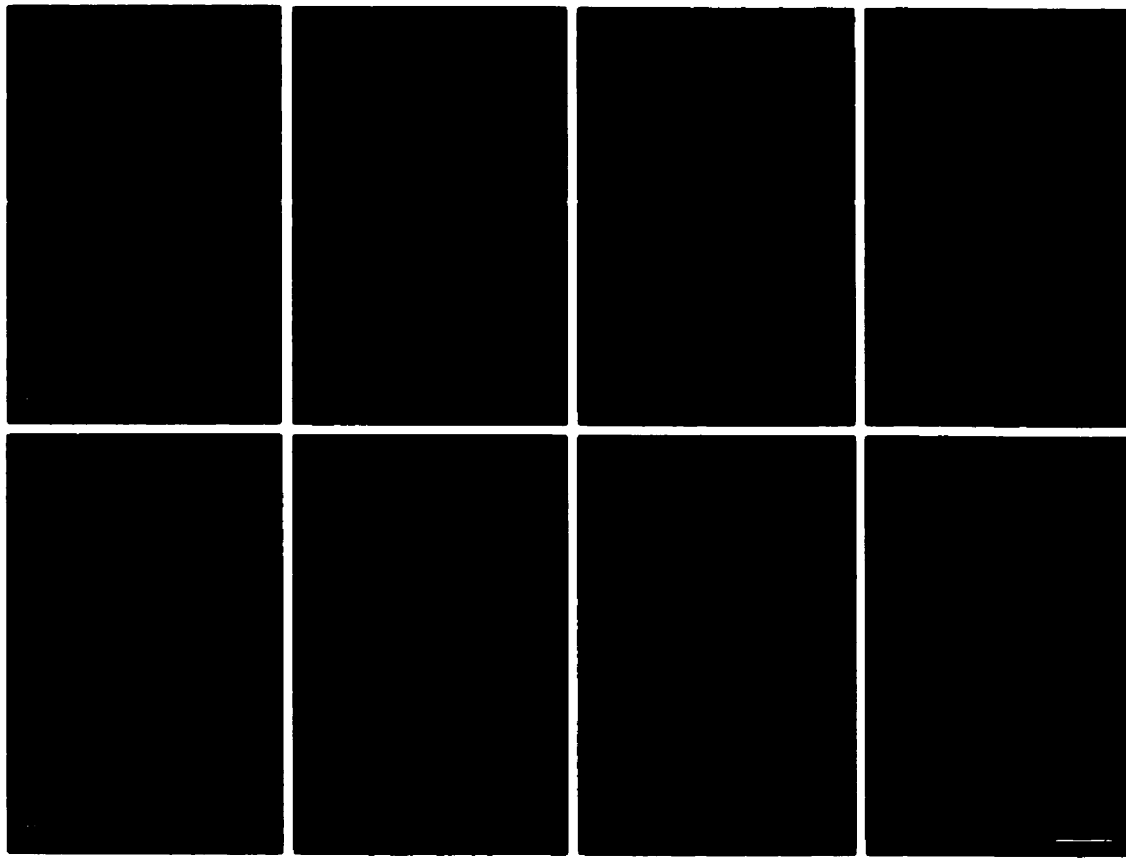

Fig. 6

Fig. 7

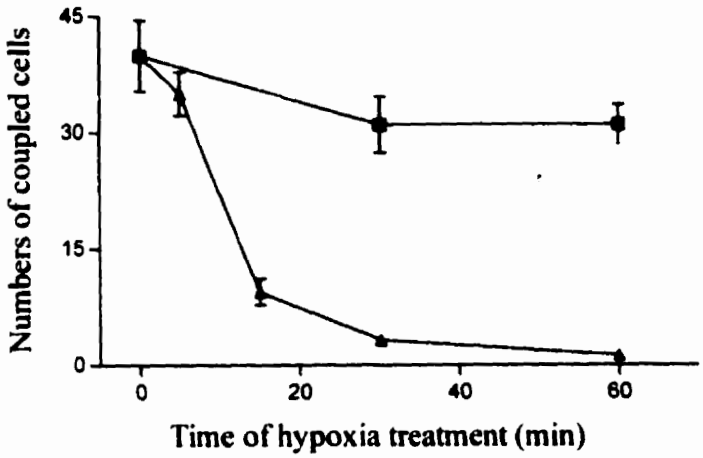
Numbers of coupled cells
45
30
15
0
0
20
40
60
Time of hypoxia treatment (min)

Fig. 8

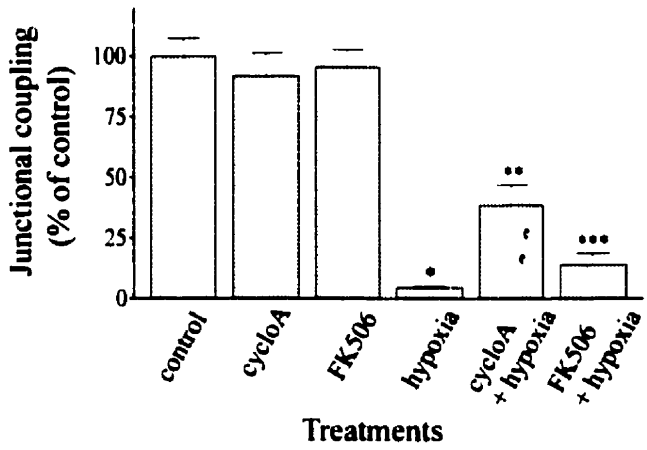
Junctional coupling
(% of control)
100
75
50
25
0
control
cycloA
FK506
hypoxia
cycloA
+ hypoxia
FK506
+ hypoxia
Treatments

Fig. 9

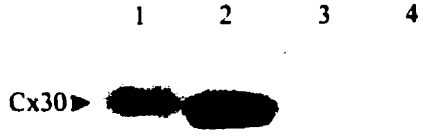

Fig. 10

GENERAL DISCUSSION

The experiments described in this thesis are part of efforts to elucidate the function of astrocytic GJIC in brain homeostasis. As a step towards this goal, we studied the regulation of astrocytic GJIC under physiological and pathological conditions. In the course of these investigations, we characterized a monoclonal anti-Cx43 antibody that selectively recognizes dephosphorylated Cx43 in cultured tracheal smooth muscle cells, cardiac myocytes, an epithelial cell line and astrocytes in vitro and in vivo (Part II, III and V). Taking advantage of this property, we used this antibody to examined the phosphorylation state of astrocytic Cx43 in vitro and in vivo under various conditions. In conjunction with immunohistochemistry and EM, we also investigated the localization of dephosphorylated Cx43 in astrocytes in vitro and in situ. Moreover, as an extension of previous studies, we investigated the status of astrocytic gap junctions in the center and the penumbral zone in focal ischemic brain. These experiments demonstrate that Cx43 in astrocytes, like cardiac myocytes, consists primarily of phosphorylated forms. Regulation of basal phosphorylation state requires collective actions of protein kinases and protein phosphatases. PP-1 and/or PP-2A may be actively involved in this process. Increased dephosphorylation of Cx43 occurs during increased neuronal activity (Part IV) and mild ischemia (Part III) in vivo and hypoxia in vitro (Part V), perhaps due to activation of calcineurin (Part V). These results suggest that Cx43 dephosphorylation is a common feature in the regulation of astrocytic GJIC under physiological and pathological conditions. Cx43 dephosphorylation is reversible in the absence of tissue injury and is followed by massive Cx43 internalization and removal of gap junctions when severe tissue injury occurs (Part III). Dephosphorylation of Cx43 may be associated with decreased GJIC in hypoxic and/or ischemic astrocytes (Part V), whereas Cx43 internalization and gap junction removal from astrocytes may result in total shutdown of astrocytic GJIC in the lesion center and are apparently dependent on severe neuronal injury (Part III). Reactive astrocytes in the area of tissue injury may express Cx43 and probably re-establish GJIC as shown by the presence of gap junctions (Part I; Alonso and Privat, 1993; Hossain et al., 1994b; Ochalski et al., 1995; Theriault et al., 1997) and dye-coupling between these cells (Anders et al., 1990; Anders and Woolery, 1992).

Thus, these and other studies suggest that regulation of astrocytic GJIC is a dynamic and programmed process.

The following discussion is to analyze current knowledge of GJIC between normal or reactive astrocytes in the context of Cx43 phosphorylation, protein phosphatase action, Cx43 internalization and gap junction degradation. Also included are some speculations concerning regulation of GJIC in astrocytes.

Phosphorylation of Cx43 and gap junction formation

The predominantly phosphorylated form of astrocytic Cx43 and the primarily junctional localization of Cx43 in brain astrocytes in situ (Part III) and in vitro (Part V) are consistent with the notion that phosphorylation of Cx43 to the P2 form (43 kDa) is required for the assembly of gap junctions (Musil et al., 1990; Musil and Goodenough, 1991). Minimal intracellular Cx43 immunolabeling with all anti-Cx43 antibodies suggests the absence of a large intracellular pool as well as the occurrence of rapid protein trafficking in these cells (Part III and V). In contrast, intense Cx43-ir was found in the cytoplasm of astrocytic processes in the spinal cord (Ochalski et al., 1997; Part IV). This portion of Cx43 likely consists of phosphorylated forms due to lack of immunorecognition by antibody 13-8300 and minimal amounts of non-phosphorylated Cx43 in the spinal cord (Part IV). Moreover, intracellular immunolabeling of Cx43 in spinal cord astrocytes is different from internalized gap junctions, which are usually annular or multivesicular profiles (Larsen and Tung, 1978; Wert and Larsen, 1990; Ochalski et al., 1995). Thus, these observations suggest the existence of an intracellular store of phosphorylated Cx43 in these astrocytes. Currently, it is uncertain whether intracellular Cx43 is a partially phosphorylated P1 form or a fully phosphorylated P2 form. Since it appears that phosphorylation of Cx43 to the P2 form occurs at the plasma membrane and is essential for gap junction assembly (Musil et al., 1990; Musil and Goodenough, 1991), this portion of Cx43 may be in the partially phosphorylated P1 form. The failure of 13-8300 to recognize this partially phosphorylated Cx43 is consistent with the notion that the epitope recognized by 13-8300 contains an early phosphorylation site (Part II). Alternatively, if intracellular Cx43 is the P2

phosphorylated form, then it may be that phosphorylation of Cx43 to the P2 form is not sufficient, even though it appears to be necessary, for gap junction assembly in spinal cord astrocytes. This possibility can be examined by comparing the phosphorylation states and sites between membrane bound Cx43 and cytoplasmic Cx43.

Calcineurin-mediated Cx43 dephosphorylation and astrocytic GJIC during ischemia and hypoxia

Reductions in oxygen and glucose supply are the major events during ischemia. The direct consequence is the reduction of ATP generation followed by the disruption of cell function and integrity. Ischemia can be mimicked in vitro by application of sodium iodoacetate and potassium cyanide to block ATP production through anaerobic and aerobic pathways, respectively. Thus, this protocol is termed in vitro ischemia, chemical hypoxia or metabolic inhibition (Gores et al., 1989; Gramolini and Renaud, 1997; Cotrina et al., 1998a; Frey et al., 1998). Cx43 dephosphorylation in hypoxic astrocytes cultured from cerebral cortex may mirror Cx43 dephosphorylation in brain astrocytes during ischemia (Part III and V).

In the course of examining the coupling state of cultured astrocytes, we improved the conventional scrape-loading technique to single cell level, referred to as single-cell-scrape-loading (SCSL) (Part V). SCSL allows a rapid, simple, reliable and quantitative evaluation of gap junctional coupling state in cultured cell monolayer without an simultaneous fluorescent microscope examination and microinjection. In conjunction with a smaller tracer, biocytin, we were able to demonstrate the rapid reduction of gap junctional coupling in hypoxic astrocytes and the partial protection of GJIC by calcineurin inhibitor FK506 and cyclosporin A (Part V).

Significant reduction in astrocytic GJIC occurred (15 min after hypoxia) prior to massive dephosphorylation of Cx43 (30 min after hypoxia) (Part V), which is in general agreement with a previous study (Cotrina et al., 1998a). Based on this observation, we have proposed that initial reduction of astrocytic GJIC was not due to massive Cx43 dephosphorylation. However, this does not exclude potential contributions of partial Cx43 dephosphorylation to the reduction in astrocytic GJIC. This is especially true when taking into account that phosphorylation at one

or several serine residues can cause significant changes in GJIC (Warn-Cramer et al., 1998), that alteration in the phosphorylation state in a small number of serine sites may go undetected by Western blotting (Warn-Cramer et al., 1998; Hossain et al., 1999a,b) and that slight dephosphorylation of Cx43 is visible at 15 min after hypoxia (Part V). On the other hand, although inhibition of calcineurin phosphatase activity by FK506 and cyclosporin A has been shown to be protective in astrocytes against Ca^{2+}-induced cell injury (Matsuda et al., 1998), we did not observe a delayed or attenuated cell death when astrocytes were subjected to longer term hypoxia in the presence of FK506 and cyclosporin A (Li and Nagy, unpublished observation). Apparently, the cytoprotective effect of FK506 and cyclosporin A in hypoxic astrocytes, if any, is minimal. Thus, the partial preservation of GJIC in hypoxic astrocytes by FK506 and cyclosporin A may be due to the concurrent inhibition of Cx43 dephosphorylation by calcineurin inhibitors.

Calmodulin-dependent regulation of GJIC

Calcineurin phosphatase activity is dependent on the binding of calcium and calmodulin (Cohen, 1989; Snyder et al., 1998; Morioka et al., 1999). Evidence for the involvement of calmodulin-dependent signaling pathways in the regulation of GJIC has been obtained in a number of studies. Gap junctional coupling in early Xenopus embryos can be disrupted by acidification of cytoplasm when exposed to high levels of CO_2. Addition of a calmodulin antagonist could substantially inhibit the low pH-induced uncoupling in these cells (Peracchia, 1984). Similar protection from calcium-induced uncoupling was seen in myometrial smooth muscle and in cardiac myocytes (Cole and Garfield, 1988; Toyama et al., 1994). Since Cx43 is a major gap junction protein in smooth muscle and in cardiac myocytes (Nagy et al., 1997b; Li et al., 1998) and calmodulin has been located in some gap junctions in cardiac myocytes by EM (Fujimoto et al., 1989), these studies suggest that GJIC in these tissue may be regulated by calmudulin-dependent mechanisms, such as alteration of Cx43 phosphorylation state by Ca2+/calmodulin-dependent protein kinases and phosphatase. Dephosphorylation of Cx43 by calcineurin described in the current study supports a role of such a signaling pathway in the

regulation of GJIC in astrocytes. Recently, CaMKII was shown to promote gap junctional coupling in neurons (Pereda et al., 1998). Since neurons do not express detectable amounts of Cx43, this study suggests that gap junctions formed by other connexins, in addition to Cx43, are also subjected to the regulation by calmodulin-dependent mechanisms.

Available data indicates that Cx43 is not a direct substrate of calcineurin. Most recently, Cruciani et al. found that calcineurin inhibitor FK506 and cyclosporin A can inhibit the dephosphorylation of hyperphosphorylated Cx43 in fibroblasts (Cruciani et al. 1999), suggesting that calcineurin may be involved in the dephosphorylation of Cx43 in these cells. However, application of these calcineurin inhibitors did not cause any visible changes in Cx43 phosphorylation state in unstimulated cells, which is consistent with our observations in normal astrocytes. These observations suggest that calcineurin is not involved in the regulation of basal phosphorylation of Cx43. Using in vitro dephosphorylation assay, these researchers found that calcineurin does not dephosphorylate immunoprecipitated Cx43. In a preliminary study, we found that incubation of calcineurin with tissue homogenate containing phosphorylated Cx43 or with immobilized Cx43 did not cause any visible changes in the phosphorylation state of Cx43 (Li and Nagy, unpublished observation). These observations suggest that Cx43 is not a direct substrate of calcineurin. Thus, it is likely that the activation of calcineurin is an intermediate step in the signaling cascade leading to Cx43 dephosphorylation. The serine phosphatase catalyzing Cx43 dephosphorylation appears to be insensitive to okadaic acid, calyculin A (Part V) and to the removal of extracellular magnesium (Li and Nagy, unpublished observation). Furthermore, this serine phosphatase may be associated with plasma membranes (see next).

Selective Cx43 dephosphorylation and GJIC

Due to cell disruption, we were not able to assay the effect of Cx43 dephosphorylation mediated by PP-1 and/or PP-2A on astrocytic GJIC. Protein dephosphorylation by PP-1 and/or PP-2A has been related to decreased GJIC in several peripheral cell types containing Cx43 gap junctions (Tripuraneni et al., 1997; Verrecchia and Herve, 1997). Inhibition of Cx43

dephosphorylation by PP-1 and PP-2A inhibitor has also been shown to preserve GJIC in epithelial cells (Guan et al., 1996). Thus, Cx43 dephosphorylation by PP-1 and/or PP-2A may be also associated with a decrease of GJIC.

Astrocytes in ischemic penumbra are characterized by strong immunolabeling of dephosphorylated Cx43, suggesting that the gap junctional coupling capacity in these cells is reduced due to ischemia insult and subsequent Cx43 dephosphorylation. A reduction in junctional coupling has been reported in ischemic heart tissue, which was also accompanied by Cx43 dephosphorylation (Huang et al., 1999). Thus, Cx43 dephosphorylation may be a common mechanism for regulating GJIC in a variety of tissues.

Localization of phosphorylated Cx43 in astrocytic processes as well as gap junctions in the spinal cord make it useful in determining cellular regions of protein phosphatase action. This is not possible in brain astrocytes due to a very small amount of intracellular Cx43 (Yamamoto et al., 1990a,b; Part III and V). The finding that intracellular Cx43 largely escaped the digestion of protein phosphatases after stimulation of sciatic nerve suggests either that protein phosphatases are located in the membrane region and preferentially act on membrane-associated junctional Cx43 or that intracellular Cx43 is protected by unknown mechanisms from the action of these enzymes (Part IV). Insight into this issue can be achieved by in vivo dephosphorylation in conjunction with Cx43 immunohistochemistry with antibody 13-8300. On the other hand, the preferential dephosphorylation of junctional Cx43 may represent an efficient mechanism of regulating GJIC in these cells. The continuous presence of dephosphorylated Cx43 at several hours after the removal of initial stimuli may indicates that dephosphorylated Cx43 may not be subjected to rapid internalization and degradation, and that basal level of Cx43 phosphorylation is not required for the stabilization of gap junctions (Part III and IV, Li and Nagy, unpublished observation).

Regulation of astrocytic GJIC by neuronal activity

Lines of evidence have suggested that astrocytic GJIC is under the regulation of neuronal activity. In Part IV, we demonstrated that increased neuronal activity by stimulation of sciatic

nerve induced Cx43 dephosphorylation in astrocytes of the spinal cord dorsal horn. This dephosphorylation shares several similarities with Cx43 dephosphorylation in brain astrocytes after ischemia and hypoxia (Part III, IV and V). First, dephosphorylation of Cx43 in these studies involves virtually total removal of most, if not all,. phosphate groups from Cx43 as shown by the exclusive detection of the non-phosphorylated form by antibody 13-8300. Second, astrocytes exhibiting Cx43 dephosphorylation are believed to be healthy cells since treatments in these experiments should not cause cell damage even though cell swelling may occur (Walz, 1989; Chen et al., 1993; Garcia et al., 1993). Third, Cx43 internalization and gap junction removal previously associated with cell injury (Vukelic et al., 1991; Hossain et al., 1994b,c; Ochalski et al., 1995; Sawchuk et al., 1995; Theriault et al., 1997) were not seen in astrocytes after these treatments. Fourth, the occurrence of Cx43 dephosphorylation in these experiments is temporally similar. Fifth, junctional Cx43 is a common target of protein phosphatases under these experimental conditions, suggesting a similar site of phosphatase action. Sixth, Cx43 dephosphorylation was accompanied by similar changes in Cx43 immunostaining pattern. Thus, dephosphorylation of Cx43 induced by increased neuronal activity may be a similar astrocytic response to that induced by mild (15 min) ischemia (Part III) and hypoxia (Part V). These observations indicate a commonality in the regulation of astrocytic GJIC under physiological and pathological conditions.

However, the postulated relationship between Cx43 dephosphorylation and astrocytic GJIC seems contradictory to some of the previous findings. For instance, Marrero and Orkand found that electrical stimulation of the optic nerve for 2 min increased dye-coupling in astrocytes in the vicinity of nerve axons (Marrero and Orkand, 1996). This increase in astrocytic GJIC was shown to be partially due to increased release of K^+ from discharging axons. In a separate study, cultured brain astrocytes exhibited increased intercellular LY transfer when $[K^+]_o$ was increased (Enkvist and McCarthy, 1994). Thus, increased neuronal activity apparently increases gap junctional coupling between astrocytes. We have observed similar stimulatory effect of high $[K^+]_o$ on GJIC in cultured astrocytes. However, we did not observe any alterations in Cx43 phosphorylation states under this experimental condition (Li

and Nagy, unpublished observation). High frequency electrical stimulation of the sciatic nerve has been shown to increase $[K^+]_o$ in spinal cord dorsal horn as well as ventral horn (Vyklicky et al., 1972; Kriz et al., 1974). The absence of Cx43 dephosphorylation in this region suggests that increase in $[K^+]_o$ alone is not sufficient for the induction of Cx43 dephosphorylation even though it can cause an increase of astrocytic GJIC in vitro and in situ (Marrero and Orkand, 1996; Enkvist and McCarthy, 1994; Li and Nagy, unpublished observation). Clearly, increases in astrocytic GJIC seen in these studies are independent of Cx43 dephosphorylation. On the other hand, the occurrence of Cx43 dephosphorylation after 15 min sciatic nerve stimulation may reflect a different astrocytic response to increased neuronal activity. This difference may be due to experimental conditions rather than astrocyte properties since K^+-induced increases in gap junctional coupling were seen in astrocytes from both white matter and gray matter. One possible explanation for this discrepancy is that transient increase in neuronal activity may induce a transient increase of $[K^+]_o$ and a transient increase of astrocytic GJIC. A long-lasting increase of neuronal activity may lead to Cx43 dephosphorylation and reduction of GJIC in astrocytes. Verification of this hypothesis requires the examination of phosphorylation states of astrocytic Cx43 after electrical stimulation with different parameters.

Functional significance of the down-regulation of astrocytic GJIC

As we have discussed in the General Introduction, a loss of dye-coupling does not necessarily suggest the absence of electrical coupling. In fact, it has been repetitively shown that electrical coupling often exists in the absence of dye-coupling (Ransom and Kettenmann, 1990; Kwak and Jongsma, 1996; Naus et al., 1997). Moreover, gap junction uncoupling is often in essence a downshift of unitary channel conductance or a reduction of the probability of channel opening. This has been shown in Cx43 gap junctions after treatments with gap junction blockers and other chemicals believed to alter Cx43 phosphorylation state (Burt and Spray, 1989; Moreno et al., 1994; Kwak et al., 1995a,b,c; Kwak and Jongsma, 1996). Thus, alteration of junctional coupling may be a re-setting of channel permeability to different molecules. The permeability of astrocytic gap junctions to LY was lost during hypoxia treatment (Part V). Inhibition of

calcineurin by cyclosporin A and FK506 did not cause any change in LY intercellular transfer (Li and Nagy, unpublished observation). However, these agents did preserve 34% and 9% of intercellular transfer of a smaller tracer, biocytin (Part V). These results suggest that channel permeability to different molecules can be differentially regulated in astrocytes. In their extensive study using a wide range of tracer molecules, Flagg-Newton and Loewenstein (1979) found that cultured cells respond to chemical hypoxia by preferentially down-regulating gap junction permeability to larger molecules, while preserving electrical coupling. Thus, astrocytes may regulate gap junction permeability to selectively restrict the intercellular flow of relatively larger molecules such as neurotransmitters and metabolites, but allow the free flow of smaller particles such as ions.

The benefit of differential regulation of intercellular flow of ions and metabolites could be several fold. First, restriction of metabolite outflow would provide local neuron and glial cells with additional energy substrates to fuel continuous neuronal activity. Second, reduction in astrocytic GJIC has been shown to be associated with increased glucose uptake, and thus might serve to overcome the shortage of energy substrate during ischemia, hypoxia and increased neuronal discharges (Giaume et al., 1997; Lavado et al., 1997). Third, these effects can occur without compromising K^+ spatial buffering due to relatively unaffected permeability to ions. Fourth, reduced GJIC may be associated with resumption of astrocyte proliferation and transformation into reactive astrocytes, as it has been suggested in peripheral cells (Xie et al., 1997). Thus, reduced astrocytic GJIC may be part of the effort of astrocytes to maintain tissue homeostasis. However, such alterations in astrocytic GJIC could also be deleterious to themselves as well as adjacent neurons. Restriction of outflow of excitatory amino acid could lead to elevation of extracellular glutamate concentration, which may accentuate the excitotoxic effects seen in ischemic tissue (Choi and Rothman, 1990). Accumulation of metabolites such as lactate can result in acidosis believed to be detrimental to cells (Siesjo, 1992). On the other hand, selective preservation of permeability to ions would allow the occurrence of spreading depression which is believed to be mediated by astrocytic gap junctions and partially responsible for spreading of ischemic injury (Nedergaard et al., 1995). Moreover, the

association of reduced GJIC with the proliferation of reactive astrocytes, if true, may indicate that this type of regulation of astrocytic GJIC could also be harmful since glial scars formed by reactive astrocytes may hinder nerve regeneration in the CNS. To test these possibilities, verification of the selective permeability of hypoxic and/or ischemic astrocytes could be a useful start.

Neuronal injury and Cx43 internalization in astrocytes

Cx43 internalization and removal of astrocytic gap junctions occur concomitantly in the CNS after brain excitotoxin lesion and spinal cord compression injury (Vukelic et al., 1991; Hossain et al., 1994b; Ochalski et al., 1995; Sawchuk et al., 1995; Theriault et al., 1997). In Part III, we demonstrated that these events also occur in the lesion center of ischemic brain. Internalization of Cx43 is often accompanied by the loss and increase of Cx43 immunostaining with antibody 18A and 16A, respectively, but not by alterations in Cx43 phosphorylation state (Hossain et al., 1994b). Increase in 16A-ir is believed to be a useful indicator of gap junction removal and Cx43 internalization in astrocytes. In all animal models so far examined, evident increase in 16A-ir has always been associated temporally and spatially with massive neuronal injury (Vukelic et al., 1991; Hossain et al., 1994a; Ochalski et al., 1995; Theriault et al., 1997). Increased 16A-ir has not been seen in healthy tissue and in the ischemic penumbra (Part III). Glutamate was seen to induce an elevation of 16A-ir in brain slices, which can be inhibited by a NMDA receptor blocker, 2-amino-5-phosphonovalerate (Li and Nagy, unpublished observations). Since astrocytes do not express a detectable amount of NMDA receptors (Hosli and Hosli, 1993; Kimelberg, 1995), this observation suggests that massive astrocytic Cx43 internalization is dependent on neuronal injury. This is consistent with NMDA-induced elevation of 16A-ir in vivo (Ochalski et al., 1995) and with the unaltered 16A-ir in hypoxic astrocytes cultured free of neurons (Li and Nagy, unpublished observations). Thus, consistent alterations in Cx43 immunostaining, Cx43 distribution and gap junction organization have been observed in a number of CNS injury models, suggesting that astrocytes regulate their GJIC in a programmed manner.

Degradation of Cx43 in cultured astrocytes occurs after prolonged hypoxia treatment (Li and Nagy, unpublished observation). This loss of Cx43 occurs in the absence of increased 16A-ir, indicating an alternative mechanism of degradation of Cx43 gap junctions. This has been implied by the rapid turnover rate of Cx43 in peripheral cell types in vitro and in situ (Laird et al., 1991, 1995; Musil and Goodenough, 1991; Beardslee et al., 1998) and the weak 16A- or 71-0700-ir in normal cardiac myocytes and astrocytes. (Laird et al., 1991, 1995; Musil and Goodenough, 1991; Yamamoto et al., 1990a,b; Ochalski et al., 1995; Li and Nagy, unpublished observations). This is perhaps also consistent with findings that Cx43 can be degraded through lysosomal as well as proteosomal pathways (Laing and Beyer, 1995; Laing et al., 1997, 1998).

Reactive astrocytes and GJIC

Initial tissue injury in the CNS is usually followed by the appearance of reactive astrocytes in the periphery of and the invasion of reactive astrocyte into the lesion center (Chen et al., 1993; Garcia et al., 1993; Eng and Ghirnikar, 1994; Theriault et al., 1997). Together with reactive microglia and macrophage, reactive astrocytes may help to remove cellular debris and finally fill the lesioned area with glial scar (Eng and Ghirnikar, 1994; Bechmann and Nitsch, 1997). Increased Cx43 immunostaining with antibody 18A was found in reactive astrocytes (Hossain et al., 1994b; Ochalski et al., 1995; Theriault et al., 1997). Consistently, gap junctions have also been found in these cells, and these gap junctions are likely functional (Anders et al., 1990; Anders and Woolery, 1992; Alonso and Privat, 1993; Hossain et al., 1994b; Ochalski et al., 1995; Theriault et al., 1997). Cx43 immunolabeling with 18A was also found in the lesion center at over 2 weeks after focal ischemia, indicating that reactive astrocytes at this stage may express Cx43 and re-establish GJIC in the lesioned region (Hossain et al., 1994b; Li and Nagy, unpublished observations). In the study of human AD brain, we found increased Cx43 immunolabeling in the processes of reactive astrocytes corresponding to the regions of senile and amyloid plaques, suggesting that human astrocytes may up-regulate Cx43 expression and GJIC in response to degenerative neural injury (Part I). Indeed, reactive astrocytes cultured from epileptic human brain display elevated coupling strength compared with control

astrocytes (Lee et al., 1995; Bordey and Sontheimer, 1998). These results suggest that reactive astrocytes are also coupled by Cx43 gap junctions in human brain.

Dynamics of astrocytic GJIC

Based on above observations and discussions, we propose a minimum of five states of astrocytic GJIC. 1) Normal astrocytes are extensively coupled (Ransom, 1995; Giaume and McCarthy; 1996; Nagy and Rash, 1999; Nagy and Dermietzel, 2000). 2) Increased junctional coupling can be induced by transient increase of neuronal activity (Giaume and McCarthy, 1996; Marrero and Orkand, 1996). 3) Reduced coupling state can be induced by prolonged increase in neuronal activity, by mild ischemia or by short-term hypoxia, possibly via Cx43 dephosphorylation (Part III, IV and V). 4) Total uncoupling in response to massive neuronal injury (Part III; Vukelic et al., 1991; Hossain et al., 1994a; Ochalski et al., 1995; Sawchuk et al., 1995; Theriault et al., 1997). 5) a gradual recovery of GJIC in reactive astrocytes infiltrating the lesioned area (Part I; Hossain et al., 1994b; Ochalski et al., 1995; Theriault et al., 1997).

In summary, we conclude that astrocytic GJIC is under the regulation of substances released from neurons under physiological and pathological conditions. The regulation appears to be a programmed process and may be achieved by alterations in the expression, phosphorylation state, distribution and degradation of Cx43 in astrocytes. The altered coupling states of astrocytes may serve to maintain ionic and metabolic homeostasis or to isolate injured tissues in the CNS. Consequently, alterations in astrocytic GJIC may also affect the excitability, metabolism and probably the viability of neurons.

REFERENCES

Ahmad, S., Diez, J. A., George, C. H. and Evans, W. H. (1999) Synthesis and assembly of connexins in vitro into homomeric and heteromeric functional gap junction hemichannels. *Biochem J.*, **339,** 247-253.

Albright, C. D., Grimley, P. M., Jones, R. T., Fontana, J. A., Keenan, K. P. and Resau, J. H. (1991) Cell-to-cell communication: a differential response to TGF-beta in normal and transformed (BEAS-2B) human bronchial epithelial cells. *Carcinogenesis,* **12,** 1993-1999.

Aldskogius, H. and Kozlova, E. N. (1998) Central neuron-glial and glial-glial interactions following axon injury. *Prog. Neurobiol.*, **55,** 1-26

Alonso, G. and Privat, A. (1993) Reactive astrocytes involved in the formation of lesional scars differ in the mediobasal hypothalamus and in other forebrain regions. *J. Neurosci. Res.*, **34,** 523-538.

Anders, J. J. (1988) Lactic acid inhibition of gap junctional intercellular communication in in vitro astrocytes as measured by fluorescence recovery after laser photobleaching. *Glia,* **1,** 371-379.

Anders, J. J., Niedermair, S., Ellis, E. and Salopek, M. (1990) Response of rat cerebral cortical astrocytes to freeze- or cobalt-induced injury: an immunocytochemical and gap-FRAP study. *Glia,* **3,** 476-486.

Anders, J. J. and Woolery, S. (1992) Microbeam laser-injured neurons increase in vitro astrocytic gap junctional communication as measured by fluorescence recovery after laser photobleaching. *Lasers Surg. Med.*, **12,** 51-62.

Anzini, P., Neuberg, D. H., Schachner, M., Nelles, E., Willecke, K., Zielasek, J., Toyka, K. V., Suter, U. and Martini, R. (1997) Structural abnormalities and deficient maintenance of peripheral nerve myelin in mice lacking the gap junction protein connexin 32. *J Neurosci.*, **17**, 4545-4551.

Atkinson, M. M., Menko, A. S., Johnson, R. G., Sheppard, J. R. and Sheridan, J. D. (1981) Rapid and reversible reduction of junctional permeability in cells infected with a temperature-sensitive mutant of avian sarcoma virus. *J. Cell Biol.*, **91**, 573-378.

Atkinson, M. M., Lampe, P. D., Lin, H. H., Kollander, R., Li, X. and Kiang, D. T. (1995) Cyclic AMP modifies the cellular distribution of connexin43 and induces a persistent increase in the junctional permeability of mouse mammary tumor cells. *J. Cell Sci.*, **108**, 3079-3090.

Avner, B. P., Delongo, J., Wilson, S. and Ladman, A. J. (1981) A method for culturing canine tracheal smooth muscle cells in vitro: morphologic and pharmacologic observations. *Anat. Rec.*, **200**, 357-370.

Azarnia, R., Larsen, W. J. and Loewenstein, W. R. (1974) The membrane junctions in communicating and noncommunicating cells, their hybrids, and segregants. *Proc. Natl. Acad. Sci. U.S.A.*, **71**, 880-884.

Azarnia, R., Reddy, S., Kmiecik, T. E., Shalloway, D. and Loewenstein, W. R. (1988) The cellular src gene product regulates junctional cell-to-cell communication. *Science*, **239**, 398-401.

Barnes, T. M. and Hekini, S. (1997) The Caenorhabditis elegans avermectin resistance and anesthetic response gene unc-9 encodes a member of a protein family implicated in electrical coupling of excitable cells. *J. Neurochem.*, **69,** 2251-2260.

Barr, L., Dewey, M. M. and Berger, W. (1965) Propagation of action potentials and the structure of the nexus in cardiac muscle. *J. Gen. Physiol.*, **48,** 797-823.

Beardslee, M. A., Laing, J. G., Beyer, E. C. and Saffitz, J. E. (1998) Rapid turnover of connexin43 in the adult rat heart. *Circ. Res.*, **83,** 629-635.

Bechmann, I. and Nitsch, R. (1997) Astrocytes and microglial cells incorporate degenerating fibers following entorhinal lesion: a light, confocal, and electron microscopical study using a phagocytosis-dependent labeling technique. *Glia,* **20,** 145-154.

Belliveau, D. J. and Naus, C. C. G. (1994) Cortical type 2 astrocytes are not dye coupled nor do they express the major gap junction genes found in the central nervous system. *Glia,* **12,** 24-34.

Belluardo, N., Trovato-Salinaro, A., Mudo, G., Hurd, Y. L. and Condorelli, D. F. (1999) Structure, chromosomal localization, and brain expression of human Cx36 gene. *J. Neurosci. Res.*, **57,** 740-752.

Bennett, M. V. L. and Goodenough, D. A. (1978) Gap junctions, electrotonic coupling, and intercellular communication. *Neurosci. Res. Prog. Bull.*, **16,** 371-486.

Bennett, M. V. L., Barrio, L. C., Bargiello, T. A., Spray, D. C., Hertzberg, E. and Saez, J. C. (1991) Gap junctions: new tools, new answers, new questions. *Neuron,* **6,** 305-320.

Bergoffen, J., Scherer, S. S., Wang, S., Scott, M. O., Bone, L. J., Paul, D. L., Chen, K., Lensch, M. W., Chance, P. F. and Fischbeck, K. H. (1993) Connexin mutations in X-linked Charcot-Marie-Tooth disease. *Science*, **262,** 2039-2042.

Berry, V., Mackay, D., Khaliq, S., Francis, P. J., Hameed, A., Anwar, K., Mehdi, S. Q., Newbold, R. J., Ionides, A., Shiels, A., Moore, T. and Bhattacharya, S. .S. (1999) Connexin 50 mutation in a family with congenital "zonular nuclear" pulverulent cataract of Pakistani origin. *Hum. Genet.*, **105,** 168-170.

Berthoud, V. M., Ledbetter, M. L. S., Hertzberg, E. L. and Saez, J. C. (1992) Connexin43 in MDCK cells: regulation by a tumor-promoting phorbol ester and Ca^{2+}. *Eur. J. Cell Biol.*, **57,** 40-50.

Berthoud, V. M., Rook, M. B., Traub, O., Hertzberg, E. L. and Saez, J. C. (1993) On the mechanisms of cell uncoupling induced by a tumor promoter phorbol ester in clone 9 cells, a rat liver epithelial cell line. *Eur. J. Cell Biol.*, **62,** 384-396.

Bevans, C. G., Kordel, M., Rhee, S. K. and Harris, A. L. (1998) Isoform composition of connexin channels determines selectivity among second messengers and uncharged molecules. *J. Biol. Chem.*, **273,** 2808-2816.

Beyer, E. C., Paul, D. L. and Goodenough, D. A. (1987) Connexin43: a protein from rat heart homologous to a gap junction protein form liver. *J. Cell Biol.*, **105,** 2621-2629.

Beyer, E. C., Kistler, J., Paul, D. L. and Goodenough, D. A. (1989) Antisera directed against connexin43 peptides react with a 43-kD protein localized to gap junctions in myocardium and other tissues. *J. Cell Biol.*, **108,** 595-605.

Beyer, E. C. (1993) Gap junctions. *Int. Rev. Cytol.*, **137C**, 1-37.

Bhat, N. R., Zhang, P. and Hogan, E. L. (1995) Thrombin activates mitogen-activated protein kinase in primary astrocyte cultures. *J. Cell. Physiol.*, **165**, 417-424.

Bickler, P. E. and Kelleher, J. A. (1992) Fructose-1,6-bisphosphate stabilizes brain intracellular calcium during hypoxia in rats. *Stroke*, **23**, 1617-1622.

Blenk, K. H., Janig, W., Michaelis, M. and Vogel, C. (1996) Prolonged injury discharge in unmyelinated nerve fibers following transection of the sural nerve in rats. *Neurosci. Lett.*, **215**, 185-188.

Boe, R., Gjertsen, B. T., Vintermyr, O. K., Houge, G., Lanotte, M. and Doskeland, S. O. (1991) The protein phosphatase inhibitor okadaic acid induces morphological changes typical of apoptosis in mammalian cells. *Exp. Cell Res.*, **195**, 237-246.

Bordey, A. and Sontheimer, H. (1998) Properties of human glial cells associated with epileptic seizure foci. *Epilepsy Res.*, **32**, 286-303.

Brink, P. R., Cronin, K., Banach, K., Peterson, E., Westphale, E. M., Seul, K. H., Ramanan, S. V. and Beyer, E. C. (1997) Evidence for heteromeric gap junction channels formed from rat connexin43 and human connexin37. *Am. J. Physiol.*, **273**, C1386-C1396.

Britz-Cunningham, S. H., Shah, M. M., Zuppan, C. W. and Fletcher, W. H. (1995) Mutations of the Connexin43 gap-junction gene in patients with heart malformations and defects of laterality. *N. Engl. J. Med.*, **332**, 1323-1329.

Bruzzone, R., Haefliger, J. A., Gimlich, R. L. and Paul, D. L. (1993) Connexin40, a component of gap junctions in vascular endothelium, is restricted in its ability to interact with other connexins. *Mol. Biol. Cell*, **4**, 7-20.

Bruzzone, B., White, T. W. and Paul, D. L. (1996) Connections with connexins: the molecular basis of direct intercellular signaling. *Eur. J. Biochem.*, **238**, 1-27.

Burt, J. M. and Spray, D. C. (1989) Volatile anesthetics block intercellular communication between neonatal rat myocardial cells. *Circ. Res.*, **65**, 829-837.

Butt, A. M. and Ransom, B. R. (1993) Morphology of astrocytes and oligodendrocytes during development in the intact rat optic nerve. *J. Comp. Neurol.*, **338**, 141-158.

Cahill, A. L. and Perlman, R. L. (1991) Activation of a microtubule-associated protein-2 kinase by insulin-like growth factor-I in bovine chromatin cells. *J. Neurochem.*, **57**, 1832-1839.

Campos de Carvalho, A. C., Roy, C., Moreno, A. P., Melman, A., Hertzberg, E. L., Christ, G. J. and Spray, D. C. (1993) Gap junctions formed of connexin43 are found between smooth muscle cells of human corpus cavernosum. *J. Urol.*, **149**, 1568-1575.

Campos de Carvalho, A. C., Roy, C., Hertzberg, E. L., Tanowitz, H. B., Kessler, J. A., Weiss, L. M., Wittner, M., Dermietzel, R., Gao, Y. and Spray, D. C. (1998) Gap junction disappearance in astrocytes and leptomeningeal cells as a consequence of protozoan infection. *Brain Res.*, **790**, 304-314.

Caspar, D. L. D., Goodenough, D. A., Makowski, L. and Phillips, W. C. (1977) Gap junction structures. I. Correlated electron microscopy and X-ray diffraction. *J. Cell Biol.*, **74,** 605-628.

Charles, A. C., Naus, C. C., Zhu, D., Kidder, G. M., Dirksen, E. R. and Sanderson, M. J. (1992) Intercellular calcium signaling via gap junctions in glioma cells. *J. Cell Biol.*, **118,** 195-201.

Charles, A. (1998) Intercellular calcium waves in glia. *Glia,* **24,** 39-49.

Charollais, A., Serre, V., Mock, C., Cogne, F., Bosco, D. and Meda, P. (1999) Loss of alpha 1 connexin does not alter the prenatal differentiation of pancreatic beta cells and leads to the identification of another islet cell connexin. *Dev. Genet.*, **24,** 13-26.

Chen, H., Chopp, M., Schultz, L., Bodzin, G. and Garcia, J. H.(1993) Sequential neuronal and astrocytic changes after transient middle cerebral artery occlusion in the rat. *J Neurol. Sci.*, **118**, 109-116.

Chisamore, B., Solc, M. and Dow, K. (1996) Excitatory amino acid regulation of astrocyte proteoglycans. *Dev. Brain Res.*, **97,** 22-28.

Choi, D. W. and Rothman, S. M. (1990) The role of glutamate neurotoxicity in hypoxic-ischemic neuronal death. *Annu. Rev. Neurosci.*, **13,** 171-182.

Cohen, P. (1989) The structure and regulation of protein phosphatases. *Annu. Rev. Biochem.*, **58,** 453-508.

Cole, W. C. and Garfield, R. E. (1988) Effects of calcium ionophore, A23187 and calmodulin inhibitors on intercellular communication in the rat myometrium. *Biol. Reprod.*, **38,** 55-62.

Condorelli, D. F., Parenti, R., Spinella, F., Trovato Salinaro, A., Belluardo, N., Cardile, V. and Cicirata, F. (1998) Cloning of a new gap junction gene (Cx36) highly expressed in mammalian brain neurons. *Eur. J. Neurosci.*, **10,** 1202-1208.

Cornell-Bell, A. H., Finkbeiner, S., Cooper, M. S. and Smith, S. J. (1990) Glutamate induces calcium waves in cultured astrocytes: long-range signaling. *Science*, **247,** 470-473.

Cotrina, M.L., Kang, J., Lin, J.H.C., Bueno, E., Hansen, T.W., He, L., Liu, Y. and Nedergaard, M. (1998a) Astrocytic gap junctions remain open during ischemic conditions. *J. Neurosci.*, **18,** 2520-2537.

Cotrina, M. L., Lin, J. H., Alves-Rodrigues, A., Liu, S., Li, J., Azmi-Ghadimi, H., Kang, J., Naus, C. C. and Nedergaard, M. (1998b) Connexins regulate calcium signaling by controlling ATP release. *Proc. Natl. Acad. Sci. U.S.A.*, **95,** 15735-15740.

Crow, D. S., Beyer, E. C., Paul, D. L., Kobe, S. S. and Lau, A. F. (1990) Phosphorylation of connexin43 gap junction protein in uninfected and Rous sarcoma virus-transformed mammalian fibroblasts. *Mol. Cell Biol.*, **10,** 1754-1763.

Cruciani, V. and Mikalsen, S. O. (1999) Stimulated phosphorylation of intracellular connexin43. *Exp. Cell Res.*, **251,** 285-298.

Cruciani, V., Kaalhus, O. and Mikalsen, S. O. (1999) Phosphatases involved in modulation of gap junctional intercellular communication and dephosphorylation of connexin43 in hamster fibroblasts: 2B or not 2B? *Exp. Cell Res.*, **252,** 449-463.

Dahl, E., Manthey, D., Chen, Y., Schwarz, H. J., Chang, Y. S., Lalley, P. A., Nicholson, B. J. and Willecke, K. (1996) Molecular cloning and functional expression of mouse connexin-30, a gap junction gene highly expressed in adult brain and skin. *J. Biol. Chem.*, **271,** 17903-17910.

Dahl, G., Werner, R., Levine, E. and Rabadan-Diehl, C. (1992) Mutational analysis of gap junction formation. *Biophys. J.*, **62,** 238-247.

Dahl, G., Nonner, W. and Werner, R. (1994) Attempts to define functional domains of gap junction proteins with synthetic peptides. *Biophys. J.*, **67,** 1816-1822.

Dahl E., Manthey D., Chen Y., Schwarz H.-J., Chang S., Lalley P. A. Nicholson B. J. and Willecke K. (1996) Molecular cloning and functional expression of mouse connexin30, a gap junction gene highly expressed in adult brain and skin. *J. Biol. Chem.* **271,** 17903-17910.

Dani, J. W., Chernjavsky, A. and Smith, S. J. (1992) Neuronal activity triggers calcium waves in hippocampal astrocyte networks. *Neuron,* **8,** 429-440.

Darrow, B. J., Laing, J. G., Lampe, P. D., Saffitz, J. E. and Beyer, E. C. (1995) Expression of multiple connexins in cultured neonatal rat ventricular myocytes. *Circ. Res.*, **76,** 381-387.

Dekker, L. R. C., Fiolet, J. W. T., VanBavel, E., Coronel, R., Opthof, T., Spaan, J. A. E. and Janse, M. J. (1996) Intracellular Ca^{2+}, intercellular electrical coupling, and mechanical activity in ischemic rabbit papillary muscle. *Circ. Res.*, **79**, 237-246.

Dermietzel, R., Yancey, S. B., Traub, O., Willecke, K. and Revel, J. P. (1987) Major loss of the 28 kD protein of gap junction in proliferating hepatocytes. *J. Cell Biol.*, **105**, 1925-1934.

Dermietzel, R., Traub, O., Hwang, T. K., Beyer, K., Bennett, M. V. L., Spray, D. C. and Willecke, K. (1989) Differential expression of three gap junction proteins in developing and mature brain tissues. *Proc. Natl., Acad. Sci. U.S.A.*, **86**, 10148-10152.

Dermietzel, R., Hertzberg, E. L., Kessler, J. A. and Spray, D. C. (1991) Gap junctions between cultured astrocytes: immunocytochemical, molecular, and electrophysiological analysis. *J. Neurosci.*, **11**, 1421-1432.

Dermietzel, R. and Spray, D. C. (1993) Gap junctions in the brain: where, what type, how many and why? *Trends Neurosci.*, **16**, 186-192.

Dermietzel, R., Farooq, M., Kessler, J. A., Althaus, H., Hertzberg, E. L. and Spray, D. C. (1997) Oligodendrocytes express gap junction proteins connexin32 and connexin45. *Glia*, **20**, 101-114.

Dewey, M. M. and Barr, L. (1962) Intercellular connections between smooth muscle cells: the nexus. *Science*, **137**, 670-672.

Diez, J. A., Elvira, M. and Villalobo, A. (1998) The epidermal growth factor receptor tyrosine kinase phosphorylates connexin32. *Mol. Cell. Biochem.*, **187**, 201-210.

Duffy, P. E., Rapport, M. and Graf, L. (1980) Glial fibrillary acid protein and Alzheimer-like dementia. *Neurology*, **30,** 778-782.

Dunia, I., Recouvreur, M., Nicolas, P., Kumar, N., Bloemendal, H. and Benedetti, E. L. (1998) Assembly of connexins and MP26 in lens fiber plasma membranes studied by SDS-fracture immunolabeling. *J. Cell Sci.*, **111,** 2109-2120.

Eddleston, M. and Mucke, L. (1993) Molecular profile of reactive astrocytes-implications for their role in neurologic disease. *Neuroscience*, **54,** 15-36.

Elfgang, C., Eckert, R., Lichtenberg-Frate, H., Butterweck, A., Traub, O., Klein, R. A., Hulser, D. F. and Willecke, K. (1995) Specific permeability and selective formation of gap junction channels in connexin-transfected Hela cells. *J. Cell Biol.*, **129,** 805-817.

el-Fouly, M. H., Trosko, J. E. and Chang, C. C. (1987) Scrape-loading and dye transfer. A rapid and simple technique to study gap junctional intercellular communication. *Exp. Cell Res.*, **168,** 422-430.

Elvira, M., Diez, J. A., Wang, K. K. and Villalobo, A. (1993) Phosphorylation of connexin-32 by protein kinase C prevents its proteolysis by mu-calpain and m-calpain. *J. Biol. Chem.*, **268,** 14294-14300.

Elvira, M., Wang, K. K. and Villalobo, A. (1994) Phosphorylated and non-phosphorylated connexin-32 molecules in gap junction plaques are protected against calpain proteolysis after phosphorylation by protein kinase C. *Biochem. Soc. Trans.*, **22,** 793-796.

Eng, A. F. and Ghirnikar, R. S. (1994) GFAP and astrogliosis. *Brain Pathol.*, **4,** 229-237.

Enkvist, M. O. and McCarthy, K. D. (1992) Activation of protein kinase C blocks astroglial gap junction communication and inhibits the spread of calcium waves. *J. Neurochem.*, **59**, 519-526.

Enkvist, M. O. and McCarthy, K. D. (1994) Astroglial gap junction communication is increased by treatment with either glutamate and high K^+ concentration. *J. Neurochem.*, **62**, 489-495.

Evans, W. H., Ahmad, S., Diez, J., George, C. H., Kendall, J. M. and Martin, P. E. M. (1999) Trafficking pathways leading to the formation of gap junctions. *Novartis Found. Sym.*, **219**, 44-59.

Fallon, R. F. and Goodenough, D. A. (1981) Five-hour half-life of mouse liver gap-junction protein. *J. Cell Biol.* **90**, 521-526.

Filson, A. J., Azarnia, R., Beyer, E. C., Loewenstein, W. R. and Brugge, J. S. (1990) *Cell Regul.*, **1**, 661-668.

Finbow, M. E. and Pitts, J. D. (1993) Is the gap junction channel – the connexon – made of connexin or ductin? *J. Cell Sci.*, **106**, 463-472.

Finbow, M. E., Harrison, M. and Phillip, J. (1995) Ductin – a proton pump component, a gap junction channel and a neurotransmitter release channel. *Bioessays*, **17**, 247-255.

Finkbeiner, S. (1992) Calcium waves in astrocytes-filling in the gaps. *Neuron*, **8**, 1101-1108.

Fishman, G. I., Moreno, A. P., Spray, D. C. and Leinwand, L. A. (1991) Functional analysis of human cardiac gap junction channel mutants. *Proc. Natl., Acad. Sci. U.S.A.*, **88,** 3525-3529.

Flagg-Newton, J. & Loewenstein, W.R. (1979) Experimental depression of junctional membrane permeability in mammalian cell culture. A study with tracer molecules in the 300 to 800 dalton range. *J. Membr.* **50,** 65-100.

Foote, C. I., Zhou, L., Zhu, X. and Nicholson, B. J. (1998) The pattern of disulfide linkages in the extracellular loop regions of connexin 32 suggests a model for the docking interface of gap junctions. *J. Cell Biol.*, **140,** 1187-1197.

Friedland, R. P., Majocha, R. E., Reno, J. M., Lyle, L. R. and Marotta, C.A. (1994) Development of an anti-Aβ monoclonal antibody for in vivo imaging of amyloid angiopathy in Alzheimer's disease. *Mol. Neurobiol.*, **9,** 117-113.

Frey, G., Lucht, M. and Schlue, W. R. (1998) ATP-inhibited K^+ channels and membrane potential of identified leech neurons. *Brain Res.*, **798,** 247-253.

Froes, M. M., Correia, A. H. P., Garcia-Abreu, J., Spray, D., Campos de Carvalho, A. C. and Mneto, V. M. (1999) Gap-junctional coupling between neurons and astrocytes in primary central nervous system cultures. *Proc. Natl. Acad. Sci. U.S.A.*, **96,** 7541-7546.

Fujimoto, K., Araki, N., Ogawa, K. S., Kondo, S., Kitaoka, T. and Ogawa, K. (1989) Ultracytochemistry of calmodulin binding sites in myocardial cells by staining of frozen thin sections with colloidal gold-labeled calmodulin. *J. Histochem. Cytochem.*, **37,** 249-256.

Fujita, M., Spray, D. C., Choi, H., Saez, J., Jefferson, D. M., Hertzberg, E., Rosenberg, L. C. and Reid, L. M. (1986) Extracellular matrix regulation of cell-cell communication and tissue-specific gene expression in primary liver cultures. *Prog. Clin. Biol. Res.* **226**, 333-360.

Furshpan, E. J. and Potter, D. D. (1959) Transmission at the giant motor synapses of the crayfish. *J. Physiol.*, **145**, 289-325.

Gabriel, H. D., Jung, D., Butzler, C., Temme, A., Traub, O., Winterhager, E. and Willecke, K. (1998) Transplacental uptake of glucose is decreased in embryonic lethal connexin26-deficient mice. *J. Cell Biol.*, **140**, 1453-1461.

Garcia, J. H., Yoshida, Y., Chen, H., Li, Y., Zhang, Z. G., Lian, J., Chen, S. and Chopp, M. (1993) Progression from ischemic injury to infarct following middle cerebral artery occlusion in the rat. *Am. J. Pathol.*, **142**, 623-635.

Gaymes, T. J., Cebrat, M., Siemion, Z. and Kay, J. E. (1997) Cyclolinopeptide A (CLA) mediates its immunosuppressive activity through cyclophilin-dependent calcineurin inactivation. *FEBS Lett.*, **418**, 224-227.

Gelb, B. D., Zhang, J., Cotter, P. D., Gershin, I. F. and Desnick, R. J. (1997) Physical mapping of the human connexin 40 (GJA5), flavin-containing monooxygenase 5, and natriuretic peptide receptor a genes on 1q21. *Genomics*, **39**, 409-411.

George, C. H., Kendall, J. M. and Evans, W. H. (1999) Intracellular trafficking pathways in the assembly of connexins into gap junctions. *J. Biol. Chem.*, **274**, 8678-8685.

Giaume, C., Fromaget, C., Aoumari, A. E., Cordier, J., Glowinski, J. and Gros, D. (1991a). Gap junctions in cultured astrocytes: single-channel currents and characterization of channel-forming protein. *Neuron*, **6**, 133-143.

Giaume, C., Marin, P., Cordier, J., Glowinski, J. and Premont, J. (1991b). Adrenergic regulation of intercellular communications between cultured striatal astrocytes from the mouse. *Proc. Natl. Acad. Sci. U.S.A.*, **88**, 5577-5581.

Giaume, C. and Venance, L. (1995). Gap junctions in brain glial cells and development. *Perspect. Dev. Neurobiol.*, **2**, 335-345.

Giaume, C. and McCarthy, K. D. (1996). Control of gap junctional communication in astrocytic networks. *Trends Neurosci.*, **8**, 319-325.

Giaume, C., Tabernero, A. and Medina, J. M. (1997). Metabolic trafficking through astrocytic gap junctions. *Glia*, **21**, 114-123.

Giepmans, B. N. and Moolenaar, W. H. (1998) The gap junction protein connexin43 interacts with the second PDZ domain of the zona occludens-1 protein. *Curr. Biol.*, **8**, 931-934.

Gilchrist, J. S., Wang, K. K., Katz, S. and Belcastro, A. N. (1992) Calcium-activated neutral protease effects upon skeletal muscle sarcoplasmic reticulum protein structure and calcium release. *J. Biol. Chem.*, **267**, 20857-20865.

Gilula, N. B., Reeves, O. R. and Steinbach, A. (1972) Metabolic coupling, ionic coupling and cell contacts. *Nature*, **235**, 262-265.

Girsch, S. J. and Peracchia, C. (1985) Lens cell-to-cell channel proteins: I. Self-assembly into liposomes and permeability regulation by calmodulin. *J. Membr. Biol.*, **83,** 217-225.

Glenner, G. G. and Wong, C. W. (1984) Alzheimer's disease: Initial report of the purification and characterization of a novel cerebrovascular amyloid protein. Biochem. *Biophys. Res. Commun.*, **120,** 885-890.

Godwin, A. J., Green, L. M., Walsh, M. P., McDonald, J. R., Walsh, D. A. and Fletcher, W. H. (1993) In situ regulation of cell-cell communication by the cAMP-dependent protein kinase and protein kinase C. *Mol. Cell. Biochem.*, **127/128,** 293-307.

Goldberg, G. S. and Lau, A. F. (1993) Dynamics of connexin43 phosphorylation in pp60v-src-transformed cells. *Biochem. J.*, **295,** 735-742.

Gong, X., Li, E., Klier, G., Huang, Q., Wu, Y., Lei, H., Kumar, N. M., Horwitz, J. and Gilula, N. B. (1997) Disruption of alpha3 connexin gene leads to proteolysis and cataractogenesis in mice. *Cell,* **91,** 833-843.

Gong, X., Baldo, G. J., Kumar, N. M., Gilula, N. B. and Mathias, R. T. (1998) Gap junctional coupling in lenses lacking alpha3 connexin. *Proc. Natl. Acad. Sci. U.S.A.*, **95,** 15303-15308.

Goodenough, D. A. and Revel, J. P. (1970) A fine structural analysis of intercellular junctions in the mouse liver. *J. Cell Biol.*, **45,** 272-290.

Goodenough, D. A. (1974) Bulk isolation of mouse hepatocyte gap junctions: Characterization of the principal protein, connexin. *J. Cell Biol.*, **61,** 557-563.

Goodenough, D. A. (1975) Methods for the isolation and structural characterization of hepatocyte gap junctions. In *Methods in Membrane Biology.* Vol. 3, E. D. Korn, ed. Plenum Publishing Corp., New York.

Goodenough, D. A., Paul, D. L. and Jesaitis, L. (1988) Topological distribution of two connexin32 antigenic sites in intact and split rodent hepatocyte gap junctions. *J. Cell Biol.*, **107**, 1817-1824.

Goodenough, D. A., Goliger, J. A. and Paul, D. L. (1996) Connexins, connexons and intercellular communication. *Ann. Rev. Biochem.*, **65**, 475-502.

Gores, G. J., Nieminen, A. L., Wray, B. E., Herman, B. and Lemasters, J. J. (1989) Intracellular pH during "chemical hypoxia" in cultured rat hepatocytes. Protection by intracellular acidosis against the onset of cell death. *J. Clin. Invest.*, **83**, 386-396.

Gorin, M. B., Yancey, S. B., Cline, J., Revel, J. P. and Horwitz, J. (1984) The major intrinsic protein (MIP) of the bovine lens fiber membrane: characterization and structure based on cDNA cloning. *Cell*, **39**, 49-59.

Gramolini, A. and Renaud, J. M. (1997) Blocking ATP-sensitive K^+ channel during metabolic inhibition impairs muscle contractility. *Am. J. Physiol.*, **272**, C1936-1946.

Grifa, A., Wagner, C. A., D'Ambrosio, L., Melchionda, S., Bernardi, F., Lopez-Bigas, N., Rabionet, R., Arbones, M., Monica, M. D., Estivill, X., Zelante, L., Lang, F. and Gasparini, P. (1999) Mutations in GJB6 cause nonsyndromic autosomal dominant deafness at DFNA3 locus. *Nat. Genet.*, **23**, 16-18.

Gruijters, W. T. (1989) A non-connexon protein (MIP) is involved in eye lens gap –junction formation. *J. Cell Sci.*, **93**, 509-513.

Guan, X. and Ruch, R. J. (1996) Gap junction endocytosis and lysosomal degradation of connexin43-P2 in WB-F344 rat liver epithelial cells treated with DDT and lindane. *Carcinogenesis*, **17**, 1791-1798.

Guan, X., Wilson, S., Schlender, K. K. and Ruch, R. J. (1996) Gap-junction disassembly and connexin43 dephosphorylation induced by 18β-glycyrrhetinic acid. *Mol. Carcinog.*, **16**, 157-164.

Guan, X., Cravatt, B. F., Ehring, G. R., Hall, J. E., Boger, D. L., Lerner, R. A. and Gilula, N. B. (1997) The sleep-inducing lipid oleamide deconvolutes gap junction communication and calcium wave transmission in glial cells. *J. Cell Biol.*, **139**, 1785-1792.

Guerrero, P. A., Schuessler, R. B., Davis, L. M., Beyer, E. C., Johnson, C. M., Yamada, K. A. and Saffitz, J. E. (1997) Slow ventricular conduction in mice heterozygous for a connexin43 null mutation. *J. Clin. Invest.*, 99, 1991-1998.

Guo, X., Ohno, Y. and Takanaka, A. (1993) Inhibition of hepatocyte gap junctional communication by 25-hydroxycholesterol may be mediated through free radicals. *Eur. J. Pharmacol.*, **248**, 337-340.

Gupta, S. K., Gallego, C., Johnson, G. L. and Heasley, L. E. (1992) MAP kinase is constitutively activated in gip2 and src transformed rat 1a fibroblasts. *J. Biol. Chem.*, **267**, 7987-7990.

Guthrie, P. B., Knappenberger, J., Segal, M., Bennett, M. V. L., Charles, A. C. and Kater, S. B. (1999) ATP released from astrocytes mediates glial calcium waves. *J. Neurosci.*, **19,** 520-528.

Guthrie, S. C. and Gilula, N. B. (1989) Gap junctional communication and development. *Trends Neurosci.*, **12,** 12-16.

Haefliger, J. A., Bruzzone, R., Jenkins, N. A., Gilbert, D. J., Copeland, N. G. and Paul, D. L. (1992) Four novel members of the connexin family of gap junction proteins. Molecular cloning, expression, and chromosome mapping. *J. Biol. Chem.*, **267,** 2057-2064.

Halayko, A. J., Salari, H., Ma, X. and Stephens, N. L. (1996) Markers of airway smooth muscle cell phenotype. *Am. J. Physiol.*, **270,** L1040-1051.

Harold, D. E. and Walz, W. (1992) Metabolic inhibition and electrical properties of type-1-like cortical astrocytes. *Neuroscience*, **47,** 203-211.

Hashimoto, T., Kawamata, T., Saito, N., Sasaki, M., Nakai, M., Niu, S., Taniguchi, T., Terashima, A., Yasuda, M., Maeda, K. and Tanaka, C. (1998) Isoform-specific redistribution of calcineurin Aα and Aβ in the hippocampal CA1 region of gerbils after transient ischemia. *J. Neurochem.*, **70,** 1289-1298.

Hasler, L., Walz, T., Tittmann, P., Gross, H., Kistler, J. and Engel, A. (1998) Purified lens major intrinsic protein (MIP) forms highly ordered tetragonal two-dimensional arrays by reconstitution. *J. Mol. Biol.*, **279,** 855-864.

Hassinger, T. D., Atkinson, P. B., Strecker, G. J., Whalen, L. R., Dudek, R. E., Kossel, A. H. and Kater, S. B. (1995) Evidence for glutamate-mediated activation of hippocampal neurons by glial calcium waves. *J. Neurosci.*, **28,** 159-170.

Hassinger, T. D., Guthrie, P. B., Atkinson, P. B., Bennett, M. V. L. and Kater, S. B. (1996) An extracellular signaling component in propagation of astrocytic calcium waves. *Proc. Natl. Acad. Sci. U.S.A.*, **93,** 13268-13273.

Hatten, M. E., Liem, R. K., Shelanski, M. L. and Mason, C.A. (1991) Astroglia in CNS injury. *Glia,* **4,** 233-243.

Haubrich, S., Schwarz, H.-J., Bukauskas, F., Lichtenberg-Frate, H., Traub, O., Weingart, R. and Willecke, K. (1996) Incompatibility of connexin40 and 43 hemichannels in gap junctions between mammalian cells is determined by intracellular domains. *Mol. Biol. Cell,* 7, 1995-2006.

He, D. S., Jiang, J. X., Taffet, S. M. and Burt, J. M. (1999) Formation of heteromeric gap junction channels by connexins 40 and 43 in-vascular smooth muscle cells. *Proc. Natl. Acad. Sci. U.S.A.*, **96,** 6495-6500.

Hedman, H. and Lundgren, E. (1992) Regulation of LFA-1 avidity in human B cells requirements for dephosphorylation events for high avidity ICAM-1 binding. *J. Immunol.*, **149,** 2295-2299.

Hennemann, H., Schwarz, H. J. and Willecke, K. (1992a) Characterization of gap junction genes expressed in F9 embryonic carcinoma cells: molecular cloning of mouse connexin31 and -45 cDNAs. *Eur. J. Cell Biol.*, **57,** 51-58.

Hennemann, H., Dahl, E., White, J. B., Schwarz, H. J., Lalley, P. A., Chang, S., Nicholson, B. J. and Willecke, K. (1992b) Two gap junction genes, connexin 31.1 and 30.3, are closely linked on mouse chromosome 4 and preferentially expressed in skin. *J. Biol. Chem.*, **267,** 17225-17233.

Hertlein, B., Butterweck, A., Haubrich, S., Willecke, K. and Traub, O. (1998) Phosphorylated carboxy terminal serine residues stabilize the mouse gap junction protein connexin45 against degradation. *J. Membr. Biol.*, **162,** 247-257.

Hertzberg, E. L., Disher, R. M., Tiller, A. A., Zhou, Y. and Cook, R. G. (1988) Topology of the Mr 27,000 liver gap junction protein. *J. Biol. Chem.*, **263,** 19105-19111.

Hidaka, S., Maehara, M., Umino, O., Lu, Y. and Hashimoto, Y. (1993) Lateral gap junction connections between retinal amacrine cells summating sustained responses. *Neuroreport,* **5,** 29-32.

Hill, C. S. T., Oh, S.-Y., Schmidt, S. A., Clark, K. J. and Murray, A. W. (1994) Lysophosphatidic acid inhibits gap-junctional communication and stimulates phosphorylation of connexin-43 in WB cells: possible involvement of the mitogen-activated protein kinase cascade. *Biochem. J.*, **303,** 475-479.

Hofer, A., Saez, J. C., Chang, C. C., Trosko, J. E., Spray, D. C. and Dermietzel, R. (1996) C-erbB2/neu transfection induces gap junctional communication incompetence in glial cells. *J. Neurosci.*, **16,** 4311-4321.

Hofer, A. and Dermietzel, R. (1998) Visualization and functional blocking of gap junction hemichannels (connexons) with antibodies against external loop domains in astrocytes. *Glia,* **24,** 141-154.

Hoh, J. H., John, S. A. and Revel, J. P. (1991) Molecular cloning and characterization of a new member of the gap junction gene family, connexin-31. *J. Biol. Chem.*, **266,** 6524-6531.

Holmes, T. C., Fadool, D. A. and Levitan, I. B. (1996) Tyrosine phosphorylation of the Kv1.3 potassium channel. *J. Neurosci.*, **16,** 1581-1590.

Honda, T. and Marotta, C. A. (1992) Arginine specific endopeptidases modify the aggregation properties of a synthetic peptide derived from Alzheimer β/A4 amyloid. *Neurochem. Res.*, **17,** 367-374.

Hosli, E. and Hosli, L. (1993) Receptors for neurotransmitters on astrocytes in the mammalian central nervous system. *Prog. Neurobiol.*, **40,** 477-506.

Hossain, M. Z., Peeling, J., Sutherland, G. R., Hertzberg, E. L. and Nagy, J. I. (1994a) Ischemia-induced cellular redistribution of the astrocytic gap junctional protein connexin43 in rat brain. *Brain Res.*, **652,** 311-322.

Hossain, M. Z., Sawchuk, M. A., Murphy, L. J., Hertzberg, E. L. and Nagy, J. I. (1994b). Kainic acid induced alterations in antibody recognition of connexin43 and loss of astrocytic gap junctions in rat brain, *Glia,* **10,** 250-265.

Hossain, M. Z., Murphy, L. J. and Nagy, J. I. (1994c) Phosphorylated forms of connexin43 predominate in rat brain: demonstration by rapid inactivation of brain metabolism. *J. Neurochem.*, **62,** 2394-2403.

Hossain, M. Z., Ernst, L. A. and Nagy, J. I. (1995) Utility of intensely fluorescent cyanine dyes (Cy3) for assay of gap junctional communication by dye-transfer. *Neurosci. Lett.*, **184,** 71-74.

Hossain, M. Z., Ao, P. and Boynton, A. L. (1998) Platelet-derived growth factor-induced disruption of gap junctional communication and phosphorylation of connexin43 involves protein kinase C and mitogen-activated protein kinase. *J. Cell. Physiol.*, **176,** 332-341.

Hossain, M. Z., Jagdale, A. B., Ao, P. and Boynton, A. L. (1999a) Mitogen-activated protein kinase and phosphorylation of connexin43 are not sufficient for the disruption of gap junctional communication by platelet-derived growth factor and tetradecanoylphorbol acetate. *J. Cell. Physiol.*, **179,** 87-96.

Hossain, M. Z., Jagdale, A. B., Ao, P., Kazlauskas, A. and Boynton, A. L. (1999b) Disruption of gap junctional communication by the platelet-derived growth factor is mediated via multiple signaling pathway. *J. Biol. Chem.*, **274,** 10489-10496.

Houghton, F. D., Thonnissen, E., Kidder, G. M., Naus, C. C., Willecke, K. and Winterhager, E. (1999) Doubly mutant mice, deficient in connexin32 and -43, show normal prenatal development of organs where the two gap junction proteins are expressed in the same cells. *Dev. Genet.*, **24,** 5-12.

Howarth, A. G., Hughes, M. R. and Stevenson, B. R. (1992) Detection of the tight junction-associated protein ZO-1 in astrocytes and other nonepithelial cell types. *Am. J. Physiol.*, **262,** C461-469.

Hsieh, C. L., Kumar, N. M., Gilula, N. B. and Francke, U. (1991) Distribution of genes for gap junction membrane channel proteins on human and mouse chromosomes. *Somat. Cell. Mol. Genet.*, **17**, 191-200.

Hu, J., Engman, L. and Cotgreave, I. A. (1995) Redox-active chalcogen-containing glutathione peroxidase mimetics and antioxidants inhibit tumor promoter-induced down-regulation of gap junctional intercellular communication between WB-F344 liver epithelial cells. *Carcinogenesis*, **16**, 1815-1824.

Huang, G. Y., Cooper, E. S., Waldo, K., Kirby, M. L., Gilula, N. B. and Lo, C. W. (1998) Gap junction-mediated cell-cell communication modulates mouse neural crest migration. *J. Cell Biol.*, **143**, 1725-1734.

Huang, X. D., Sandusky, G. E. and Zipes, D. P. (1999) Heterogeneous loss of connexin43 protein in ischemic dog hearts. *J. Cardiovasc. Electrophysiol.*, **10**, 79-91.

Husoy, T., Mikalsen, S.-O. and Sanner, T. (1993) Phosphatase inhibitors, gap junctional intercellular communication and [^{125}I]-EGF binding in hamster fibroblasts. *Carcinogenesis*, **14**, 2257-2265.

Itahana, K., Tanaka, T., Morikazu, Y., Komatu, S., Ishida, N. and Takeya, T. (1998) Isolation and characterization of a novel connexin gene, Cx-60, in porcine ovarian follicles. *Endocrinology*, **139**, 320-329.

Janeczko, K. (1991) The proliferative response of S-100 protein-positive glial cells to injury in the neonatal rat brain. *Brain Res.*, **564**, 86-90.

Janeczko, K. (1993) Co-expression of GFAP and vimentin in astrocytes proliferating in response to injury in the mouse cerebral hemisphere. A combined autoradiographic and double immunocytochemical study. *Int. J. Dev. Neurosci.*, **11**, 139-147.

Jansen, L. A. M., De Vrije, T. and Jongen, W. M. F. (1996) Differences in the calcium-mediated regulation of gap junctional intercellular communication between a cell line consisting of initiated cells and a carcinoma-derived cell line. *Carcinogenesis*, **17**, 2311-2319.

Jarvis, L. J. and Louis, C. F. (1992) The permeability of reconstituted liposomes containing the purified lens fiber cell integral membrane proteins MP20, MP26 and MP70. *J. Membr. Biol.*, **130**, 251-263.

Jennissen, H. P. (1995) Ubiquitin and the enigma of intracellular protein degradation. *Eur. J. Biochem.*, **231**, 1-30.

Jiang, J. X. and Goodenough, D. A. (1996) Heteromeric connexons in lens gap junction channels. *Proc. Natl. Acad. Sci. U.S.A.*, **93**, 1287-1291.

John, S. A., Saner, D, Pitts, J. D., Holzenburg, A., Finbow, M. E. and Lal, R. (1997) Atomic force microscopy of arthropod gap junctions. *J. Struct. Biol.*, **120**, 22-31.

Johnston, M. F., Simon, S. A. and Ramon, F. (1980) Interaction of anaesthetics with electrical synapses. *Nature*, **286**, 498-500.

Juneja, S. C., Barr, K. J., Enders, G. C. and Kidder, G. M. (1999) Defects in the germ line and gonads of mice lacking connexin43. *Biol. Reprod.*, **60**, 1263-1270.

Kadle, R., Zhang, J. T. and Nicholson, B. J. (1991) Tissue-specific distribution of differentially phosphorylated forms of Cx43. *Mol. Cell Biol.* **11**, 363-369.

Kandel, E. R., Siegelbaum, S. A. and Schwartz, J. H. (1991) Synaptic transmission. In Kandel, E. R., Schwartz, J. H. and Jessell, T. M (eds), *Principles of Neural Science*, Elsevier, New York, pp. 123-134.

Kandler, K. and Katz, L. C. (1995) Neuronal coupling and uncoupling in the developing nervous system. *Curr. Opin. Neurol.*, **5**, 98-105.

Kanemitsu, M. Y. and Lau, A. F. (1993) Epidermal growth factor stimulates the disruption of gap junctional communication and connexin43 phosphorylation independent of 12-0-tetradecanoylphorbol 13-acetate-sensitive protein kinase C: the possible involvement of mitogen-activated protein kinase. *Mol. Biol. Cell*, **4**, 837-848.

Kanemitsu, M. Y., Jiang, W. and Eckhart, W. (1998) Cdc2-mediated phosphorylation of the gap junction protein, connexin43, during mitosis. *Cell Growth Diff.*, **9**, 13-21.

Kanno, Y. and Loewenstein, W. R. (1964) Intercellular diffusion. *Science*, **143**, 959-960.

Kardami, E., Stoski, R. M., Doble, B. W., Yamamoto, T., Hertzberg, E. L. and Nagy, J. I. (1991) Biochemical and ultrastructural evidence for the association of basic fibroblast growth factor with cardiac gap junctions. *J. Biol. Chem.*, **226**, 19551-19557.

Kasuya, Y., Abe, Y., Hama, H., Sakurai, T., Asada, S., Masaki, T. and Goto, K. (1994) Endothelin-1 activates mitogen-activated protein kinases through two independent signalling pathways in rat astrocytes. *Biochem. Biophys. Res. Commun.*, **204**, 1325-1333.

Kelsell, D. P., Dunlop, J., Stevens, H. P., Lench, N. J., Liang, J. N., Parry, G., Mueller, R. F. and Leigh, I. M. (1997) Connexin 26 mutations in hereditary non-syndromic sensorineural deafness. *Nature*, **387**, 80-83.

Kenins, P. (1982) Responses of single nerve fibers to capsaicin applied to the skin. *Neurosci. Letts.*, **29**, 83-88.

Kennelly, P. J. and Krebs, E. G. (1991) Consensus sequences as substrate specificity determinants for protein kinases and protein phosphatases. *J. Biol. Chem.*, **266**, 15555-15558.

Kettenmann, H., Orkand, R. K. and Schachner, M. (1983) Coupling among identified cells in mammalian nervous system cultures. *J. Neurosci.*, **3**, 506-516.

Kettenmann, H. and Ransom, B. R. (1988) Electrical coupling between astrocytes and between oligodendrocytes studied in mammalian cell cultures. *Glia*, **1**, 64-73.

Kim, D. Y., Kam, Y., Koo, S. K. and Joe, C. O. (1999) Gating connexin 43 channels reconstituted in lipid vesicles by mitogen-activated protein kinase phosphorylation. *J. Biol. Chem.*, **274**, 5581-5587.

Kimelberg, H. K. and Kettenmann, H. (1990) Swelling-induced changes in electrophysiological properties of cultured astrocytes and oligodendrocytes. I. Effects on membrane potentials, input impedance and cell-cell coupling. *Brain Res.*, **529**, 255-261.

Kimelberg, H. K. (1995) Receptors on astrocytes-what possible functions? *Neurochem. Int.*, **26**, 27-40.

Kirchhoff, S., Nelles, E., Hagendorff, A., Kruger, O., Traub, O. and Willecke, K. (1998) Reduced cardiac conduction velocity and predisposition to arrhythmias in connexin40-deficient mice. *Curr. Biol.*, **8**, 299-302.

Kleber, A. G., Riegger, C. B. and Janse, M. J. (1987) Electrical uncoupling and increase of extracellular resistance after induction of ischemia in isolated, arterially perfused rabbit papillary muscle. *Circ. Res.*, **61**, 271-279.

Koizumi, J., Yoshida, Y., Nakazawa, T. and Ooneda, G. (1986) Experimental studies of ischemic brain edema. 1. A new experimental model of cerebral embolism in rats in which recirculation can be introduced in the ischemic area. *Jpn. J. Stroke*, **8**, 1-8.

Kojima, T., Mitaka, T., Mizuguchi, T. and Mochizuki, Y. (1996) Effects of oxygen radical scavengers on connexins 32 and 26 expression in primary cultures of adult rat hepatocytes. *Carcinogenesis*, **17**, 537-544.

Konietzko, U. and Muller, C. M. (1994) Astrocytic dye coupling in rat hippocampus: topography, developmental onset, and modulation by protein kinase C. *Hippocampus*, **4**, 297-306.

Kreutziger, G. O. (1968) a. Freeze-etching of intercellular junctions of mouse liver. *Proc. Electron Microsc. Soc. Am.*, **26**, 234.

Kriz, N., Sykova, E., Ujec, E. and Vyklicky, L. (1974) Changes of extracellular potassium concentration induced by neuronal activity in the spinal cord of the cat. *J. Physiol.*, **238**, 1-15.

Kuffler, S. W. and Potter, D. D. (1964) Glia in the leech central nervous system: physiological properties and neuron-glia relationship. *J. Neurophysiol.*, **27**, 290-320.

Kumagai, N., Morii, N., Fujisawa, K., Yoshimasa, T., Nakao, K. and Narumiya, S. (1993) Lysophosphatidic acid induces tyrosine phosphorylation and activation of MAP-kinase and focal adhesion kinase in cultured Swiss 3T3 cells. *FEBS Lett.*, **329**, 273-276.

Kumar, N. M. and Gilula, N. B. (1986) Cloning and characterization of human and rat liver cDNAs coding for a gap junction protein. *J. Cell Biol.*, **103**, 767-776.

Kumar, N. M. and Gilula, N. B. (1996) The gap junction communication channel. *Cell*, **84**, 381-388.

Kumar, N. M. (1999) Molecular biology of the interactions between connexins. *Novartis Found. Sym.*, **219**, 6-21.

Kunzelmann, P., Blumcke, I., Traub, O., Dermietzel, R. and Willecke, K. (1997) Coexpression of connexin45 and -32 in oligodendrocytes of rat brain. *J. Neurocytol.*, **26**, 17-22.

Kunzelmann, P., Schroder, W., Traub, O., Steinhauser, C., Dermietzel, R. and Willecke, K. (1999) Late onset and increasing expression of the gap junction protein connexin30 in adult murine brain and long-term cultured astrocytes. *Glia*, **25**, 111-119.

Kwak, B. R., Saez, J. C., Wilders, R., Chanson, M., Fishman, G. I., Hertzberg, E. L., Spray, D. C. and Jongsma, H. J. (1995a) Effects of cGMP-dependent phosphorylation on rat and human connexin43 gap junction channels. *Pflugers Arch.*, **430**, 770-778.

Kwak, B. R., Hermans, M. M. P., De Jonge, H. R., Lohmann, S. M., Jongsma, H. J. and Chanson, M. (1995b) Differential regulation of distinct types of gap junction channels by similar phosphorylating conditions. *Mol. Biol. Cell*, **6**, 1707-1719.

Kwak, B. R., van Veen, T. A., Analbers, L. J. and Jongsma, H. J. (1995c) TPA increases conductance but decreases permeability in neonatal rat cardiomyocyte gap junction channels. *Exp. Cell Res.*, **220**, 456-463.

Kwak, B. R. and Jongsma, H. J. (1996) Regulation of cardiac gap junction channel permeability and conductance by several phosphorylating conditions. *Mol. Cell. Biochem.*, **157**, 93-99.

Kwak, B. R. and Jongsma, H. J. (1999) Selective inhibition of gap junction channel activity by synthetic peptides. *J. Physiol.*, **516**, 679-685.

Lafarga, M., Berciano, M. T., Saurez, I., Andres, M. A. and Berciano, J. (1993) Reactive astroglia-neuron relationships in the human cerebellar cortex: a quantitative, morphological and immunocytochemical study in Creutzfeldt-Jakob disease. *Int. J. Dev. Neurosci.*, **11**, 199-213.

Laing, J. G. and Beyer, E. C. (1995) The gap junction protein connexin43 is degraded via the ubiquitin proteasome pathway. *J. Biol. Chem.*, **270**, 26399-26403.

Laing, J. G., Tadros, P. N., Westphale, E. M. and Beyer, E. C. (1997) Degradation of connexin43 gap junctions involves both the proteasome and the lysosome. *Exp. Cell Res.*, **236**, 482-492.

Laing, J. G., Tadros, P. N., Green, K., Saffitz, J. E. and Beyer, E. C. (1998) Proteolysis of connexin43-containing gap junctions in normal and heat-stressed cardiac myocytes. *Cardiovas. Res.*, **38,** 711-718.

Laird, D. W. and Revel, J. P. (1990) Biochemical and immunochemical analysis of the arrangement of connexin43 in rat heart gap junction membranes. *J. Cell Sci.*, **97,** 109-117.

Laird, D. W., Puranam, K. L. and Revel, J. P. (1991) Turnover and phosphorylation dynamics of connexin43 gap junction protein in cultured cardiac myocytes. *Biochem. J.*, **273,** 67-72.

Laird, D. W., Castillo, M. and Kasprzak, L. (1995) Gap junction turnover, intracellular trafficking, and phosphorylation of connexin43 in brefeldin A-treated rat mammary tumor cells. *J. Cell Biol.*, **131,** 1193-1203.

Laird, D. W. (1996) The life cycle of a connexin: gap junction formation, removal, and degradation. *J. Bioenerg. Biomembr.*, **28,** 311-318.

Laird, J. M. A. and Bennett, G. J. (1993) An electrophysiological study of dorsal horn neurons in the spinal cord of rats with an experimental peripheral neuropathy. *J. Neurophysiol.*, **69,** 2072-2085.

Lampe, P. D. (1994) Analyzing phorbol ester effects on gap junctional communication: a dramatic inhibition of assembly. *J. Cell Biol.*, **127,** 1895-1905.

Lampe, P. D., Kurata, W. E., Warn-Cramer, B. J. and Lau, A. F. (1998) Formation of a distinct connexin43 phosphoisoform in mitotic cells is dependent upon p34cdc2 kinase. *J. Cell Sci.*, **111,** 833-841.

Larsen, W. J. and Tung, H. N. (1978) Origin and fate of cytoplasmic gap junctional vesicles in rabbit granulosa cells. *Tissue & Cell*, **10**, 585-598.

Laskawi, R., Rohlmann, A., Landgrebe, M. and Wolff, J.R. (1997) Rapid astroglial reactions in the motor cortex of adult rats following peripheral facial nerve lesions. *Eur. Arch. Oto. Rhino. Laryngol.*, **254**, 81-85.

Lau, A. F., Hatch-Pigott, V. and Crow, D. S. (1991) Evidence that heart connexin43 is a phosphoprotein. *J. Mol. Cell. Cardiol.*, **23**, 659-663.

Lau, A. F., Kanemitsu, M. Y., Kurata, W. E., Danesh, S. and Boynton, A. L. (1992) Epidermal growth factor disrupts gap-junctional communication and induces phosphorylation of connexin43 on serine. *Mol. Biol. Cell*, **3**, 865-874.

Lau, A. F., Kurata, W. E., Kanemitsu, M. Y., Loo, L. W. M., Warn-Cramer, B. J., Eckhart, W. and Lampe, P. D. (1996) Regulation of connexin43 function by activated tyrosine protein kinases. *J. Bioenerg. Biomembr.*, **28**, 359-368.

Lavado, E., Sanchez-Abarca, L. I., Tabernero, A., Bolanos, J. P. and Medina, J. M. (1997) Oleic acid inhibits gap junction permeability and increases glucose uptake in cultured rat astrocytes. *J. Neurochem.*, **69**, 721-728.

Lazarini, F., Strosberg, A. D., Couraud, P. O. and Cazaubon, S. M. (1996) Coupling of ETB endothelin receptor to mitogen-activated protein kinase stimulation and DNA synthesis in primary cultures of rat astrocytes. *J. Neurochem.*, **66**, 459-465.

Lee, S. H., Magge, S., Spencer, D. D., Sontheimer, H. and Cornell-Bell, A. H. (1995) Human epileptic astrocytes exhibit increased gap junction coupling. *Glia*, 15, 195-202.

Leybaert, L., Paemeleire, K., Strahonja, A. and Sanderson, M. J. (1998) Inositol-trisphosphate-dependent intercellular calcium signaling in and between astrocytes and endothelial cells. *Glia*, **24**, 398-407.

Li, H., Liu, T. F., Lazrak, A., Peracchia, C., Goldberg, G. S., Lampe, P. D. and Johnson, R. G. (1996) Properties and regulation of gap junctional hemichannels in the plasma membranes of cultured cells. *J. Cell Biol.*, **134**, 1019-1030.

Li, J., Hertzberg, E. L. and Nagy, J. I. (1997). Connexin32 in oligodendrocytes and association with myelinated fibers in mouse and rat brain. *J. Comp. Neurol.*, **379**, 571-591.

Li, W., Ochalski, P. A. Y., Brimijoin, S., Jordan, L. M. and Nagy, J. I. (1995) C-terminals on motoneurons: electron microscope localization of cholinergic markers in adult rats and antibody-induced depletion in neonates. *Neuroscience*, **65**, 879-891.

Li, W. E. I., Hertzberg, E. L. and Nagy, J. I. (1996) Astrocytic connexin43 in rat brain after focal ischemia. *Soc. Neurosci. Abstr.*, **22**, 1023.

Li, W. E. I., Ochalski, P. A. Y., Hertzberg, E. L. and Nagy, J. I. (1998). Immunorecognition, ultrastructure and phosphorylation of astrocytic gap junctions and connexin43 in rat brain after cerebral focal ischemia. *Eur. J. Neurosci.*, **10**, 2444-2463.

Li, W. E. I. and Nagy, J. I. (2000a) Activation of primary afferent fibers in rat sciatic nerve alters the phosphorylation state of connexin43 at astrocytic gap junctions in spinal cord: Evidence for junction regulation by neuronal-glial interactions. *Neuroscience*, submitted.

Li, W. E. I. and Nagy, J. I. (2000b) Connexin43 phosphorylation state and gap junctional intercellular communication in cultured astrocytes following hypoxic treatments and inhibition of protein phosphatases. *Eur. J. Neurosci.*, submitted.

Li, Y., Chopp, M., Jiang, N., Yao, F. and Zaloga, C. (1995a) Temporal profile of in situ DNA fragmentation after transient middle cerebral artery occlusion in the rat. *J. Cereb. Blood Flow Metab.*, **15**, 389-397.

Li, Y., Chopp, M., Jiang, N., Zhang, Z. G. and Zaloga, C. (1995b) Induction of DNA fragmentation after 10 to 120 minutes of focal cerebral ischemia in rats. *Stroke*, **26**, 1252-1258.

Little, T. L., Beyer, E. C. and Duling, B. R. (1995) Connexin 43 and connexin 40 gap junctional proteins are present in arteriolar smooth muscle and endothelium in vivo. *Am. J. Physiol.*, **268**, H729-739.

Little, T. L., Xia, J. and Duling, B. R. (1995) Dye tracers define differential endothelial and smooth muscle coupling patterns within the arteriolar wall. *Circ. Res.*, **76**, 498-504.

Llinas, R. R. (1985) Electronic transmission in the mammalian central nervous system. In Bennett, M. V. L. and Spray, D. C. (eds) *Gap Junctions*,. Cold Spring Harbor Laboratory. New York, pp337-353.

Lo, C. W. (1996) The role of gap junction membrane channels in development. *J. Bioenerg. Biomembr.*, **28**, 379-385.

Loewenstein, W. R. and Kanno, Y. (1964) Studies on an epithelial (gland) cell junction. I. Modifications of surface membrane permeability. *J. Cell Biol.*, **22,** 565-586.

Loewenstein, W. R. (1975) Permeable junctions. *Cold Spring Harbor Symp. Quant. Biol.*, **40,** 49-63.

Loewenstein, W. R. (1981) Junctional intercellular communication: The cell-to-cell membrane channel. *Physiol. Rev.*, **61,** 829-913.

Longa, E. Z., Weinstein, P. R., Carlson, S. and Cummins, R. (1989) Reversible middle cerebral artery occlusion without craniectomy in rats. *Stroke*, **20,** 84-91.

Loo, L. W. M., Berestecky, J. M., Kanemitsu, M. Y. and Lau, A. F. (1995) pp60src-mediated phosphorylation of connexin 43, a gap junction protein. *J. Biol. Chem.*, **270,** 12751-12761.

Lynn, B., Ye, W. and Cotsell, B. (1992) The actions of capsaicin applied topically to the skin of the rat on C-fiber afferents, antidromic vasodilatation and substance P levels. *Br. J. Pharmacol.*, **107,** 400-406.

Mackay, D., Ionides, A., Kibar, Z., Rouleau, G., Berry, V., Moore, A., Shiels, A. and Bhattacharya, S. (1999) Connexin46 mutations in autosomal dominant congenital cataract. *Am. J. Hum. Genet.*, **64,** 1357-1364.

Majocha, R. E., Benes, F. M., Reifel, R. L., Rodenrys, A. M. and Marotta, C. A. (1988) Laminar-specific distribution and infrastructural detail of amyloid in the Alzheimer cortex visualized by computer-enhanced imaging of unique epitopes, *Proc. Natl. Acad. Sci. U.S.A.*, **85,** 6182-6186.

Majocha, R. E., Tate, B. and Marotta, C. A. (1992a) PC12 cells release stimulatory factors after transfection with β/A4 C-terminal DNA of the Alzheimer amyloid precursor protein. *Cell. Mol. Neurobiol.*, **18,** 99-113.

Majocha, R. E., Reno, J. M., Van Haight, C., Lyle, L. R., Friedland, R. P. and Marotta, C.A. (1992b) Development of a monoclonal antibody specific for β/A4 amyloid in Alzheimer's disease brain for application to in vivo imaging of amyloid angiopathy. *J. Nucl. Med.*, **33,** 2184-2189.

Makowski, L., Caspar, D. L. D., Phillips, W. C. and Goodenough, D. A. (1977) Gap junction structures. II. Analysis of the X-ray diffraction data. *J. Cell Biol.*, **74,** 629-645.

Mandel, M., Moriyama, Y., Hulmes, J. D., Pan, Y.-C., Nelson, H. and Nelson, N. (1988) cDNA sequence encoding the 16 kDa proteolipid of chromaffin granules implies gene duplication in the evolution of H+-ATPases. *Proc. Natl. Acad. Sci. U.S.A.*, **85,** 5521-5524.

Mandybur, T. I. and Chuirazzi, B. A. (1990) Astrocytes and the plaques of Alzheimer's disease. *Neurology*, **40,** 635-639.

Manthey, D., Bukauskas, F., Lee, C. G., Kozak, C. A. and Willecke, K. (1999) Molecular cloning and functional expression of the mouse gap junction gene connexin-57 in human HeLa cells. *J. Biol. Chem.*, **274,** 14716-14723.

Mantz, J., Cordier, J. and Giaume, C. (1993) Effects of general anesthetics on intercellular communication mediated by gap junctions between astrocytes in primary culture. *Anesthesiology*, **78,** 892-901.

Marrero, H. and Orkand, R. K. (1996) Nerve impulses increase glial intercellular permeability. *Glia*, **16**, 285-289.

Martin, R. L., Lloyd, H. G. E. and Cowan, A. I. (1994) The early events of oxygen and glucose deprivation: setting the scene for neuronal death? *Trend Neurosci.*, **17**, 251-257.

Massa, P. T. and Mugnaini, E. (1982) Cell junctions and intermembrane particles of astrocytes and oligodendrocytes: a freeze-fracture study. *Neuroscience*, **7**, 523-538.

Massa, P. T. and Mugnaini, E. (1985) Cell-cell junctional interactions and characteristic plasma membrane features of cultured rat glial cells. *Neuroscience*, **14**, 695-709.

Masters, C. L., Simms, G., Weinman, N. A., Multhaup, G., McDonald, B. L. and Beyreuther, I. (1985) Amyloid plaque core protein in Alzheimer's disease and Down syndrome. *Proc. Natl. Acad. Sci. U.S.A.*, **82**, 4245-4249.

Matsuda, T., Takuma, K., Asano, S., Kishida, Y., Nakamura, H., Mori, K., Maeda, S. and Baba, A. (1998) Involvement of calcineurin in Ca^{2+} paradox-like injury of cultured rat astrocytes. *J. Neurochem.*, **70**, 2004-2011.

McCarthy, K. D. and DeVellis, J. (1980) Preparation of separate astroglial and gligodendroglial cell cultures from rat cerebral tissue. *J. Cell Biol.*, **85**, 890-902.

Meda, P. (1996) The role of gap junction membrane channels in secretion and hormonal action. *J. Bioenerg. Biomembr.*, **28**, 369-377.

Mesaeli, N., Lamers, J. M. and Panagia, V. (1992) Phosphoinositide kinases in rat heart sarcolemma: biochemical properties and regulation by calcium. *Mol. Cell. Biochem.*, **117,** 181-189.

Meyer, D. J., Yancey, S. B. and Revel, J. P. (1981) Intercellular communication in normal and regenerating rat liver: a quantitative analysis. *J. Cell Biol.* **91**, 505-523.

Meyer, R. A., Laird, D. W., Revel, J.-P. and Johnson, R. G. (1992) Inhibition of gap junction and adhesions junction assembly by connexin and A-CAM antibodies. *J. Cell Biol.*, **119,** 179-189.

Micevych, P. E. and Abelson, L. (1991) Distribution of mRNAs coding for liver and heart gap junction proteins in the rat central nervous system. *J. Comp. Neurol.*, **305,** 96-118.

Mignon, C., Fromaget, C., Mattei, M. G., Gros, D., Yamasaki, H. and Mesnil, M. (1996) Assignment of connexin 26 (GJB2) and 46 (GJA3) genes to human chromosome 13q11-->q12 and mouse chromosome 14D1-E1 by in situ hybridization. *Cytogenet. Cell. Genet.*, **72,** 185-186.

Mikalsen, S.-O., Husoy, T., Vikhamar, G. and Sanner T. (1997) Induction of phosphotyrosine in the gap junction protein, connexin43. *FEBS Lett.*, **401,** 271-275.

Milks, L. C., Kumar, N. M., Houghten, R., Unwin, N. and Gilula, N. B. (1988) Topology of the 32-kd liver gap junction protein determined by site-directed antibody localizations. *EMBO J.*, **7,** 2967-2975.

Moennikes, O., Buchmann, A., Ott, T., Willecke1, K. and Schwarz, M. (1999) The effect of connexin32 null mutation on hepatocarcinogenesis in different mouse strains. *Carcinogenesis*, **20,** 1379-1382.

Moreno, A. P., Saez, J. C., Fishman, G. I. and Spray, D. C. (1994) Human connexin43 gap junction channels: regulation of unitary conductances by phosphorylation. *Circ. Res.*, **74,** 1050-1057.

Morioka, M., Hamada, J.-I., Ushio, Y. and Miyamoto, E. (1999) Potential role calcineurin for brain ischemia and traumatic injury. *Prog. Neurobiol.*, **58,** 1-30.

Mugnaini, E. (1986) Cell junctions of astrocytes, ependyma, and related cells in the mammalian central nervous system, with emphasis on the hypothesis of a generalized functional syncytium of supporting cells. In Fedoroff, S. and Vernadakis, A. (eds), *Astrocytes*, Vol., 1, Academic Press, New York, pp. 329-371.

Muller, T., Moller, T., Neuhaus, J. and Kettenmann, H. (1996) Electrical coupling among Bergmann glial cells and its modulation by glutamate receptor activation. *Glia*, **17,** 274-284.

Musil, L. S., Cunningham, B. A., Edelman, G. M. and Goodenough, D. A. (1990) Differential phosphorylation of the gap junction protein connexin43 in junctional communication-competent and –deficient cell lines. *J. Cell Biol.*, **111,** 2077-2088.

Musil, L. S. and Goodenough, D. A. (1991) Biochemical analysis of connexin43 intracellular transport, phosphorylation, and assembly into gap junctional plaques. *J. Cell Biol.*, **115,** 1357-1374.

Musil, L. S. and Goodenough, D. A. (1993) Multisubunit assembly of an integral plasma membrane channel protein, gap junction connexin43, occurs after exit from the ER. *Cell*, **74**, 1065-1077.

Mussini, J., Biral, D., Marin, O., Furlan, S. and Salvatori, S. (1999) Myotonic dystrophy protein kinase expressed in rat cardiac muscle is associated with sarcoplasmic reticulum and gap junctions. *J. Histochem. Cytochem.*, **47**, 383-392.

Nadarajah, B., Thomaidou, D., Evans, W. H. and Parnavelas, J. G. (1996) Gap junctions in the adult cerebral cortex: Regional differences in their distribution and cellular expression of connexins. *J. Comp. Neurol.*, **376**, 326-342.

Nagy, J. I., Yamamoto, T., Sawchuk, M. A., Nance, D. M. and Hertzberg, E. L. (1992) Quantitative immunohistochemical and biochemical correlates of connexin43 localization in rat brain. *Glia*, **5**, 1-9.

Nagy, J. I., Hossain, M. Z., Lynn, B. D., Li, W., Hertzberg, E. L. and Marotta, C.A. (1995) Connexin43 (Cx43) and gap junctions in PC12 cells overexpressing β/A4 amyloid and Cx43 elevation in Alzheimer's disease. *Soc. Neurosci. Abst.*, **21**, 1717.

Nagy, J. I., Hossain, M. Z., Hertzberg, E. L. and Marotta, C.A. (1996a). Induction of connexin43 and gap junctional communication in PC12 cells overexpressing the carboxy terminal region of amyloid precursor protein. *J. Neurosci. Res.*, **44**, 124-132.

Nagy, J. I., Li, W. E. I., Doble, B. W., Hochman, S., Hertzberg, E. L. and Kardami, E. (1996b) Detection of dephosphorylated Cx43 in brain, heart and in spinal cord after nerve stimulation. *Soc. Neurosci. Abstr.*, **22**, 1023.

Nagy, J. I., Li, W., Hertzberg, E. L. and Marotta, C. A. (1996c). Elevated connexin43 immunoreactivity at sites of amyloid plaques in Alzheimer's disease. *Brain Res.*, **717**, 173-178.

Nagy, J. I., Ochalski, P. A. Y., Li, J. and Hertzberg, E. L. (1997a). Evidence for the co-localization of another connexin with connexin43 at astrocytic gap junctions in rat brain. *Neuroscience*, **78**, 533-548.

Nagy, J. I., Li, W. E. I., Roy, C., Doble, B. W., Gilchrist, J., Kardami, E. and Hertzberg, E. L. (1997b) Selective monoclonal antibody recognition and cellular localization of an unphosphorylated form of connexin43. *Exp. Cell Res.*, **236**, 127-136.

Nagy, J. I., Patel, D., Ochalski, P. A. Y. and Stelmack, G. L. (1999a). Connexin30 in rodent, cat and human brain: selective expression in gray matter astrocytes, co-localization with connexin30 at gap junctions and late developmental appearance. *Neuroscience*, **88**, 447-468.

Nagy, J. I. and Rash, J. E. (1999b) Connexins and gap junctions of astrocytes and oligodendrocytes in the CNS. *Brain Res. Rev.* In press.

Nagy, J. I. and Dermietzel, R. (2000) Gap junctions and connexins in the mammalian central nervous system. In *Advances in Molecular and Cell Biology* (ed. Hertzberg E. L.) Vol. 18, JAI, New York. In press.

Naus, C. C. G., Hearn, S., Zhu, D., Nicholson, B. J. and Shivers, R. R. (1993) Ultrastructural analysis of gap junctions in C6 glioma cells transfected with connexin43 cDNA. *Exp. Cell Res.*, **206**, 72-84.

Naus, C. C. G., Bechberger, J. F., Zhang, Y., Venance L., Yamasaki, H., Juneja, S. C., Kidder, G. M. and Giaume, C. (1997) Altered gap junctional communication, intercellular signaling, and growth in cultured astrocytes deficient in connexin43. *J. Neurosci. Res.*, **49**, 528-540.

Nedergaard, M. (1994). Direct signaling from astrocytes to neurons in cultures of mammalian brain cells. *Science*, **263**, 1768-1771.

Nedergaard, M., Cooper, A. J. L. and Goldman, S. A. (1995) Gap junctions are required for the propagation of spreading depression. *J. Neurobiol.*, **28**, 433-444.

Nelles, E., Butzler, C., Jung, D., Temme, A., Gabriel, H. D., Dahl, U., Traub, O., Stumpel, F., Jungermann, K., Zielasek, J., Toyka, K. V., Dermietzel, R. and Willecke, K. (1996) Defective propagation of signals generated by sympathetic nerve stimulation in the liver of connexin32-deficient mice. *Proc. Natl. Acad. Sci. U.S.A.*, **93**, 9565-9570.

Newman, E. A. (1985) Regulation of potassium levels by glial cells in the retina. *Trends Neurosci.* **8**, 156-159.

Newman, E. A. and Zahs, K. R. (1997) Calcium waves in retinal glial cells. *Science*, **275**, 844-847.

Newman, E. A. and Zahs, K. R. (1998) Modulation of neuronal activity by glial cells in the retina. *J. Neurosci.*, **18**, 4022-4028.

Nicholson, B. J., Hunkapillar, M. W., Grim, L. B., Hood, L. E. and Revel, J.-P. (1981) Rat liver gap junction protein: properties and partial sequence. *Proc. Natl. Acad. Sci. U.S.A.*, **78**, 7594-7598.

Nicholson, B., Dermietzel, R., Teplow, D., Traub, O., Willecke, K. and Revel, J. P. (1987) Two homologous protein components of hepatic gap junctions. *Nature*, **329**, 732-734.

O'brian, J., Al-Ubaidi, M. R. and Ripps, H. (1996) Connexin35: A gap junctional protein expressed preferentially in the skate retina. *Mol. Biol. Cell*, **7**, 233-243.

Ochalski, P. A. Y., Hossain, M. Z., Sawchuk, M. A., Hertzberg, E. L. and Nagy, J. I. (1995). Astrocytic gap junction removal, connexin43 redistribution and epitope masking at excitatory amino acid lesion sites in rat brain. *Glia*, **14**, 279-294.

Ochalski, P. A. Y., Frankenstein, U. N., Hertzberg, E. L. and Nagy, J. I. (1997). Connexin43 in rat spinal cord: localization in astrocytes and identification of heterotypic astro-oligodendrocytic gap junctions. *Neuroscience*, **76**, 931-945.

Oelze, I., Kartenbeck, J., Crusius, K. and Alonso, A. (1995) Human papillomavirus type 16 E5 protein affects cell-cell communication in an epithelial cell line. *J. Virol.*, **69**, 4489-4494.

Ogata, T., Nakamura, Y., Tsuji, K., Shibata, T. and Kataoka, K. (1995) A possible mechanism for the hypoxia-hypoglycemia-induced release of excitatory amino acids from cultured hippocampal astrocytes. *Neurochem. Res.*, **20**, 737-743.

Oh, S. Y., Grupen, C. G. and Murray, A. W. (1991) Phorbol ester induces phosphorylation and down-regulation of connexin 43 in WB cells. *Biochim. Biophys. Acta.*, **1094**, 243-245.

Omori, Y. and Yamasaki, H. (1999) Gap junction proteins connexin32 and connexin43 partially acquire growth-suppressive function in HeLa cells by deletion of their C-terminal tails. *Carcinogenesis*, **20**, 1913-1918.

Orkand, R. K., Nicholls, J. G. and Kuffler, S. W. (1966) Effect of nerve impulses on the membrane potential of glial cells in the central nervous system of amphibia. *J. Neurophysiol.*, **29,** 788-806.

Orkand, R. K. (1986) Introductory remarks: Glial-interstitial fluid exchange. *Ann. N. Y. Acad. Sci.*, **481,** 269-272.

Osipchuk, Y. and Cahalan, M. (1992) Cell-to-cell spread of calcium signals mediated by ATP receptors in mast cells. *Nature*, **359,** 241-244.

Ou, C. W., Orsino, A. and Lye, S. J. (1997) Expression of connexin-43 and connexin-26 in the rat myometrium during pregnancy and labor is differentially regulated by mechanical and hormonal signals. *Endocrinology*, **138,** 5398-5407.

Pappas, G. D. and Bennett, M. V. L. (1966) Specialized junctions involved in electrical transmission between neurons. *Ann. N. Y. Acad. Sci.*, **137,** 495-508.

Parpura, V., Basarsky, T. A., Liu, F., Jeftinija, K., Jeftinija, S., and Haydon, P.G. (1994). Glutamate-mediated astrocyte-neuron signaling. *Nature*, **369,** 744-747.

Pastor, A., Kremer, M., Moller, T., Kettenmann, H. and Dermietzel, R. (1998) Dye coupling between spinal cord oligodendrocytes: differences in coupling efficiency between gray and white matter. *Glia*, **24,** 108-120.

Payton, B. W., Bennett, M. V. L. and Pappas, G. D. (1969) Temperature-dependence of resistance at an electronic synapse. *Science*, **165,** 594-597.

Paul, D. L. (1986) Molecular cloning of cDNA for rat liver gap junction protein. *J. Cell Biol.*, **103,** 123-134.

Paul, D. L., Ebihara, L., Takemoto, L. J., Swenson, K. I. and Goodenough, D. A. (1991) Connexin46, a novel lens gap junction protein, induces voltage-gated currents in nonjunctional plasma membrane of Xenopus oocytes. *J. Cell Biol.*, **115,** 1077-1089.

Peracchia, C. (1980) Structural correlates of gap junction permeation. *Int. Rev. Cytol.*, **66,** 81-146.

Peracchia, C. and Bernardini, G. (1984) Gap junction structure and cell-to-cell coupling regulation: is there a calmodulin involvement? *Fed. Proc.*, **43,** 2681-2691.

Peracchia, C. and Girsch, S.J. (1985) Permeability and gating of lens gap junction channels incorporated into liposomes. *Curr. Eye Res.*, **4,** 431-439.

Peracchia, C., Wang, X., Li, L. and Peracchia, L.L. (1996) Inhibition of calmodulin expression prevents low-pH-induced gap junction uncoupling in Xenopus oocytes. *Pflugers Arch.*, **431,** 379-387.

Pereda, A. E., Bell, T. D., Chang, B. H., Czernik, A. J., Nairn, A. C., Soderling, T. R. & Faber, D. S. (1998) Ca^{2+}/calmodulin-dependent kinase II mediates simultaneous enhancement of gap-junctional conductance and glutamatergic transmission. *Proc. Natl. Acad. Sci. U.S.A.*, **95,** 13272-13277.

Perez Velazquez, J. L., Frantseva, M., Naus, C. C. G., Bechberger, J. F., Juneja, S. C., Velumian, A., Carlen, P. L., Kidder, G. M. and Mills, L. R. (1996) Development of

astrocytes and neurons in cultured brain slices from mice lacking connexin43. *Dev. Brain Res.*, **97**, 293-296.

Peters, J. M. (1994) Proteasomes: protein degradation machines of the cell. *Trends Biochem. Sci.*, **19**, 377-382.

Peters, N. S., Coromilas, J., Severs, N. J. and Wit, A. L. (1997) Disturbed connexin43 gap junction distribution correlates with the location of reentrant circuits in the epicardial border zone of healing canine infarcts that cause ventricular tachycardia. *Circulation*, **95**, 988-996.

Petrov, T., Howarth, A. G., Krukoff, T. L. and Stevenson, B. R. (1994) Distribution of the tight junction-associated protein ZO-1 in circumventricular organs of the CNS. *Mol. Brain Res.*, **21**, 235-246.

Peusner, K. D. and Giaume, C. (1994) The first developing "mixed" synapses between vestibular sensory neurons mediate glutamate chemical transmission. *Neuroscience*, **58**, 99-113.

Phelan, P., Bacon, J. P., Davies, J. A., Stebbings, L. A., Todman, M. G., Avery, L., Baines, R. A., Barnes, T. M., Ford, C., Hekimi, S., Lee, R., Shaw, J. E., Starich, T. A., Curtin, K. D., Sun, Y. A. and Wyman, R. J. (1998) Innexins: a family of invertebrate gap junction proteins. *Trends Genet.*, **14**, 348-349.

Pitts, B. J. R. (1979) Stoichiometry of sodium-calcium exchange in cardiac sarcolemmal vesicles. Coupling to the sodium pump. *J. Biol. Chem.*, **254**, 6232-6235.

Postma, F. R., Hengeveld, T., Alblas, J., Giepmans, B. N. G., Zondag, G. C. M., Jalink, K. and Moolenaar, W. H. (1998) Acute loss of cell-cell communication caused by G protein-coupled receptors: A critical role of c-Src. *J. Cell Biol.*, **140,** 1199-1209.

Pshenichkin, S. P. and Wise, B. C. (1995) Okadaic acid increases nerve growth factor secretion, mRNA stability, and gene transcription in primary cultures of cortical astrocytes. *J. Biol. Chem.*, **270,** 5994-5999.

Puranam, K. L., Laird, D. W. and Revel, J. P. (1993) Trapping an intermediate form of connexin43 in the Golgi. *Exp. Cell Res.*, **206,** 85-92.

Raff, M. C. (1989) Glial cell diversification in the rat optic nerve. *Science*, **243,** 1450-1455.

Randriamampita, C. and Tsien, R. Y. (1995) Degradation of a calcium influx factor (CIF) can be blocked by phosphatase inhibitors or chelation of Ca^{2+}. *J. Biol. Chem.*, **270,** 29-32.

Ransom, B. R. and Kettenmann, H. (1990) Electrical coupling, without dye coupling between mammalian astrocytes and oligodendrocytes in cell cultures. *Glia*, **3,** 258-266.

Ransom, B. R. (1995) Gap junctions. In Kettenmann, H. and Ransom, B. R. (eds) *Neuroglia*, Oxford University Press, New York. pp299-318.

Rash, J. E., Dillman, R. K., Bilhartz, B. L., Duffy, H. S., Whalen, L. R., and Yasumura, T. (1996). Mixed synapses discovered and mapped throughout mammalian spinal cord. *Proc. Natl. Acad. Sci. U.S.A.*, **93,** 4235-4239.

Rash, J. E., Duffy, H. S., Dudek, F. E., Bilhartz, B. L., Whalen, L. R., and Yasumura, T. (1997). Grid-mapped freeze-fracture analysis of gap junctions in gray and white matter of

adult rat central nervous system, with evidence for a "panglial syncytium" that is not coupled to neurons. *J. Comp. Neurol.*, **388,** 265-292.

Reaume, A. G., De Sousa, P. A., Kulkarni, S., Langille, B. L., Zhu, D., Davies, T. C., Juneja, S. C., Kidder, G. M. and Rossant, J. (1995) Cardiac malformation in neonatal mice lacking connexin43. *Science,* **267,** 1831-1834.

Reuss, B. and Unsicker, K. (1998) Regulation of gap junction communication by growth factors from non-neural cells to astroglia: A brief review. *Glia,* **24,** 32-38.

Revel, J. P. and Karnovsky, M. J. (1967) Hexagonal arrays of subunits in intercellular junctions of the mouse heart and liver. *J. Cell Biol.*, **33,** C7-C12.

Revel, J. P., Hoh, J. H., John, S. A., Laird, D. W., Puranam, K. and Yancey, S. B. (1992) Aspects of gap junction structure and assembly. *Semin. Cell Biol.*, **3,** 21-28.

Richard, G., Smith, L. E., Bailey, R. A., Itin, P., Hohl, D., Epstein Jr, E. H., GiGiovanna, J. J., Compton, J. G. and Bale, S. J. (1998) Mutations in the human connexin gene GJB3 cause erythrokeratodermia variabilis. *Nat. Genet,* **20,** 366-369.

Robertson, J. D. (1963) The occurrence of a subunit pattern in the unit membranes of club endings in Mauthner cell synapses in goldfish brains. *J. Cell Biol.*, **19,** 201-221.

Robinson, S. R., Hampson, E. C. G. M., Munro, M. N. and Vaney, D. I. (1993) Unidirectional coupling of gap junctions between neuroglia. *Science,* **262,** 1072-1074.

Rohlmann, A., Laskawi, R., Hofer, A., Dobo, E., Dermietzel, R. and Wolff, J.R. (1993) Facial nerve lesions lead to increased immunostaining of the astrocytic gap junction protein (connexin43) in the corresponding facial nucleus of rats. *Neurosci. Lett.*, **154**, 206-208.

Rohlmann, A., Laskawi, R., Hofer, A., Dermietzel, R. and Wolff, J. R. (1994) astrocytes as rapid sensors of peripheral axotomy in the facial nucleus of rats. *Neuroreport*, **36**, 409-412.

Rose, C. R. and Ransom, B. R. (1997) Gap junctions equalize intracellular Na^+ concentration in astrocytes. *Glia* **20**, 299-307.

Saez, J. C., Spray, D. C., Nairn, A. C., Hertzberg, E. L., Greenngard, P. and Bennet, M. V. L. (1986) cAMP increases junctional conductance and stimulates phosphorylation of 27 kDa principal gap junction polypeptide. *Proc. Natl. Acad. Sci. U.S.A.*, **83**, 2473-2477.

Saez, J. C., Connor, J. A., Spray, D. C. and Bennett, M. V. L (1989a) Hepatocyte gap junctions are permeable to the second messenger, inositol 1,4,5-trisphosphate, and to calcium ions. *Proc. Natl. Acad. Sci. U.S.A.*, **86**, 2708-2712.

Saez, J. C., Gregory, W. A., Watanabe, T., Dermietzel, R., Hertzberg, E. L., Reid, L., Bennett, M. V. L. and Spray, D. C. (1989b) cAMP delays disappearance of gap junctions between pairs of rat hepatocytes in primary culture. *Am. J. Physiol.* **257**, C1-11.

Saez, J. C., Nairn, A. C., Czernik, A. J., Spray, D. C., Hertzberg, E. L., Greengard, P. and Bennett, M. V. (1990) Phosphorylation of connexin 32, a hepatocyte gap-junction protein, by cAMP-dependent protein kinase, protein kinase C and Ca^{2+}/calmodulin-dependent protein kinase II. *Eur. J. Biochem.*, **192**, 263-273.

Saez, J. C., Berthoud, V. M., Moreno, A. P. and Spray, D. C. (1993) Gap junctions: Multiplicity of controls in differentiated and undifferentiated cells and possible functional implications. In Shenolikar, S. and Nairn, A. C. (eds), *Advances in Second Messenger and Phosphoprotein Research.*, Vol. 27, Raven Press, New York, pp. 163-198.

Saez, J. C., Nairn, A. C., Czernik, A. J., Fishman, G. I., Spray, D. C. and Hertzberg, E. L. (1997) Phosphorylation of connexin43 and the regulation of neonatal rat cardiac myocyte gap junctions. *J. Mol. Cell. Cardiol.*, **29,** 2131-2145.

Sawchuk, M. A., Hossain, M. Z., Hertzberg, E. L., and Nagy, J. I. (1995). In situ transblot and immunocytochemical comparisons of astrocytic connexin43 responses to NMDA and kainic acid in rat brain. *Brain Res.*, **683,** 153-157.

Scemes, E., Dermietzel, R. and Spray, D. C. (1998) Calcium waves between astrocytes from Cx43 knockout mice. *Glia*, **24,** 65-73.

Scherer, S. S., Deschenes, S. M., Xu, Y.-T., Grinspan, J. B., Fischbeck, K. H. and Paul, D. L. (1995) Connexin32 is a myelin-related protein in the PNS and CNS. *J. Neurosci.*, **15,** 8281-8294.

Scherer, S. S., Xu, Y. T., Nelles, E., Fischbeck, K., Willecke, K. and Bone, L. J. (1998) Connexin32-null mice develop demyelinating peripheral neuropathy. *Glia*, **24,** 8-20

Schousboe, A., Westergaard, N., Waagepetersen, H. S., Larsson, O. M., Bakken, I. J. and Sonnewald, U. (1997) Trafficking between glia and neurons of TCA cycle intermediates and related metabolites. *Glia*, **21,** 99-105.

Seminario, M.-C., Sterbinsky, S. A. and Bochner, B. S. (1998) β1 Integrin-dependent binding of Jurkat cells to fibronectin is regulated by a serine-threonine phosphatase. *J. Leukoc. Biol.*, **64**, 753-758.

Severs, N. J. (1999) Cardiovascular disease. *Novartis Found. Sym.*, **219**, 188-211.

Shiels, A., Mackay, D., Ionides, A., Berry, V., Moore, A. and Bhattacharya, S. (1998) A missense mutation in the human connexin50 gene (GJA8) underlies autosomal dominant "Zonular Pulverulent" cataract, on chromosome 1q. *Am. J. Hum. Genet.*, **62**, 526-532.

Shiosaka, S., Yamamoto, T., Hertzberg, E. L. and Nagy, J. I. (1989) Gap junction protein in rat hippocampus: Correlative light and electron microscope immunohistochemical localization. *J. Comp. Neurol.*, **281**, 282-297.

Shubeita, H. E., Thorburn, J. and Chien, K. R. (1992) Microinjection of antibodies and expression vectors into living myocardial cells. Development of a novel approach to identify candidate genes that regulate cardiac growth and hypertrophy. *Circulation*, **85**, 2236-2246.

Siesjo, B. K. (1992) Pathophysiology and treatment of focal cerebral ischemia. Part I: Pathophysiology. *J. Neurosurg.*, **77**, 169-184.

Simon, A. M., Goodenough, D. A., Li, E. and Paul, D. L. (1997) Female infertility in mice lacking connexin 37. *Nature*, **385**, 525-529.

Simon, A. M., Goodenough, D. A. and Paul, D. L. (1998) Mice lacking connexin40 have cardiac conduction abnormalities characteristic of atrioventricular block and bundle branch block. *Curr. Biol.*, **8**, 295-298.

Simpson, I., Rose, B. and Loewenstein, W. R. (1977) Size limit of molecules permeating the junctional membrane channels. *Science*, **195**, 294-296.

Singer, S. J. and Nicolson, G. L. (1972) The fluid mosaic model of the structure of cell membranes. *Science*, **175**, 720-731.

Singh, M. V., Bhatnagar, R. and Malhotra, S. K. (1997) Inhibition of connexin 43 synthesis by antisense RNA in rat glioma cells. *Cytobios.*, **91**, 103-123.

Snyder, S. H., Lai, M. M. and Burnett, P. E. (1998) Immunophilins in the nervous system. *Neuron*, **21**, 283-294.

Sonnewald, U., Westergaard, N. and Schousboe, A. (1997) Glutamate transport and metabolism in astrocytes. *Glia*, **21**, 56-63.

Sontheimer, H., Minturn, J. E., Black, J. A., Waxman, S. G. and Ransom, B. R. (1990) Specificity of cell-cell coupling in rat optic nerve astrocytes in vitro. *Proc. Natl. Acad. Sci. U.S.A.*, **87**, 9833-9837.

Sosinsky, G. (1995) Mixing of connexins in gap junction membrane channels. *Proc. Natl. Acad. Sci. U.S.A.*, **92**, 9210-9214.

Sotelo, C. and Korn, H. (1978) Morphological correlates of electrical and other interactions through low-resistance pathways between neurons of the vertebrate central nervous system. *Int. Rev. Cytol.*, **55**, 67-107.

Spray, D. C., Moreno, A. P., Kessler, J. A. and Dermietzel, R. (1991) Characterization of gap junctions between cultured leptomeningeal cells. *Brain Res.*, **568,** 1-14.

Starich, T. A., Lee R. Y., Panzarella, C., Avery, L. and Shaw, J. E. (1996) eat-5 and unc-7 represent a multigene family in Caenorhabditis elegans involved in cell-cell coupling. *J. Cell Biol.*, **134,** 537-548.

Stewart, W. W. (1978) Functional connections between cells as revealed by dye-coupling with a highly fluorescent naphthalimide tracer. *Cell,* **14,** 741-759.

Sun, F. F., Fleming, W. E. and Taylor, B. M. (1993) Degradation of membrane phospholipids in the cultured human astroglial cell line UC-11MG during ATP depletion. *Biochem. Pharmacol.*, **45,** 1149-1155.

Swenson K. I., Jordan, J. R., Beyer, E. C. and Paul, D. L. (1989) Formation of gap junctions by expression of connexins in Xenopus oocyte pairs. *Cell,* **57,** 145-155.

Swenson, K. I., Piwnica-Worms, H., McNamee, H. and Paul, D. L. (1990) Tyrosine phosphorylation of the gap junction protein connexin43 is required for the pp60v-src-induced inhibition of communication. *Cell Regul.*, **1,** 989-1002.

Szolcsanyi, J. (1987) Selective responsiveness of polymodal nociceptors of the rabbit ear to capsaicin, bradykinin and ultraviolet radiation. *J. Physiol.*, **388,** 9-23.

Tabernero, A., Giaume, C. and Medino, J. M. (1996) Endothelin-1 regulates glucose utilization in cultured rat astrocytes by controlling intercellular communication through gap junctions. *Glia,* **16,** 187-195.

Takens-Kwak, B. R. and Jongsma, H. J. (1992) Cardiac gap junctions: three distinct single channel conductances and their modulation by phosphorylating treatments. *Pflugers Arch.*, **422**, 198-200.

Temme, A., Buchmann, A., Gabriel, H. D., Nelles, E., Schwarz, M. and Willecke, K. (1997) High incidence of spontaneous and chemically induced liver tumors in mice deficient for connexin32. *Curr. Biol.*, **7**, 713-716.

Teranishi, T. and Negishi, K. (1994) Double-staining of horizontal and amacrine cells by intracellular injection with lucifer yellow and biocytin in carp retina. *Neuroscience*, **59**, 217-226.

Theriault, E., Frankenstein, U. N., Hertzberg, E. L. and Nagy, J. I. (1997) Connexin43 and astrocytic gap junctions in the rat spinal cord after acute compression injury. *J. Comp. Neurol.*, **382**, 199-214.

Thomas, S. A., Schuessler, R. B., Berul, C. I., Beardslee, M. A., Beyer, E. C., Mendelsohn, M. E. and Saffitz, J. E. (1998) Disparate effects of deficient expression of connexin43 on atrial and ventricular conduction: evidence for chamber-specific molecular determinants of conduction. *Circulation*, **97**, 686-691.

Tom-Moy, M., Madison, J. M., Jones, C. A., de Lanerolle, P. and Brown, J. K. (1987) Morphologic characterization of cultured smooth muscle cells isolated from the tracheas of adult dogs. *Anat. Rec.*, **218**, 313-328.

Tournier, C., Pomerance, M., Gavaret, J. M. and Pierre, M. (1994) MAP kinase cascade in astrocytes. *Glia*, **10**, 81-88.

Toyama, J., Sugiura, H., Kamiya, K., Kodama, I., Terasawa, M. and Hidaka, H. (1994) Ca(2+)-calmodulin mediated modulation of the electrical coupling of ventricular myocytes isolated from guinea pig heart. *J. Mol. Cell. Cardiol.*, **26,** 1007-1015.

Toyofuku, T., Yabuki, M., Otsu, K., Kuzuya, T., Hori, M. and Tada, M. (1998) Direct association of the gap junction protein connexin-43 with ZO-1 in cardiac myocytes. *J. Biol. Chem.*, **273,** 12725-12731.

Traub, O., Druge, P. M. and Willecke, K. (1983) Degradation and resynthesis of gap junction protein in plasma membranes of regenerating liver after partial hepatectomy or cholestasis. *Proc. Natl. Acad. Sci. U.S.A.*, **80**, 755-759.

Traub, O., Look, J., Dermietzel, R., Brummer, F., Hulser, D. and Willecke, K. (1989) Comparative characterization of the 21-kD and 26-kD gap junction proteins in murine liver and cultured hepatocytes. *J. Cell Biol.*, **108,** 1039-1051.

Tripuraneni, J., Koutsouris, A., Pestic L., De Lanerolle, P. & Hecht, G. (1997) The toxin of diarrheic shellfish poisoning, okadaic acid, increases intestinal epithelial paracellular permeability. *Gastroenterology*, **112,** 100-108.

Tsacopoulos, M. and Magistretti, P. J. (1996) Metabolic coupling between glia and neurons. *J. Neurosci.*, **16,** 877-885.

Umino, O., Maehara, M., Hidaka, S., Kita, S. and Hashimoto, Y. (1994) The network properties of bipolar-bipolar cell coupling in the retina of teleost fishes. *Vis. Neurosci.*, **11,** 533-548.

Unger, V. M., Kumar, N. M., Gilula, N. B. and Yeager, M. (1997) Projection structure of a gap junction membrane channel at 7 Å resolution. *Nat. Struct. Biol.*, **4**, 39-43.

Unger, V. M., Kumar, N. M., Gilula, N. B. and Yeager, M (1999) Electron cryo-crystallography of a recombinant cardiac gap junction channel. *Novartis Found. Symp.*, **219**, 22-37.

Van Camp, G., Coucke, P., Speleman, F., Van Roy, N., Beyer, E. C., Oostra, B. A. and Willems, P. J. (1995) The gene for human gap junction protein connexin37 (GJA4) maps to chromosome 1p35.1, in the vicinity of D1S195. *Genomics*, **30**, 402-403.

Veenstra, R. D. (1996) Size and selectivity of gap junction channels formed from different connexins. *J. Bioenerg. Biomembr.*, **28**, 327-337.

Venance, L., Cordier, J., Monge, M., Zalc, B., Glowinski, J. and Giaume, C. (1995a) Homotypic and heterotypic coupling mediated by gap junctions during glial cell differentiation in vitro. *Eur. J. Neurosci.*, **7**, 451-461.

Venance, L., Piomelli, D., Glowinski, J. and Giaume, C. (1995b) Inhibition by anandamide of gap junctions and intercellular calcium signalling in striatal astrocytes. *Nature*, **376**, 590-594.

Verrecchia, F. and Herve, J. C. (1997) Reversible blockade of gap junctional communication by 2,3-butanedione monoxime in rat cardiac myocytes. *Am. J. Physiol.*, **272**, C875-885.

Verrecchia, F., Duthe, F., Duval, S., Duchatelle, I., Sarrouilhe, D. & Herve, J.C. (1999) ATP counteracts the rundown of gap junctional channels of rat ventricular myocytes by promoting protein phosphorylation. *J. Physiol.*, **516,** 447-459.

Vinade, L. and Rodnight, R. (1996) The dephosphorylation of glial fibrillary acidic protein (GFAP) in the immature rat hippocampus is catalyzed mainly by a type 1 protein phosphatase. *Brain Res.*, **732,** 195-200.

Vukelic, J. I., Yamamoto, T., Hertzberg, E. L. and Nagy, J. I. (1991) Depletion of connexin43-immunoreactivity in astrocytes after kainic acid-induced lesions in rat brain. *Neurosci. Lett.*, **130,** 120-124.

Vyklicky, L., Sykova, E., Kriz, N. and Ujec, E. (1972) Post-stimulation changes of extracellular potassium concentration in the spinal cord of the rat. *Brain Res.*, **45,** 608-611.

Wachym, P. A., Popper, P., Abelson, L. A., Ward, P. H. and Micevych, P. E. (1991) Molecular biology of the vestibular system. *Acta Otolaryngol.*, **481,** 141-149.

Wall, P. D., Waxman, S. and Basbaum, A. (1974) Ongoing activity in peripheral nerve: injury discharge. *Exp. Neurol.*, **45,** 576-589.

Walz, W. and Hertz, L. (1983) Functional interactions between neurons and astrocytes. II. Potassium homeostasis at the cellular level. *Prog. Neurobiol.*, **20,** 133-183.

Walz, W. (1989) Role of glial cells in the regulation of the brain ion microenvironment. *Prog. Neurobiol.* **33,** 309-333.

Warn-Cramer, B. J., Lampe, P. D., Kurata, W. E., Kanemitsu, M. Y., Loo, L. W. M., Eckhart, W. and Lau, A. F. (1996) Characterization of the mitogen-activated protein kinase phosphorylation sites on the connexin-43 gap junction protein. *J. Biol. Chem.*, **271,** 3779-3786.

Warn-Cramer, B. J., Cottrell, G. R., Burt, J. M. and Lau, A. F. (1998) Regulation of connexin-43 gap junctional intercellular communication by mitogen-activated protein kinase. *J. Biol. Chem.*, **273,** 9188-9196.

Warner, A., Clements, D. K., Parikh, S., Evans, W. H. and DeHaan, R. L. (1995) Specific motifs in the external loops of connexin proteins can determine gap junction formation between chick heart myocytes. *J. Physiol.*, **488,** 721-728.

Warner, A. (1999) Interactions between growth factors and gap junctional communication in developing systems. *Novartis Foundation Symposium,* **219,** 60-75.

Weidmann, S. (1952) The electrical constants of Purkinje fibres. *J. Physiol.*, **118,** 348-360.

Wera, S. and Hemmings, B. A. (1995) Serine/threonine protein phosphatases. *Biochem. J.*, **311,** 17-29.

Wert, S. E. and Larsen, W. J. (1990) Preendocytotic alterations in cumulus cell gap junctions precede meiotic resumption in the rat cumulus-oocyte complex. *Tissue Cell,* **22,** 827-851.

White, T. W., Bruzzone, R., Goodenough, D. A. and Paul, D. L. (1992) Mouse Cx50, a functional member of the connexin family of gap junction proteins, is the lens fiber protein MP70. *Mol. Biol. Cell,* **3,** 711-720.

White, T. W., Bruzzone, R., Wolfram, S., Paul, D. L. and Goodenough, D. A. (1994) Selective interactions among the multiple connexin proteins expressed in the vertebrate lens: the second extracellular domain is a determinant of compatibility between connexins. *J. Cell Biol.*, **125**, 879-892.

White, T. W., Bruzzone, B. and Paul, D. L. (1995a) The connexin family of intercellular channel forming proteins. *Kidney Int.*, **48**, 1148-1157.

White, T. W., Paul, D. L., Goodenough, D. A. and Bruzzone, R. (1995b) Functional analysis of selective interactions among rodent connexins. *Mol. Biol. Cell*, **6**, 459-470.

White, T. W., Goodenough, D. A. and Paul, D. L. (1998) Targeted ablation of connexin50 in mice results in microphthalmia and zonular ulverulent cataracts. *J. Cell Biol.*, **143**, 815-825.

White, W. W. and Paul, D. L. (1999) Genetic diseases and gene knockouts reveal diverse connexin functions. *Annu. Rev. Physiol.*, **61**, 283-310.

Wiesinger, H., Hamprecht, B. and Dringen, R. (1997) Metabolic pathways for glucose in astrocytes. *Glia*, **21**, 22-34.

Willecke, K., Heynkes, R., Dahl, E., Stutenkemper, R., Hennemann, H., Jungbluth, S., Suchyna, T. and Nicholson, B. J. (1991) Mouse connexin37: cloning and functional expression of a gap junction gene highly expressed in lung. *J. Cell Biol.*, **114**, 1049-1057.

Wolburg, H. and Rohlmann, A. (1995) Structure-function relationships in gap junctions. *Int. Rev. Cytol.*, **157**, 315-373.

Wolff, J. R., Stuke, K., Missler, M., Tytko, H., Schwarz, P., Rohlmann, A. and Chao, T. I. (1998) Autocellular coupling by gap junctions in cultured astrocytes: A new view on cellular autoregulation during process formation. *Glia*, **24**, 121-140.

Woolf, C. J. and Fitzgerald, M. (1983) The properties of neurones recorded in the superficial dorsal horn of the rat spinal cord. *J. Comp. Neurol.*, **221**, 313-328.

Woolf, C. J. and King, A. E. (1987) Physiology and morphology of multireceptive neurons with C-afferent fiber inputs in the deep dorsal horn of the rat lumbar spinal cord. *J. Neurophysiol.*, **58**, 460-479.

Wu ,Y., Taylor, B. M. and Sun, F. F. (1996) Alterations in reactive oxygen, pH, and calcium in astrocytoma cells during lethal injury. *Am. J. Physiol.*, **270**, C115-124.

Xia, J.-H., Liu, C.-Y., Tang, B.-S., Pan, Q., Huang, L., Dai, H.-P., Zhang, B.-R., Xie, W., Hu, D.-X., Zheng, D., Shi, X.-L., Wang, D.-A., Xia, K., Yu, K.-P., Liao, X.-D., Feng, Y., Yang, Y.-F., Xiao, J.-Y., Xie, D.-H. and Huang, J.-Z. (1998) Mutations in the gene encoding gap junction protein β-3 associated with autosomal dominant hearing impairment. *Nature Genetics*, **20**, 370-373.

Xie, H., Laird, D. W., Chang, T.-H. and Hu, V. W. (1997) A mitosis-specific phosphorylation of the gap junction protein connexin43 in human vascular cells: biochemical characterization and localization. *J. Cell Biol.*, **137**, 203-210.

Yamamoto, T., Shiosaka, S., Whittaker, M. E., Hertzberg, E. L. and Nagy, J. I. (1989) Gap junction protein in rat hippocampus: Light microscope immunohistochemical localization. *J. Comp. Neurol.*, **281**, 262-281.

Yamamoto, T., Ochalski, A., Hertzberg, E. L. and Nagy, J. I. (1990a) LM and EM immunolocalization of the gap junctional protein connexin 43 in rat brain. *Brain Res.*, **508,** 313-319.

Yamamoto, T., Ochalski, A., Hertzberg, E. L. and Nagy, J. I. (1990b) On the organization of astrocytic gap junctions in rat brain as suggested by LM and EM immunohistochemistry of connexin43 expression. *J. Comp. Neurol.*, **302,** 853-883.

Yamamoto, T., Hertzberg, E. L. and Nagy, J. I. (1990c) Epitopes of gap junctional proteins localized to neuronal subsurface cisterns. *Brain Res.*, **527,** 135-139.

Yamamoto, T., Hertzberg, E. L. and Nagy, J. I. (1991) Subsurface cisterns in α-motoneurons of the rat and cat: Immunohistochemical detection with antibodies against connexin32. *Synapse*, **8,** 119-136.

Yamamoto, T., Vukelic J., Hertzberg, E. L. and Nagy, J. I. (1992) Differential anatomical and cellular patterns of connexin43 expression during postnatal development of rat brain. *Dev. Brain Res.*, **66,** 165-180.

Yamasaki, H., Omori, Y., Krutovskikh. V., Zhu, W., Mironov, N., Yamakage, K. and Mesnil, M. (1999) Connexins in tumour suppression and cancer therapy. *Novartis Found. Symp.*, **219,** 241-260.

Yancey, S. B., Nicholson, B. J. and Revel, J. P. (1981) The dynamic state of liver gap junctions. *J. Supramol. Struct. Cell Biochem.* **16,** 221-232.

Yancey, S. B., John, S. A., Lal, R., Austin, B. J. and Revel, J.-P. (1989) The 43-kD polypeptide of heart gap junctions: immunolocalization, topology and functional domains. *J. Cell Biol.*, **108,** 2241-2254.

Yee, A. G. and Revel, J. P. (1978) Loss and reappearance of gap junctions in regenerating liver. *J. Cell Biol.* **78**, 554-564.

Yuste, R., Nelson, D. A., Rubin, W. W. and Katz, L. C. (1995) Neuronal domains in developing neocortex: Mechanisms of coactivation. *Neuron*, **14,** 7-17.

Zahs, K. R. and Newman, E. A. (1997) Asymmetric gap junctional coupling between glial cells in the rat retina. *Glia*, **20,** 10-22.

Zhang, J.-T. and Nicholson, B. J. (1989) Sequence and tissue distribution of a second protein of hepatic gap junctions, Cx26, as deduced from its cDNA. *J. Cell Biol.*, **109,** 3391-3401.

Zhou, L., Kasperek, E. M. and Nicholson, B. J. (1999) Dissection of the molecular basis of pp60v-src induced gating of connexin 43 gap junction channels. *J. Cell Biol.*, **144,** 1033-1045.

Zhu, D., Caveney, S., Kidder, G. M. and Naus, C. C. G. (1991) Transfection of C6 glioma cells with connexin 43 cDNA: Analysis of expression, intercellular coupling, and cell proliferation. *Proc. Natl. Acad. Sci. U.S.A.*, **88,** 1883-1887.

Zimmer, D. B., Green, C. R., Evans, W. H. and Gilula, N. B. (1987) Topological analysis of the major protein in isolated intact rat liver gap junctions and gap junction-derived single membrane structures. *J. Biol. Chem.*, **262,** 7751-7763.